

One-Dimensional Models for Organic Magnetic Materials

Thesis by

Simon Joshua Jacobs

In Partial Fulfillment of the Requirements for the Degree
of Doctor of Philosophy

California Institute of Technology
Pasadena, California

1994

(Submitted July 23, 1993)

"...were the value of \hbar to go to zero, the loss of the science of magnetism is one of the catastrophes that would overwhelm the universe."

C. Kittel

To My Parents

Acknowledgement

While writing this thesis I drew heavily on the technical and English skills of Kraig Anderson, Scott Silverman, Jeff Clites, Anthony West, and Bruce Hietbrink. Despite my own 48-hour-day efforts, without their help I would have been sunk. Thanks, guys.

My time in graduate school has in large part resembled playing in a chemistry sandbox because I was almost always creating something new and making a big mess in the process. My advisor Dennis Dougherty has had enough guts, money, or both to leave me with my toys, and I am grateful to him for the chance to make my own way. I am also thankful that he had the sense to take the 14 projects I was once working on simultaneously and whittle down to a more manageable number like 4. He has been a moderating influence on my obsession with the new and different, and he actually has gotten me to *finish* some things. This has provided a different type of challenge. Dennis also understands that life extends beyond chemistry, even for graduate students, and he has been understanding and patient with me as I have endured growing pains while here at Caltech.

Other faculty have also had influence on me. Angelo Di Bilio got me going with EPR simulation, and Sunney Chan had some good suggestions when I ran into trouble. Bob Grubbs and Seth Marder are thanked for their guidance and for their assistance in securing my postdoctoral position. Thanks also go to Rudy Marcus and Andy Myers for serving as members of my thesis committee.

My predecessors in the Dougherty group left quite a legacy that I was fortunate to have the chance to build on. I am especially grateful to those I knew personally, who had patience enough to put up with an obnoxious kid that they might teach him the ropes. Frank Coms, Dave Kaisaki, Rakesh Jain, and Dave Stauffer all deserve mention.

Each of my biradical coworkers has added something to my experience and knowledge. Dave Shultz provided inspiration, perspiration, commiseration, and

publication. Without his influence, I would still be struggling to finish this work. Ed Stewart was great to talk to about new synthetic approaches, although he can chew your ear off like a buzz saw; his frequent companionship at three o' clock in the morning rather obviated the need for caffeine. Kraig Anderson has always been able to provide a reasonably sane opinion about most things scientific and otherwise. Mick Murray and Piotr Kaszynski provided many new conundrums related to the MPMS that led to the better ways to do things chronicled here. Scott Silverman and Jeff Clites have asked multiple times "Why do we do it *that* way," providing a constant reminder of fundamentals as well as some much-appreciated enthusiasm.

Julie Novak's origination of and Rakesh Jain's contributions to the bis(TMM) work are acknowledged, as is the most excellent cameraderie and work of Dr. David Shultz. Anthony West asked a key question that led to the now-famous $1/9$ Heisenberg scaling factor. Randy Lee, Dave Nichols, Rakesh Jain, and Joe Ho are to thank for their contributions to the polymer project.

My learning experience in graduate school has extended far beyond chemistry. Certain events have had a curious and not always kind way of sneaking up on me. Special friends have provided companionship, support and understanding: Dave and Lisa Shultz, Kraig Anderson, Pat Kearney, Jamie Schlessman, Joel Schwartz, Andri Friedli, Piotr Kaszynski, Jeff Clites, Randy Lee, and Dian Buchness.

Diversion-has been important to my sanity. For several golf games I thank Dave Mack, Jong Soon Koh, Milan Mrksich, and George Best, as well as Bob Blake and crew. Softball has always been an important part of summer; thanks especially go to all the members of Chumly's Petting Zoo, to past managers Ed Stewart, Pat Kearney, and Spud Stauffer, as well as Jon Forman and Scott Silverman for taking over the managing chores.

Finally, thanks go to my parents for their unfailing love and support through everything that I have experienced, enjoyed, and endured to reach this goal.

Abstract

In the preparation of small organic paramagnets, these structures may conceptually be divided into spin-containing units (SCs) and ferromagnetic coupling units (FCs). The synthesis and direct observation of a series of hydrocarbon tetraradicals designed to test the ferromagnetic coupling ability of *m*-phenylene, 1,3-cyclobutane, 1,3-cyclopentane, and 2,4-adamantane (a chair 1,3-cyclohexane) using Berson TMMs and cyclobutanediyls as SCs are described. While 1,3-cyclobutane and *m*-phenylene are good ferromagnetic coupling units under these conditions, the ferromagnetic coupling ability of 1,3-cyclopentane is poor, and 1,3-cyclohexane is apparently an antiferromagnetic coupling unit. In addition, this is the first report of ferromagnetic coupling between the spins of localized biradical SCs.

The poor coupling of 1,3-cyclopentane has enabled a study of the variable temperature behavior of a 1,3-cyclopentane FC-based tetraradical in its triplet state. Through fitting the observed data to the usual Boltzman statistics, we have been able to determine the separation of the ground quintet and excited triplet states. From this data, we have inferred the singlet-triplet gap in 1,3-cyclopentanedyl to be 900 cal/mol, in remarkable agreement with theoretical predictions of this number.

The ability to simulate EPR spectra has been crucial to the assignments made here. A powder EPR simulation package is described that uses the Zeeman and dipolar terms to calculate powder EPR spectra for triplet and quintet states.

Methods for characterizing paramagnetic samples by SQUID magnetometry have been developed, including robust routines for data fitting and analysis. A precursor to a potentially magnetic polymer was prepared by ring-opening metathesis polymerization (ROMP), and doped samples of this polymer were studied by magnetometry. While the present results are not positive, calculations have suggested modifications in this structure which should lead to the desired behavior.

Source listings for all computer programs are given in the appendix.

Table of Contents

Acknowledgement	v
Abstract	vii
List of Figures	x
List of Tables	xi
List of Schemes	xi
 Chapter 1 – Introduction	 1
The Origin of Magnetic Behavior	6
Spin Wavefunctions, the Heisenberg Hamiltonian, and High-Spin Organic Molecules. The Paradigm of the Ferromagnetic Coupling Unit.	9
Biradicals and Related Structures	12
Scope of This Work.	18
Chapter 2 – Evaluation of Potential Ferromagnetic Coupling Units: the Bis(TMM) Approach to High-Spin Organic Molecules	22
Summary.	23
Synthesis.	24
Model.	31
EPR Spectroscopy of High-Spin Molecules	33
EPR Results.....	37
Summary and Conclusions.....	48
Experimental	50
Chapter 3 – Synthesis and EPR Spectroscopy of a Bis(cyclobutanediyl)	62
Background	63
Synthesis	65
Model	67
EPR Results.....	69

Summary and Outlook	74
Experimental	75
Chapter 4 – Complete Computer Simulation of Quintet- and Triplet-State EPR Spectra.....	78
EPR Spectroscopy as a Diagnostic Tool.....	79
Methods for Computer Simulation of EPR Spectra.....	80
The Resonance Condition and EPR Absorption	81
The EPR Hamiltonian	86
Description of Programs	88
Miscellaneous Programs	91
Chapter 5 – Methods for Magnetic Measurements on Polymer Systems and the Study of PDPMC•, a Potentially Magnetic Organic Polymer	93
Polymer Synthesis and Characterization.....	96
Magnetic Behavior of Polymer-Based Paramagnets	99
Magnetic Measurements: Theory and Models	99
The Measurement.....	104
The Meaning of S.....	109
Creating Spins	110
Experimental	116
References	130
Appendix - Source Listings of Computer Programs	139

List of Figures

1-1 Magnetic behaviors	9
1-2 Design of high-spin assemblies	11
2-1 Heisenberg energy level diagrams	32
2-2 Constituent D -tensors of 2	35
2-3 EPR spectra obtained on photolysis of 1(N₂)₂	40
2-4 EPR spectra obtained on photolysis of 2(N₂)₂	41
2-5 EPR spectra obtained on photolysis of 3(N₂)₂	42
2-6 EPR spectra obtained on photolysis of 4(N₂)₂	44
2-7 Plot of EPR signal intensity vs. photolysis time for 4(N₂)₂ and 53	45
2-8 EPR spectra of 3 obtained at 40 K	46
2-9 Plot of IT vs. T for ³3	47
3-1 EPR spectra obtained upon brief photolysis of 5(N₂)₂	70
3-2 EPR spectra obtained upon extended photolysis of 5(N₂)₂	71
3-3 Simulated EPR spectra of ³5(N₂) and ⁵5	72
5-1 The Brillouin Function	102
5-2 Experimental SQUID coil arrangement.....	105
5-3 SQUID scan voltage trace	107
5-4 Sample holder design.....	107
5-5 SQUID trace of a zero-moment sample.....	109
5-6 Plot of best-fit <i>S</i> -value vs. mole fraction for a quintet/triplet mixture.....	110
5-7 DISCOVER-computed geometries of 4-mers of PDPMC-H and 64	115

List of Tables

1-1 Biradical substructures in 1-5	19
2-1 Observed zfs parameters for monoazo triplet biradicals	39
2-2 Predicted and experimental <i>D</i> -values for tettraradicals	43

List of Schemes

1-1 Preparation of Berson TMMs	16
2-1 Protection/deprotection synthesis of bisfulvenes	27
2-2 BF ₃ ·Et ₂ O synthesis of bisfulvenes	29
2-3 Preparation of 1(N₂)₂–4(N₂)₂	30
3-1 Synthesis of 5(N₂)₂	66
5-1 Synthesis of diarylmethylenecyclobutenes	98
5-2 Synthesis of biphenylenemethylenecyclobutenes	114

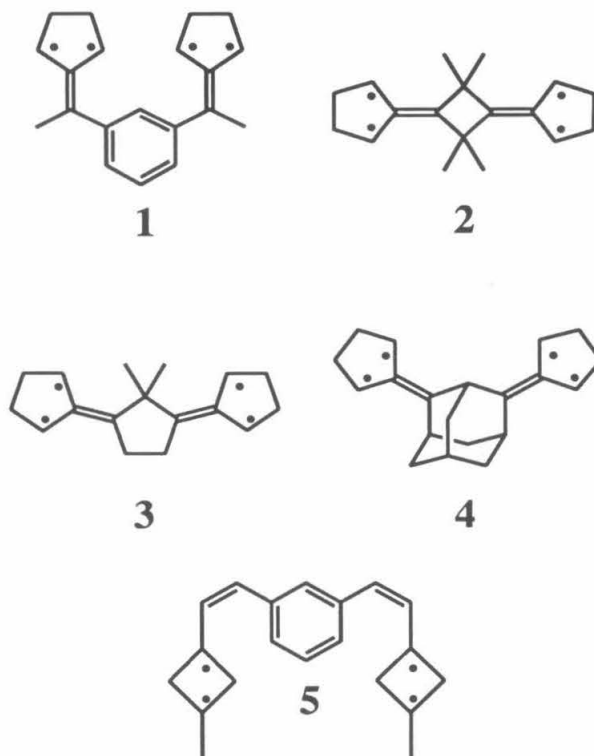
Chapter 1 - Introduction

Chemists have considered the intermediacy of free radicals in a wide variety of organic reactions ever since Kekulé and Lewis formulated their models of bonding in organic compounds.^{1,2} While simple radicals are interesting in their own right, the preparation of organic polyradicals and study of their magnetic behavior is a new and challenging endeavor.³⁻⁸ Cooperative, high-spin interactions among the angular momenta of unpaired electrons in these molecules are responsible for their magnetic behavior. The study of these molecules allows magnetic structure-property relationships to be established on a very basic level. Organic chemistry thus offers a fundamentally new, *ab initio* approach to magnetism that complements the phenomenological, top-down models of solid-state physicists and others who have long studied magnetic behavior.^{9,10} The focus of the present work is on the magnetic interactions of the radical centers in molecules with two, four, or more unpaired electrons—biradicals, tetraradicals, and polyradicals—whose synthesis represents a first step towards the preparation of rationally designed organic magnetic materials.^{5,11-14} The synthesis of organic magnets will ultimately rely on the ability of chemists to build ordered molecular and macromolecular structures containing free radical centers in which cooperative magnetic interactions are effected over a macroscopic distance.

This work is concerned in part with the synthesis of tetraradicals **1-5** and direct observation of these species by matrix-isolation electron paramagnetic resonance (EPR) spectroscopy.¹⁵ Matrix isolation conditions are required not only to stabilize these highly reactive hydrocarbon species, but also to suppress intermolecular spin-exchange phenomena that occur when two high-spin species interact in nonrigid media. These phenomena preclude the observation of the EPR spectra of high-spin species in almost all cases.¹⁵

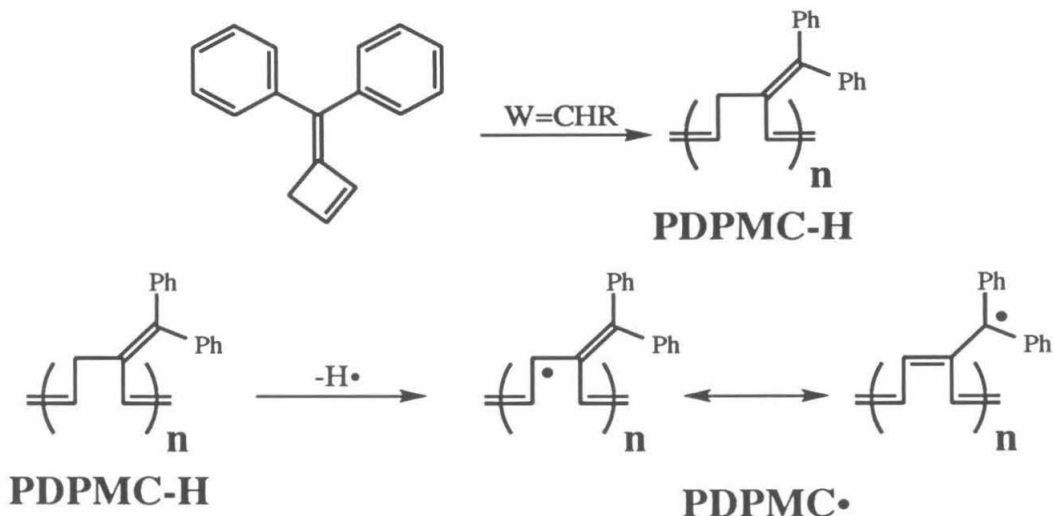
The EPR spectra observed under matrix-isolation conditions are highly anisotropic due to spin-spin dipolar interactions, which are unique to a given spin state and tensorial in nature. Proper interpretation of the EPR spectra through visual inspection

and computer simulation allows determination of the components of the dipolar tensor and the nature of the associated spin state. Cooperative magnetic behavior among all four electrons of a tetraradical results in a quintet ground state that is easily characterized by EPR.

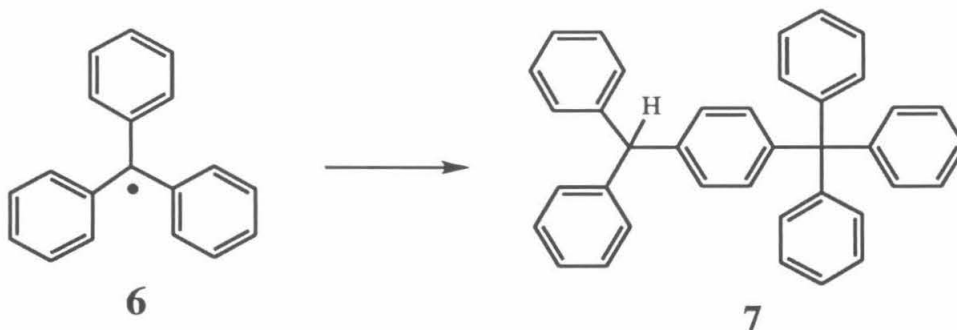


The EPR studies described here were intended to elucidate fundamental magnetic behavior of a variety of polyradicals, and matrix-isolation conditions were ideal to the intent. However, the reactivity of the radical centers is an important consideration in the design of practical organic magnetic materials. The thermodynamic instability inherent to the unsatisfied valence of a free radical leads to high reactivity unless kinetic stabilization is provided by delocalization and/or steric protection.^{1,2} A variety of strategies for stabilizing radical centers are available, and stable organic magnetic materials are being pursued in our laboratory and elsewhere.¹⁶⁻²⁴ In Chapter 5 we describe the synthesis of the polymer poly(diphenylmethylenecyclobutene) **PDPMC-H** by ring-opening metathesis polymerization (ROMP),²⁵ and magnetization studies on this

polymer after a variety of treatments designed to abstract hydrogen atoms to produce **PDPMC•**.

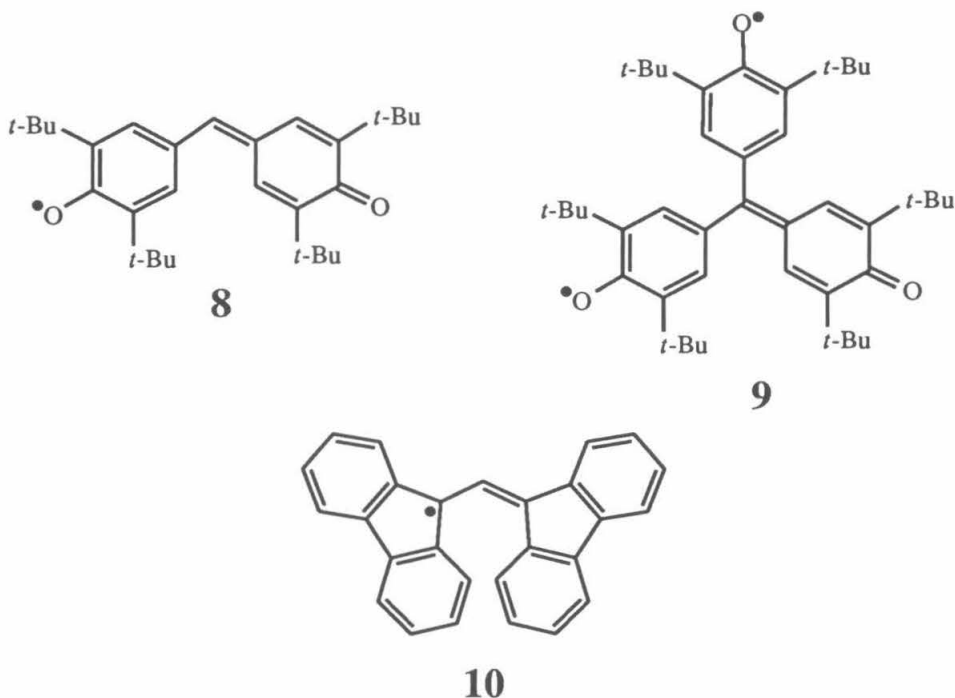


We anticipated that the spins in **PDPMC•** might be kinetically stable based on the work of Gomberg, who in 1900 reported the generation of triphenylmethyl, **6**, by reduction of trityl chloride with zinc. This radical is remarkably kinetically stable in the solid state.²⁶ In solution, however, despite the presence of both delocalization and steric protection, **6** slowly dimerizes to **7**. More recent work has shown that perchlorinated polyarylmethyl radicals are indefinitely stable.²⁷⁻²⁹

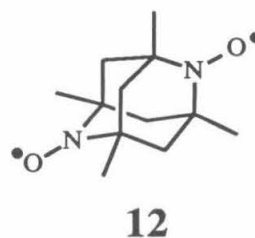
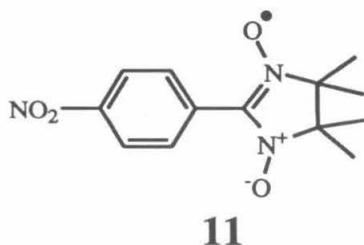


Future efforts toward the development of organic magnetic materials will require additional stable free radical components. One such radical, **8**, first synthesized by Galvin Coppinger and commonly known as galvinoxyl, owes its stability, like that of **6**,

to delocalization and steric protection.³⁰⁻³² A related structure with a high-spin ground state is Yang's biradical, **9**.^{33,34} The synthesis of this molecule demonstrated the feasibility of making thermally stable high-spin structures. In 1932, a report of the synthesis of **10**, another very stable radical, was rejected by the editors of Journal of the American Chemical Society, only to be accepted 25 years later when the free-radical character of this molecule was proven by EPR spectroscopy.^{35,36} The foregoing example illustrates both the impact of the development of EPR on the study of free radicals and the widely held and mostly correct view of free radicals as highly reactive species. Recent studies highlight the growing use of heteroatom-supported radicals such as nitroxides and phenoxides as stable radical components.³⁷⁻⁴¹ Much research remains to be done on stable radical species so that a wide range of magnetic building blocks may be developed.



As noted above, the presence or absence of intermolecular spin-spin interactions giving rise to long-range order in organic solids will ultimately determine their magnetic behavior. Recent reports of ferromagnetic behavior in crystals of **11** and **12**, therefore, hold much promise for the field.^{40,42}



The Origin of Magnetic Behavior.

While many scientists throughout history have tried to explain magnetism, all were doomed to failure until the advent of quantum mechanics. The bulk magnetic behavior of all materials is due to electron spin—a purely quantum mechanical phenomenon that was not adequately described until the 1920s. The first evidence for the intrinsic angular momentum of the electron came from the results of the Stern-Gerlach experiment, a cornerstone of quantum theory.⁴³⁻⁴⁵ In this experiment, a collimated beam of atoms with non-zero angular momentum is passed through an inhomogeneous magnetic field that deflects the atoms according to the orientation of their magnetic moments. Stern and Gerlach employed silver atoms, which have $L=0$ and $S=1/2$, the same as an electron. After emerging from the magnetic field, the atoms are collected at a detector. If the atoms are classical particles, then any orientation of their magnetic moments is possible, and a random distribution of atoms is detected. Instead, Stern and Gerlach observed that atoms emerge from the field at only two orientations, corresponding to only two discrete values of the magnetic moment. The results of the Stern-Gerlach experiment demonstrate the quantization of magnetic states of atoms with non-zero angular momentum.

In 1925, Uhlenbeck and Goudsmit proposed the idea of intrinsic electronic angular momentum, or spin, in order to explain the "anomalous" Zeeman effect.^{46,47} This effect is the splitting of the energy levels of an atom with $S > 0$ by an applied magnetic field—the "anomaly" that makes EPR possible. Uhlenbeck and Goudsmit's hypothesis was expanded into a complete theory by Pauli⁴⁸ and confirmed by the natural evolution of electron spin in Dirac's relativistic formulation of quantum mechanics.⁴⁹

According to nonrelativistic quantum theory,⁴³⁻⁴⁵ the magnetic dipole moment associated with electron spin may be written as $\vec{\mu}_e = g_e \left(\frac{-e}{2m_e} \right) \mathbf{S}$, where g_e is the Landé g -factor which in nonrelativistic theory equals 2. The experimentally determined value is $g_e \approx 2.00232$, and the slight difference is due to relativistic and radiative effects. The energy E of this dipole in an external magnetic field \mathbf{H} is given by $E = -\vec{\mu}_e \cdot \mathbf{H}$. The quantization of the electron spin means that the spin is either up or down with respect to the external field, i.e., the dot product $\mathbf{S} \cdot \mathbf{H} = \pm \hbar/2 = \hbar m_s$ is dichotomic, and $E = g_e \beta H m_s$ is quantized ($\beta \equiv \frac{e\hbar}{2m_e} = 9.274 \times 10^{-24}$ J/T is the Bohr magneton).

Of course, electron spin is purely a quantum mechanical phenomenon of relativistic origin, and one can really only say that an electron has intrinsic angular momentum \mathbf{S} . If the electron were actually a charged particle spinning about its axis, its dipole moment would be given by a classical expression: g_e would be equal to 1. The term "spin" is only a convenient expression for something with no classical counterpart.

The overall magnetic moment of a sample is the sum of the individual orbital and spin magnetic moments of its constituent electrons. Orbital angular momenta, fixed by the molecular axes, do not reorient to the direction of a magnetic field. In randomly oriented samples such as those under consideration here, the orbital contributions average nearly to zero; their only contribution is the very weak diamagnetic term discussed below.

The electron spin contribution, \mathbf{M}_{spin} , to the magnetic moment of a sample is $\mathbf{M}_{spin} = \sum_{all\ e^-} \tilde{\mu}_e$. One may quickly conclude that electrons in filled shells do not

contribute to \mathbf{M}_{spin} , since the total electronic angular momentum in a filled shell is zero. Therefore, the first requirement for a significant magnetic moment is the presence of *unpaired* electrons. Based on this criterion, all molecules may be classed as either paramagnets, which have unpaired electrons and thus interact favorably with the magnetic field, or diamagnets, which have filled shells and experience only a weakly repulsive orbital interaction. Diamagnetism is a universal property of matter that results from a weakly repulsive interaction of core electrons with a magnetic field. Even paramagnets have a diamagnetic contribution to their magnetic moments, but the paramagnetic contributions are normally orders of magnitude larger.

In order to achieve bulk magnetism, unpaired electrons alone are not enough. In addition, one must first provide some interaction mechanism by which the individual electronic moments may interact cooperatively with those nearby; these individual interactions serve to create magnetic order over a macroscopic distance.^{9,10} A purely paramagnetic substance, one with no cooperative spin-spin interactions, contains only a random ensemble of rapidly reorienting moments. Such a substance has no net moment in the absence of an applied field. Because the individual moments are noninteracting, paramagnetism has been described as the magnetic analog of ideal gas behavior.¹⁰

Figure 1-1 shows several possible types of magnetic behavior. The presence of interelectronic interactions in three dimensions leads to bulk magnetic behavior.⁹ The ideal case is a ferromagnet, whose spins are aligned rigorously parallel to one another. A ferromagnet has a magnetization \mathbf{M} even in the absence of an external field. The opposite case is an antiferromagnet, which has perfect antiparallel spin alignment in three dimensions and zero moment in any applied magnetic field. A simple extension of these terms allows the definition of *ferromagnetic coupling* as the interaction of two spins in parallel or high-spin fashion and *antiferromagnetic coupling* as the interaction of two

spins in antiparallel or low-spin fashion. A ferrimagnet comprises two spin angular momenta of different magnitudes coupled antiferromagnetically, and its bulk behavior resembles that of a ferromagnet. It should be noted that these and all bulk magnetic behaviors are critical phenomena, and above some critical magnetic phase temperature, all of these materials act as paramagnets.⁹

○ **DIAMAGNETIC - no spins, i.e., closed shell**
all matter has diamagnetic component



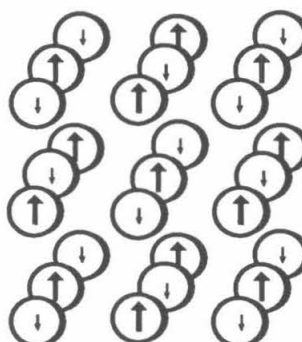
PARAMAGNETIC



FERROMAGNETIC



ANTIFERROMAGNETIC



FERRIMAGNETIC

Figure 1-1. Types of magnetic behavior

Spin Wavefunctions, the Heisenberg Hamiltonian, and High-Spin Organic Molecules. The Paradigm of the Ferromagnetic Coupling Unit.

As mentioned above, electron spin is a consequence of relativity and is taken into account naturally only within the scope of the relativistic Dirac formalism. In

Schrödinger quantum mechanics, spin is included as somewhat of an afterthought, and electron spin angular momentum is included in the total wavefunction as a separate spin wavefunction that multiplies the spatial wavefunction. The Fermi statistics governing electron behavior require the product wavefunction to be antisymmetric with respect to the interchange of any two electrons; this requirement is known as the Pauli Principle. According to the Pauli Principle, the symmetric or antisymmetric nature of the spin wavefunction must complement the symmetry of the spatial wavefunction.^{43,44}

$$\begin{aligned}\Psi_{total} &= \Psi_{spatial} \Psi_{spin} \\ A &= A \bullet S \\ A &= S \bullet A\end{aligned}$$

The Schrödinger-Pauli treatment of spatial and spin components in this equation relies on the unimportance of spin-orbit coupling. Spin-orbit coupling provides only a small perturbation to the wavefunction for almost all light atoms, and is negligible for the hydrocarbons that are the focus of the present work. One might conclude that the Schrödinger-Pauli representation is a good approximation. In the study of high-spin molecules, this treatment offers an advantage: for a given molecular geometry, a spin-only Hamiltonian—the Heisenberg Hamiltonian—can be employed to model the energy spectrum of covalent spin states.^{9,10,50}

The Heisenberg Hamiltonian models the pairwise interaction of spins. The Hamiltonian operator has the form $\hat{\mathcal{H}} = -2J_{ij} \hat{S}_i \bullet \hat{S}_j$, where \hat{S}_i and \hat{S}_j are the operators for spins $|i\rangle$ and $|j\rangle$, and J_{ij} is the Heisenberg exchange parameter that describes the nature of the coupling. When the coupling between the spins is ferromagnetic, $J_{ij} > 0$; when the coupling is antiferromagnetic, $J_{ij} < 0$. In this model, all information regarding the influence of the spatial part of the wavefunction on the relative energies of the spin states formed by interaction of $|i\rangle$ and $|j\rangle$ is contained in the exchange parameter J_{ij} . The interplay of the overlap and exchange terms (see below) of the spatial wavefunctions

associated with the different possible spin states formed by the combination of $|i\rangle$ and $|j\rangle$ determines the sign and magnitude of J_{ij} .

In the absence of spin-orbit coupling, the value of J_{ij} for the coupling of any two angular momenta through a given molecular fragment is constant, i.e., *all $|i\rangle$ and $|j\rangle$ are coupled by the same J_{ij}* . This model enables one to develop the paradigm of a *ferromagnetic coupling unit*—a molecular fragment for which $J_{ij} > 0$ —and to divide a high-spin organic molecule conceptually into a sequence of spin-containing units and ferromagnetic coupling units. This concept is depicted in Figure 1-2a; the infinite one-dimensional extension has obvious applications to polymers.

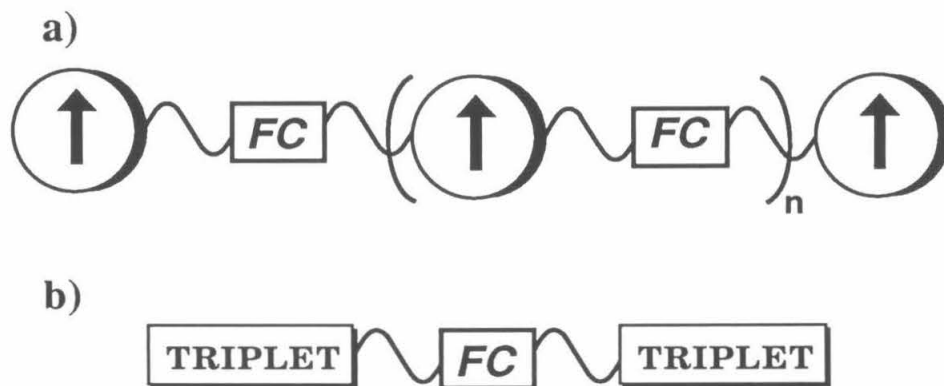


Figure 1-2. (a) General design of high-spin assemblies. (b) Design of quintet ground state tetraradicals.

In our work, candidates for ferromagnetic coupling units and spin-containing units were selected based on earlier studies of biradicals,^{12,51-55} which are among the simplest cases in which spin control is an issue.⁶ A biradical may be analyzed according to the paradigm of Figure 1-2a; simple radicals are the spin-containing units, and the structure linking them is the ferromagnetic coupling unit. Modeling the behavior of the lowest two biradical states with the Heisenberg Hamiltonian leads to the conclusion that the Heisenberg term $2J_{ij}$ is equal to the singlet-triplet gap. This relationship can be used in conjunction with the Heisenberg Hamiltonian and the results of *ab initio* calculations of

singlet-triplet gaps in biradicals to predict the spin-state energy spacing in tetradicals from theoretical results (see Chapter 2).

Biradicals and Related Structures.

All biradicals relevant to the present study are homosymmetric biradicals,⁵⁶ in which the unpaired electrons occupy two p -type orbitals, χ_l and χ_r . In the molecular orbital model and Schrödinger formalism, the interaction of two electrons gives rise to two formally non-bonding molecular orbitals (NBMOs). The first, slightly bonding MO ϕ_s is formed by the in-phase combination of χ_l and χ_r , while the second, weakly antibonding MO ϕ_a is formed by the out of phase combination of χ_l and χ_r .

$$\phi_s = \frac{1}{\sqrt{2+2S_{lr}}}(\chi_l + \chi_r); \quad \phi_a = \frac{1}{\sqrt{2-2S_{lr}}}(\chi_l - \chi_r)$$

In the limit of zero overlap ($S_{lr} = 0$), ϕ_s and ϕ_a are exactly degenerate. A biradical has been defined as a molecule with two degenerate or nearly degenerate NBMOs,^{12,56} and thus we are interested in cases where S_{lr} is small.

Population of ϕ_s and ϕ_a with two electrons gives rise to six configurations. Three of these configurations are components of the triplet state, while the remaining three correspond to three singlet states: a covalent state, a singly-excited ionic state, and a doubly-excited ionic state. The two ionic singlet states are very high in energy and are not considered. The covalent singlet is properly described by a two-configuration wavefunction, while the triplet can be described by a single configuration wavefunction that is independent of S_{lr} .

$${}^1\Psi = \lambda \phi_s^2 - \sqrt{1-\lambda^2} \phi_a^2; \quad \lambda = \sqrt{\frac{1+S_{lr}}{2}}$$

$${}^3\Psi = \frac{1}{\sqrt{2}}(\phi_s\phi_a - \phi_a\phi_s)$$

Of these two states, the singlet has $S=0$, and thus no spin-associated magnetic behavior, while the triplet has $S=1$ and a spin-associated magnetic dipole moment. Here

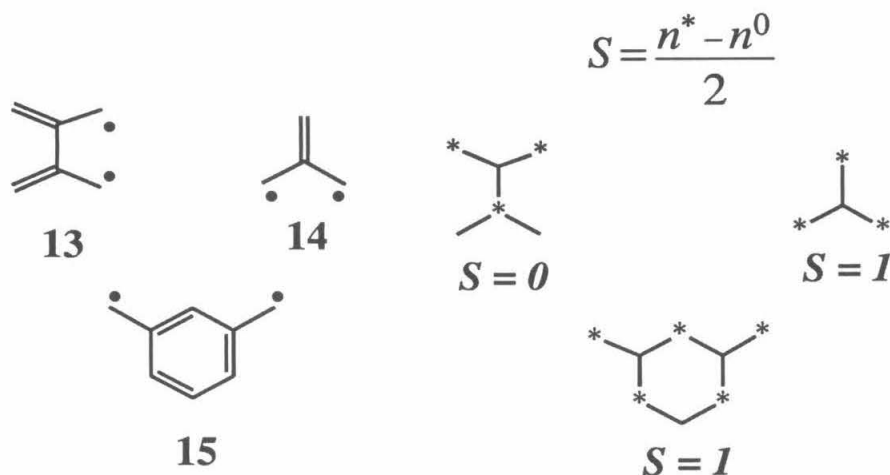
specifically, and in the general case as well, *maximizing cooperative magnetic interactions in organic molecules is equivalent to obtaining a ground state with the highest possible spin.*

The relative energies of the triplet and covalent singlet wavefunctions are determined by the interplay of exchange and overlap.^{56,57} Significant overlap between the two p-type orbitals of a biradical strongly favors the singlet state because overlap is a bonding interaction, and the electrons in a bond are spin-paired. Exchange is a purely quantum-mechanical interaction that arises as a consequence of electron spin.⁴³ The effect of exchange is to correlate the motion of electrons with the same spin. This correlation minimizes Coulomb repulsion and thus lowers the interelectronic interaction energy. No correlation occurs for a singlet, and thus exchange interactions preferentially stabilize the triplet state. The exchange interaction is significant only when the radical centers are close enough together that their electrons interact substantially. Overlap is generally a stronger effect than exchange, and a significant exchange interaction between closely-spaced radical centers results in a triplet ground state only when the overlap $S_{lr} \approx 0$. These conditions are fulfilled only in special circumstances, and thus triplet ground state biradicals are rare.

Biradicals may be divided into two structural classes: delocalized and localized.⁵⁸ In a delocalized biradical, the two unpaired electrons are in classical π -conjugation with one another, while in a localized biradical the centers are isolated from one another, although each may have a delocalizing substituent. The manner in which the zero-overlap/significant exchange condition is fulfilled is different for these two classes.

In any delocalized biradical, the overlap S_{lr} between the NBMOs is zero due to topology. Delocalized biradicals may be further divided into two topological classes: those with NBMOs confined to two different sets of atoms, called *disjoint* NBMOs, and those with NBMOs that span a common set of atoms, termed *nondisjoint* NBMOs.⁵⁹ The atoms of an alternant hydrocarbon (AH) may be divided conceptually into two sets,

starred and nonstarred, such that no two adjacent atoms are in the same set. For an AH delocalized biradical, Borden and Davidson showed that if the populations of the two sets are equal, then the biradical NBMOs are disjoint, while if the number of starred atoms exceeds the number of unstarred atoms, the NBMOs are nondisjoint.⁵⁹

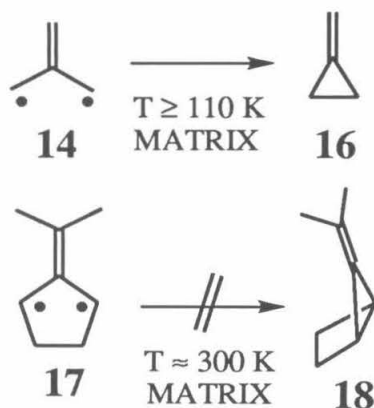


In a biradical with disjoint NBMOs, such as tetramethylethane (TME, **13**), the exchange interaction is small, and a near degeneracy of singlet and triplet states results. In biradicals with nondisjoint NBMOs, typified by trimethylenemethane (TMM, **14**) and *m*-benzoquinodimethane (*m*-BQM or *m*-xylylene, **15**), the exchange interaction is strong, and a triplet ground state is predicted. In an extension of this work, Ovchinnikov developed a simple equation based on topology rules that predicts the ground spin state of any alternant hydrocarbon: $S = \frac{n^* - n^0}{2}$, where n^* is the number of starred atoms and n^0 is the number of unstarred atoms.⁶⁰

There is much debate regarding the nature of the ground state of TME, **13**. High-level theoretical results have in the past predicted a singlet ground state,⁶¹ but a triplet EPR spectrum attributable to TME has been observed.^{62,63} The most recent results from theory suggest that the ground state is geometry-dependent; at the triplet's optimized geometry, the triplet lies *ca.* 1 kcal/mol below the singlet, but the global minima are essentially degenerate.^{64,65} TME is typical of the general class of delocalized biradicals

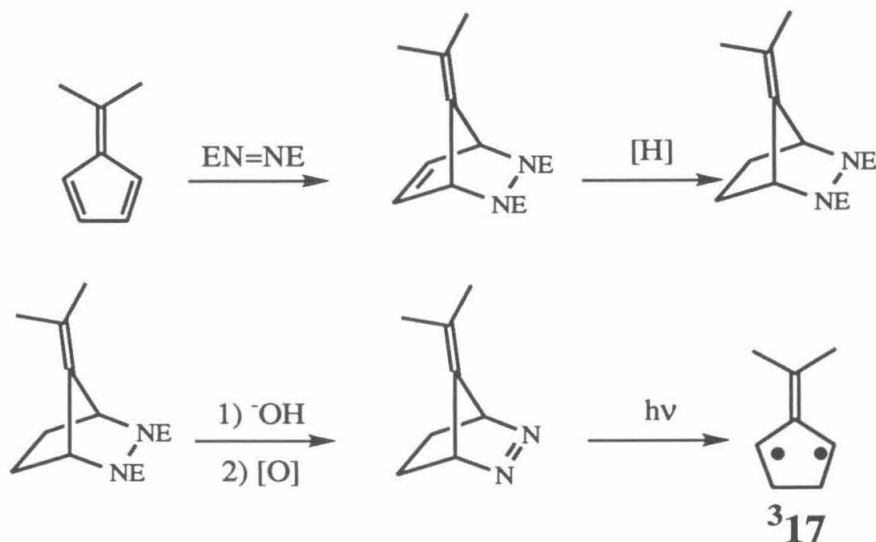
with disjoint NBMOs, whose members show no substantial preference for either high-spin or low-spin ground states. We remove this class of molecules from consideration because we are interested in producing molecules and materials with a strong high-spin preference.

A large body of experimental and computational work confirms the strong high-spin preference of **14** and its derivatives. The magnitude of the singlet-triplet gap has so far precluded experimental determination, but the calculated triplet preference is *ca.* 15 kcal/mol.⁶⁶ Dowd initiated investigations in the matrix-isolation EPR spectroscopy of this high-spin species in 1966,^{52,67} and subsequently reported rapid unimolecular decay at temperatures in the range 110-140 K, corresponding to an activation energy of 7 kcal/mol.⁶⁸ Triplet TMM is 15 kcal/mol higher in energy than its closed-shell isomer methylenecyclopropane, **16**, and the low-temperature decay can be attributed to this relative thermodynamic instability.⁶⁹ Singlet TMM has yet to be detected.



The triplet biradical ³**17** is the prototypical member of a class of exceptionally stable, easily prepared, and well characterized triplet biradicals known as Berson TMMs.^{53,70} The ethano-bridge modification of TMM makes ³**17** more stable than its lowest-energy closed shell isomer **18** by *ca.* 7 kcal/mol,⁷¹ and ring closure is not observed under matrix conditions. In fact, ³**17** is the thermodynamic unimolecular sink^{72,73} and is stable to near room temperature in rigid media.⁷⁴ It is said to be a "strain-protected"

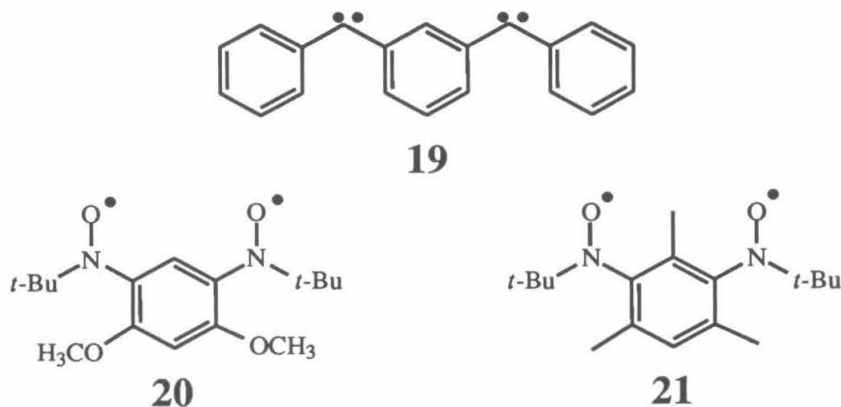
TMM.⁷⁰ An experimental determination puts **117** at least 14 kcal/mol above **317** in energy,⁷³ in agreement with theory.⁶⁶ Appropriate diazene precursors to this type of TMM are readily available from a simple sequence of azodicarboxylate addition to a fulvene, reduction of the endocyclic double bond, cleavage of the carbamates, and oxidation of the resulting hydrazine (Scheme 1-1).⁷⁴ The synthesis and EPR spectroscopy of a wide variety Berson TMMs have been reported.^{70,74}



Scheme 1-1

Biradical **15** is the parent member of the class of *m*-phenylene-linked high-spin molecules that lies at the heart of the investigation of the magnetic properties of organic materials. The first evidence for coupling according to the paradigm of Figure 1-2a was obtained by Itoh in 1967,⁷⁵ and independently by Wasserman in the same year.⁷⁶ Both observed the EPR spectrum of the quintet ground state of **19**. Itoh and Iwamura have since taken advantage of the ferromagnetic coupling ability of *m*-phenylene and the paradigm of Figure 1-2a to build a wide array of oligo(carbenes) and oligo(nitrenes) with high-spin ground states.^{14,77,78} In these molecules, the individual n- π interactions ensure local high-spin coupling at a divalent center, while *m*-phenylene enforces ferromagnetic

coupling along the chain. Recently, Iwamura^{37,39} and Rassat^{40,79,80} have turned to nitroxide radicals as stable spin-containing units. *m*-Phenylene often couples these radical centers ferromagnetically, but not as rigorously as it does in hydrocarbons. **20** and **21**, which are severely twisted molecules, have singlet ground states.^{79,81} Rajca has synthesized several poly(arylmethyl) polyradical structures that rely on *m*-phenylene as a coupling unit. Despite significant twisting in these molecules, ferromagnetic coupling is

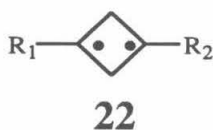


robust and can produce molecules with up to $S = 5$.²³ Results of investigations in our group indicate a geometric dependence of the coupling ability of *m*-phenylene for TMM spin-containing units.⁸² The reasons for the apparent variation in the ferromagnetic coupling ability of *m*-phenylene are not presently understood.

1,3-Cyclobutanediyls,^{54,83,84} **22**, and 1,3-cyclopentanediyIs,^{58,85-89} **23**, are the only types of localized biradicals that have been shown to have triplet ground states. The first EPR observation of cyclopentanediyI in 1975 seemed to open a new field of investigation.⁸⁵ However, in further investigations it was determined that minor perturbations of the cyclopentane skeleton led to species which gave only weak EPR signals or none at all.⁵⁸ Work on the smaller homolog 1,3-cyclobutanediyl was carried out in the Dougherty group.^{83,84} While the parent compound **22a** and other derivatives unsubstituted at the radical-carrying carbons are not observed upon photolysis in the EPR cavity at 4 K, presumably due to tunneling behavior, it has been demonstrated that 1,3-

disubstituted-1,3-cyclobutanediyls constitute the first general class of EPR-observable localized biradicals.^{54,83} Further work in the Dougherty group has explored the chemistry of 1,3-diarylcyclopentanediyIs which, contrary to expectations based on the earlier published reports, are remarkable stable.⁸⁶⁻⁸⁹

In a significant theoretical study, Goldberg and Dougherty computed the singlet and triplet energies for various C-C-C bond angles in trimethylene, and found the triplet to be the ground state at geometries such as those enforced in cyclobutane and cyclopentane rings.⁵⁷ The near degeneracy of NBMOs required for a triplet ground state in these localized triplet biradicals is due to a combination of through-space and through-bond effects.^{56,57} In MO terms (see above), ϕ_s undergoes symmetry-allowed mixing with the π -CH₂ orbital(s) of the intervening methylene(s) such that it is nearly degenerate with ϕ_a , and the proximity of the radical centers induces substantial exchange interactions that favor a triplet ground state.



- a) $R_1 = R_2 = H$
- b) $R_1 = R_2 = \text{alkyl}$
- c) $R_1 = R_2 = Ph$
- d) $R_1 = R_2 = CH=CH_2$
- e) $R_1 = Et; R_2 = CH=CH_2$
- f) $R_1 = Ph; R_2 = Me$



- a) $R_1 = R_2 = H$
- b) $R_1 = R_2 = Ar$

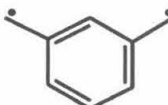
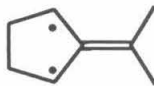



Scope of This Work.

In the present work, we have used the model of Figure 1-2b to design tetraradicals with quintet ground states and have employed the Heisenberg Hamiltonian to model the relative energies of the tetraradical states. In particular, we have developed a general strategy for evaluating the ferromagnetic coupling ability of a wide number of organic fragments that we term the "bis(TMM) approach." We have chosen to use a Berson TMM as a spin-containing unit because of its outstanding properties that are discussed

above. Chapter 2 describes the investigation of the ferromagnetic coupling abilities of *m*-phenylene, 1,3-cyclobutane, 1,3-cyclopentane, and chair 1,3-cyclohexane in compounds **1-4**.

An important distinction between the classes of localized and delocalized biradicals may be drawn upon brief inspection of Table 1-1, which presents data from previous studies on biradicals pertinent to the present work: according to theory, nondisjoint delocalized biradicals have triplet preferences roughly an order of magnitude

Table 1-1. Biradicals substructures in compounds **1-5**.

Biradical	ΔE_{ST} (kcal/mol) ^a	$ D/hc $ (cm ⁻¹)
 15	10 ⁹⁰	0.011 ⁹¹
 17	15 ⁶⁶	0.026 ^{70,74}
 22a	1.7 ^{57,92,93}	0.112 ^{b,83}
 23a	0.9 ^{57,93,94}	0.084 ^{58,85}
 24	-1.3 ^c	- ^{95,96}

^aFrom *ab initio* calculations

^b*D* for 1,3-dimethyl-1,3-cyclobutanediyl

^cPresent work

larger than those in localized biradicals. As an outcome of our investigations, we have provided for the first time direct experimental evidence for the magnitude of the high-spin preference of a localized biradical.

1,3-Cyclopentane is a relatively weak ferromagnetic coupling unit, and as a consequence we have been able to elucidate the energy spectrum of **3** through characterization of its triplet state by variable-temperature EPR. We have found excellent correlation between the quintet-triplet separation and the value of the exchange parameter J_{ij} predicted by the calculated singlet-triplet gap in cyclopentanediy1.^{57,93,94} The ability to characterize not only the nature, but also the magnitude of the coupling in **3**, and by inference in **23a**, is an additional benefit of the bis(TMM) strategy, which continues to be exploited in the Dougherty group.^{82,97}

Chapter 3 describes the synthesis and EPR spectroscopy of **5**, a molecule in which two 1,3-cyclobutanediyls are linked vinylogously through *m*-phenylene. While cyclobutanediyls are not nearly as robust as TMMs, this particular molecule provides a further test of the ferromagnetic coupling ability of *m*-phenylene. Molecule **5** may also be thought of as a model for introducing units into a magnetic material that interrupt conjugation but still provide spin communication.

Our results demonstrate that hydrocarbon tetraradicals **1-3** and **5** join a very limited number of previously synthesized quintet ground state organic species, while **4** is a ground state singlet. Other quintets that have been prepared include, in addition to those already mentioned above: a quintet bis-*m*-quinomethane generated by photolysis of a strained diketone precursor,^{98,99} a tetrakisgalvinoxyl that has been well characterized spectroscopically,^{100,101} the tetraradical tetraanion of tetra(9,10-anthrylene),¹⁰² and a novel tribenzobarrelene-based biscarbene structure.¹⁰³

The ability to interpret EPR spectra has been crucial to assigning quintet ground states to tetraradical structures. Our best tool for this task is complete simulation of quintet-state and triplet-state EPR spectra. The methods and computer programs used to

accomplish EPR spectral simulation are discussed separately in Chapter 4. In addition, simple relationships between the D-values of biradicals and tetraradicals may be derived for structures such as **1-5**, which are composed of two triplet biradical subunits, by simple computation of the spin-spin Hamiltonian terms.⁵⁰ These values allow one to predict, *a priori*, the D-values of the quintet and triplet states of these tetraradicals. This technique serves to further bolster our spectral assignments, and makes confident assignment of the EPR signals due to **33** and **55** possible.

We have also investigated the synthesis of macromolecular structures that exhibit cooperative spin behavior according to the model of Figure 1-2a.^{5,13,16,104-107} In Ovchinnikov's presentation of his topological model, special note was made of polyradicals which would have ground states directly proportional to their lengths.⁶⁰ Ring-opening metathesis polymerization²⁵ (ROMP) of diphenylmethylenecyclobutene provides a novel polymer **PDPMC-H** that is a precursor to such a structure. Monomer and polymer synthesis, and attempts to prepare **PDPMC•**, are discussed in Chapter 5.

In the study of polymeric systems such as **PDPMC•**, EPR is no longer informative. Instead we have employed magnetization measurements in the presence of an applied field in order to ascertain the degree of paramagnetism in these samples.^{8,10} Magnetization measurements have been performed on a Quantum Design Magnetic Property Measurement System (MPMS). This instrument consists of a superconducting quantum interference device (SQUID)-based magnetometer equipped with a superconducting, ± 5.5 Tesla variable-field magnet. The magnet is used to magnetize the paramagnetic samples; the magnetization is then detected by the magnetometer. Development of the methodology used to make magnetic measurements and the extraction of information on sample paramagnetism through computer analysis of data from these magnetization experiments is also discussed in Chapter 5.

**Chapter 2 - Evaluation of Potential Ferromagnetic Coupling Units:
the Bis(TMM) Approach to High-Spin Organic Molecules**

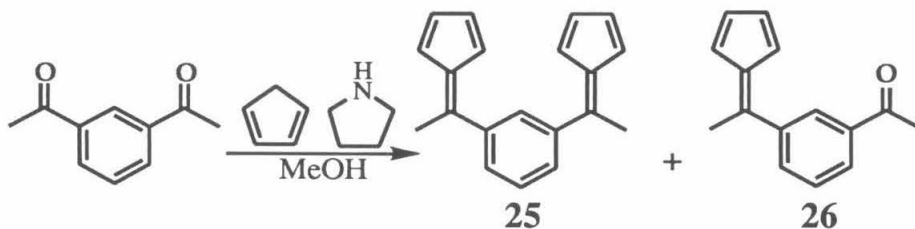
Summary. Triplet trimethylenemethanes of the Berson type can be generated by photolysis of appropriate bicyclic azoalkanes under cryogenic matrix-isolation conditions.^{70,74} Fulvenes, which are the synthetic precursors to these diazenes, can in turn be prepared from carbonyl compounds.¹⁰⁸ The preparation of bis(TMMs) requires an extension to the synthesis of bisfulvene structures that is simple in conception but has been difficult in the particular cases of the molecules studied here.

The bisfulvenes derived from 1,3-cycloalkanediones required for this study are difficult to prepare in large quantities because direct syntheses of these bisfulvenes are not possible under standard conditions: retroaldol condensations preclude their formation. Our initial approach, a sequential introduction of fulvenes to suitably protected derivatives, is arduous and suffers from loss of material due to the high reactivities of fulvenes. However, we have discovered a new direct synthesis of bisfulvenes from diketones. Although the yields are not good, the quantities of bisfulvenes obtained are sufficient to enable the synthesis of the bisdiazenes required for EPR experiments.

Biradicals and tetraradicals are generated by extrusion of dinitrogen upon photolysis of the diazene $n\text{-}\pi^*$ chromophore, and EPR spectroscopy is used to characterize the species produced. In addition to visual inspection, which is not at all conclusive for spin-state assignment in these cases, we have developed a series of computer programs for the simulation of triplet-state and quintet-state EPR spectra. These are described fully in Chapter 3. We have also developed a model that allows for *a priori* prediction of the **D**-tensors of the spin states of tetraradicals **1-3** based on a simple geometric analysis. The predictions agree well with the observed spectra, and have allowed us to assign two observed EPR lines to ³**3**. Modeling of the observed thermal behavior of **3** with the Heisenberg Hamiltonian has allowed us to determine the energetic separation of the ground quintet and first excited triplet states of **3**. The strength of the interaction correlates well with the computationally determined singlet-triplet gap in cyclopentanediy **23a**.

Synthesis. Several alternatives involving cyclopentadiene derivatives are available for the synthesis of fulvenes from carbonyl compounds.¹⁰⁸ The most straightforward is the simple condensation with an alkali metal cyclopentadienide, prepared *in situ* from cyclopentadiene (CpH) and either n-butyllithium to provide CpLi or sodium hydride to give CpNa. A newer reagent, cyclopentadienylmagnesium bromide, CpMgBr, has been described by Stille and Grubbs.¹⁰⁹ This reagent is prepared by refluxing methylmagnesium bromide with cyclopentadiene in tetrahydrofuran and can be isolated as a polymeric THF complex. A conveniently handled white solid, this reagent produces fulvenes reliably, even with a number of sterically hindered ketones, and is the reagent of choice when an organometallic reagent is required.

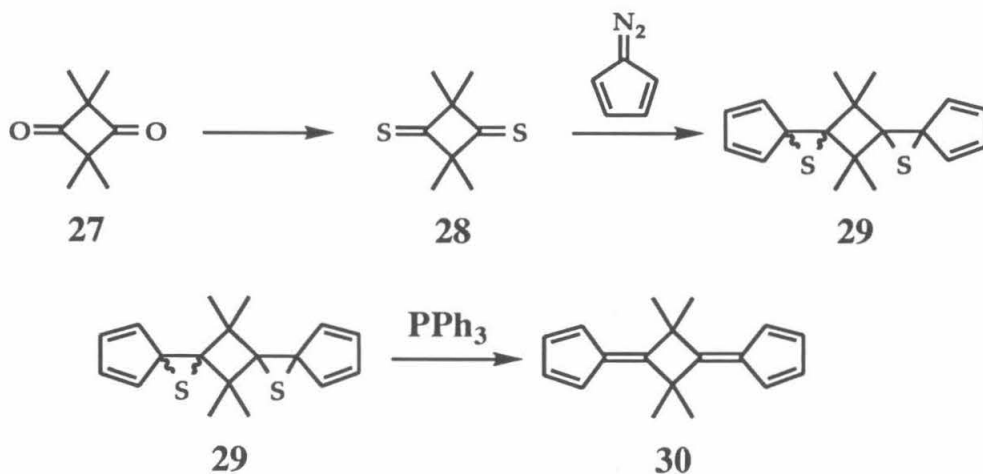
A quite simple alternative to these condensations, discovered by Little and Stone,¹¹⁰ is the condensation of the carbonyl component with cyclopentadiene and pyrrolidine in methanol. These conditions often give very high yields of fulvenes. The preparation of **25** highlights the simplicity of this reaction. Stirring 1,3-diacetylbenzene with 5 equiv of CpH and 3 equiv of pyrrolidine in methanol for 30 h at room temperature gives **25** in 51% yield. The remaining monofulvene **26** is easily recycled.



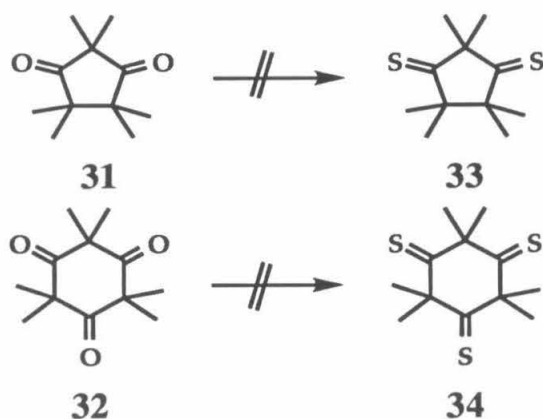
Unfortunately, the preparation of the other bisfulvenes needed for this study could not be accomplished as easily. While the ketone moieties in 1,3-diacetylbenzene react as separate entities, the reactivities of the two ketones in 1,3-cycloalkanediones are intimately connected. Blocking 2,2-dimethyl substitution is required to avoid problems with enolization in these β -diketones and, in addition, subjecting these compounds to

nucleophilic conditions invariably leads to ring-opened products due to retroaldol reactions.¹¹¹ Therefore, alternative syntheses are required.

Several published reports have established a general route to compounds with a central cyclobutane ring through dipolar cycloaddition to dithione **28**.¹¹¹⁻¹¹³ Freund and Hünig accomplished the preparation of bisfulvene **30** by dual dipolar cycloaddition of diazocyclopentadiene to **28** and desulfurization of the resulting bisthiirane, **29**, with triphenylphosphine.¹¹² We have succeeded in synthesizing small quantities of **30** in this manner. Unfortunately, the addition reaction requires several weeks at room temperature to produce appreciable quantities of **29**, while heating is precluded by the explosive nature of diazocyclopentadiene.



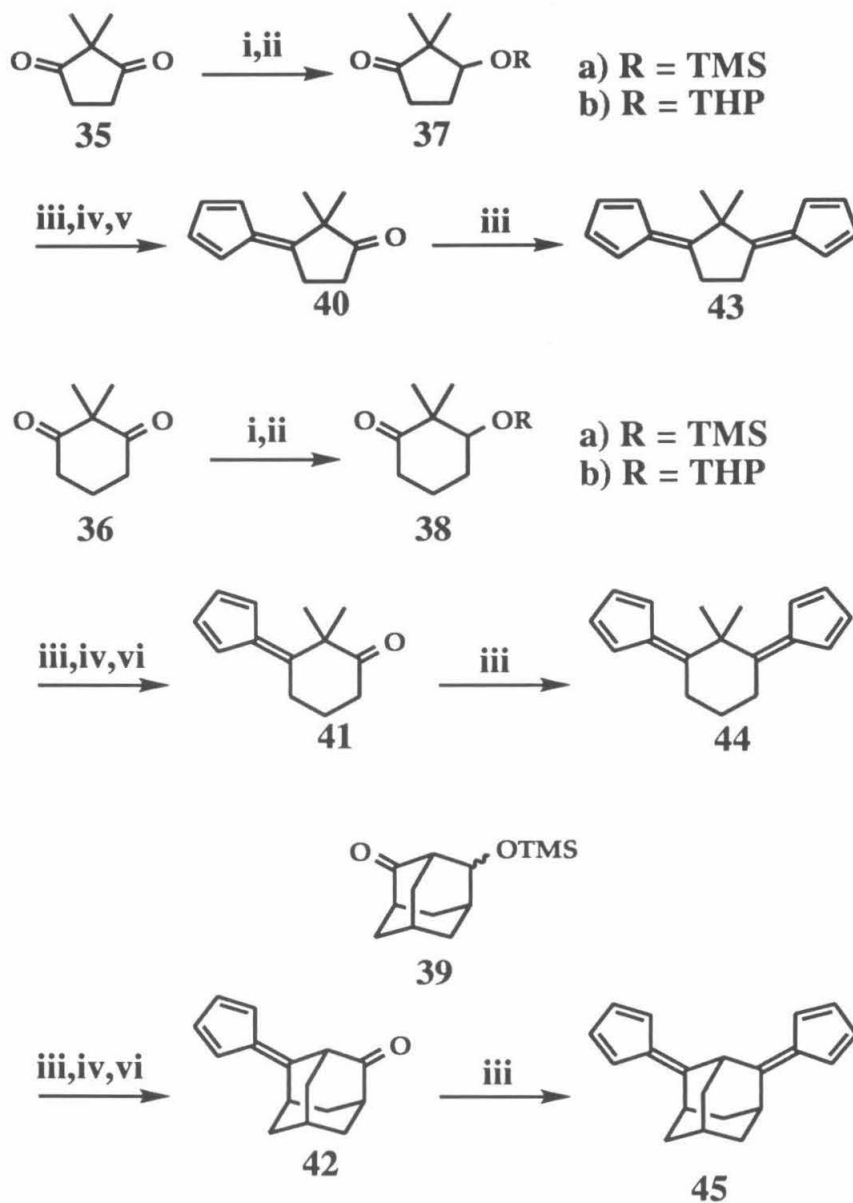
Due to the success of the above method, we have also investigated the synthesis of other dithiones related to the 1,3-cyclopentane and 1,3-cyclohexane ferromagnetic coupling units (FCs). Although treatment of **27** with either of the standard reagents P_4S_{10} ¹¹⁴ or Laewesson's reagent¹¹⁵ produces **28** in good yield, we have obtained no evidence for the conversion of compounds **31** or **32** to thiones by treatment with these reagents. We note that oxo- and alkylidene-disubstituted cyclobutanes have special electronic properties due to the short transannular distance,¹¹⁶ and these properties may well lend special reactivity to **27**.



Unable to produce the necessary thiones, we have investigated a protection/deprotection route to the bisfulvenes **43** and **44** (Scheme 2-1). Dione starting materials **35** and **36** are selectively reduced by atmospheric pressure hydrogenation over Adams' catalyst.¹¹⁷ Reaction of **37** and **38** with chlorotrimethylsilane and hexamethyldisilazane yields the protected derivatives **37a** and **38a**, which are then condensed with CpMgBr. We have also employed THP protecting groups in **37b** and **38b**, but have found cleavage of the THP ethers to be difficult in the presence of fulvenes. In contrast, we have found that the mild reagent triethylamine trihydrofluoride in CH₃CN¹¹⁸ effects clean deprotection of the silyl derivatives to the intermediate alcohols. Oxidations employing either tetra(*n*-propyl)ammonium perruthenate¹¹⁹ (TPAP) or the Swern reagents^{120,121} have been used. The latter is far superior, giving almost quantitative yields. The optimized combination of these reactions gives an overall yield of 25% for the five steps from the diones to the fulvene-ketones.

When treated with CpMgBr in THF at reflux, **40** gives the intermediate magnesium salt as evidenced by TLC, but this intermediate eliminates to bisfulvene **43** only in low yield. The difficulty in this step is presumably due to steric repulsions between the methyl groups and fulvene hydrogens in **43**. We have not been able to effect

SCHEME 2-1



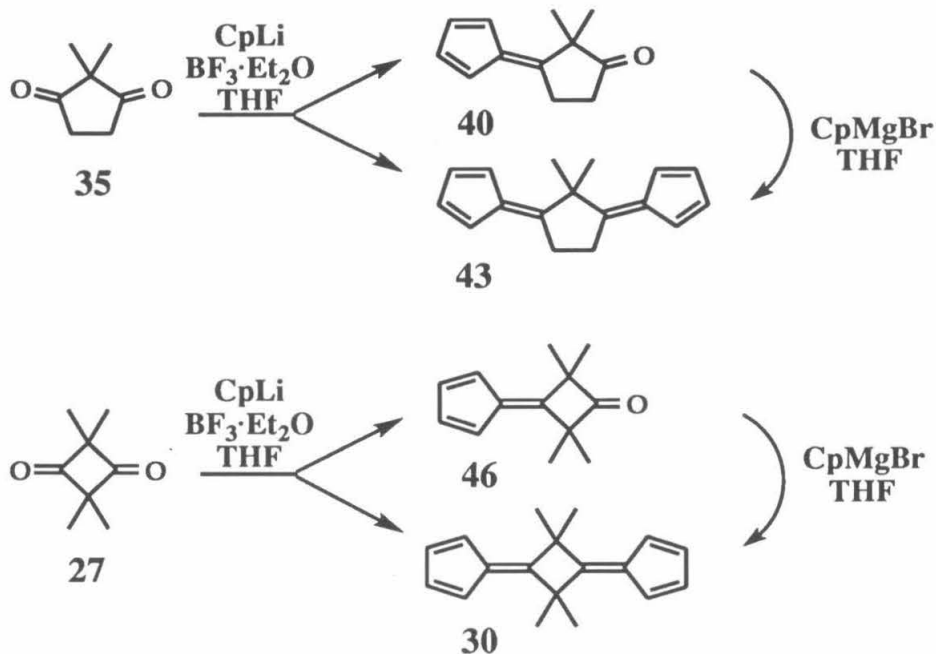
elimination of the intermediate magnesium salt formed by CpMgBr addition to **41** under a variety of conditions. Apparently, steric effects completely preclude the formation of **44**.

The inability to synthesize **44** has caused us to turn to the adamantyl ring system, which has significant advantages: there are no steric interactions to worry about, the exocyclic fulvene bonds in the intermediate compounds cannot tautomerize easily, and the adamantane skeleton imparts a high degree of crystallinity to these derivatives. The first aspect makes formation of fulvenes easier, while the latter two aspects lend resistance to decomposition and polymerization reactions that seems to further plague the preparation of **42** and **43**. Indeed, we are able to make bisfulvene **45** in good overall yield. The known compound 8-hydroxy-2-adamantanone¹²² is protected to give **39**, and the synthesis proceeds as above.

The instability of the intermediates in the synthesis of **43** has caused us to continue a search for simpler syntheses of this compound. In a perusal of the literature for oxophilic reagents that might preclude the retro-aldol condensation in the reaction of cyclopentadienides with **35**, we discovered a report of the ring-opening reactions of oxetanes and tetrahydrofurans with n-BuLi in the presence of BF₃•Et₂O.¹²³ Reasoning that it might be the role of the boron trifluoride to precomplex the oxygen in these compounds, thereby promoting electrophilicity and capturing the developing oxy-anion, we have tried similar conditions with **35**. We have discovered that when BF₃•Et₂O is included in the reactions of CpLi or CpNa with this compound, appreciable quantities of ring-retained fulvenes **40** and **43** and *no ring-opened products* are formed. The major product of this reaction is **40**; small and varying amounts of **43** are also produced. The modest yields obtained in this reaction (32% **40**, 14% **43**) are attributed to the joint presence of a strong Lewis acid and highly reactive fulvene moieties. The fulvene **40** may be converted to **43** with CpMgBr. We have found that this reaction works with **27**

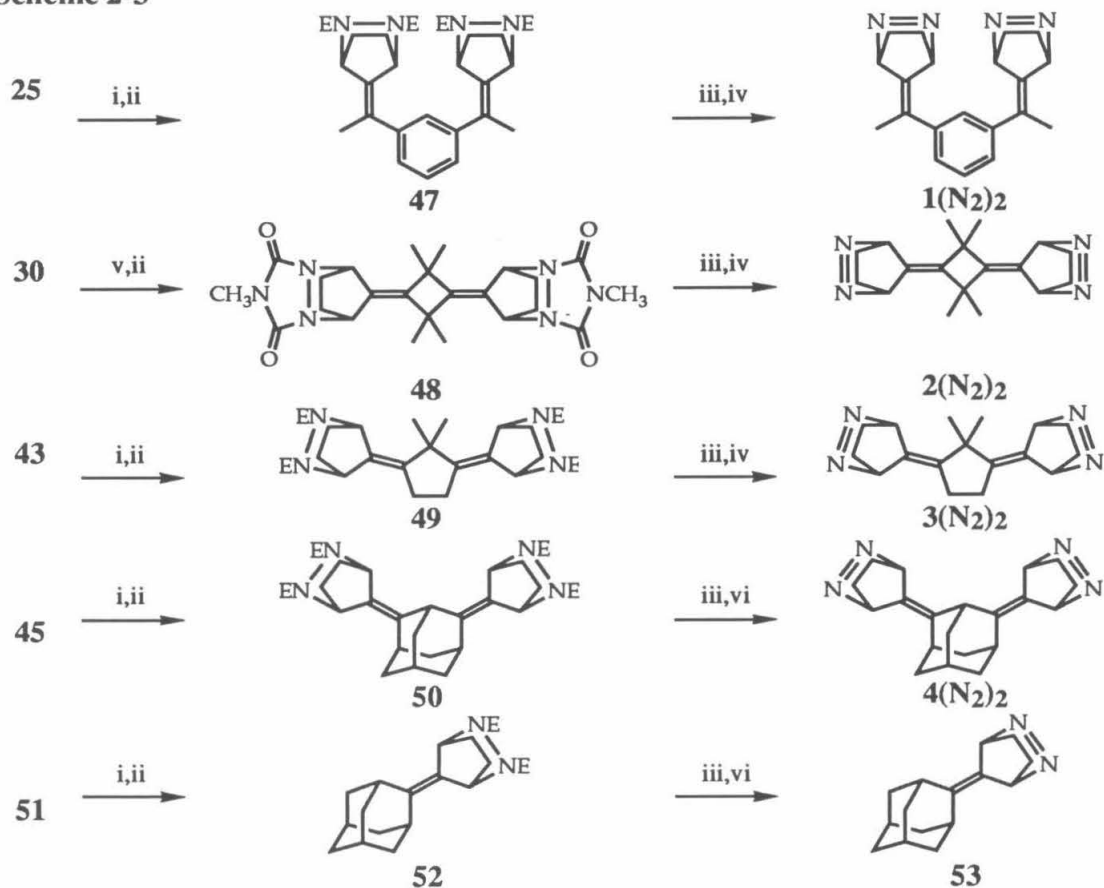
as well, and provides a convenient, time-saving synthesis of monofulvene **46** and bisfulvene **30**. These results are summarized in Scheme 2-2.

SCHEME 2-2



Elaboration of fulvenes into diazenes occurs through a straightforward series of transformations that we have adapted to the synthesis of bisdiazenes.^{74,124} Although we have had to make minor modifications in some cases, we have tried to establish a standard protocol for this sequence (Scheme 2-3). Diels-Alder reaction of the two fulvene subunits with dimethyl azodicarboxylate (DMAD) is the first step. We have found that separation of the dual Diels-Alder adducts from excess DMAD on a flash silica column gives clean products for which we can monitor the succeeding reduction easily by ^1H NMR. Bisfulvene **30** does not react with DMAD, again presumably due to poor steric interactions, and thus we employ reaction with N-methyltriazolinedione (MTAD). This highly reactive dienophile gives the desired dual Diels-Alder products. All of these compounds are produced as mixtures of diastereomers.

Scheme 2-3



Legend. (i) DMAD, CH₂Cl₂ (ii) PADC, AcOH, CH₂Cl₂ (iii) KOH, i-ProH, Δ (iv) NiOx, CH₂Cl₂, 0 °C (v) MTAD, hexane/ether (vi) a) CuCl₂ b) NH₄OH.

The endocyclic olefin linkages in these compounds are reduced with diimide generated from potassium azodicarboxylate (PADC) and acetic acid in methylene chloride.¹²⁴ The generation of diimide is slow, and some yellow PADC always remains when these reactions are quenched with water. Quenching leads to significant gas evolution. It is not clear how much reduction actually occurs at this stage. Nevertheless, we are able to isolate clean samples of the reduced double Diels-Alder adducts, **47-50**, and overreduction is not encountered. When reduction is not complete, as determined by the presence of alkene resonances in the ¹H NMR spectrum, the reaction mixture is simply resubmitted to the reaction.

Transformations of **47-50** to **1(N₂)₂-4(N₂)₂** complete the syntheses. Hydrolyses of the diazene-masking groups are accomplished with KOH in refluxing 2-propanol. Cooling to room temperature and stirring with solid NaHCO₃ leads to decarboxylation. Dark brown reaction mixtures result and are evaporated to dryness under high vacuum. Water is added, and the mixtures are extracted with methylene chloride. The methylene chloride solutions are treated with nickel peroxide, NiO_x,^{55,58,125,126} at 0 °C to effect oxidations to the bisdiazenes. This method is successful except in the case of the adamantyl-based molecules, which give multiple products upon NiO_x oxidation. We point to the high reactivity of NiO_x in a hydrogen-abstracting sense and the number of bridgehead positions in adamantane to explain the results we obtain in these cases.¹²⁶ Molecules containing the adamantane skeleton can be oxidized successfully to the diazene copper complexes using CuCl₂, and these complexes give diazenes when treated with NH₄OH.^{58,127}

Bisdiazene precursors **1(N₂)₂-4(N₂)₂** are converted to the corresponding tetraradicals **1-4** by photolysis in a matrix of either MTHF or 1,2-propanediol at low temperature in the cavity of an EPR spectrometer. The results of the photolyses are described in the EPR section below.

Model. A tetraradical is distinguished by four electrons in four nearly degenerate nonbonding molecular orbitals. These give rise to 70 possible electronic configurations that can be assigned to 36 states: 20 singlets, 15 triplets, and *one* quintet. In a hydrocarbon tetraradical, ionic states are expected to be very high in energy and these may be disregarded. There are six possible covalent states: two singlets, three triplets, and one quintet. When combining two biradicals to form a tetraradical, the situation is further simplified if the biradicals are "robust triplets," with their singlet states too high-lying to be thermally populated at any reasonable temperature. If such biradicals are employed, then triplet-triplet coupling is solely responsible for the resulting spin states, which then number only three: a quintet (Q), a triplet (T), and a singlet (S). Purposely

limiting the number of states available to the system in this way allows questions regarding the FC to be answered experimentally with relative ease. This simplification of the energy spectra of the tetradicals produced by choice of Berson TMMs as SCs is a significant advantage of our strategy.

The contributions of the three triplet spin states to the spin states of the tetradical may be computed by means of the Clebsch-Gordan, or vector-coupling coefficients.^{15,128} The highest m_s eigenfunctions of each spin state are given in eq 1-3. As discussed in Chapter 1, the interaction of the two triplet subunits may be modeled by the Heisenberg Hamiltonian (eq 4).⁵⁰ The exchange parameter J , *due to the FC*, determines the ground state of the resulting tetradical. If $J > 0$, high-spin or ferromagnetic coupling occurs and **Q** is the ground state, while if $J < 0$, low-spin or antiferromagnetic coupling occurs, and **S** is the ground state. Application of the Heisenberg Hamiltonian to the spin functions of eq 1-3 leads to an energy expression given in eq 5 and depicted in Figure 1.

$$\mathbf{Q} = |1\rangle|1\rangle \quad (1)$$

$$\mathbf{T} = \frac{1}{\sqrt{2}}(|1\rangle|0\rangle - |0\rangle|1\rangle) \quad (2)$$

$$\mathbf{S} = \frac{1}{\sqrt{3}}(|1\rangle|-1\rangle - |0\rangle|0\rangle + |-1\rangle|1\rangle) \quad (3)$$

$$\hat{H} = -2J \hat{S}_1 \cdot \hat{S}_2 \quad (4)$$

$$E_s = -J(S(S+1) - 4) \quad (5)$$

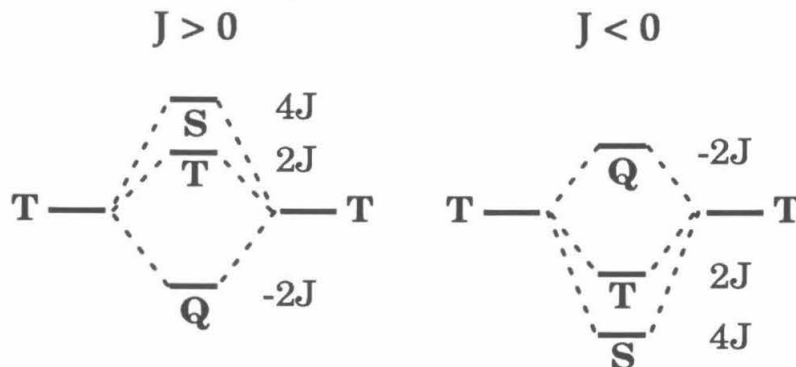


Figure 1. Heisenberg energy level diagrams for two interacting triplet biradicals.

EPR Spectroscopy of High-Spin Molecules. A brief review of quintet and triplet state EPR spectroscopy will assist in the interpretation of the experimental spectra.^{15,129} For a quintet (triplet) there are five (three) energy levels with $m_s=0,\pm1,\pm2$ ($m_s=0,\pm1$). These energy levels are distinct even in the absence of an applied magnetic field due to a dipolar coupling among (between) the electron spins. This coupling is described by a zero-field splitting (zfs) tensor, **D**, which is characteristic of a particular species. The **D**-tensor is represented by two scalar parameters in the EPR Hamiltonian, D and E , which can be deduced from the observed spectra.

The EPR resonance fields of a single molecule in a sample are highly dependent on the orientation of its **D**-tensor with respect to the applied magnetic field. The randomly oriented molecules in a frozen matrix give rise to a virtually infinite number of absorptions; thus the EPR absorption spectra are broad. However, molecules in similar orientations, with one of their **D**-tensor axes nearly aligned with the magnetic field (the canonical orientations), all have roughly the same absorption spectrum. This gathering of resonances leads to a peak in the derivative of the absorption, and for this reason, EPR spectra are normally recorded in derivative mode.

EPR selection rules allow four (two) $\Delta m_s=1$ transitions. There are then 4 transitions x 3 canonical orientations = 12 ($2 \times 3 = 6$) lines that might be detected. Total spectral width is $6D$ ($2D$), and at X-band (≈ 9.27 GHz) the linewidths in the experimental spectra described here are large enough in comparison with D that fewer than 12 lines are observed. Additionally, the small D -values of these spectra preclude the occurrence of off-axis extra lines that have been used to assign EPR spectra in other cases.¹³⁰ The practical effect of these factors is to complicate assignment of the observed spectra to a quintet spin state.

A formally forbidden "half-field" $\Delta m_s=2$ transition is also observed in the spectra of quintet and triplet states due to the perturbation of the selection rules by the zfs tensor; large zfs leads to greater intensity of the transition. We observe distinct lines in this

region for some quintets. This feature of quintet spectra is a useful diagnostic probe, especially in the present systems, in which triplets are converted slowly into quintets by photolysis.

In addition to these basic spectral features, we have two powerful tools to assist in the spin-state assignment of EPR spectra. The first is a complete simulation of the powder spectrum. The effective EPR spin Hamiltonian used in these simulations is

$$\hat{\mathcal{H}} = g\beta\mathbf{H} \cdot \hat{\mathbf{S}} + D(\hat{S}_z^2 - (S(S+1)/3)) + E(\hat{S}_x^2 - \hat{S}_y^2) \quad (6)$$

in which terms of fourth order and higher in $\hat{\mathbf{S}}$ are neglected and an isotropic g -tensor is assumed. A detailed description of the manner and methods used for these simulations is given in Chapter 4.

Our assignments are also substantially bolstered by our ability to predict D -values for the spin states of a tetraradical composed of two coupled triplet biradicals. For tetraradicals composed of two biradical subunits such as **1-5**, the Hamiltonian for the dipolar interactions among the four electrons in zero field can be written

$$\hat{\mathcal{H}} = \hat{\mathbf{S}}_A \cdot \mathbf{D}^A \cdot \hat{\mathbf{S}}_A + \hat{\mathbf{S}}_B \cdot \mathbf{D}^B \cdot \hat{\mathbf{S}}_B + \hat{\mathbf{S}}_A \cdot \mathbf{D}^{AB} \cdot \hat{\mathbf{S}}_B \quad (7)$$

where \mathbf{D}^A and \mathbf{D}^B are the \mathbf{D} -tensors of biradicals A and B, \mathbf{D}^{AB} is the \mathbf{D} -tensor that describes the dipolar interaction between the two biradical subunits, and $\hat{\mathbf{S}}$ is shorthand notation for the collection of spin operators $[\hat{S}_x, \hat{S}_y, \hat{S}_z]$. To first order, the interaction occurs only when there are spins on both carbons of the FC. In a bis(TMM), according to Hückel theory, this is the case $\left(\frac{2}{3}\right)\left(\frac{2}{3}\right) = \left(\frac{4}{9}\right)$ of the time. Therefore the interaction tensor \mathbf{D}^{AB} is determined by scaling the tensor of the corresponding biradical by $\left(\frac{4}{9}\right)$.

The zero-field splitting tensors of the tetraradical quintet and triplet states can be obtained by setting the zfs Hamiltonian of eq 1 equal to the zfs Hamiltonian for the resulting tetraradicals written in terms of the total spin \mathbf{S} (expanded form, eq 8). By computing the energies of the tetraradical eigenfunctions using these Hamiltonians, one can arrive at eq

9 and 10, the relationships between the **D**-tensors of the tetraradical states and the individual interactions that contribute to them. Eq 9 and 10 have been presented by Itoh.⁵⁰ These equations have obvious value in a predictive sense for tetraradicals and higher-spin species for which the **D**-tensors of the constituent subunits are known.

$$\hat{\mathcal{H}} = \left(-Z_A \hat{S}_{Az}^2 - \gamma_A \hat{S}_{Ay}^2 - \chi_A \hat{S}_{Ax}^2 \right) + \left(-Z_A \hat{S}_{Az}^2 - \gamma_A \hat{S}_{Ay}^2 - \chi_A \hat{S}_{Ax}^2 \right) + \left(-Z_A \hat{S}_{Az} \hat{S}_{Bz} - \gamma_A \hat{S}_{Ay} \hat{S}_{By} - \chi_A \hat{S}_{Ax} \hat{S}_{Bx} \right) = \left(-Z \hat{S}_z^2 - \gamma \hat{S}_y^2 - \chi \hat{S}_x^2 \right) \quad (8)$$

$$\mathbf{D}^Q = \frac{\mathbf{D}^A + \mathbf{D}^B}{6} + \frac{\mathbf{D}^{AB}}{3} \quad (9)$$

$$\mathbf{D}^T = \frac{\mathbf{D}^A + \mathbf{D}^B}{2} + \mathbf{D}^{AB} \quad (10)$$

In all paramagnets, the axis of highest symmetry is also usually a magnetic axis.^{15,129} The tetraradical states are therefore most likely quantized along the C_2 axes of **2** and **3**. Furthermore, the C_3 axis of the TMM is its principal magnetic Z-axis. The geometries of tetraradicals **2** and **3** are very convenient, because the principal axis of the TMM subunits are out of the plane, while the interelectronic axis is a logical choice for the Z-axis of a localized biradical (Figure 2-2). The arrangement of the TMM and localized units in **2** and **3** means that the constituent **D**-tensors are diagonal in a coincident set of coordinates. This situation allows the expected *D*-values to be computed easily.

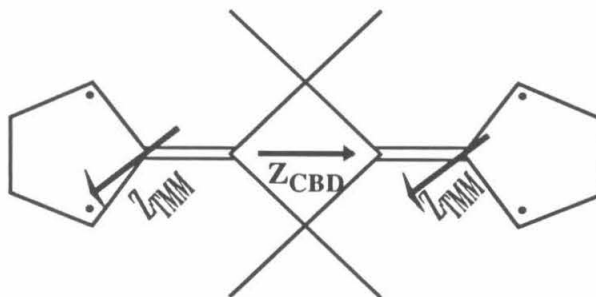


Figure 2-2. Illustration of the diagonal **D**-tensor directions of constituents of **2**.

The detailed calculation of the D -value of **52** (eq 11-15) serves as an example. In order to calculate the contributions to the tetraradical zfs tensors \mathbf{D}^Q and \mathbf{D}^T of eq 9 and 10 correctly, we must add the proper components of \mathbf{D}^{CBD} (the \mathbf{D} -tensor of cyclobutanediyl) and \mathbf{D}^{TMM} (the \mathbf{D} -tensor of TMM) together. The Z-axis of \mathbf{D}^{CBD} corresponds to the X-axis of \mathbf{D}^{TMM} . In order to add them properly, we apply a cyclic permutation to the components of \mathbf{D}^{CBD} . The tensors, now expressed in the same coordinate system, can be added together according to eqs 9 and 10. In predicting the D -values, a case-unbiased simplification is provided by arbitrarily assuming $E = 0$ for all of the components.

The predicted D -values for triplet and quintet tetraradicals computed by this procedure are shown in Table 2-2 along with the values we have determined experimentally. For **2** and **3** we expect our predictions and the experimental D -values to coincide. For **1**, the agreement will be rather ambiguous in meaning, especially when one considers that the m -phenylene interaction has a very small effect on the overall D -value (Table 1-1). The D -value predicted for **1** reflects a limiting case where the interaction through the ferromagnetic coupling unit has nearly no effect on the observed EPR spectra. Additionally, the evidence now available suggests it is likely that **1** is somewhat twisted, and the assumption of identical spin-quantization axes becomes questionable.⁸²

$$\mathbf{D}^A = \mathbf{D}^B = \mathbf{D}^{TMM} (\text{cm}^{-1}) = \begin{pmatrix} 0.00867 & 0 & 0 \\ 0 & 0.00867 & 0 \\ 0 & 0 & -0.0173 \end{pmatrix} \quad (11)$$

$$\mathbf{D}^{AB} = \left(\frac{4}{9}\right) \mathbf{D}^{CBD} = \left(\frac{4}{9}\right) \begin{pmatrix} -0.0373 & 0 & 0 \\ 0 & -0.0373 & 0 \\ 0 & 0 & 0.0747 \end{pmatrix} \quad (12)$$

$$\mathbf{D}^Q = \left(\frac{1}{6}\right) 2 \begin{pmatrix} 0.00867 & 0 & 0 \\ 0 & 0.00867 & 0 \\ 0 & 0 & -0.00173 \end{pmatrix} + \left(\frac{1}{3}\right) \left(\frac{4}{9}\right) \begin{pmatrix} 0.0747 & 0 & 0 \\ 0 & -0.0373 & 0 \\ 0 & 0 & -0.0373 \end{pmatrix} \quad (13)$$

$$\mathbf{D}^Q = \begin{pmatrix} 0.0140 & 0 & 0 \\ 0 & -0.00264 & 0 \\ 0 & 0 & -0.0113 \end{pmatrix} \quad (14)$$

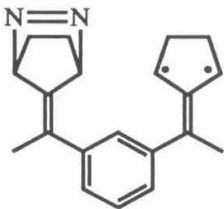
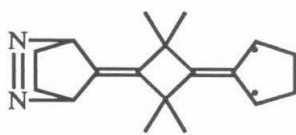
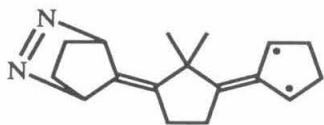
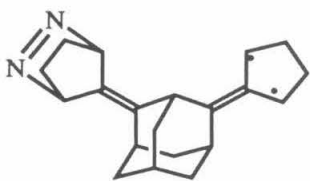
$$\left| \frac{D^Q}{hc} \right| = \frac{3}{2} 0.0140 \text{ cm}^{-1} = 0.0210 \text{ cm}^{-1} \quad (15)$$

EPR Results. Solutions of individual bisdiazenes are frozen at cryogenic temperatures and photochemical extrusion of N_2 is effected by irradiation of the diazene $n\text{-}\pi^*$ chromophore. Initial photolysis of $\mathbf{1}(\text{N}_2)_2 - \mathbf{4}(\text{N}_2)_2$ produces EPR spectra whose carriers are easily and unambiguously identified as triplet TMMs.^{70,74} Further photolysis alters the EPR spectra, producing noticeable differences between the initial and final spectra.

Figure 2-3a shows the EPR spectrum obtained upon initial photolysis of $\mathbf{1}(\text{N}_2)_2$ in MTHF at 77 K. The six lines in the $\Delta m_s = 1$ region and the $\Delta m_s = 2$ transition (not shown) identify the carrier of this EPR signal as the triplet biradical $\mathbf{1}(\text{N}_2)$ (Table 2-1). The zero field splitting parameters for this biradical are $|D|/hc = 0.0205 \text{ cm}^{-1}$ and $|E|/hc = 0.0023 \text{ cm}^{-1}$, in accord with values reported by Berson for similar molecules.⁷⁰ Figures 2-3b – 2-3d show the evolution of the recorded EPR spectra as this sample is subjected to further photolysis. The spectrum obtained after extended photolysis is well reproduced by computer simulation, shown in Figure 2-3e, employing a quintet Hamiltonian with $S=2$, $|D|/hc = 0.0076 \text{ cm}^{-1}$, $|E|/hc = 0.0003 \text{ cm}^{-1}$. We therefore assign this spectrum to $\mathbf{51}$.

Initial EPR spectra obtained after compounds $2(\text{N}_2)_2$ - $4(\text{N}_2)_2$ are irradiated are shown in Figures 2-4a, 2-5a, and 2-6a. Each is typical of a TMM,^{70,74} and the signal carriers are assigned as $2(\text{N}_2) - 4(\text{N}_2)$. The zfs parameters of these triplet biradicals are listed in Table 2-1. Figure 2-4b shows the EPR spectra obtained after extended photolysis of a sample of $2(\text{N}_2)_2$ in MTHF at 70 K. We assign the new fine structure peaks to 52 , with $|D|/hc = 0.0207 \text{ cm}^{-1}$ and $|E|/hc = 0.0047 \text{ cm}^{-1}$. A simulation of a quintet spectrum with these parameters is shown in Figure 2-4c. Comparison of the spectra in Figures 2-4b and 2-4c reveals that formation of **2** is incomplete and some $^32(\text{N}_2)$ remains in the matrix. A sum of simulated spectra representing a 1:1 mixture of $^32(\text{N}_2)$ and 52 (Figure 2-4d) matches the experimental spectrum exactly. Analogous spectra from the extended photolysis of $3(\text{N}_2)_2$ in MTHF at 4 K are shown in Figures 2-5b – 2-5d; for 53 , $|D|/hc = 0.0178 \text{ cm}^{-1}$ and $|E|/hc = 0.0047 \text{ cm}^{-1}$. Our spectral assignments are thoroughly consistent with the D -values of 51 , 52 , and 53 calculated from eq 9 (Table 2-2).

Table 2-1. Observed zfs parameters for monoazo triplet biradicals.

Species	$ D/hc $ (cm ⁻¹)	$ E/hc $ (cm ⁻¹)
 1(N₂)	0.0205	0.0023
 2(N₂)	0.0256	0.0044
 3(N₂)	0.0254	0.0035
 4(N₂)	0.0252	0.0039

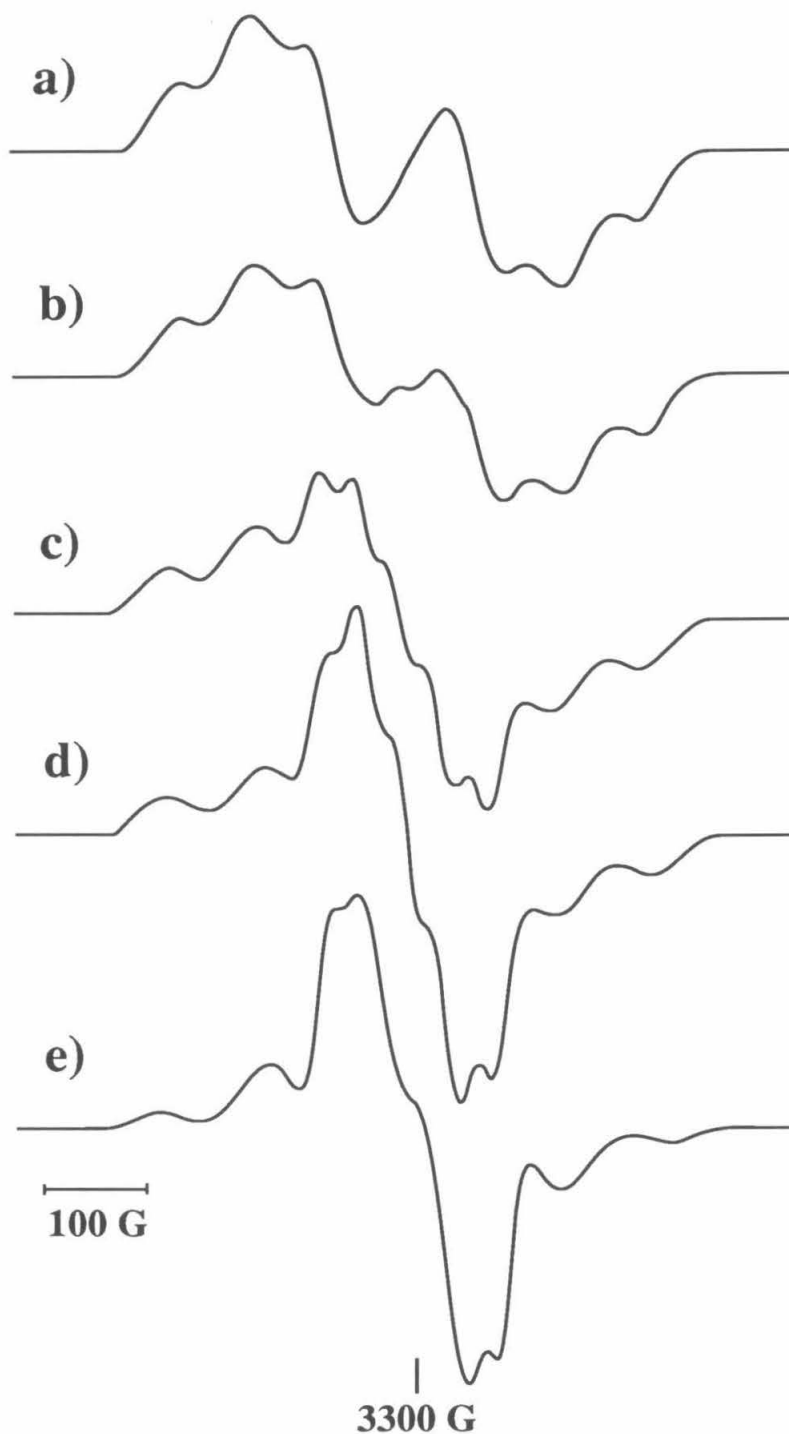


Figure 2-3. EPR spectra: (a)-(d) obtained from photolysis of $1(\text{N}_2)_2$ at 77 K; (a) 15 min hn; (b) 90 min hn; (c) 450 min hn; (d) 900 min hn. (e) Simulated quintet with $|D|/hc = 0.0076 \text{ cm}^{-1}$ and $|E|/hc = 0.0003 \text{ cm}^{-1}$.

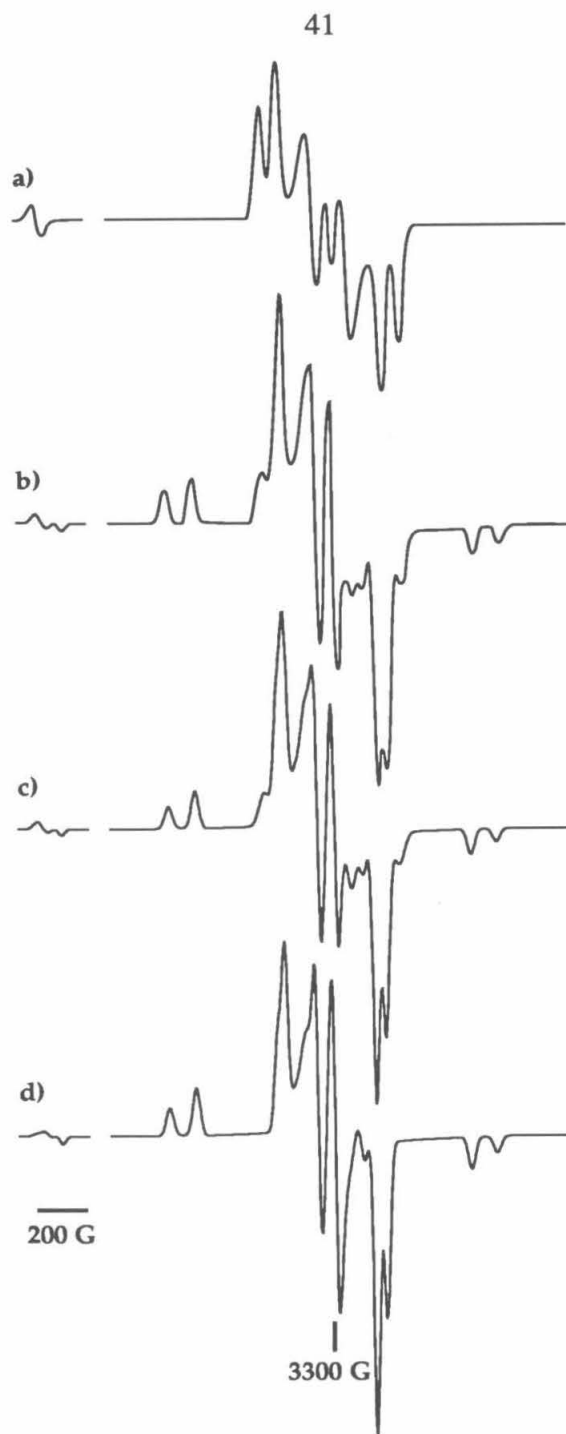


Figure 2-4. EPR spectra: (a) obtained after 30 s photolysis of $2(\text{N}_2)_2$ at 70 K, assigned to $^3\text{2}(\text{N}_2)$ (b) obtained after 353 min photolysis of $2(\text{N}_2)_2$ at 70 K, assigned to a mixture of $^3\text{2}(\text{N}_2)$ and $^5\text{2}$ (c) mixture of simulations of $^3\text{2}(\text{N}_2)$ and $^5\text{2}$ (see d) representing a 1:1 molar ratio. (d) simulation of spectrum of $^5\text{2}$ with zfs parameters $|D|/hc = 0.0207 \text{ cm}^{-1}$ and $|E|/hc = 0.0047 \text{ cm}^{-1}$.

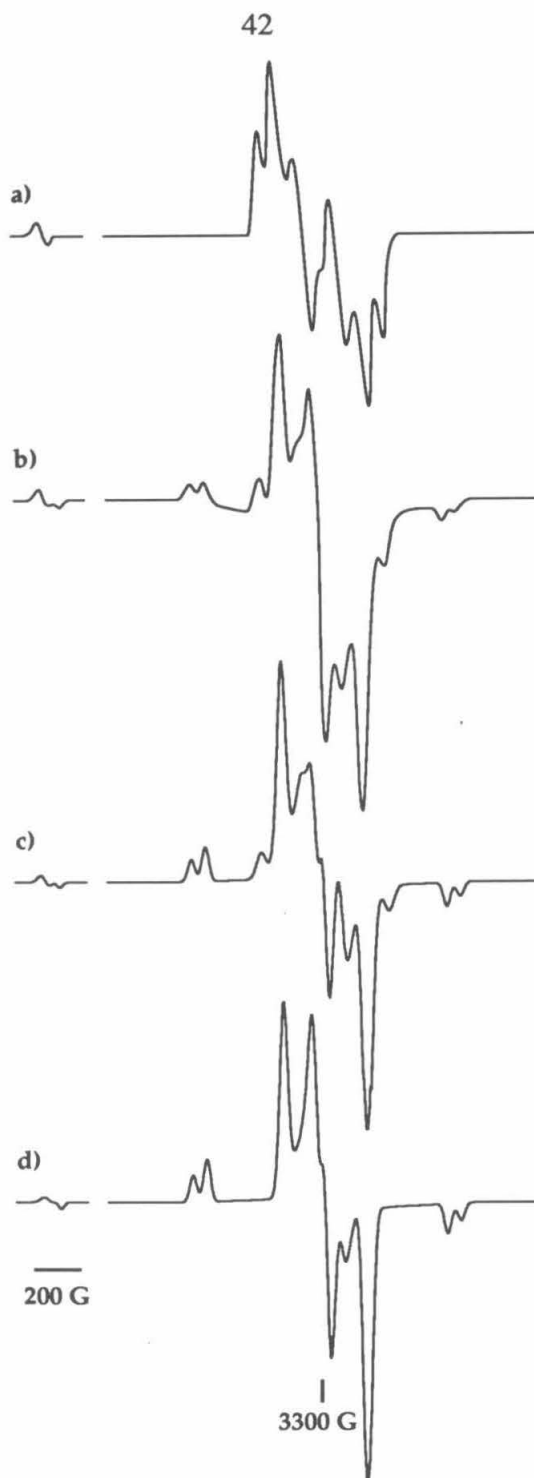


Figure 5. EPR spectra: (a) obtained after 60 s photolysis of $3(\text{N}_2)_2$ at 4 K, assigned to $^3\text{N}_2$ (b) obtained after 650 min photolysis of $3(\text{N}_2)_2$ at 4 K, assigned to a mixture of $^3\text{N}_2$ and $^5\text{N}_2$ (c) mixture of simulations of $^3\text{N}_2$ and $^5\text{N}_2$ (see d) representing a 1:1 molar ratio. (d) simulation of spectrum of $^5\text{N}_2$ with zfs parameters $|D|/hc = 0.0178 \text{ cm}^{-1}$ and $|E|/hc = 0.0047 \text{ cm}^{-1}$.

Table 2-2. Predicted and experimental D -values for tetraradicals.

Species	$\frac{D^A(=D^B)}{hc}$	$\frac{D^{AB}}{hc}$	$\left \frac{D^Q}{hc} \right $ (cm ⁻¹)		$\left \frac{D^T}{hc} \right $ (cm ⁻¹)	
	(cm ⁻¹)	(cm ⁻¹)	calc.	expt'l.	calc.	expt'l.
1	0.020	0.0053	0.0078	0.0076	0.029	--
2	0.026	-0.049	0.020	0.021	0.037	--
3	0.026	-0.037	0.016	0.018	0.030	0.036
4	0.026	-0.031 ^a	0.015	--	0.028	--

^a Calculated by scaling values from **22b** and **23a** by the distance calculated for **24** using a $1/r^3$ relationship. See refs 15, 83, 85.

In contrast to the results for **2(N₂)₂** and **3(N₂)₂**, when **4(N₂)₂** is irradiated for a prolonged period at either 4 K or 77 K, no new fine structure appears. During an extended photolysis period, the amplitude of the observed triplet signal decreases (Figures 2-6b–2-6d). The intensity of the EPR signal resulting from irradiation of **4(N₂)₂** can be measured as a function of photolysis time. In separate experiments, MTHF solutions of monodiazene **53** and **4(N₂)₂** were irradiated at 50 K. For the conversion of **53** to **54**, first-order growth of the triplet signal is observed ($k_A = 0.015 \text{ min}^{-1}$) with a very slight decay upon extended photolysis ($k_D = 2 \times 10^{-5} \text{ min}^{-1}$) (Figure 2-7). The intensity profile of the EPR signal from the photolysis of **4(N₂)₂** (Figure 2-7) strongly suggests that the carrier of this signal is the first product in a two-step unimolecular decomposition ($k_1 = 0.004 \text{ min}^{-1}$, $k_2 = 0.011 \text{ min}^{-1}$).¹³¹ From these results, we conclude that the extended photolysis of **4(N₂)₂** produces tetraradical **4**, but that **4** is EPR silent because it has a **singlet** ground state. Of course, it is conceivable that

photodecomposition of $4(\text{N}_2)$ differs in some way from that of the large number of related, previously studied structures,⁷⁰ but we consider this possibility highly unlikely.

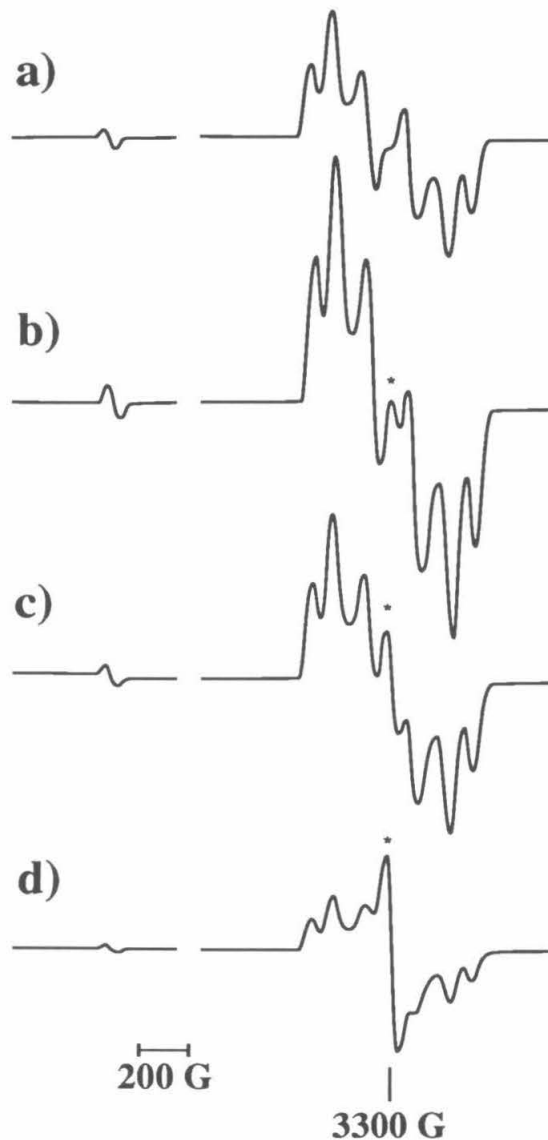


Figure 2-6. EPR spectra resulting from photolysis of $4(\text{N}_2)_2$ at 77 K. Irradiation times: (a) 30 min (b) 190 min (c) 300 min (d) 607 min. All spectra were recorded at the same receiver gain setting. Small doublet impurity is marked *.

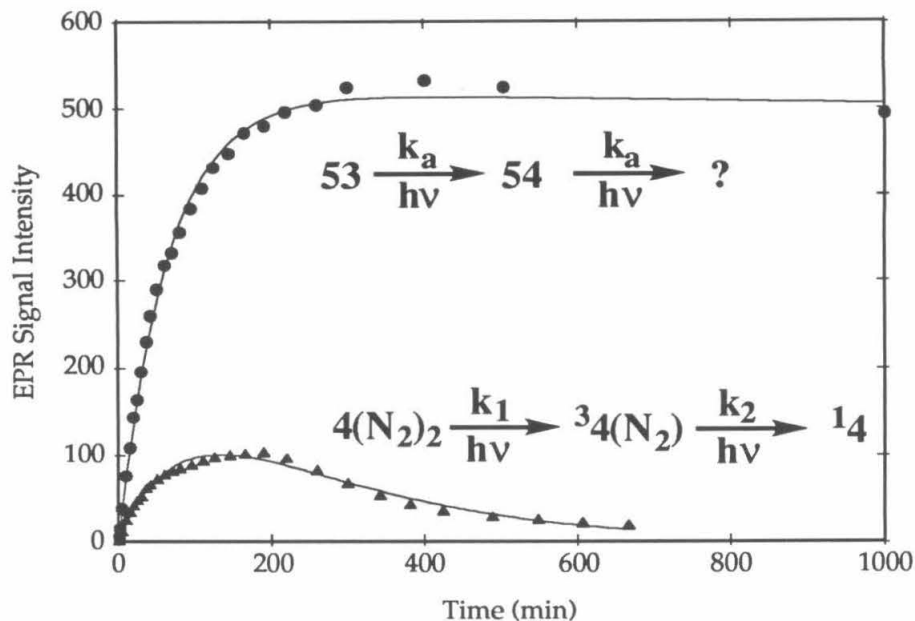


Figure 2-7. Plot of EPR signal intensity vs. photolysis time at 50 K for **53** and $4(N_2)_2$.

Variable-Temperature Studies. The quintet states of tetraradicals **1-3** are all readily observed at temperatures as low as 3.8 K, strongly suggesting a quintet ground state in each case. Monitoring signal intensity as the temperature is raised can provide information on the energetic magnitude of this preference. Tetraradical **1** is quite stable thermally, and raising the temperature as high as 135 K (1,2-propanediol matrix) produces only intensity changes consistent with conventional Curie behavior. Thus the preference for a quintet ground state in **1** is at least 1350 cal/mol (see eq 19, below).

When samples of **2** in 1,2-propanediol are warmed, Curie behavior is also observed, but only up to 85 K. At this temperature, the signals due to **52** disappear over a period of a few minutes. A similar irreversible decay of **53** signals is seen at temperatures above 120 K.

However, when samples of **3** in 1,2-propanediol are observed in the 4 - 100 K range, two new peaks symmetrically displaced from the center of the $\Delta m_s=1$ region appear in the higher temperature spectra. A spectrum recorded at 40 K is shown in Figure 2-8. These changes are reversible — the new peaks completely disappear upon recooling. Thus $^5\mathbf{3}$ is in thermal equilibrium with an EPR active species. Referring to the state energy diagram of Figure 2-1, the obvious candidate for the EPR active species is $^3\mathbf{3}$. As computed from eq 10 and shown in Table 2-2, $^3\mathbf{3}$ should have $|D|/hc = 0.036 \text{ cm}^{-1}$. If the two new peaks correspond to the outer lines of a triplet spectrum, then $|D|/hc = 0.030 \text{ cm}^{-1}$ for the triplet species. We consider such agreement compelling and conclude that $^5\mathbf{3}$ is in equilibrium with $^3\mathbf{3}$ and $^1\mathbf{3}$. Fitting the change in the observed triplet signal intensity vs. temperature (Figure 2-9) allows us to estimate J as 50 cal/mol, and so the energy separation between $^5\mathbf{3}$ and $^3\mathbf{3}$ is $\Delta E_{QT}=200 \text{ cal/mol}$.

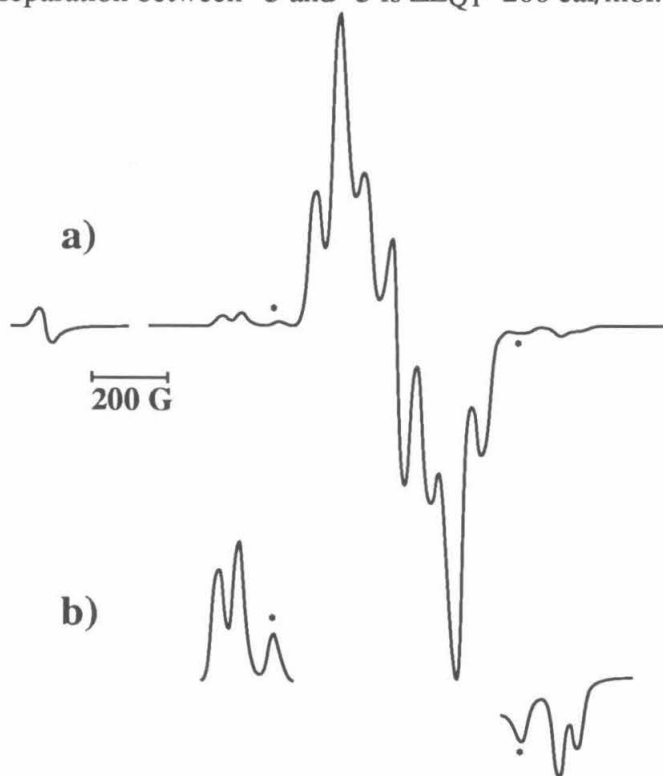


Figure 2-8. EPR spectra of Figure 2-5 recorded at 40 K. (a) normal gain setting (b) gain increased 10x. * marks peaks due to $^3\mathbf{3}$.

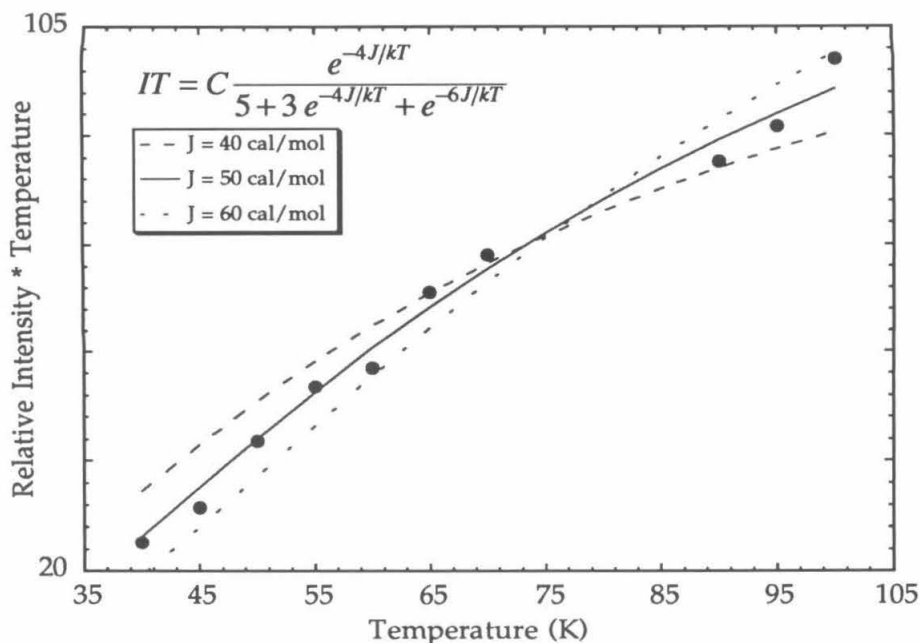


Figure 2-9. Plot of IT (the product of relative EPR signal intensity and temperature) vs. T for ^{33}S . The curves shown for different J are the best fits of the data to the equation shown, which incorporates both Boltzmann and Curie effects.

We have found that the spin state energies of the tetraradicals can be reconciled with *ab initio* calculations of the singlet-triplet gaps (ΔE_{ST}) in the corresponding biradicals (Table 1-1). Modeling a biradical with the Heisenberg Hamiltonian (eq 4) gives $2J$ as the **S-T** gap (eq 16). This J transfers directly to a bis(TMM), except it must be scaled by $\frac{1}{3} \cdot \frac{1}{3} = \frac{1}{9}$ since only $\frac{1}{3}$ of the total TMM spin density is on the FC carbons. Combining this factor with eq 5 gives eq 17. Combining eqs 16 and 17 gives eq 18, relating the **Q-T** gap of a bis(TMM) to the **S-T** gap of the biradical that corresponds to the FC.

$$\Delta E_{ST} = 2J \quad (16)$$

$$\Delta E_{QT} = 4J/9 \quad (17)$$

$$\Delta E_{QT}/\Delta E_{ST} = 2/9 \quad (18)$$

$$\Delta E_{QT}/kT \leq 5.0 \quad (19)$$

For cyclopentadienyl, $\Delta E_{ST}=900$ cal/mol ($J=450$ cal/mol) has been calculated.^{57,94} Application of eq 18 predicts $\Delta E_{QT}=200$ cal/mol in **3**, in remarkable agreement with experiment. Certainly the agreement is fortuitous to some extent, as the calculated S-T gap has some uncertainty and spin polarization effects in the TMM unit have been ignored. Using the S-T gaps of Table 1-1, Q-T gaps of 2,200 cal/mol for **1** and 380 cal/mol for **2** are obtained. Our experience with **33** shows that one can expect to observe the excited T state when eq 19 is satisfied. For **1**, this requires a temperature of 222 K, precluding observation of **31** in the matrices employed to date ($T<140$ K). The temperature range in which **32** might be observable is quite close to where irreversible thermal decay sets in.

We have computed ΔE_{ST} for trimethylene at a geometry analogous to **4**. This geometry was obtained by MM2 geometry optimization of bisfulvene **42**, followed by isolation of the desired three-carbon fragment and attachment of hydrogens at the optimized bond and dihedral angles, but normal C-H bond lengths (1.10 Å). This trimethylene has a 1.3 kcal/mol preference for a *singlet* ground state at the same level of theory used for the other biradicals discussed above. The results of these calculations are completely consistent with the Goldberg and Dougherty model concerning the origin of the spin state energy differences, which emphasizes the role of through-bond coupling, the importance of the C1-C2-C3 angle, and the C1-C3 distance. This computed ΔE_{ST} is, of course, consistent with the apparent singlet ground state of tetraradical **4**.

Summary and Conclusions

The scope of *m*-phenylene as a ferromagnetic coupling unit has been expanded. Previous efforts have focused primarily on one-center spin-containing units such as carbenes and simple radicals. The quintet ground state of **1** establishes that delocalized biradicals are also ferromagnetically coupled by this unit. In Chapter 3, we show that *m*-phenylene also serves as an FC for localized biradicals. Our work directed toward the “polaronic ferromagnet” has established that radical cations are also ferromagnetically

coupled by *m*-phenylene.¹⁰⁵⁻¹⁰⁷ Thus, this FC appears to have broad potential in the design of high-spin and potentially magnetic materials.

The results on **2-4** allow several conclusions concerning potential "localized"⁵⁸ FCs. Based on the results for **2**, 1,3-cyclobutane appears to be an effective FC. The thermal instability of **2** above 85 K could signal a liability in this unit, but further work will be required to quantify the effect. In contrast, the results for **3** and **4** indicate that 1,3-cyclopentane is a fairly weak ferromagnetic coupling unit, and 1,3-cyclohexane (chair) is an *antiferromagnetic* coupling unit. Thus, neither seems well-suited to producing very high spin arrays or magnetic materials.

An encouraging aspect of our findings is the remarkable success of eq 9 and 10 in predicting zfs values for tetraradicals, and the equivalent performance of eq 18 in predicting state energy orderings for **3**. The quantitative nature of these predictions will facilitate study of a wide array of tetraradical structures.

A few comments about the "bis(TMM)" approach are appropriate. First, it must be emphasized that, conceptually, the strategy is directly analogous to the polycarbene approach that has been exploited by Itoh, Iwamura, and others.^{7,8,23} There are some practical advantages to the bis(TMM) approach. First, the Berson TMMs we have used are less reactive than diaryl carbenes, especially with regard to H-atom abstraction from matrices.¹³³ Second, there is more design flexibility with this approach, in that biscarbene analogues of **2-4** would be unrealistic targets. Finally, the quantitative modeling of the bis(TMM)s described above opens the way for many further studies of tetraradicals. The results on **2-4** demonstrate that the bis(TMM) approach can also provide information about simple biradicals. This includes information that would be difficult to obtain from direct studies of the biradicals themselves, either because the biradicals are not thermally stable (**3** vs **23a**) or because the biradicals themselves have never been observed (**4** vs **24**). This work continues in the Dougherty group.

Experimental

General. Unless otherwise noted, reactions were run under an atmosphere of dry argon or nitrogen. Tetrahydrofuran, diethyl ether, dioxane, and benzene were distilled from sodium benzophenone ketyl. Methylene chloride and acetonitrile were distilled from CaH_2 . TLC was performed on 0.25 mm silica pre-coated glass plates visualized under UV light and/or with vanillin stain. Flash chromatography was performed on 230-400 mesh silica gel. 70 eV EI Mass spectral data were obtained on a Hewlett-Packard 5890/5970 GC/MS. High resolution mass spectral analyses were performed by the Mass Spectral Facility at the University of California, Riverside. NMR spectra were obtained on JEOL GX-400, GE QE-300, or Varian EM-390 spectrometers and referenced to residual protio solvent. EPR spectra were obtained on a Varian E-Line Century Series spectrometer operating at X-band ($\nu \approx 9.27$ GHz). EPR samples were prepared in either 2-MTHF (vacuum transferred from sodium-benzophenone ketyl) or propylene glycol (dried over Na_2SO_4 , then distilled under partial vacuum/argon) in the strict absence of oxygen. A liquid nitrogen-filled finger dewar was employed for 77 K experiments. Variable temperature control in EPR experiments was achieved with a ^4He -cooled Oxford Instruments ESR-900 cryostat. The filtered (307-386 nm pass), focused output of either a 1000 W Hg-Xe arc lamp or 500 W Hg arc lamp was used for photolysis of samples in the EPR cavity. Lamps, housings, lenses and power supplies were obtained from Oriel Corporation, Stamford, CT. Filters were obtained from Schott Optical Glass Company, Duryea, PA.

Cyclopentadienylmagnesium bromide-THF complex ($\text{CpMgBr} \cdot \text{THF}_n$) was prepared according to the procedure of Stille and Grubbs. The effective molecular weight of this white solid complex was found to be *ca.* 400 g/mol by NMR integration against a mesitylene standard.

Bisfulvene 25. 1,3-Diacetylbenzene (2.52 g, 15.5 mmol), cyclopentadiene (7 ml, 85.4 mmol), and methanol (40 ml) were combined in a 100 ml round bottomed flask.

Pyrrolidine (4.2 ml, 50.3 mmol) was added dropwise and the mixture stirred at room temperature for 30 h. The reaction was quenched by dropwise addition of glacial acetic acid (3 ml). The solvent was removed by rotoevaporation and the residue partitioned between ether (200 ml) and water (100 ml). The aqueous phase was saturated with NaCl and extracted with ether (2 x 100 ml). The combined organics were washed with water (100 ml) and saturated aqueous NaCl (50 ml), and dried over MgSO₄ and filtered. The solvent was removed by rotoevaporation and the residue chromatographed on silica gel (20% ether/petroleum ether). The first-eluted orange band provided **25** as an orange solid (2.04 g, 51%). ¹H NMR (CDCl₃) δ 2.50 (s, 6H), 6.10-6.25 (m, 2H), 6.35-6.70 (m, 6H), 7.35 (s, 4H).

Preparation of 30 with CpLi/BF₃•Et₂O. Cyclopentadienyllithium (16.1 g, 200 mmol) was dissolved in 500 ml THF and the mixture cooled to -78 °C. Boron trifluoride etherate (25 ml, 203 mmol) was added via cannula and the mixture stirred at -78 °C for 30 min. A solution of **27** (7.0 g, 50 mmol) in THF (150 ml) was added via cannula. The mixture was stirred 15 min at -78 °C and then the cooling bath was removed. The mixture was allowed to warm to room temperature and stir for 40 h, and then poured into 600 ml of saturated aqueous NH₄Cl. The organic layer was separated and dried over MgSO₄, filtered, and the solvent removed by rotary evaporation. Chromatography on silica gel with 10% benzene/petroleum ether provided bisfulvene **30** (243 mg, 2%): ¹H NMR (GX-400, CDCl₃) 1.69 (s, 12 H), 6.39 (d, *J*=4 Hz, 4H), 6.50 (d, *J*=4 Hz, 4H) ¹³C NMR (GX-400, CDCl₃) 30.03, 120.21, 130.95, 137.42, 171.79. Increasing the polarity to 100% benzene gave **12** (4.8 g, 50%): ¹H NMR (GX-400, CDCl₃) 1.50 (s, 12 H), 6.38 (d, *J*=4 Hz, 2H), 6.52 (d, *J*=4 Hz, 2H).

Conversion of 46 to 30 with CpMgBr. **46** (1.36 g, 7.2 mmol) and CpMgBr (7.2 g, 18 mmol) were refluxed in dioxane for 3 h. The reaction mixture was filtered to remove magnesium salts, which were washed well with ether, and the organic layer was washed with saturated aqueous NH₄Cl and dried over MgSO₄. Filtration and removal of

solvent left 2.5 g of brown residue which was chromatographed on silica gel using 10% benzene/petroleum ether as eluent to yield **13** (80 mg, 3.6%).

Preparation of 40 and 43 with CpLi/BF₃•Et₂O. Cyclopentadiene (9 ml, 110 mmol) was dissolved in 150 ml tetrahydrofuran and the solution cooled in an ice bath. A solution of *n*-butyllithium in hexanes (32 ml, 2.5 M, 80 mmol) was added over a period of 10 min to yield a milky white slurry. BF₃•Et₂O (10 ml, 80 mmol) was added to the stirred, cooled slurry over 1 min via syringe. The mixture turned clear and orange upon complete addition. Solid **14** (2.5 g, 20 mmol) was then added, causing the color to become very dark orange. The mixture was stirred for 15 min and then poured into water (200 ml). This mixture was saturated with sodium chloride and extracted with portions of ether (100 ml) until no more color entered the organic phase. The combined organic extracts were dried over MgSO₄. The treatment with MgSO₄ turned the color of the solution from brown to orange. Filtration and removal of solvent gave a residue which was chromatographed on silica gel. Gradient elution (5-20% ether/petroleum ether) gave bisfulvene **16** (600 mg, 14%) as the first yellow band: ¹H NMR (GX-400, CDCl₃) δ 1.82 (s, 6H), 3.16 (s, 4H), 6.45 (m, 2H), 6.54 (m, 2H), 6.68 (m, 2H); ¹³C NMR (GX-400, CDCl₃) δ 32.00, 33.40, 49.99, 119.81, 122.68, 129.45, 131.91, 137.88, 167.74; MS (70 eV EI) : *m/z* 222 (M⁺), 207 (base peak), 192, 165. The second yellow band eluted was ketofulvene **15** (1.1 g, 32%); MS (70 eV EI) *m/z* 174 (M⁺, base peak), 131, 117.

Bisfulvene 43 from monofulvene 40. **15** (1.1 g, 6.3 mmol) was refluxed in 100 ml tetrahydrofuran with CpMgBr•THF_n (4.9 g, 12 mmol) for 4 h and then stirred overnight at room temperature. The reaction mixture was poured into water (200 ml). The mixture was saturated with NaCl and extracted with portions of ether (100 ml) until no more color entered the organic layer. The combined organic layers were dried over MgSO₄, filtered, rotovapped, and chromatographed on silica gel. Gradient elution (0-3% ether/petroleum ether) allowed separation of **40** (200 mg, 14%).

TMS Ether 39. 2-Hydroxy-9-adamantanone (13.8 g, 83 mmol) was suspended in hexane, and trimethylsilyl chloride (3.7 ml, 29.1 mmol), and hexamethyldisilazide (6.1 ml, 29.1 mmol) were added via syringe. The reaction was monitored by TLC (2% methanol/methylene chloride). After 12 h, the reaction mixture was filtered, and concentrated to give **39** as a white solid (17.5g, 89%), which was used without purification. MS (70 eV EI) m/z 237 (M^+), 223 (base peak).

Fulvene 42. Adamantanone-TMS ether **39** (4.77 g, 20 mmol) was added to a tetrahydrofuran solution of $CpMgBr \cdot THF_n$ (12 g, ca. 30 mmol) and brought to reflux. The reaction was monitored by TLC (2:1 petroleum ether/ether). After 18 h, the reaction mixture was cooled to room temperature, poured onto cracked ice, and diluted with ether. The resulting mixture was washed with saturated NH_4Cl (2 x 100 ml) and saturated aqueous $NaCl$ (2 x 100 ml). The organic phase was dried with $MgSO_4$ and concentrated. The bright yellow residue was chromatographed on silica gel (4:1 petroleum ether/ether). The first yellow band was collected and evaporated to give 4.1 g (71%) fulvene MS (70 eV EI) m/z 286 (M^+), 73 (base peak). The second band proved to be the deprotected alcohol (1.0 g, 21%); MS (70 eV EI) m/z 214 (M^+). The TMS ether (4.1 g, 14 mmol) was dissolved in 50 ml acetonitrile. Triethylamine tris(hydrofluoride) (4.7 ml, 28 mmol) was added via syringe. The reaction was complete within 30 min as judged by TLC (2:1 petroleum ether/ether). The reaction mixture was diluted with 100 ml ether and poured into a separatory funnel containing 200 ml saturated NH_4Cl . The layers were separated, and the organic layer was washed with water (2 x 150 ml), saturated $NaHCO_3$, and saturated $NaCl$. The solution was dried with $MgSO_4$ and concentrated to give 2.9 g (95%) of alcohol as a bright yellow solid which was used immediately in the next step. Freshly distilled oxalyl chloride (1.3 ml, 14.9 mmol) was added to anhydrous DMSO (2.1 ml, 29.7 mmol) dissolved in 50 ml dry methylene chloride at $-78^\circ C$. The mixture was stirred for 15 min, and a methylene chloride solution of the alcohol obtained in the last step (2.9 g, 13.5 mmol) was added over 10 min. After stirring for 1 h at $-78^\circ C$, freshly

distilled triethylamine (10 ml, 68 mmol) was added, and the reaction was warmed to room temperature. The reaction mixture was filtered to remove insoluble salts (Et_3NHCl) and was washed with saturated aqueous NH_4Cl (3 x 100 ml) and saturated aqueous NaCl (2 x 100 ml). The organic phase was dried with MgSO_4 and concentrated to give 2.7 g (93%) bright yellow crystals. The product was analyzed by GC/MS and used immediately in the next step. MS (70 eV EI) m/z 212 (M^+ , base peak).

Bisfulvene 45. Crude ketone **42** (2.7 g, 12.7 mmol) and a THF solution of $\text{CpMgBr}\cdot\text{THF}_n$ (7.7 g, 19.1 mmol) were heated to reflux. The reaction was followed by TLC (2:1 petroleum ether/ether). After 22 h, the reaction mixture was cooled to room temperature, poured onto cracked ice and diluted with ether. The resulting mixture was washed with sat aq NH_4Cl (2 x 100 ml) and sat aq NaCl (2 x 100 ml). The organic phase was dried with MgSO_4 and concentrated to yield 1.8 g (53%) of bright yellow crystals of bisfulvene **21**. ^1H NMR (QE-300, CDCl_3) δ 2.04-2.18 (m, 9 H), 3.38 (bs, 2 H), 4.59(bs, 1H), 6.48-6.55 (m, 6 H), 6.55 (m, 2 H); ^{13}C NMR (QE-300, CDCl_3) δ 28.3, 36.7, 39.3, 40.8, 43.0, 45.9, 119.2, 119.9, 131.3, 131.5, 136.7, 161.7; MS (70 eV EI) m/z 260 (M^+).

Fulvene 51. This compound was prepared using the procedure for bisfulvene **25**. ^1H NMR (QE-300, CDCl_3) δ 1.85-2.15 (m, 12 H), 3.29 (bs, 1 H), 6.58 (m, 4 H); ^{13}C NMR (QE-300, CDCl_3) δ 28.12, 36.86, 37.15, 40.06, 119.27, 130.29, 135.65, 167.03; MS (70 eV EI) m/z 198 (M^+).

Preparation of reduced Diels-Alder adducts, representative procedure. Bisfulvene **40** (140 mg, 0.63 mmol) was treated with dimethyl azodicarboxylate (DMAD, 184 mg, 1.26 mmol) in methylene chloride (20 ml) at room temperature and the mixture allowed to stand 15 min. The solvent was removed and the product purified by column chromatography with 3/1 ethyl acetate:petroleum ether. This product was dissolved in methylene chloride, the mixture was cooled in an ice bath, and stirring begun as solid potassium azodicarboxylate (1.22 g, 6.3 mmol) was added. A solution of acetic acid

(0.72 ml, 12.6 mmol) in methylene chloride (5 ml) was added dropwise over 0.5 h. Stirring was continued overnight as the ice bath warmed. The reaction was quenched by the addition of water (10 ml). Additional methylene chloride (25 ml) was added, and the mixture separated. The aqueous phase was extracted with methylene chloride (2x25 ml), and the combined organics dried over anhydrous K_2CO_3 . Filtration, removal of solvent, and chromatography (75% ethyl acetate/petroleum ether) allowed isolation of the white solid product isomeric tetrakis carbamates **48** (163 mg, 46%).

Data for compounds that were prepared in this fashion:

Note: Due to slow rotation of the amide linkages, ^{13}C NMR spectra of these compounds taken in $CDCl_3$ displayed poor resolution up to 50 °C, and thus only 1H NMR spectra are reported. These compounds were also characterized by exact mass analysis. The corresponding bisdiazenes were characterized by ^{13}C and 1H NMR (see below).

47: 1H NMR (EM-390, $CDCl_3$) d 1.5-2.0 (bs, 8 H), 2.10 (s, 6 H), 3.67 (s, 6 H), 3.75 (s, 6 H), 4.60 (bs, 2 H), 4.90 (bs, 2 H), 7.00 (d, $J=5$ Hz, 2 H), 7.10 (s, 1 H), 7.30 (t, $J=5$ Hz, 1 H); HRMS (M^+) calcd. for $C_{28}H_{34}N_4O_8$ 554.2377, obsd 554.2379.

48: 1H NMR (GX-400, $CDCl_3$) d 1.20 (s, 12 H), 1.80 (m, 4 H), 2.05 (m, 4 H), 2.95 (s, 6 H), 4.68 (s, 4H).

49: 1H NMR (EM-390, $CDCl_3$) d 1.21 (overlapping s & d, 6H), 1.70 (bs, 4H), 2.38 (bs, 4H), 3.65 (bs, 12H), 4.56 (bs, 2H), 4.94 (bs, 2H); HRMS (MH^+) calcd. for $C_{25}H_{35}N_4O_8$ 519.2455, obsd 519.2482.

50: 1H NMR (EM-390, $CDCl_3$) d 1.2 (m, 4 H), 1.4-2.2 (m, 13 H), 2.65 (bs, 2 H), 3.40 (bs, 1 H), 3.75 (bs, 12 H), 4.80 (bs, 4 H); HRMS (M^+) calcd. for $C_{28}H_{36}N_4O_8$ 556.2533, obsd 556.2532.

52. 1H NMR (EM-390, $CDCl_3$) d 1.0-2.0 (m, 16 H), 2.5 (bs, 2 H), 3.6 (bs, 6 H), 4.7 (bs, 2 H); MS (70 eV EI) m/z 346 (M^+), 198 (base peak).

Preparation of bisdiazenes. Representative procedure. **47** (275 mg, 495 mmol) was heated to reflux for 2 h with 85% KOH (1.0 g) in Ar-purged 2-propanol (10 ml). The mixture was allowed to cool to room temperature and solid NaHCO₃ (2.0 g) was added. After stirring overnight at room temperature, the 2-propanol was removed under high vacuum. Water (25 ml) was added, and the aqueous phase extracted with methylene chloride (3x25 ml). The brown solution of hydrazine was dried over Na₂SO₄, decanted, and cooled to 0 °C. Nickel peroxide (1.0 g) was added and the mixture stirred 1 h at 0 °C. Filtration through celite and removal of solvent provided **1(N₂)₂** (130 mg, 82%).

Data for bisdiazenes:

1(N₂)₂: ¹H NMR (QE-300, CDCl₃) δ 1.05-1.30 (m, 4 H), 1.65-1.81 (m, 4 H), 2.00 (2s, 6 H), 5.23 (m, 2 H), 5.48 (d, *J*=2.3 Hz, 2 H), 6.82 (m, 1 H), 7.00 (m, 2 H), 7.27 (t, *J*=7.7 Hz); ¹³C NMR (QE-300, CDCl₃) δ 19.81, 21.05, 21.10, 21.27, 21.29, 74.35, 74.43, 74.50, 124.51, 124.55, 126.20, 126.25, 126.37, 126.41, 128.03, 140.61, 141.81; UV λ_{max}=342 nm.

2(N₂)₂ (*syn* isomer only): ¹H NMR (QE-300, CDCl₃) δ 1.05 (m, 4 H), 1.23 (s, 12 H), 1.62 (m, 4 H), 5.25 (s, 4H); ¹³C NMR (QE-300, CDCl₃) δ 21.29, 21.33, 26.55, 27.47, 28.40, 46.52, 73.77, 73.82, 134.82, 142.59; UV λ_{max}=342 nm.

3(N₂)₂ (*syn* and *anti* isomers): ¹H NMR (QE-300, CDCl₃) δ 1.10 (m, 4 H), 1.21 (s) and 1.23 (d, *J*=5 Hz) (6 H total), 1.63 (m, 4 H), 2.31 (m, 4 H), 5.57 (s, 2 H), 5.24 and 5.25 (2 overlapping s, 2 H); ¹³C NMR (QE-300, CDCl₃) δ 20.86, 20.91, 21.36, 28.42, 28.99, 29.46, 29.54, 29.65, 45.32, 45.35, 72.44, 72.48, 75.95, 76.00, 135.38, 139.20; UV λ_{max}=342 nm.

4(N₂)₂: ¹H NMR (QE-300, CDCl₃) δ 1.0-1.18 (m, 4H), 1.38-1.5 (m, 4 H), 1.58-2.0 (m, 8 H), 2.56 (s, 2 H), 3.14 (s, 1 H), 5.28-5.41 (m, 4 H); ¹³C NMR (QE-300, CDCl₃) δ 21.22, 21.18, 21.28, 21.32, 21.40, 27.68, 27.71, 34.13, 34.24, 37.29, 37.64, 38.05,

39.84, 39.94, 39.99, 40.83, 41.04, 72.62, 72.77, 73.02, 73.10, 73.15, 131.75, 131.83, 132.27, 133.27, 134.14, 134.24; UV λ_{max} =342 nm.

53. ^1H NMR (QE-300, CDCl_3) δ 1.07 (m, 2 H), 1.55-1.89 (m, 14 H), 2.53 (bs, 2 H), 5.38 (s, 2 H); ^{13}C NMR (QE-300, CDCl_3) δ 21.47, 27.92, 28.09, 34.54, 36.75, 38.42, 39.31, 73.07, 130.85, 136.02; UV λ_{max} =342 nm.

Calculations on trimethylene in adamantane geometry. The structure of bisfulvene **21** was energy minimized with the MM2 force field as implemented in Macromodel. The geometry of the C8-C1-C2 fragment thus obtained was frozen, and all the carbon atoms were replaced by hydrogen atoms maintaining the bond and dihedral angles, but shortening the bond lengths to 1.10 Å. The coordinates of this trimethylene were then submitted to Gaussian 90 for single point calculations using the D95V basis set (Dunning's basis set). The GVB(1/2) singlet energy was -116.9555789 Hartrees and the ROHF triplet energy was -116.9534734 Hartrees, indicating a singlet ground state and a singlet-triplet gap of 1.3 kcal/mol.

Matched O.D. photolysis of $4(\text{N}_2)_2$ and **53.** MTHF solutions of $4(\text{N}_2)_2$ with $A(342 \text{ nm}) = 1.4$ and **31** with $A(342 \text{ nm}) = 1.3$ were prepared. The solutions were pipetted into quartz EPR tubes fitted with vacuum stopcocks and submitted to five freeze-pump-thaw cycles. Samples were irradiated sequentially at 50 K using the same source and filter combination. Plots of signal intensity vs. photolysis time are shown in Figure 7.

Variable temperature EPR study of **3.** An EPR sample of $3(\text{N}_2)_2$ in 1,2-propanediol was photolyzed for 6 h at 50 K. The temperature was raised briefly (~5 min) to 120 K in order to anneal the sample, and spectra taken at decreasing temperatures down to 10 K.

Other procedures for older routes.

31. NaH (3.81 g 60% dispersion in oil, 2.29 g, 95.2 mmol) was washed free of mineral oil with pentane and suspended in 30ml THF under Ar and cooled to 0 °C. Compound **28** (2.00 g, 15.9 mmol) and methyl iodide (13.5 g, 95.2 mmol) in 20 ml THF were added dropwise to the cooled suspension over 25 min. The cooling bath was removed and the brown mixture stirred overnight at room temperature. The reaction was quenched by dilution with pentane and careful addition of water. The layers were separated, and the organic layer was dried over MgSO₄, filtered, and rotovapped. Flash chromatography (20% ether/petroleum ether) yielded 0.5 g white crystals. ¹H NMR(EM-390, CDCl₃): δ 1.09 (s, 6H); 1.00 (s, 12 H). GC/MS M⁺ m/z=182.

Attempted reaction of 31 with P₄S₁₀. **46** (428 mg, 2.35 mmol) was dissolved in pyridine (15 ml) and P₄S₁₀ (523 mg, 1.18 mmol) was added. After no apparent reaction at room temperature, the temperature was raised to 90 °C. GC/MS and TLC analysis showed no evidence for the desired conversion. After 24 h at 90 °C, no reaction had occurred.

31a. 3-Hydroxy-2,2-dimethylcyclopentanone was prepared by the atmospheric pressure hydrogenation of **28** (6.32 g, 50 mmol) using PtO₂ as the catalyst and 2-propanol as the solvent. Filtration of the catalyst and removal of solvent gave a quantitative yield. GC/MS: M⁺ m/z=128. The ketoalcohol was dissolved in hexanes (50 ml) and hexamethyldisilazane (2.15 g, 2.81 ml, 13.3 mmol) was added. Chlorotrimethylsilane (1.45 g, 1.69 ml, 13.3 mmol) was added to this stirred mixture dropwise. An exothermic reaction occurred, and ammonium chloride precipitated. After stirring overnight, the mixture was filtered, washing through with additional hexane, and the solvent was removed by rotary

evaporation. Distillation provided 8.58 g (86%) of **31**, bp 56 °C (0.5 mmHg). ¹H NMR (EM-390, CDCl₃): d 3.87 (dt, 1 H), 2.5-1.6 (m, 4H), 0.91 (s, 6H), 0.89 (s, 6H), 0.06 (s, 9H).

40. CpMgBr (20.0 g, 50 mmol) was dissolved in THF (100 ml) and **31a** (5.00 g, 40 mmol) was added. The mixture was heated under reflux for 96 h, cooled to room temperature, stirred for 72 h, and quenched by addition of sat aq NH₄Cl (100 ml). The layers were separated and the aqueous phase extracted with ether (100 ml, 50 ml). The combined organics were dried over MgSO₄, filtered, and rotovapped. The residue was extracted with a mixture of 2% ether in petroleum ether, and the washings filtered through silica gel and evaporated to give 5.00 g (80%) of crude product. GC/MS: M⁺ m/z = 248. This material (1.1 g, 4.44 mmol) was dissolved in CH₃CN (50 ml) and triethylamine tris(hydrofluoride) (3 ml) was added. After stirring for 4 h at room temperature, TLC (20% ethyl acetate/petroleum ether) indicated complete conversion. The reaction mixture was diluted with sat aq NaHCO₃ (50 ml) and extracted with CH₂Cl₂ (100 ml, 50 ml). The combined organics were dried over MgSO₄, filtered, and the solvent removed by rotary evaporation. The residue was chromatographed on silica gel (15% ethyl acetate/petroleum ether) to yield 435 mg (56%) of the desired alcohol. GC/MS: M⁺ m/z=176. This material (228 mg, 1.30 mmol) was dissolved in CH₂Cl₂ (10 ml) and N-methylmorpholine-N-oxide (230 mg, 1.95 mmol) and activated 3A molecular sieve powder (2.5 g) was added. Tetrapropylammonium perruthenate (22 mg, 0.065 mmol) was added and the mixture stirred at 20 °C for 14 h. The reaction mixture was applied directly to the top of a silica gel column packed in 20% ether/petroleum ether solvent, and the yellow band was eluted using this solvent. Removal of solvent from the yellow fractions provided 64 mg (25% for the oxidation, 11.2% overall) **40**.

38b. 3-Hydroxy-2,2-dimethylcyclopentanone was prepared by the atmospheric pressure hydrogenation of **36** (10.0 g, 36 mmol) using PtO_2 as the catalyst and 2-propanol as the solvent. Filtration of the catalyst and removal of solvent gave a quantitative yield. This material was converted to its tetrahydropyranyl ether by stirring with dihydropyran (6.2 g, 6.7 ml, 74 mmol) and p-toluenesulfonic acid monohydrate (130 mg, 0.7 mmol) in CH_2Cl_2 (100 ml). The mixture was washed with sat aq NaHCO_3 and the solvent was removed by rotary evaporation. Chromatography of the residue on silica gel provided 14.7 g (93%) **38b** as a slightly yellow oil.

41. CpMgBr (25.0 g, 62.5 mmol) was dissolved in THF (50 ml) and **38b** (5.00 g, 22 mmol) was added. The mixture was heated under reflux for 4 days, cooled to room temperature, and poured into water. This mixture was stirred with solid sodium chloride and decanted into a separatory funnel. The layers were separated and the aqueous phase extracted with ether (100 ml, 50 ml). The combined organics were dried over MgSO_4 , filtered, and evaporated. The residue was chromatographed on silica gel using 10% ether/petroleum ether to provide 2.7 g (45%) of the product as a yellow oil. This material (2.7 g, 9.8 mmol) was dissolved in ethanol and treated with a solution of trifluoroacetic acid in THF. The mixture was heated to 55 °C for 2 h and then cooled to room temperature. Ether (100 ml) was added, and the mixture was poured into sat aq NaHCO_3 . The layers were separated and the organic phase was washed with sat aq NaCl (3x100 ml) and water (3x100 ml) and dried (MgSO_4). Chromatography on silica gel provided 1.31 g (73%) of the alcohol.

A solution of the alcohol (1.31 g, 6.88 mmol) in CH_2Cl_2 was added to the reagent prepared from DMSO (1.1 ml, 15.2 mmol) and oxallyl chloride (0.66 ml, 7.6

mmol) in CH_2Cl_2 (50 ml) at $-60\text{ }^\circ\text{C}$. Stirring was continued for 1 h at $-60\text{ }^\circ\text{C}$, and then triethylamine (4.8 ml, 34.4 mmol) was added, and the mixture was allowed to warm to room temperature. Sat aq NaCl (100 ml) was added and the layers were separated. The organic layer was washed with water (3x100 ml) and dried (MgSO_4) and filtered through a plug of silica gel. Removal of solvent provided 1.20 g (93%, 30% overall) **35**.

Chapter 3 - Synthesis and EPR Spectroscopy of a Bis(cyclobutanediyl)

Background. In 1975, Buchwalter and Closs reported generation of the triplet biradical 1,3-cyclopentanediy, **23a**, by extrusion of nitrogen from 2,3-diazabicyclohept-2-ene and observation of the biradical by matrix-isolation EPR spectroscopy.⁸⁵ In contrast to all other biradicals studied by EPR until that time, the radical centers in cyclopentanediy are not in classical π -conjugation with one another. The term "localized" biradical has been defined based on this criterion.⁵⁸ Buchwalter and Closs later reported the results of further investigations.⁵⁴ Cyclopentanediy decays to bicyclopentane in a process that is temperature independent between 1.3 and 20 K, strongly implicating a tunneling process. They established the activation barrier for this reaction as 2.3 kcal/mol. They also described investigations of EPR spectroscopy with variously substituted derivatives, in which they found simple substitution of the cyclopentane framework to lead to the observation of either weak EPR signals or no signal at all.

**22**

- a) $R_1 = R_2 = H$
- b) $R_1 = R_2 = \text{alkyl}$
- c) $R_1 = R_2 = Ph$
- d) $R_1 = R_2 = CH=CH_2$
- e) $R_1 = Et$; $R_2 = CH=CH_2$
- f) $R_1 = Ph$; $R_2 = Me$

**23**

- a) $R_1 = R_2 = H$
- b) $R_1 = R_2 = Ar$

In a later theoretical study, Goldberg and Dougherty calculated the spin preferences of **23a**, its next smaller homolog 1,3-cyclobutanediyl, **22a**, and its acyclic analog, trimethylene.⁵⁷ The results of these calculations indicated that 1,3-cyclobutanediyl prefers a triplet ground state by 1.7 kcal/mol and cyclopentanediy also has a triplet preference, but of only 0.9 kcal/mol. The results of their study of trimethylene indicated that it also has a triplet ground state at intermediate C-C-C angles and close C1-C3 distances. They attributed these high-spin preferences to the effects of

through-bond coupling. In conjunction with these theoretical studies, synthetic efforts toward direct observation of **22a** were undertaken.¹³⁴

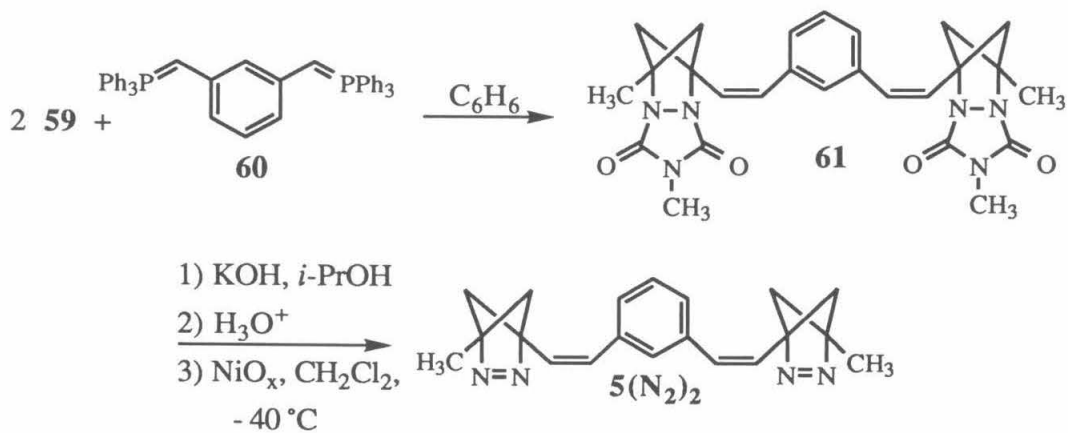
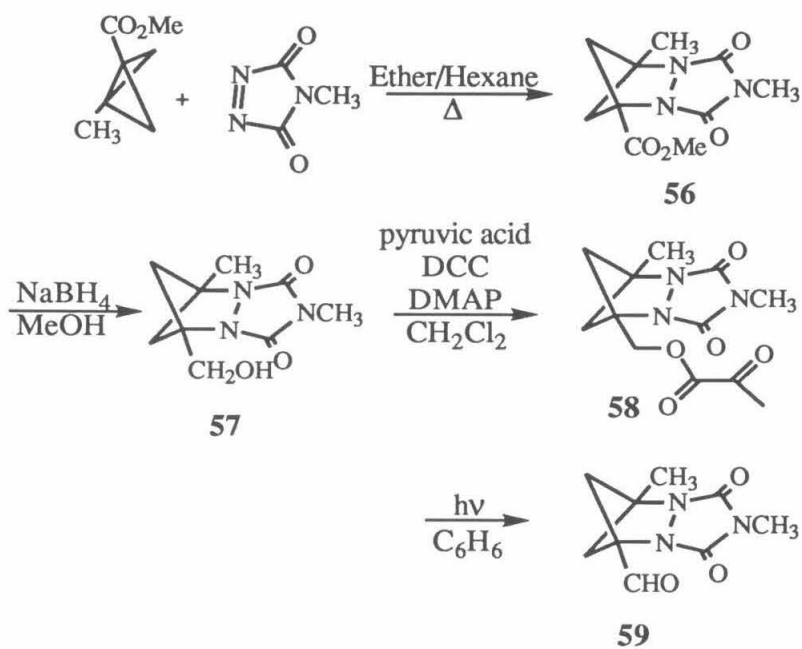
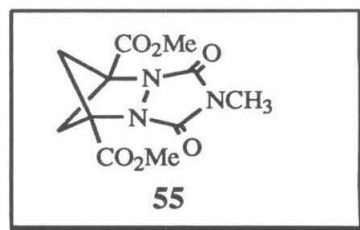
The parent compound **22a** cannot be observed by EPR spectroscopy, presumably due to a facile, bond-forming tunneling process to give bicyclobutane—such a process would be analogous to the established decomposition pathway of cyclopentadienyl. However, 1,3-dimethyl-1,3-cyclobutanediyl was observed in 1984.⁸³ The family of 1,3-disubstituted-1,3-cyclobutanediyls has been shown to form a general class of observable, localized biradicals. The study of these compounds has led to new structural information about biradicals, as well as a new model for matrix-decay kinetics.⁸⁴ This work has established a general synthetic route to these compounds based on the addition of N-methyltriazolinedione (MTAD) to the central bond of a bicyclobutane.^{55,58} The urazoles so produced have proven remarkably stable to a multitude of reaction conditions and have allowed a wide variety of derivatives to be prepared.

The pursuit of magnetic organic materials requires high-spin species.³⁻⁸ When electron spins are coupled throughout a material, bulk magnetism results. As a fundamentally new, bottom-up approach to magnetism, organic chemistry requires well defined and easily modified building blocks in order to fully establish magnetic structure-property relationships on a molecular level. The well characterized, easily synthesized class of 1,3-cyclobutanediyls offers a new set of such building blocks. In Chapter 2, we described the success of 1,3-cyclobutane as a ferromagnetic coupling unit (FC), capable of coupling the spins of two biradical spin containing units (SCs). In the paradigm of Figure 1-2, of course, there is an alternative role for cyclobutanediyl—that of SC. Here we explore the coupling of the electron spins of 1,3-cyclobutanediyls connected through *m*-phenylene^{7,23} in a vinylogous fashion. We do so via the synthesis and study of tetraradical **5**. The work described in the previous chapter, as well as the contributions from other researchers, has established *m*-phenylene as a robust ferromagnetic coupling

unit. We chose it to ensure that success or failure of our design could be attributed to the cyclobutanediyl fragment.

Synthesis.⁵⁸ 2,3-diazabicyclo[2.2.1]-hex-2-enes are the direct photochemical precursors to 1,3-cyclobutanediyls. These compounds are prepared from precursor urazoles, which ultimately derive from the addition of MTAD to a bicyclobutane. For this work, we required an unsymmetrically substituted urazole, which we discovered could be obtained from 3-methyl-1-carbomethoxybicyclobutane. Thermal addition of MTAD to this compound produces urazole **56** in 56% yield. This moderate yield stands in stark contrast to the case of 1,3-dimethylbicyclobutane, which gives approximately a 10% yield, and 1,3-dicarbomethoxybicyclobutane, which does not react with MTAD thermally, but does so photochemically to give compound **55**. Taken together, these current findings and past results seem to imply a dipolar addition mechanism for the thermal reaction.

The transformations used here are patterned after the successful reactions of diester urazole **55**, which serves as a useful intermediate in the preparation of several 1,3-cyclobutanediyls. Because the chemistry of **55** and its derivatives has already been established, elaboration of **56** into $5(\text{N}_2)_2$ is straightforward (Scheme 3-1). We require aldehyde **59** for the synthesis of **61** through a double-Wittig reaction. Earlier efforts toward the synthesis of the dialdehyde derivative of **55** have revealed it to be sensitive to hydration. The water-free pyruvate photolysis method of Binkley¹³⁵ has been employed to circumvent this problem. Reduction of the ester group in **56** proceeds with NaBH_4 in ethanol at room temperature to give the alcohol **57** in nearly quantitative yield. Esterification of this alcohol with pyruvic acid in the presence of DCC as a dehydrating agent results in formation of the pyruvate ester **58**, also in nearly quantitative yield. Photolysis of a dilute benzene solution of **58** with Pyrex-filtered light provides the aldehyde **59**. After reduction in volume, this solution is added directly to the bisylid **60**



Scheme 3-1

prepared from α,α' -bis(triphenylphosphonium)-*m*-xylene dibromide and *n*-BuLi in benzene.

The Wittig reaction gives predominantly *cis* stereochemistry in the product bisurazole **61** that may be rationalized by considering the model proposed by Vedejs.¹³⁶ The oxaphosphetane intermediate formed on the path to the *cis* isomer has the phosphorous ligands away from the aldehyde substituents, while for the *trans* isomer, they are forced together. In the case of aldehyde **59** and a triphenyl-substituted phosphorous ylid, this requires a very sterically unfavorable arrangement. We have assigned the stereochemistry based on the 12 Hz olefin ¹H NMR coupling constant, and on the 17 Hz coupling constant which we observe for a minor fraction of the product, which is formed as the *trans* isomer. The Wittig condensation proceeds in 50% yield based on starting pyruvate. We have therefore established a viable route to many unsymmetrically substituted urazoles that may prove useful in the future.

Hydrolysis and oxidation of the bisurazole proceed as they do normally for urazoles of this general structure.⁵⁸ Partial hydrolysis with KOH, followed by decarboxylation effected with 3 N HCl, leads to a mixture of bissemicarbazides that is oxidized at low temperature. The oxidation and all subsequent manipulations of **5(N₂)₂** must be carried out below -40 °C in order to avoid decomposition of the bisdiazene. We have found that purification of this bisdiazene may be effected by trituration with pentane at low temperature to yield a white solid.

Model. Tetraradical **5** is another example of a molecule for which the Heisenberg Hamiltonian may be employed to model spin state behavior.⁵⁰ This model is fully discussed in Chapters 1 and 2, and we simply present the results of the treatment here. Tetraradical **5** is expected to have a quintet ground state based on the paradigm of Figure 1-2b. The coupling of the two cyclobutanediyl subunits by the *m*-phenylene coupling unit occurs with a magnetic exchange parameter, *J*. Based on the results of the studies in

Chapter 2 and the results of others in the field,^{7,23} we expect J to be greater than zero and anticipate that ferromagnetic coupling will result in a quintet ground state in **5**.

In addition, due to the composition of **5**, we are able to predict the EPR spectra we should observe with a high degree of accuracy. In our previous work on cyclobutanediyls, it was demonstrated that the D -values in the series decrease with the spin density present at the cyclobutane carbons. We were able to establish a linear relationship between the observed and calculated D -values by employing a simple point-dipole approximation.⁵⁸ By employing this relationship along with experimentally determined spin densities,¹³⁷ we are able to predict the D -value for the monoazo triplet biradical as 0.060. Furthermore, using the model of Chapter 2, since \mathbf{D}^A and $\mathbf{D}^B \gg \mathbf{D}^{AB}$, the approximate expression for the D -value of the tetraradical is $D_Q = D^A/3$. Thus we expect that the D -value of the quintet state of the tetraradical should be 0.020 cm⁻¹. This is equivalent to stating that there is **no dipolar coupling** between the electrons of the two separate cyclobutanediyl fragments. If this seems strange, one should remember that dipolar coupling is merely a small perturbative correction to the overall energy. For example, the sign and magnitude of J determine the energy of a given electronic state much more strongly than the zfs does. Given the localized nature of two cyclobutanediyl electrons α to the methyl groups in **5**, and given also the localization of spin densities of styryl radicals away from the benzene ring, $D^{AB} = 0$ seems a very good approximation.

Since the outer $\Delta m_s = 1$ lines of a triplet EPR spectrum are separated by $2D$, while the outer lines of a quintet EPR spectrum are separated by $6D$, we expect the quintet and triplet spectra to be coincident. The only features that will allow us to unambiguously assign a quintet ground state will be peaks due to the inner quintet lines, associated with transitions between the middle m_s states. Fortunately, we also have the ability to fully simulate quintet and triplet powder EPR spectra (Chapter 4). This expertise is an indispensable aid in the study of **5**.

EPR Results. When a solution of **5**(N₂)₂ is photolyzed in the cavity of an EPR spectrometer at 4 K, high-spin species develop rapidly. EPR spectra are apparent after just 1 s of photolysis. This distinction is important, because the predominant feature of the spectra taken after short photolysis times is a $\Delta m_s = 2$ transition (Figure 3-1a). The carrier of this signal must be spin state with $S \geq 1$. The hyperfine splitting observed in this transition is typical of a cyclobutanediyl, and the particular pattern observed here strongly resembles that of the analogous compound 1-vinyl-3-ethylcyclobutanediyl **22e**.⁵⁸ In this feature of the EPR spectra, which relies on delocalization and spin density, the aryl ring of **5** is really only a minor perturbation with respect to structure **22e**, and we therefore expect it to exhibit a similar hyperfine pattern. Based on the analysis of the hyperfine splitting and the species present in the matrix, we are confident that a cyclobutanediyl-based species gives rise to this transition.

As photolysis is continued, new fine structure grows into the $\Delta m_s = 1$ region of the spectra. The new lines quickly become larger than the $\Delta m_s = 2$ transition (fig 3-1b-d). At long photolysis times, the spectra are dominated by the central fine-structure features (Figure 3-2). The outer four lines of the $\Delta m_s = 1$ region, if they should be for a triplet, correspond to $|D/hc| = 0.057 \text{ cm}^{-1}$ and $|E/hc| = 0.0009 \text{ cm}^{-1}$, in good agreement with the prediction above. A simulation of a triplet EPR spectrum with these zfs parameters is shown in Figure 3-3a. It can be seen that a triplet state clearly cannot account for all of the fine structure observed. The obvious candidate for the species giving rise to these additional lines is **55**. If **55** is responsible for the fine structure observed, then $|D/hc| = 0.019 \text{ cm}^{-1}$ and $|E/hc| = 0.00035 \text{ cm}^{-1}$, again in good agreement with our predictions. A simulation of a quintet EPR spectrum with these spin-Hamiltonian parameters is shown in Figure 3-3b.

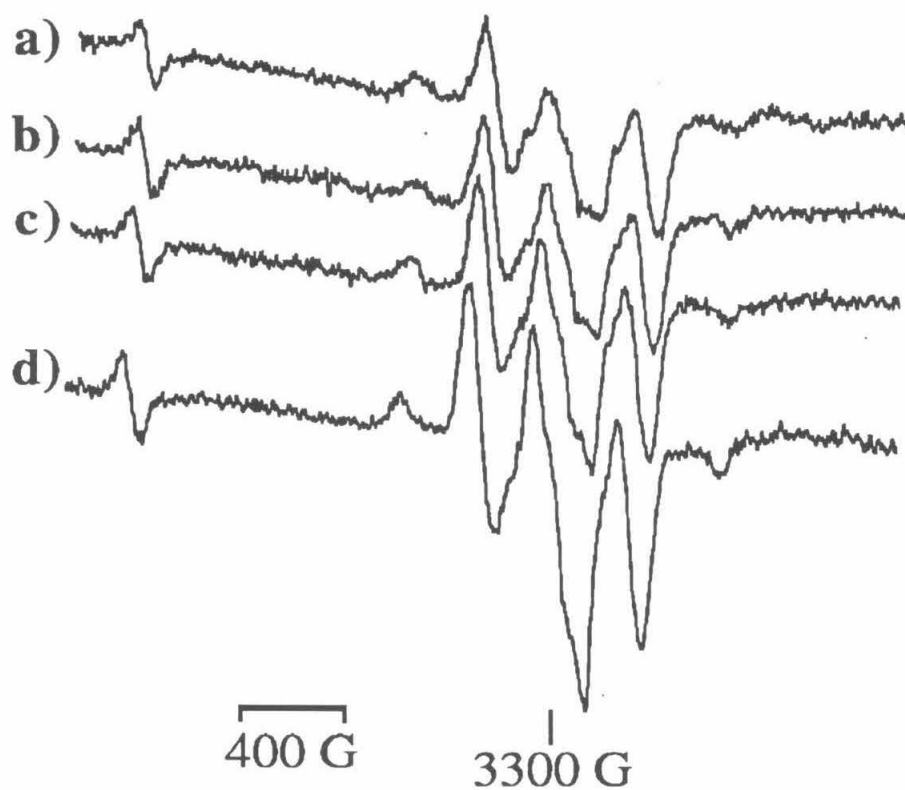


Figure 3-1. EPR spectra produced upon photolysis of $5(\text{N}_2)_2$ at 4 K. Photolysis times (a) 75 s (b) 90 s (c) 120 s (d) 180 s.

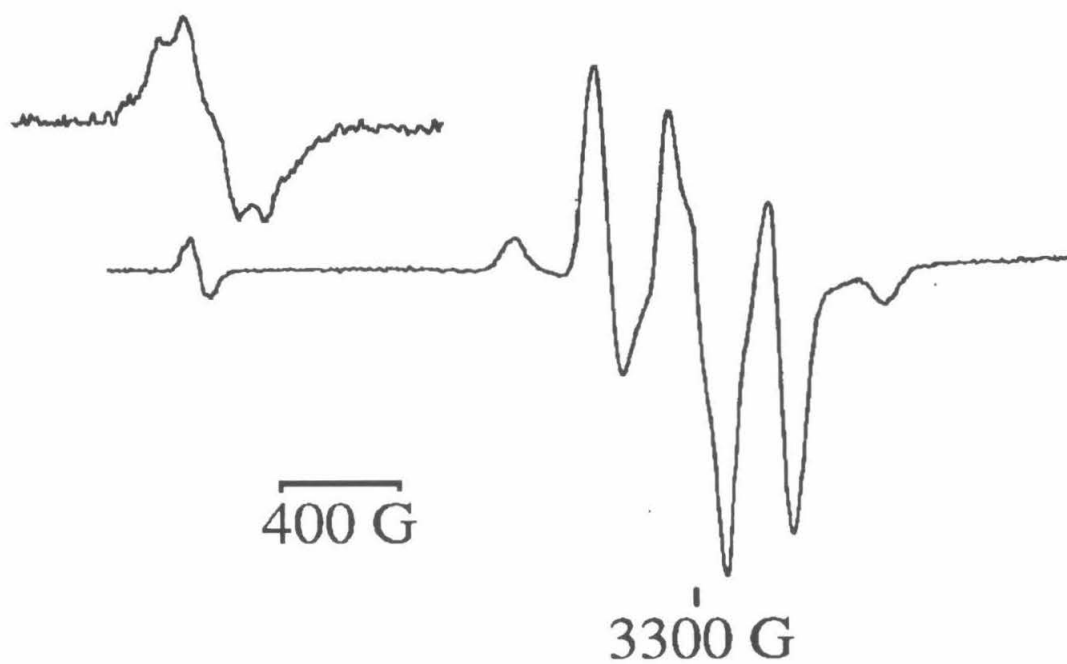


Figure 3-2. EPR spectra obtained after 80 min photolysis of $5(\text{N}_2)_2$ at 4 K.

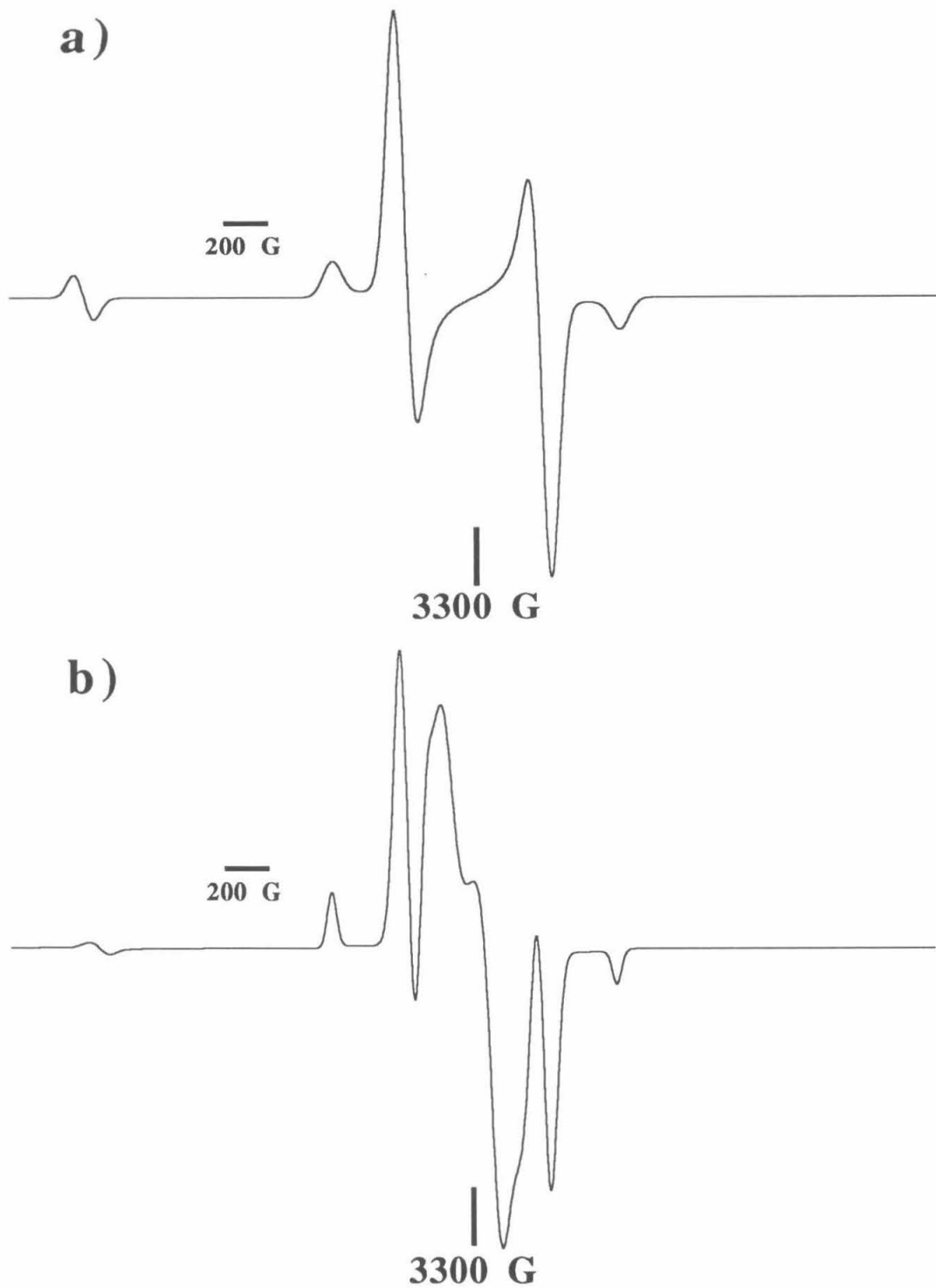


Figure 3-3. (a) Simulated triplet EPR spectrum with $|D/hc| = 0.057 \text{ cm}^{-1}$, $|E/hc| = 0.0009 \text{ cm}^{-1}$. (b) Simulated quintet EPR spectrum with $|D/hc| = 0.0193 \text{ cm}^{-1}$, $|E/hc| = 0.00035 \text{ cm}^{-1}$.

We find the agreement between the experimental and simulated spectra to be compelling, and thus assign the additional fine structure to $^5\mathbf{5}$. The temperature of 3.8 K at which these signals are observed makes it highly probable that the quintet is the ground state of $\mathbf{5}$.

It is rather difficult to discern whether any $^3\mathbf{5}(\text{N}_2)$ is present in this case because the spin-Hamiltonian parameters for the two states cause complete coincidence of the outer lines of the $\Delta m_s=1$ region, which are the *only* lines of the triplet EPR spectrum in this region. Indeed, the proper interpretation of the results of these EPR experiments was not clear to us for quite some time after completion of the experimental study. It was not until we gained experience with related high-spin structures and complete powder spectral simulation through the work described in Chapter 2 that we could confidently make the assignments we do here. The initial growth followed by leveling off of the $\Delta m_s=2$ transition suggests that triplet is indeed formed first, but the rapid (relative to the molecules studied in Chapter 2) appearance of a strong quintet EPR signal suggests that the quintet is easily formed as well. It would be exceedingly difficult to perform a meaningful spectral subtraction in this case, but we can state that the general appearance of the $\Delta m_s=1$ region closely matches the intensities of the lines in the spectrum of the simulated quintet.

This conclusion leads us to consider the possibility of a dominant single photon double deazotization similar to those observed with polydiazocompounds.¹³⁸ In earlier work, we have estimated that a localized biradical is formed with approximately 39 kcal/mol of excess energy, localized mostly on the hydrocarbon fragment.¹³⁹ The thermal deazotization of 2,3-diazabicyclo[2.2.1]hex-2-ene has been determined to require 33.7 kcal/mol of activation.¹³⁴ Bisdiazene $\mathbf{5}(\text{N}_2)_2$ is significantly less thermally stable than this compound, and we find it entirely reasonable that intramolecular energy transfer could lead to loss of a second molecule of N_2 from an excited monoazo triplet biradical. Further work is required to evaluate this possibility.

Summary and Outlook. We have synthesized tetraradical **5** under matrix-isolation conditions and established through EPR study that *m*-phenylene acts as a ferromagnetic coupling unit in this molecule. This result is entirely in accord with expectations based on the history of *m*-phenylene,^{75,76,7,23} but at the same time this work represents further extension of the scope of *m*-phenylene and provides illustration of the multiple possible roles for localized biradicals in spin-containing structures. Furthermore, we have demonstrated that with sufficient knowledge and experience, one can closely predict all of the EPR spectra obtained in this series of experiments. The agreement of the experimental spectra with our expectations, or vice versa, merely illustrates the detail in which it is now possible to understand the behavior of these systems; much of this newfound understanding is due to the work discussed here.

Although cyclobutanediyls are not nearly as robust as TMMs, further studies should be undertaken in order to more fully establish the nature of multiple deazotization. In the bis(TMM) strategy, the inability to achieve multiple deazotization is likely to be a limiting factor, given that we obtain 1:1 tetraradical:biradical mixtures after 6 h of photolysis of **2**(N₂)₂ and **3**(N₂)₂. In this regard, mixed systems of TMMs and cyclobutanediyls may provide intriguing alternatives. It is certainly true that the syntheses of multiple azo precursors to cyclobutanediyls are established, and furthermore that the various intermediate urazoles may be manipulated with virtual impunity. The difficulty in handling the azo compounds required for these studies will be rewarded by the answers to questions about the chemistry of high-spin molecules that their synthesis and study will provide.

Experimental

Ester Urazole 55. A solution of 2.00 g (14.8 mmol) 3-methyl-1-carbomethoxybicyclobutane in 500 ml hexanes was heated to reflux with magnetic stirring. A solution of 2.63 g (23.3 mmol) 4-methyltriazoline-3,5-dione (MTAD) in 125 ml diethyl ether was added dropwise over 2 h, and heating and stirring were continued until the starting material was consumed as monitored by TLC (50% ethyl acetate/petroleum ether). Some precipitate, which contained in part the desired product, had formed by this time. The solution was decanted and the precipitate extracted with methylene chloride. The combined solutions were rotoevaporated and the residue recrystallized from ethyl acetate to yield **27** (1.42 g). Flash chromatography on the mother liquor (50% ethyl acetate/petroleum ether) afforded a further 0.59 g product (total yield 57%). ^1H NMR (GX-400, CDCl_3): δ 3.88 (s, 3H), 3.05 (s, 3H), 2.16 (m, 4H), 1.80 (s, 3H). ^{13}C NMR (GX-400, CDCl_3): δ 165.49, 160.01, 70.38, 69.17, 52.85, 46.47, 25.70, 15.52. HRMS calcd. for $\text{C}_{10}\text{H}_{13}\text{N}_3\text{O}_4$ 239.0906, obsd. 239.0903.

Aldehyde 56. Ester urazole **55** (1.41 g, 0.91 mmol) was suspended with stirring in 40 ml of methanol and NaBH_4 (350 mg, 9.3 mmol) added in portions at a rate sufficient to maintain reflux. The reaction was monitored by TLC (10% methanol/methylene chloride) and was complete in less than 5 min. The mixture was hydrolyzed by addition of 3N HCl to $\text{pH} \leq 2$. The mixture was evaporated to dryness and partitioned between water (25 ml) and methylene chloride (25 ml). The aqueous phase was extracted with methylene chloride (2x25 ml) and the combined extracts were washed with water (25 ml) and dried over MgSO_4 . Filtration and rotoevaporation left the product alcohol (1.28 g, 97%). ^1H NMR (QE-300, CDCl_3): δ 4.01 (δ , $J=6.5$ Hz, 2H), 3.65 (t, $J=6.5$ Hz, 1H), 2.98 (s, 3H), 1.92 (m, 2H), 1.76 (m, 2H), 1.72 (s, 3H). ^{13}C NMR (QE-300, CDCl_3): δ 160.99, 159.45, 73.10, 70.44, 59.95, 45.14, 25.59, 15.48. HRMS calcd. for $\text{C}_9\text{H}_{13}\text{N}_3\text{O}_3$ 211.0957, obsd. 211.0969.

The alcohol (1.12 g, 5.3 mmol), 4-pyrrolidinopyridine (80 mg, 0.53 mmol), and pyruvic acid (0.70 g, 8.0 mmol) were dissolved in 40 ml methylene chloride. A solution of dicyclohexylcarbodiimide (1.64 g, 8.0 mmol) in 25 ml methylene chloride was added with stirring. Dicyclohexylurea precipitated immediately. The reaction was complete as monitored by TLC (50% ethyl acetate/petroleum ether). Stirring was continued for one hour, and the mixture was filtered through glass wool. The filtrate was evaporated and chromatographed on oven-dried silica gel (50% ethyl acetate/petroleum ether) to yield 1.38 g (93%) pyruvate ester. ^1H NMR (GX-400, CDCl_3): δ 4.85 (s, 2H), 3.02 (s, 3H), 2.47 (s, 3H), 2.07 (m, 2H), 1.84 (m, 2H), 1.78 (s, 3H). ^{13}C NMR (GX-400, CDCl_3): δ 190.8, 160.0, 159.9, 70.6, 69.9, 61.7, 45.3, 26.7, 25.6, 15.5. HRMS calcd. for $\text{C}_{12}\text{H}_{15}\text{N}_3\text{O}_5$ 281.1012, obsd. 281.1016.

A solution of 202 mg pyruvate in 250 ml benzene was photolyzed in a photochemical reactor with Pyrex filtered output from a Hanovia 450 W medium pressure source. Progress of the reaction was monitored by TLC (10% methanol/methylene chloride). After 2 h the reaction was complete, and the volume of the solution was reduced to 20 ml by rotoevaporation.

Bisurazole 57. Aldehyde **56** obtained above was added to a solution of (1,3-phenylene)-bis(methylenetriphenylphosphorane) prepared by addition of 0.24 ml of a solution of 2.67 M *n*-BuLi in hexanes to a suspension of 255 mg (1,3-phenylene)-bis(methyltriphenylphosphonium) dibromide in 20 ml benzene. The red color of the ylide was dispersed almost immediately. The product was evident by TLC (10% methanol/methylene chloride) as a spot which stains intensely blue with vanillin, $R_f=0.3$. The reaction was stirred for 0.5 h and then quenched by the addition of 20 ml of 5% HCl. The aqueous phase was separated and extracted with ether (2x20 ml). The combined organic phases were washed with 5% HCl, sat. aq. NaHCO_3 , and water and dried over MgSO_4 . Filtration, removal of solvent, and column chromatography (50% ethyl acetate/petroleum ether) allowed isolation of the desired bisurazole (81 mg, 50% yield) as

a mixture of isomers, predominantly Z,Z. ^1H NMR (GX-400, CDCl_3): δ 7.05-7.30 (m, 4H), 6.83 (d, $J = 12$ Hz, 2H), 6.05 (d, $J = 12$ Hz, 2H), 2.98 (s, 6H), 1.68 (m, 8H), 1.57 (s, 6H). HRMS calcd. for $\text{C}_{26}\text{H}_{28}\text{N}_6\text{O}_4$ 488.2172, obsd. 488.2150.

5(N₂)₂. **Note:** The thermal instability of **5(N₂)₂** necessitated that the oxidation and subsequent operations be carried out at temperatures below -40 °C. A solution of **57** (55 mg, .112 mmol) in Ar-purged 2-propanol (3 ml) was prepared and purged with Ar for 1 min and then heated to 52 °C for 40 min. The temperature was reduced to 40 °C and the solvent was removed with a stream of Ar. The resulting paste was cooled to 0 °C and treated with Ar-purged 3N HCl. 2 ml were required to effect complete decarboxylation to the semicarbazides. To ensure decarboxylation, the mixture was warmed to 40 °C for 10 min. The mixture was then cooled again in ice and neutralized with Ar-purged 1N NH_4OH . This required approximately 1 ml. The aqueous solution was extracted with 0.5 ml and then 4x1 ml CH_2Cl_2 . The extracts were passed via cannula into an oven-dried Schlenk tube through a column of MgSO_4 held in a transfer pipette. The yellow solution was cooled with an acteonitrile slush bath and nickel peroxide (600 mg) was added. This did not complete the oxidation, indicating a poor quality of nickel peroxide. Fresh nickel peroxide was added until TLC indicated complete reaction. The mixture was filtered through Celite at low temperature and the solvent removed. The residue was triturated with pentane to provide a white solid. The yield was of course not determined due to the experimental conditions. **5(N₂)₂**: ^1H NMR (GX-400, CDCl_3 , -40 °C) δ 7.16 (t, $J=7.2$ Hz, 1 H), 7.08 (d, $J=7.2$ Hz, 2 H), 7.02 (s, 1 H), 6.83 (d, $J=12$ Hz, 2 H), 6.14 (d, $J=12$ Hz, 2 H), 2.23 (d, $J=6.4$ Hz, 4 H), 1.66 (s, 6 H), 1.60 (d, $J=6.4$ Hz, 4 H); UV $\lambda_{\text{max}}=346$ nm.

**Chapter 4 - Complete Computer Simulation of Quintet- and Triplet-State
EPR Spectra**

EPR Spectroscopy as a Diagnostic Tool

Electron paramagnetic resonance (EPR) spectroscopy was first used to study matrix-isolated high-spin species over 30 years ago.^{139,140} It is now routinely used to observe high-spin species directly.^{6,7,12,15,51} EPR spectra convey a great deal of information regarding the electronic structure of their carriers in the form of their spin-Hamiltonian zero-field splitting parameters. In the case of organic biradicals, the spin-Hamiltonian parameters D and E can often be obtained, or at least closely approximated, by simple inspection of experimental spectra. For a triplet ground state biradical, data obtained in this manner are usually sufficient for reporting purposes.⁵¹ The presence of a triplet state is usually confirmed by a "half-field" transition; evidence for the triplet as ground state is either a linear Curie plot or simply the observation of the triplet spectrum at very low temperature, usually 4 K. Control over experimental conditions ensures that there is only one paramagnetic species in the matrix, and assignment of the observed EPR spectrum is routine.⁵¹

The study of tetraradicals produced by twofold extrusion of N_2 from a bisdiazene precursor often involves more complicated situations, in which multiple high-spin species, including quintets, may be present in the cryogenic matrix (see Chapters 2 and 3). Under these circumstances, unambiguous assignment of the observed spectra is impossible without additional theoretical and computational tools. A series of FORTRAN computer programs has been developed to simulate triplet-state and quintet-state EPR spectra for any combination of spin-Hamiltonian parameters. Simulation of the experimental spectra through the use of these programs ensures correct spectral assignments. The details of these programs are outlined below, and source listings can be found in the Appendix.

Methods for Computer Simulation of EPR Spectra

The computer simulation of EPR spectra has been practiced since the early 1960s.¹⁴¹⁻¹⁴⁴ Three basic methods have been described, differing in the way that the eigenvalues and eigenvectors of the Hamiltonian matrix are calculated. The original approach, which may only be applied to triplet simulation, involved exact solution of the resonance condition.¹⁴¹⁻¹⁴⁴ This method is possible because the characteristic polynomial of the triplet-state Hamiltonian matrix is third order, and a closed-form solution for the roots of such a polynomial is known.

A more straightforward but computationally more intensive approach is simple diagonalization of the Hamiltonian matrix. This method has received widespread attention in the literature.¹⁴⁵⁻¹⁵⁰ Its practicality depends largely on the computing power available. A Hamiltonian matrix for a system of spin S requires approximately $8(2S+1)^3$ floating point operations (flops) to diagonalize,¹⁵¹ and approximately $10 S$ diagonalizations are required at each of 8100 orientations. The number of flops then rises roughly as $5 \times 10^6 S^4$.

A final method, on which a number of papers has appeared, is a perturbational approach wherein analytic expressions are derived for the resonance fields and transition probabilities.^{130,152,153} This approach requires a substantial amount of painstaking algebra. Once the algebra is done, however, a simple means of calculating the desired EPR spectra is available. The appeal and success of this method have been illustrated in the computation of powder spectra of septet and nonet states.¹⁵³

We take the simple diagonalization approach and apply it both to triplets and to quintets in the present work. The parallel development of these two programs has obvious advantages. Our computing resources are sufficient to make the diagonalization approach entirely reasonable for quintets; a full simulation requires approximately 12-15 minutes of CPU time on our Silicon Graphics 4D/220GT computer.

The Resonance Condition and EPR Absorption^{130,141-150,153}

In EPR, a paramagnetic sample is placed in a magnetic field \mathbf{H} and the absorption Q of microwave energy applied perpendicular to \mathbf{H} is measured. There are several effects that cooperate to give rise to the absorption phenomenon that need to be considered in order to gain the understanding necessary to simulate spectra.

When a paramagnetic sample in thermal equilibrium is placed in a magnetic field \mathbf{H} , the spin sublevels of its constituent molecules become energetically distinct through magnetic interaction with the field. The magnetic dipole moment operator for an electron is $\hat{\mu} = -\frac{g\beta}{\hbar}\hat{\mathbf{S}}$, and the Hamiltonian operator $\hat{\mathcal{H}}$ for its interaction with \mathbf{H} is of the magnetic dipole moment of an electron with \mathbf{H} is given by $\hat{\mathcal{H}} = -\hat{\mu} \cdot \mathbf{H} = g\beta \mathbf{H} \cdot \hat{\mathbf{S}}$. For molecules with more than one electron, there is also an energy term that results from dipolar interaction among the electrons. The Hamiltonian operator $\hat{\mathcal{H}}$ for a paramagnetic molecule with $S \geq 1$ and an isotropic g -tensor in the applied field \mathbf{H} includes not only the dipolar term for interaction with \mathbf{H} , but also the spin-spin dipolar interaction term that may be characterized by the tensor \mathbf{D} (eq 1).

$$\hat{\mathcal{H}} = g\beta \mathbf{H} \cdot \hat{\mathbf{S}} + \hat{\mathbf{S}} \cdot \mathbf{D} \cdot \hat{\mathbf{S}} = g\beta \mathbf{H} \cdot \hat{\mathbf{S}} + D \left(\hat{S}_z^2 - \hat{S}^2/3 \right) + E \left(\hat{S}_x^2 - \hat{S}_y^2 \right) \quad (1)$$

The spin eigenstates of this molecule, denoted $|1\rangle, |2\rangle, \dots, |2S+1\rangle$, may be written as linear combinations of the pure \hat{S}_z eigenstates $|m_s\rangle$, where $-S \leq m_s \leq S$ (eq 2).

$$|i\rangle = \sum_{m_s} C_{i,m_s} |m_s\rangle \quad (2)$$

Of course, the energy of state $|i\rangle$ in the field \mathbf{H} and the coefficients C_{i,m_s} connecting $|i\rangle$ to the pure \hat{S}_z spin basis set vary with the strength of \mathbf{H} and its direction with respect to the molecule. The Hamiltonian and state energy levels are discussed in further detail below.

When a beam of electromagnetic radiation with energy $h\nu$ and oscillating magnetic field $e^{2\pi i\nu t}\mathbf{H}_1$ is applied perpendicular to the magnetic field \mathbf{H} , a molecule may absorb a photon and be promoted from a state $|i\rangle$ to a higher-energy state $|j\rangle$ if the resonance condition

$$|E_i(\mathbf{H}) - E_j(\mathbf{H})| = h\nu \quad (3)$$

is met. This absorption is termed a *magnetic dipole transition*, because the magnetic dipole moments associated with states $|i\rangle$ and $|j\rangle$ are different. In any sample, the transition is not observed as a sharp spike, but rather over a distribution of resonance frequencies that may be represented by a normalized function. The finite width of the distribution may be attributed to unresolved hyperfine effects, matrix-site effects, and other higher-order effects.

The likelihood of a magnetic dipole transition from state $|i\rangle$ to state $|j\rangle$ for a single molecule in the sample under the influence of external magnetic field $\mathbf{H} + e^{2\pi i\nu t}\mathbf{H}_1$ is the square of the matrix element M_{ij} connecting the two states.

$$M_{ij}^2(\mathbf{H}, \mathbf{H}_1) = |\langle i | \hat{\mathcal{H}}_1(\mathbf{H}_1) | j \rangle|^2 \quad (4)$$

The dependence of M_{ij} on \mathbf{H} is due to the dependence of the composition of the eigenstates $|i\rangle$ and $|j\rangle$ on \mathbf{H} already discussed. The overall equation for the probability P_{ij} of EPR absorption from state $|i\rangle$ to state $|j\rangle$ may be written as the product of the dipole transition probability and the distribution function.

$$P_{ij} = M_{ij}^2(\mathbf{H}, \mathbf{H}_1) f(h\nu - h\nu_0) \quad (5)$$

The distribution function $f(h\nu - h\nu_0)$ is normally assigned either Lorentzian or Gaussian shape.¹⁵ For high-spin organic molecules, the choice of Gaussian lineshape is predominant.^{130,141-144,153} Gaussian lineshape functions are traditionally expressed in terms of their half-width at half-height Γ ; the form of a Gaussian distribution centered at $h\nu_0$ is

$$f(h\nu - h\nu_0) = \sqrt{\frac{\ln 2}{\pi}} \Gamma^{-1} \exp(-(\ln 2)(h\nu - h\nu_0)^2 / \Gamma^2). \quad (6a)$$

Γ is related to σ , the peak-to-peak width of the derivative of the Gaussian line.¹⁵

$$\Gamma = \sqrt{2 \ln 2} \sigma \approx 1.177 \sigma$$

The expression for the Gaussian lineshape in terms of σ is

$$f(h\nu - h\nu_0) = \sqrt{\frac{1}{2\pi}} \sigma^{-1} \exp(-(h\nu - h\nu_0)^2 / 2\sigma^2). \quad (6b)$$

Because EPR spectra are actually recorded in derivative mode, σ has more direct relevance to the recorded spectra than Γ , and we employ σ in our work.

Equation 6b is written for a frequency-swept experiment, but in a normal EPR experiment the field is swept while the frequency is held constant. For simulation purposes it is necessary to write the Gaussian lineshape in field variables; however, there is a difference in the linewidths for frequency-swept and field-swept experiments. The relationship between them has been shown to be

$$\sigma_H = \left| \frac{\partial H_0}{\partial h\nu} \right| \sigma_\nu, \quad (7)$$

where H_0 is the center of the field-swept peak and $\frac{\partial H_0}{\partial h\nu}$ is the value of $\frac{\partial H}{\partial h\nu}$ at H_0 .^{145,146} When eq 7 is taken into account, the form of the derivative of the lineshape required to simulate spectra, expressed in terms of field variables, is

$$\frac{\partial f(H - H_0)}{\partial H} = -\frac{(H - H_0)}{\sigma_H^3 \sqrt{2\pi}} \left| \frac{\partial H_0}{\partial h\nu} \right| \exp(-(H - H_0)^2 / 2\sigma_H^2). \quad (8)$$

In the normal spectrometer arrangement, \mathbf{H}_1 is perpendicular to \mathbf{H} , which means that the orientation of the two fields with respect to the molecular magnetic axes (X,Y,Z) may be described by one set of Euler angles (θ, ϕ, χ). The angle between \mathbf{H} and the Z magnetic axis of the molecule is θ , the angle the projection of \mathbf{H} on the XY plane makes

with the X axis is ϕ , and the angle that the \mathbf{H}_1 - \mathbf{H} plane makes with the YZ plane is χ . The direction of \mathbf{H} may be described by the first two Euler angles, while the third is required to define the direction of \mathbf{H}_1 .

$$\mathbf{H} = H \begin{pmatrix} \sin \theta \cos \phi \\ \sin \theta \sin \phi \\ \cos \theta \end{pmatrix} ; \quad \mathbf{H}_1 = H_1 \begin{pmatrix} \cos \theta \cos \phi \cos \chi - \sin \phi \sin \chi \\ \cos \theta \sin \phi \cos \chi + \cos \phi \sin \chi \\ \sin \theta \cos \chi \end{pmatrix}$$

In terms of these Euler angles, the formula for the derivative of the absorption spectrum is

$$\frac{\partial Q}{\partial H} = \sum_{i < j} - \int_0^\pi d\chi \int_0^\pi d\phi \int_0^\pi \sin \theta d\theta M_{ij}^2(\mathbf{H}, \mathbf{H}_1) \frac{\partial f(H - H_0)}{\partial H}. \quad (9)$$

Simulation of spectra requires performing the integrations and summation of eq 9.

Because only \mathbf{H}_1 is dependent on χ , it is possible to separate and perform the integral with respect to χ in eq 9, which leaves the *average* transition probability $\langle M_{ij} \rangle$ in what becomes a double integral expression. Elimination of one integration before submitting the simulation to the computer greatly reduces the computer time needed. The integral expression for the average transition probability is given by

$$\langle M_{ij} \rangle = \int_0^\pi d\chi M_{ij}^2(\mathbf{H}, \mathbf{H}_1) = \int_0^\pi d\chi \left| \langle i | \hat{\mathcal{H}}_1(\mathbf{H}_1) | j \rangle \right|^2. \quad (10)$$

The necessary Hamiltonian, assuming an isotropic g -tensor, is given by

$$\hat{\mathcal{H}}_1(\mathbf{H}_1) = -g\beta\mathbf{H}_1 \cdot \hat{\mathbf{S}} = -g\beta H_1 \begin{bmatrix} (\cos \theta \cos \phi \cos \chi - \sin \phi \sin \chi) \hat{S}_x + \\ (\cos \theta \sin \phi \cos \chi + \cos \phi \sin \chi) \hat{S}_y - \\ \sin \theta \cos \chi \hat{S}_z \end{bmatrix}. \quad (11)$$

Evaluating the integral of eq 10 using the trigonometric identity

$$\int_0^\pi \cos^2 \chi \, d\chi = \int_0^\pi \sin^2 \chi \, d\chi = \frac{\pi}{2}$$

yields for the average transition probability

$$\langle M_{ij} \rangle = \frac{\pi}{2} g^2 \beta^2 H_1^2 \left[\frac{\left| \langle i | \cos \theta \cos \phi \hat{S}_x + \cos \theta \sin \phi \hat{S}_y - \sin \theta \hat{S}_z | j \rangle \right|^2 + \left| \langle i | \sin \phi \hat{S}_x - \cos \phi \hat{S}_y | j \rangle \right|^2}{\left| \langle i | \sin \phi \hat{S}_x - \cos \phi \hat{S}_y | j \rangle \right|^2} \right]. \quad (12)$$

In addition to the use of the average transition probability, other computational devices employed include approximation of the integrals in eq 9 by discrete summations with a small step size (usually 1°) and integration only over the range of 0 to 90° for each θ and ϕ due to the symmetry properties of the EPR Hamiltonian.¹⁴⁶ With these approximations, the computationally tractable expression actually *used* to simulate spectra becomes

$$\frac{\partial Q}{\partial H} = - \sum_{i < j} \sum_{\phi=0^\circ}^{90^\circ} \sum_{\theta=0^\circ}^{90^\circ} \sin \theta \, \Delta \theta \, \Delta \phi \, \langle M_{ij} \rangle \frac{(H - H_0)}{\sigma_H^3 \sqrt{2\pi}} \left| \frac{\partial H_0}{\partial h\nu} \right| \exp\left(- (H - H_0)^2 / 2\sigma_H^2\right). \quad (13)$$

A stepwise approach to the evaluation of eq 13 is necessary. Each set of values (θ, ϕ) represents a different orientation of the molecule with respect to the external field \mathbf{H} . At each orientation, the resonance condition of eq 3 must be solved exactly for all $i < j$ (the Gaussian broadening is applied later). Eq 3, rewritten as

$$h(\mathbf{H}) = |E_i(\mathbf{H}) - E_j(\mathbf{H})| - h\nu = 0, \quad (14)$$

defines a root-finding problem of a function of the field \mathbf{H} , which can be solved by iterative regression. The function $h(\mathbf{H})$ can be evaluated by diagonalization of the matrix EPR Hamiltonian (see below). Once a root H_0 of $h(\mathbf{H})$, i.e., a resonance field, is found,

the average transition probability may be calculated according to eq 12. The factor $\left| \frac{\partial H_0}{\partial h\nu} \right|$ may be evaluated according to the Feynman-Hellman theorem,¹⁴⁹ which states that the partial derivative of the energy with respect to any quantity may be computed by applying the partial derivative of the Hamiltonian operator to the wavefunction, and thus

$$\frac{\partial H}{\partial h\nu} = \left(\frac{\partial E}{\partial H} \right)^{-1} = \left(\langle i | \frac{\partial \hat{H}}{\partial H} | i \rangle - \langle j | \frac{\partial \hat{H}}{\partial H} | j \rangle \right)^{-1} = (g\beta m_i - g\beta m_j)^{-1} = (g\beta \Delta m_s)^{-1}. \quad (15)$$

The EPR Hamiltonian

The EPR Hamiltonian (eq 1) employed in this work includes only Zeeman and dipolar terms.

$$\hat{\mathcal{H}} = g\beta \mathbf{H} \cdot \hat{\mathbf{S}} + \hat{\mathbf{S}} \cdot \mathbf{D} \cdot \hat{\mathbf{S}} = g\beta \mathbf{H} \cdot \hat{\mathbf{S}} + D \left(\hat{S}_z^2 - \hat{S}^2/3 \right) + E \left(\hat{S}_x^2 - \hat{S}_y^2 \right) \quad (1)$$

Several approximations shown in the past to be valid for high-spin organic molecules are used here.^{141-144,152,153} First, the g -tensor is assumed to be isotropic and its magnitude equal to the free-electron g -value. Second, although terms involving \mathbf{S}^4 and \mathbf{S}^6 are group-theoretically allowed, they are ignored. For the small spin-Hamiltonian parameters encountered in this work, these higher-order terms are not expected to make significant contributions to the spectra.

Expansion of the first term of eq 1 leads to

$$\hat{\mathcal{H}} = g\beta H \left(\sin \theta \cos \phi \hat{S}_x + \sin \theta \sin \phi \hat{S}_y + \cos \theta \hat{S}_z \right) + D \left(\hat{S}_z^2 - \hat{S}^2/3 \right) + E \left(\hat{S}_x^2 - \hat{S}_y^2 \right) \quad (16)$$

where θ and ϕ are the Euler angles defined above between the magnetic field axes and the principal magnetic axes of the molecule. For a triplet, the necessary matrices for the spin operators are

$$\hat{S}_x = \begin{pmatrix} 0 & 1/\sqrt{2} & 0 \\ 1/\sqrt{2} & 0 & 1/\sqrt{2} \\ 0 & 1/\sqrt{2} & 0 \end{pmatrix}; \quad \hat{S}_y = \begin{pmatrix} 0 & -i/\sqrt{2} & 0 \\ i/\sqrt{2} & 0 & -i/\sqrt{2} \\ 0 & i/\sqrt{2} & 0 \end{pmatrix}; \quad \hat{S}_z = \begin{pmatrix} 1 & 0 & 0 \\ 0 & 0 & 0 \\ 0 & 0 & -1 \end{pmatrix}$$

The Hamiltonian matrix may then be written

$$\hat{\mathcal{H}} = \begin{pmatrix} g\beta H \cos \theta - D/3 & (g\beta H/\sqrt{2})\sin \theta e^{-i\phi} & E \\ (g\beta H/\sqrt{2})\sin \theta e^{i\phi} & -2D/3 & (g\beta H/\sqrt{2})\sin \theta e^{-i\phi} \\ E & (g\beta H/\sqrt{2})\sin \theta e^{i\phi} & -g\beta H \cos \theta - D/3 \end{pmatrix}$$

For a quintet state, the spin matrices are

$$\hat{S}_x = \begin{pmatrix} 0 & 1 & 0 & 0 & 0 \\ 1 & 0 & \sqrt{3/2} & 0 & 0 \\ 0 & \sqrt{3/2} & 0 & \sqrt{3/2} & 0 \\ 0 & 0 & \sqrt{3/2} & 0 & 1 \\ 0 & 0 & 0 & 1 & 0 \end{pmatrix}; \quad \hat{S}_y = \begin{pmatrix} 0 & -i & 0 & 0 & 0 \\ i & 0 & -i\sqrt{3/2} & 0 & 0 \\ 0 & \sqrt{-3/2} & 0 & -i\sqrt{3/2} & 0 \\ 0 & 0 & \sqrt{-3/2} & 0 & -i \\ 0 & 0 & 0 & i & 0 \end{pmatrix};$$

$$\hat{S}_z = \begin{pmatrix} 2 & 0 & 0 & 0 & 0 \\ 0 & 1 & 0 & 0 & 0 \\ 0 & 0 & 0 & 0 & 0 \\ 0 & 0 & 0 & -1 & 0 \\ 0 & 0 & 0 & 0 & -2 \end{pmatrix}$$

and the Hamiltonian matrix is

$$\hat{\mathcal{H}} = \begin{pmatrix} 2D + 2g\beta H \cos \theta & g\beta H \sin \theta e^{-i\phi} & \sqrt{6}E & 0 & 0 \\ g\beta H \sin \theta e^{i\phi} & -D + g\beta H \cos \theta & \sqrt{3/2}g\beta H \sin \theta e^{-i\phi} & 3E & 0 \\ \sqrt{6}E & \sqrt{3/2}g\beta H \sin \theta e^{i\phi} & -2D & \sqrt{3/2}g\beta H \sin \theta e^{-i\phi} & \sqrt{6}E \\ 0 & 3E & \sqrt{3/2}g\beta H \sin \theta e^{i\phi} & -D - g\beta H \cos \theta & g\beta H \sin \theta e^{-i\phi} \\ 0 & 0 & \sqrt{6}E & g\beta H \sin \theta e^{i\phi} & 2D - 2g\beta H \cos \theta \end{pmatrix}$$

Diagonalization of these matrices for any set of values (θ, ϕ, H) yields the energies of the magnetic sublevels of a molecule at that orientation and in that magnetic field, from which the eigenvectors in the basis of the \hat{S}_z eigenfunctions may be determined.

Description of Programs

JQ and JT

These two programs share the same structure; they differ only in the version of the spin Hamiltonian matrix used. These programs use an input file JQ.INP or JT.INP with the following format:

```
TITLE (60 Character String)
D(cm-1) E(cm-1)
gxx gyy gzz LOWFIELD(kG) HIGHFIELD(kG)
θmin θmax Δθ ϕmin ϕmax Δϕ
v(GHz) SCREEN
```

TITLE is simply an allowance for a comment line. LOWFIELD and HIGHFIELD indicate the range in which the simulator should search for solutions to the resonance condition. SCREEN is a Boolean that, if true, will print the stick spectrum on the screen (the screen output can be redirected to a file using by using a '>' in the UNIX command line). The program actually allows for an anisotropic g -tensor, but in all of our simulations we set $g_{xx} = g_{yy} = g_{zz} = 2.0023$.

In order to cover the summation limits of eq 13, the angles θ and ϕ are swept from 0° to 90° in small, user-defined increments (usually 1°). At each orientation, transition fields between each pair of energy levels must be found. Only the $\Delta m_s=1$ and $\Delta m_s=2$ transitions are calculated. When solving for the field at which a transition between two energy levels occurs, the field is varied according to the secant method of iterative regression¹⁵⁴ and the energy levels of the Hamiltonian are computed until eq 14 is satisfied. Of course, each regression step requires a diagonalization of the Hamiltonian matrix. The routine used for diagonalization is a FORTRAN adaptation of HHERM, a routine developed by Wilkinson to solve eigenvalue problems for Hermitian matrices.¹⁵⁵ This routine employs QR factorization¹⁵⁵ and calls the subroutine QRSTD to perform the factorization.

Secant method iterative regression is a simple bracketing method of finding the root of an equation.¹⁵⁴ In this method, the function is assumed to be linear between the two iterative points, and the next point is taken where that line crosses the ordinate. We expect $h(\mathbf{H})$ to be smooth and monotonic function of \mathbf{H} for any fixed (θ, ϕ) because the Zeeman term is the leading term in the Hamiltonian. Thus this method is expected to converge in all instances. Its order of convergence is the "golden ratio" of 1.618... . In practice, seldom are more than five iterations required, showing that $h(\mathbf{H})$ is truly a well-behaved function.

It is crucial to computing time that the secant method does not require derivative computation. Diagonalization of the Hamiltonian matrix is by far the slowest step in the whole procedure, requiring $8(2S+1)^3$ flops.¹⁵¹ N steps of secant method regression require only N diagonalizations of the Hamiltonian matrix, whereas the widely-used Newton-Raphson derivative technique¹⁵⁴ would require $2N$ diagonalizations and severely hamper performance of the simulator. Even though the order of convergence of the Newton-Raphson technique is 2, a direct comparison showed that the secant method is roughly twice as fast. A full discussion of root-finding methods is available.¹⁵⁴

Once the resonance field is found, the subroutine CORA,¹⁵⁵ which calculates the eigenvectors of a symmetric tridiagonal matrix, is used to compute the C_{i,m_s} and C_{j,m_s} corresponding to the two energy levels involved in the transition. The eigenvectors $|i\rangle$ and $|j\rangle$ are used in turn to calculate the transition probability $\langle M_{ij} \rangle$ according to eq 12. When evaluating this quantity, it is faster in practice to work with the pair of spin operators \hat{S}_+ and \hat{S}_- instead of \hat{S}_x and \hat{S}_y because the former are composed of only $2S$ elements each while the latter have $4S$ elements each. The relationships among these operators are given by

$$\begin{aligned} S_+ &= S_x + iS_y; \quad S_- = S_x - iS_y \\ S_x &= \frac{1}{2}(S_+ + S_-); \quad S_y = \frac{1}{2i}(S_+ - S_-) \end{aligned}$$

The calculation to this point provides "stick" spectra, so named because the transitions and corresponding intensities found by the procedure described above resemble an assembly of individual spikes of different lengths at different values of the magnetic field. The values of $i, j, H, \langle M_{ij} \rangle, \left| \frac{\partial H_0}{\partial h\nu} \right|, \theta$, and ϕ for these stick spectra are stored in the output file JQ.OUT or JT.OUT.

JQS and JTS

These programs perform the complete lineshape simulation. Experimental spectra are reproduced poorly by an isotropic linewidth, and thus a transition-dependent diagonal

linewidth tensor $\sigma_{ij} = \begin{pmatrix} \sigma_{ij}^{xx} & 0 & 0 \\ 0 & \sigma_{ij}^{yy} & 0 \\ 0 & 0 & \sigma_{ij}^{zz} \end{pmatrix}$ is used. For any given set of zfs parameters,

several different trial-and-error attempts usually have to be made with different linewidths to closely reproduce the experimental spectra, and having all of the stick spectral information stored in JQ.OUT or JT.OUT is convenient. The linewidth for any transition is calculated according to

$$\sigma_{ij}(\theta, \phi) = \frac{|\sigma_{ij} \cdot \mathbf{H}|}{H} = \sqrt{(\sigma_{ij}^{xx} \sin \theta \cos \phi)^2 + (\sigma_{ij}^{yy} \sin \theta \sin \phi)^2 + (\sigma_{ij}^{zz} \cos \theta)^2}.$$

The linewidth parameters and desired spectral resolution are provided by the user in the file JTS.INP or JQS.INP. These files have the format

$$\begin{array}{ccc}
 \sigma_{zz}^{12} & \sigma_{xx}^{12} & \sigma_{yy}^{12} \\
 \sigma_{zz}^{13} & \sigma_{xx}^{13} & \sigma_{yy}^{13} \\
 & \vdots & \\
 \sigma_{zz}^{1S} & \sigma_{xx}^{1S} & \sigma_{yy}^{1S} \\
 \sigma_{zz}^{23} & \sigma_{xx}^{23} & \sigma_{yy}^{23} \\
 & \vdots & \\
 \sigma_{zz}^{2S} & \sigma_{xx}^{2S} & \sigma_{yy}^{2S} \\
 & \vdots & \\
 & \vdots & \\
 \sigma_{zz}^{(S-1)S} & \sigma_{xx}^{(S-1)S} & \sigma_{yy}^{(S-1)S}
 \end{array}$$

LOWFIELD HIGHFIELD NPOINT

The individual entries are the components of the linewidth tensor for each transition, given in Gauss. The spectrum is computed between the limits of LOWFIELD and HIGHFIELD with resolution (HIGHFIELD - LOWFIELD)/NPOINT.

The contribution to eq 13 is calculated for every line in the stick spectrum over a distance 5σ in either direction from the resonance field, and the individual contributions are summed together to provide the simulated spectrum in the file JQS.OUT or JTS.OUT.

Miscellaneous Programs

The programs QTP and TTP can be run on the input files JQ.INP or JT.INP, respectively, to identify the transition number and molecular axis associated with the spectral turning points. This information is quite useful for assigning linewidth parameters in the complete simulation. The program ORDFIELDS provides the turning points for quintet spectra for input in JQ.INP in ascending order, and this information can be useful in some cases when trying to assign the zfs parameters. The programs PLOT and HARDCOPY allow one to view the simulated spectra and linewidth parameters in

the files JQS.OUT/JTS.OUT and JQS.INP/JTS.INP on the Silicon Graphics terminal and to print them out on the attached Laserwriter. The appropriate command lines are

```
plot jqs.out jqs.inp <cr>
```

```
plot jts.out jts.inp <cr>
```

```
hardcopy jqs.out jqs.inp <cr>
```

```
hardcopy jts.out jts.inp <cr>
```

PLOT and HARDCOPY are written in C for easy access to the Silicon Graphics Shared Graphics Libraries.

**Chapter 5 - Methods for Magnetic Measurements on Polymer Systems and the
Study of PDPMC•, a Potentially Magnetic Organic Polymer**

The preparation of magnetic organic materials remains a significant intellectual and experimental challenge.³⁻⁸ Bulk magnetism requires unpaired (non-bonding) electrons. Each of the unpaired electrons has an associated magnetic moment. Aligning these moments in three dimensions produces bulk magnetism. Reaching this objective in organic systems requires solutions to two difficult challenges. The first is maintaining the presence of non-bonding electrons. Unpaired electrons must be present as radical centers in organic structures, yet most radicals are kinetically unstable species.^{1,2} Once suitable radicals are in hand, the electron spins must be aligned through control of the molecular framework. Both intermolecular and intramolecular spin coupling are crucial to bulk magnetic behavior. Present understanding of intermolecular coupling is based on McConnell's overlapping spin-density model.¹⁵⁶⁻¹⁵⁸ Spin-density alignment leading to cooperative magnetic behavior in organic systems will rely on crystal and solid engineering techniques. While at present this might seem a daunting prospect, several important results indicate promise for the field. Cooperative magnetic behaviors have been observed in charge-transfer complexes of transition-metal sandwich-complexes and 2,3,5,6-tetracyanoquinone (TCNQ),^{21,159} in resins prepared from oxidation of polycyclic aromatic hydrocarbons with 2,3-dichloro-5,6-dicyanoquinone (DDQ),²² and two molecular crystals: *p*-nitrophenylnitronylnitroxide **11** and 2,6-adamantanedinitroxide **12**.⁴⁰⁻⁴²

We have been working toward an understanding of the molecular structures that give rise to cooperative intramolecular spin-spin coupling.^{6,13,104-107} A paradigm we have found useful is shown in Figure 1-2. The spin-containing unit (SC) may be any structure that contains unpaired electrons. The more crucial element is the ferromagnetic coupling unit (FC). *m*-Phenylene has proven its versatility as an FC in a number of studies. Other FCs our model studies have proven viable include 1,3-cyclobutane and 1,3-cyclopentane. The present work demonstrates the use of 1,1-ethylene as an FC. This choice of FC is well preceded. The simplest example of 1,1-ethylene as an FC is of

course trimethylenemethane (TMM). TMM and its derivatives have been studied for over 25 years.^{52,58} In addition, Iwamura recently found 1,1-ethylene to be effective in the coupling of two nitrene or nitroxide centers to give high-spin ground state molecules.^{37,39}

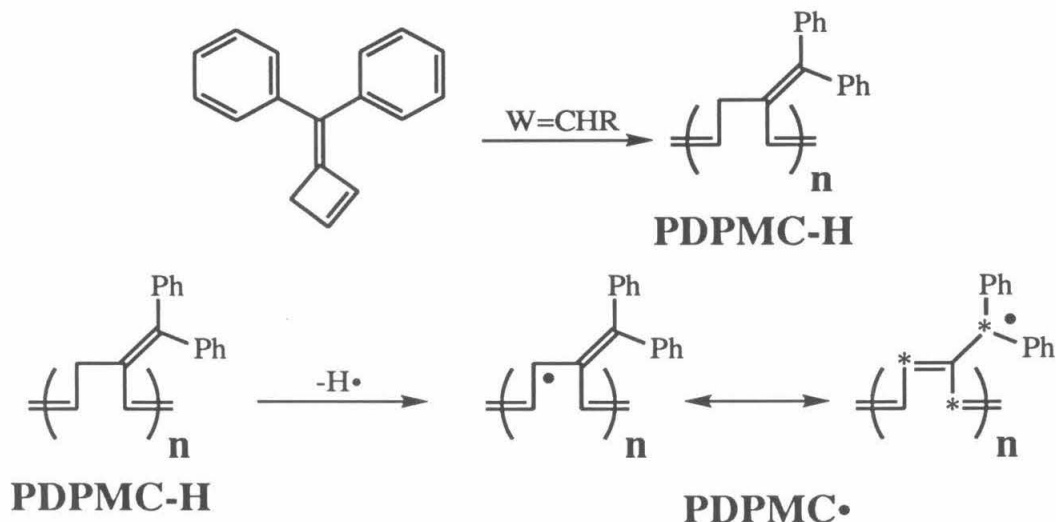
The topological coupling approach to magnetic organic materials has been explored theoretically by Ovchinnikov, who developed a model for alternant hydrocarbons.⁶⁰ For an alternant hydrocarbon, the ground spin state is given by

$$S = \frac{n^* - n^0}{2}$$

where n^* is the number of starred atoms and n^0 is the number of unstarred atoms (Chapter 1). The well-known work of Itoh and Iwamura has established the topological coupling of carbenes as a viable approach to very high-spin paramagnetic organic molecules.^{7,8,137} A slightly different topological coupling approach to very high-spin structures has been adopted by Rajca, who employs simple triarylmethyl radicals as SCs.²³ Both groups have successfully employed *m*-phenylene as an FC to construct oligomeric structures with high spin ground states.

High-spin ground states and radical stability are the two necessary factors for persistent magnetic behavior in organic materials. Preparation of polymers designed to meet these requirements deserves attention as a possible route to organic magnetic materials. In presenting his model for topological coupling, Ovchinnikov specifically stated that polymers with one excess starred atom per repeat unit would have spin ground states S directly proportional to their lengths.⁶⁰ **PDPMC•** is a polyacetylene substituted every five carbons with a diphenylmethyl radical group. Application of Ovchinnikov's rule indicates that **PDPMC•** should have a ground spin state S proportional to its length. Because the SCs in **PDPMC•** are related to triphenylmethyl, a very stable free radical, the SCs in **PDPMC•** should be kinetically stable.^{23,26} We have synthesized the polymer **PDPMC-H**, a precursor polymer to **PDPMC•**, and several of its simply-substituted

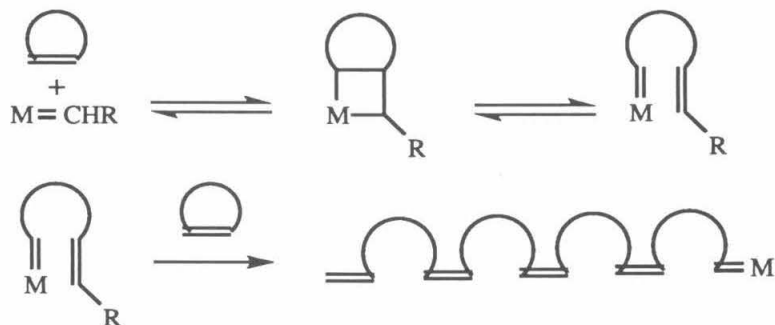
derivatives by ring-opening metathesis polymerization (ROMP).²⁵ We report here on the preparation of **PDPMC-H** and its derivatives and attempts to convert **PDPMC-H** into **PDPMC•**, a polymer potentially having magnetic properties.



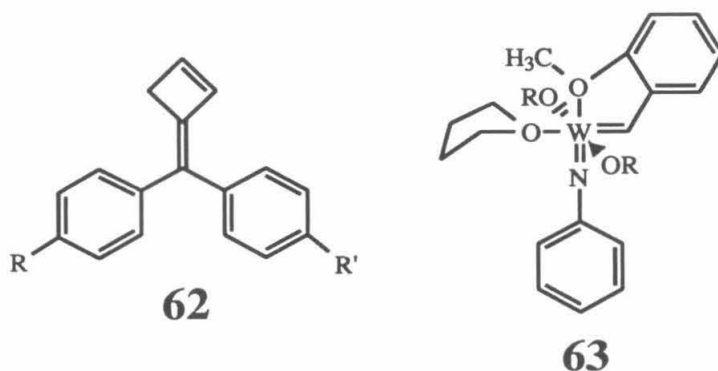
Polymer Synthesis and Characterization

The ROMP of strained cyclic olefins with well-defined metal alkylidene catalysts has proven to be a versatile route to a variety of polymers. Metathesis involves formal [2+2] addition of a metal carbene to an olefin, followed by a productive formal [2+2] cycloreversion. When the olefin metathesized is in a ring, polymer formation results.

Ring-Opening Metathesis Polymerization



We have found that polymerization of diarylmethylenecyclobutenes **62** with a tungsten alkylidene catalyst **63** developed in these laboratories¹⁶⁰ proceeds in a strictly head-to-tail fashion and leads to polymers with the **PDPMC-H** structure.

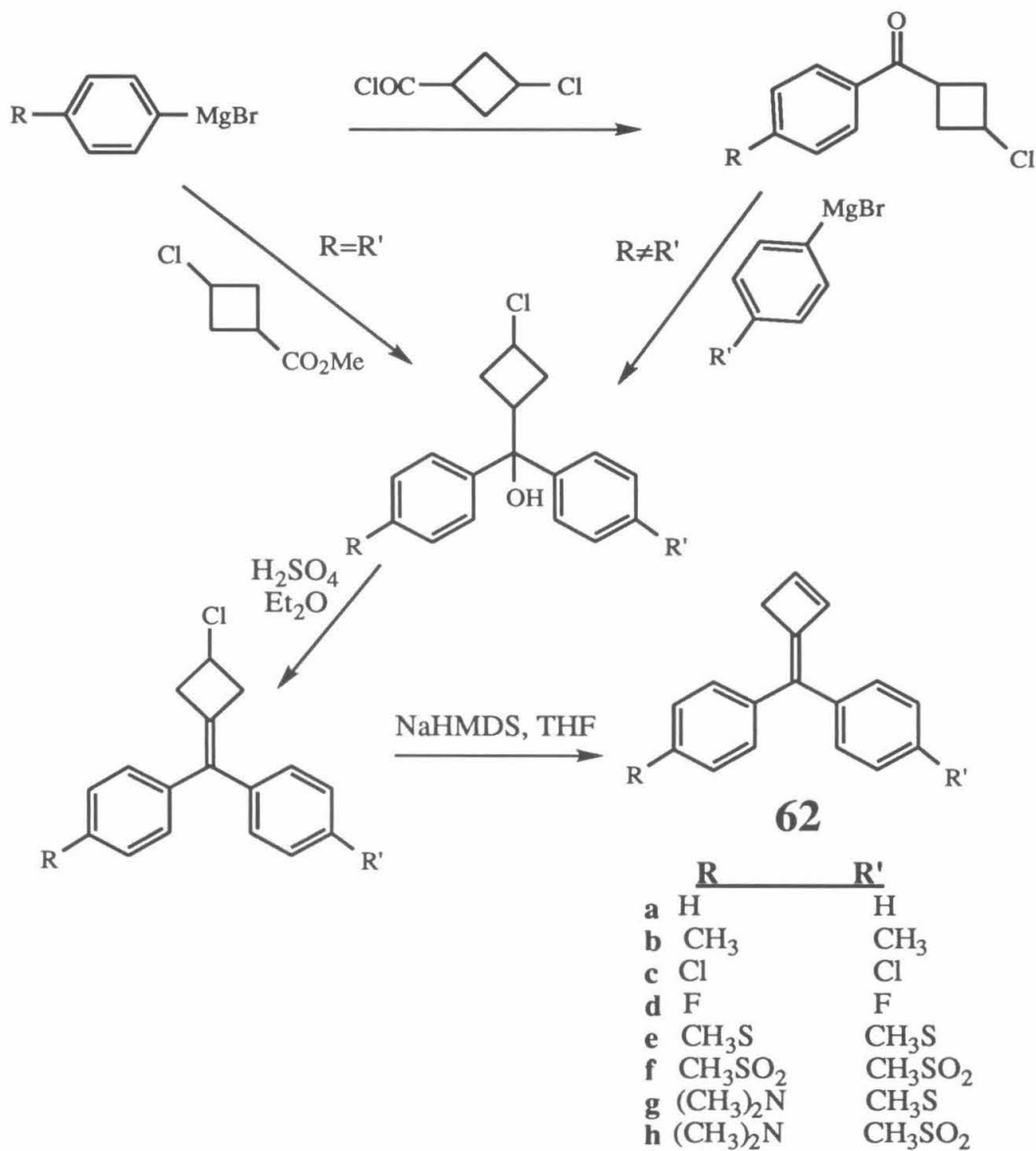


A general synthesis of diarylmethylenecyclobutenes proceeds from 3-chlorocyclobutanecarboxylic acid¹⁶¹ as shown in Scheme 5-1. For symmetric diarylmethylene groups, esterification followed by reaction with two equivalents of a Grignard reagent and dehydration of the crude alcohol with concentrated sulfuric acid in ether provide the desired 3-chlorodiarylmethylenecyclobutenes in 15-60% yield for the two steps. Conversion of the 3-chlorocyclobutanecarboxylic acid to the acid chloride and reaction with one equivalent of Grignard reagent at low temperature provide the 3-chlorocyclobutyl aryl ketones in good yield, providing a way to introduce unsymmetric diarylmethylene groups. Reaction with a second Grignard reagent and dehydration proceeds smoothly. The dienes are extremely labile, whereas the precursor chlorides are all crystalline solids. We therefore have established a two-step, one-pot procedure for elimination of the chloride and *in situ* polymerization of the olefin. Treatment of a solution of the chloride in THF with sodium hexamethyldisilazide conveniently provides a THF solution of the diene, to which a THF solution of the catalyst **63** is then added.

The disappearance of monomer is monitored by TLC. After polymerization has proceeded to a high degree of conversion, the polymer is precipitated into methanol and collected by centrifugation. Further washings with methanol are performed to remove catalyst residues. ¹H and ¹³C NMR analysis indicates regiospecific head-to-tail ROMP polymerization. GPC analysis reveals highly variable molecular weights for this polymerization, indicative of highly reactive monomers. **PDPMC-H** prepared in this

manner contains no paramagnetic substances, as determined by magnetization measurements (see below).

Scheme 5-1



Magnetic Behavior of Polymer-Based Paramagnets

PDPMC• and its derivatives were designed as one-dimensional models for organic magnets. While intermolecular coupling is important to the overall magnetic behavior, it has not yet been designed into this system. Accordingly, we treat these polymers as paramagnetic. The response of an assembly of paramagnets to an applied field may be divided into paramagnetic and diamagnetic terms.^{9,10} The paramagnetic response is due to the unpaired electrons in the sample while the diamagnetic response is due to the repulsion of the magnetic field by the core electrons of the sample. The diamagnetic response is weak, linear with applied field, and independent of temperature, while the paramagnetic response is strong and dependent on both field and temperature. The behavior of a paramagnetic sample at low temperature reveals an average spin state S that scales roughly with the average length of cooperative magnetic interactions down the polymer chain. A value of S significantly greater than $1/2$ indicates cooperative behavior among several unpaired electrons and demonstrates the success of the design.

Magnetic Measurements: Theory and Models^{9,10}

We employed a Quantum Design Magnetic Property Measurement System for magnetic measurements. In this instrument, a ± 5.5 Tesla variable field magnet surrounds a gradient, second-derivative array SQUID magnetometer designed to reject the field due to the superconducting magnet with high accuracy. The magnetic field is necessary to provide magnetization to the paramagnetic samples, which have no permanent moment in the absence of an applied field. The field is applied in the same direction along which the sample is measured, which we denote as the z -direction. From Chapter 1, we know that the projections of the spins of the sample along the axis of the applied field are quantized, with energy $E = -\vec{\mu} \cdot \mathbf{H} = g\beta H_z m_s$. The measured magnetization in the z -direction is $M_z = \sum \mu_{z_i}$, where $\mu_z = -\frac{\partial E}{\partial H_z}$ and the sum is over all molecules in the sample. The population of the m_s states is governed by Boltzmann statistics, and therefore the population of the state m_s , P_{m_s} , is given by

$$P_{m_s} = \frac{e^{-Em_s/kT}}{\sum_{m_s=-S}^S e^{-Em_s/kT}}$$

The average magnetic moment of a single molecule in the sample is $\langle \mu_z \rangle = \frac{\sum P_i \mu_{zi}}{\sum P_i}$, or

$$\langle \mu_z \rangle = \frac{\sum_{m_s=-S}^S g\beta m_s e^{-gbHm_s/kT}}{\sum_{m_s=-S}^S e^{-gbHm_s/kT}}$$

This expression is an exact derivative of the magnetic partition function, W , of one molecule.

$$\langle \mu_z \rangle = \frac{kT}{W} \frac{\partial W}{\partial H_z} = kT \frac{\partial \ln W}{\partial H_z}$$

The quantity $\eta = \frac{g\beta H_z}{kT}$ is a measure of the strength of the magnetic field relative to the thermal energy available to the system. If η is large, the field has a large effect on the population of m_s states; if it is small, the field has a negligible effect. The partition function, W , may be written in terms of η as

$$W = \sum_{-S}^S e^{-\eta m_s} = \frac{e^{-\eta S} - e^{\eta(S+1)}}{1 - e^{\eta}} = \frac{e^{-\eta(S+1/2)} - e^{\eta(S+1/2)}}{e^{-\eta/2} - e^{\eta/2}} = \frac{\sinh\left(S + \frac{1}{2}\right)\eta}{\sinh \frac{\eta}{2}},$$

and thus

$$\langle \mu_z \rangle = kT \frac{\partial \ln W}{\partial H_z} = kT \frac{\partial \ln W}{\partial \eta} \frac{\partial \eta}{\partial H_z} = g\beta \frac{\partial \ln W}{\partial \eta} = \frac{g\beta}{W} \frac{\partial W}{\partial \eta}$$

$$\begin{aligned}
&= \frac{g\beta}{\frac{\sinh(S+1/2)\eta}{\sinh \eta/2}} \left[\frac{(S+1/2) \cosh(S+1/2)\eta}{\sinh \eta/2} - \frac{1}{2} \frac{\sinh(S+1/2)\eta}{\sinh^2 \eta/2} \cosh \eta/2 \right] \\
&= g\beta \left[(S+1/2) \cosh(S+1/2)\eta - (1/2) \coth \eta/2 \right]
\end{aligned}$$

The field and temperature dependence of the magnetization are collected in the Brillouin function, given by

$$B_S(\eta) = \frac{1}{S} \left[(S+1/2) \cosh(S+1/2)\eta - (1/2) \coth \eta/2 \right].$$

In terms of this function,

$$\langle \mu_z \rangle = g\beta S B_S(\eta), \text{ and } \mathbf{M} = N \langle \mu_z \rangle = Ng\beta S B_S(\eta).$$

The behavior of the Brillouin function is shown in Figure 1. The quantity $Ng\beta S$ defines a saturation magnetization, M_{sat} , the maximum moment the sample can achieve. This moment is achieved when all of the individual moments are aligned with the applied field

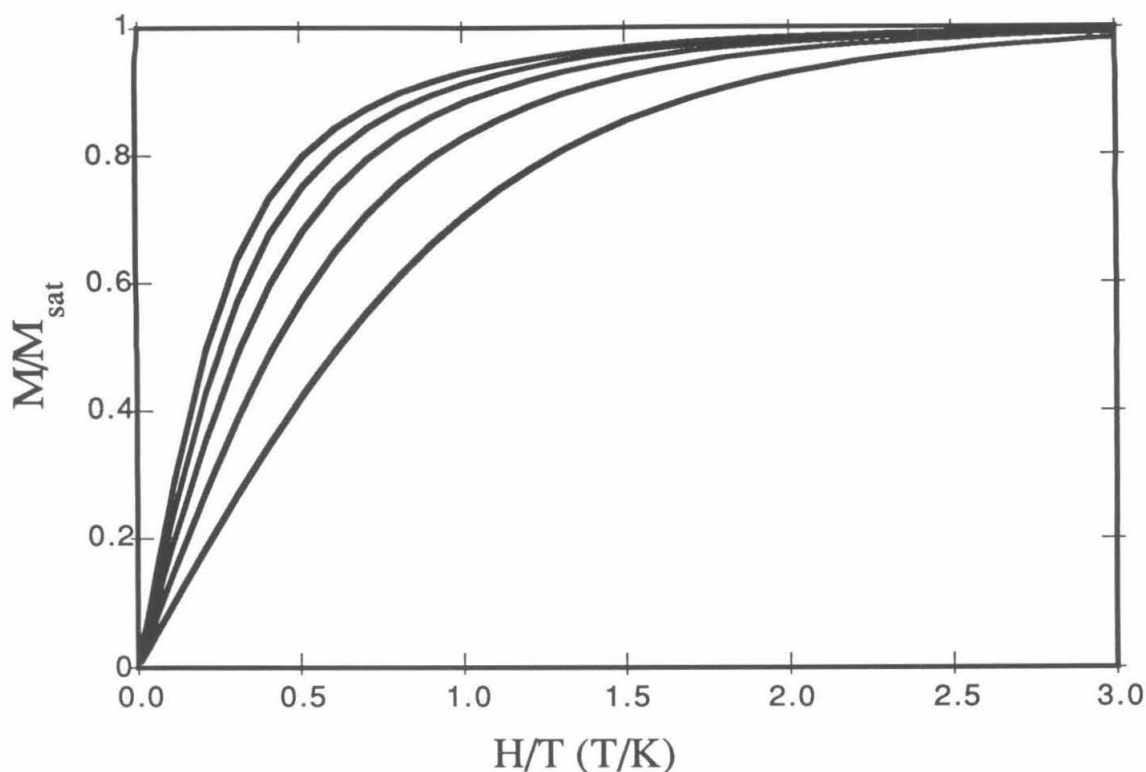


Figure 5-1. The Brillouin function for $S=1$ (lowest curve), 2, 3, 4, 5 (highest curve).

and thus occupy their lowest possible m_s states. The behavior of the Brillouin function shows that this happens only under conditions of very high magnetic field and very low temperature. The value of the MPMS is that it allows us to make measurements under these conditions. Its field ranges up to 5.5 T and its temperature down to 1.7 K, making it possible to achieve $\eta = 4.35$.

A polymer sample may be characterized by an S -value by performing a "saturation plot" determination, in which the moment is measured as a function of H/T at low temperature (typically at 1.8 K). We recall from Chapter 1 that in addition to the paramagnetic moment discussed above, all matter has a weak diamagnetic contribution to the observed magnetic moment. This diamagnetic response is linear with the field and

negative: $M_{dia} = \chi_{dia}H$, $\chi_{dia} < 0$. The observed moment is a sum of diamagnetic and paramagnetic contributions $M_{obs} = M_{dia} + M_{para} = \chi_{dia}H + Ng\beta SB_S(\eta)$.

We are faced with the problem of extracting an S -value from the saturation data according to this equation. Rewritten in terms of η and M_{sat} , this equation is $M_{obs} = \chi_{dia}T\eta + M_{sat}B_S(\eta)$. To determine S , M_{sat} , and χ_{dia} from experimental data, we minimize the merit function

$$\chi^2(S, M_{sat}, \chi_{dia}) = \sum_i \left(M_{obs_i} - M_{calc_i}(S, M_{sat}, \chi_{dia}) \right)^2$$

according to the Levenberg-Marquardt method for nonlinear parameter estimation.¹⁵⁴

The Levenberg-Marquardt method varies smoothly between steepest descent and conjugate gradient minimizations. When χ^2 is large, the steepest descent method is used to calculate the next set of parameters \mathbf{a}_{next} from the current set \mathbf{a}_{cur} . The iterative relation is

$$\mathbf{a}_{next} = \mathbf{a}_{cur} - \text{constant} \times \nabla \chi^2(\mathbf{a}_{cur})$$

The conjugate gradient method is based on a local approximation of the merit function as a quadratic form.

$$\chi^2(\mathbf{a}) = \gamma - \mathbf{d} \cdot \mathbf{a} + \frac{1}{2} \mathbf{a} \cdot \mathbf{D} \cdot \mathbf{a}$$

Near the minimum of χ^2 , the minimizing set of parameters \mathbf{a}_{min} can be determined directly from the current set \mathbf{a}_{cur} by

$$\mathbf{a}_{min} = \mathbf{a}_{cur} + \mathbf{D}^{-1} \cdot \left[-\nabla \chi^2(\mathbf{a}_{cur}) \right]$$

We have written a computer program, 3PFIT, that uses the Levenberg-Marquardt procedure in order to obtain the best fit of the three adjustable parameters S , M_{sat} , and χ_{dia} to the experimental data (source listing in Appendix).

In field and temperature conditions in which the ratio H/T is low, which for these measurements may be defined as $H/T \leq 0.4$ Tesla/Kelvin, the Brillouin function is

approximately linear and the paramagnetic magnetization can be adequately described by the simple equation

$$M_{para} = \frac{N g^2 \beta^2 S(S+1) H}{3kT}$$

In this approximation the magnetization is a linear function of the field. This relationship allows definition of the paramagnetic susceptibility, $\chi_{para} = \frac{N g^2 \beta^2 S(S+1)}{3kT}$, and one can write

$$\chi_{para} = \frac{C}{T}$$

This is the famous Curie equation.

If the moment of a sample is measured as a function of temperature, the observed moment is

$$M_{obs} = (\chi_{para} + \chi_{dia})H = \frac{C}{T}H + \chi_{dia}H$$

and the y-intercept of a plot of M_{obs} vs. $1/T$ gives the diamagnetic susceptibility. In practice this value of χ_{dia} can differ from that obtained using 3PFIT. This is due to the fact that the merit function χ^2 in 3PFIT is most likely very shallow around its minimum, i.e., there are a number of different combinations of S , M_{sat} , and χ_{dia} that all give roughly the same value of χ^2 . This is not surprising, since the Brillouin function and diamagnetic magnetization are both featureless, monotonic functions of H . For this reason, the diamagnetic susceptibility obtained from analysis of the Curie plot, when such data is available, should be viewed as a more reliable estimate of the sample diamagnetism.

The Measurement

According to Faraday's Law, the magnetic flux in a closed conductor loop due to a magnetized paramagnet produces an emf in the loop which may be measured as a voltage. The superconducting quantum interference device (SQUID) is based on a Josephson junction, which is very sensitive to changes in the magnetic flux and thus

measures moments with high accuracy. The second-derivative r.f. SQUID detector used in the MPMS comprises a Josephson junction coupled to four superconducting loops wound in opposing, second-derivative fashion as shown in Figure 5-2. Quantum Design claims that their SQUID detector is accurate to 5×10^{-8} emu·G/cm, a small fraction of a flux quantum (one flux quantum $\equiv h/2e = 2.067 \times 10^{-11}$ Wb = 2.067×10^{-3} emu·G/cm).

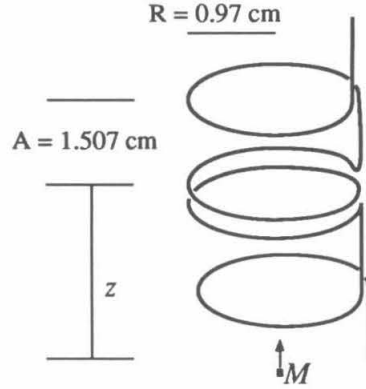


Figure 5-2. Experimental SQUID coil arrangement showing actual coil radius R and detector coil separation A . The current through the four loop circuit is measured as a function of the displacement z in order to determine the moment M . M is approximated as a point dipole in determining the response curve.

The magnetic flux Φ in a superconducting coil of radius R due to a point dipole with moment M oriented along the normal axis of the loop at a distance z from the loop is given by

$$\Phi = \frac{2\pi MR^2}{(z^2 + R^2)^{\frac{3}{2}}}$$

For the array employed in the MPMS, the equation for the voltage due to the total flux in the superconducting detection loops, arranged as in Figure 5-2 is

$$V = \frac{FMR^2}{2} \left(\frac{-1}{((z-A)^2 + R^2)^{\frac{3}{2}}} + \frac{2}{((z)^2 + R^2)^{\frac{3}{2}}} + \frac{-1}{((z+A)^2 + R^2)^{\frac{3}{2}}} \right)$$

where A is the separation of the top and bottom loops from the set of central loops and F is the SQUID calibration factor, which for our instrument is $F = 8384.14 \frac{\text{Volt}\cdot\text{cm}}{\text{emu}\cdot\text{G}}$. This number has been determined empirically by Quantum Design. The maximum sensitivity of the instrument may be gotten by dividing the detection limit of the voltmeter attached to the SQUID, which is 1.5×10^{-4} V, by this calibration factor. The result is 1.8×10^{-8} emu·G/cm. At $z = 0$, since $R = 0.97$, a moment of roughly 1.8×10^{-8} emu·G will be detected by the MPMS. Of course, the limiting factors at this sensitivity will not be due to the instrument, but rather to difficulties in providing a homogeneous background signal. All of the samples we measure have moments on the order of 10^{-4} and higher, simply due to the sample holder arrangement (see below).

A single scan of a sample is performed by a unidirectional motion of the sample in the direction of the magnetic field. Any motion of the sample that causes a deflection of the flux in any loop will be detected. The sample motion is detected if a magnetically inhomogeneous region of the sample is moved close to or through the coils. In this scan, the "sample" that is detected is actually any change in the "background" of the detector. The voltage trace from a typical scan is shown in Figure 5-3. Several scans are averaged to produce one data point.

Due to the second-derivative nature of the pickup coils, it is possible to design a sample holder that is invisible to the instrument except in the sample region. The criterion for a successful sample-holder design is simply that the regions of the sample holder that pass through the detection coils during a scan must have a uniform magnetic susceptibility. We designed the sample holders drawn in Figure 5-4. These holders,

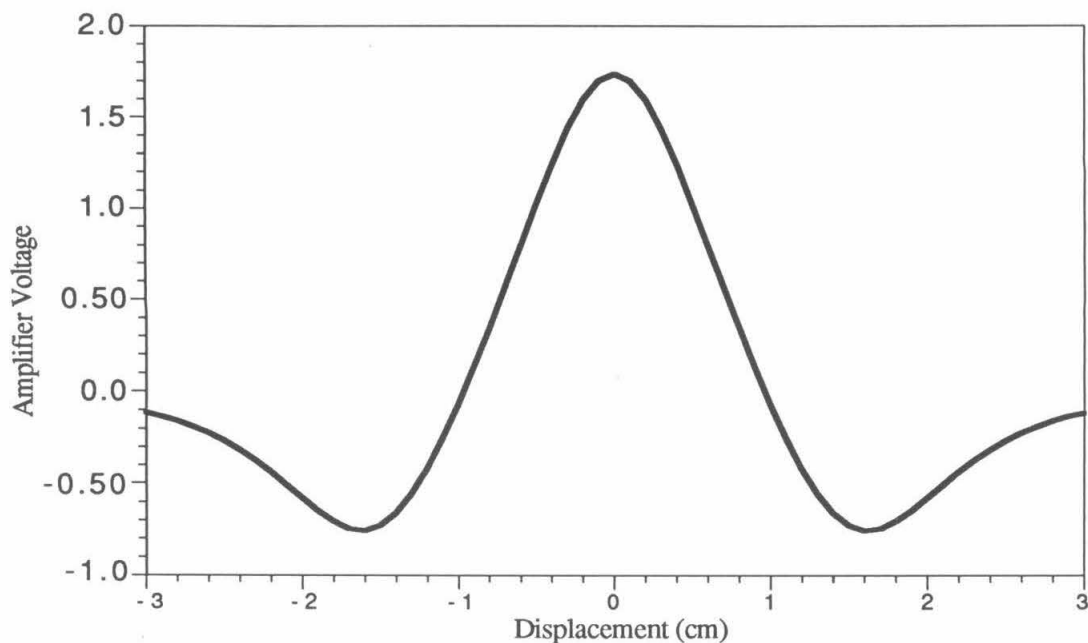


Figure 5-3. Voltage trace produced during a single scan of the sample through the SQUID coils.

constructed from Delrin poly(formaldehyde) or Lucite Plexiglas resin, are magnetically homogeneous except in the sample region. The diamagnetic polymer provides the background signal. Because this material is diamagnetic, the sample space region, which is significantly less dense than the remainder of the extruded polymer rod even when it contains a sample, appears to the instrument as a "paramagnetic" signal. This signal is actually the *absence of diamagnetic material*. This phenomenon is very helpful in our

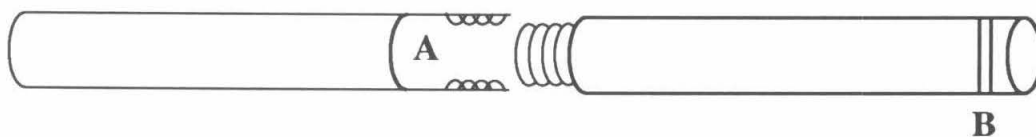


Figure 5-4. Sample Holder Designed for use with the MPMS. The sample fits in the space marked A. The remainder of the holder provides a uniform background for the measurement. The hole at B provides for attachment to the sample support rod.

measurements on the paramagnetic polymer systems that interest us, because it ensures that the observed moment never changes sign. In the past, we have had a great deal of trouble with samples whose diamagnetic and paramagnetic contributions to the observed moment were similar. In these cases, when the observed moment passes through zero, the centerings of the diamagnetic and paramagnetic contributions to the observed moment are usually not spatially coincident, and the trace of the SQUID response is not interpretable within the point-dipole approximation (Figure 5-5). Use of these holders greatly simplifies measurement and analysis of magnetic properties.

In addition, samples tend to become off-center either during a long run or during variable-temperature experiments in which the relative magnitudes of the diamagnetic and paramagnetic contributions change substantially with temperature. We have found that the software provided with the MPMS instrument by the manufacturer, Quantum Design, does not correct well for off-center samples when computing the moment from a voltage trace. We have, therefore, written our own computer fitting procedure which converts the raw voltage data to a magnetic moment. This program is the SQUID DATA CONVERTER (see Appendix). Here again, the Marquardt method is used to fit a function, in this case one with five parameters. These parameters are the moment, the offset of the sample from proper centering, and three terms of a quadratic correction that arise due to slight drift during the measurement.

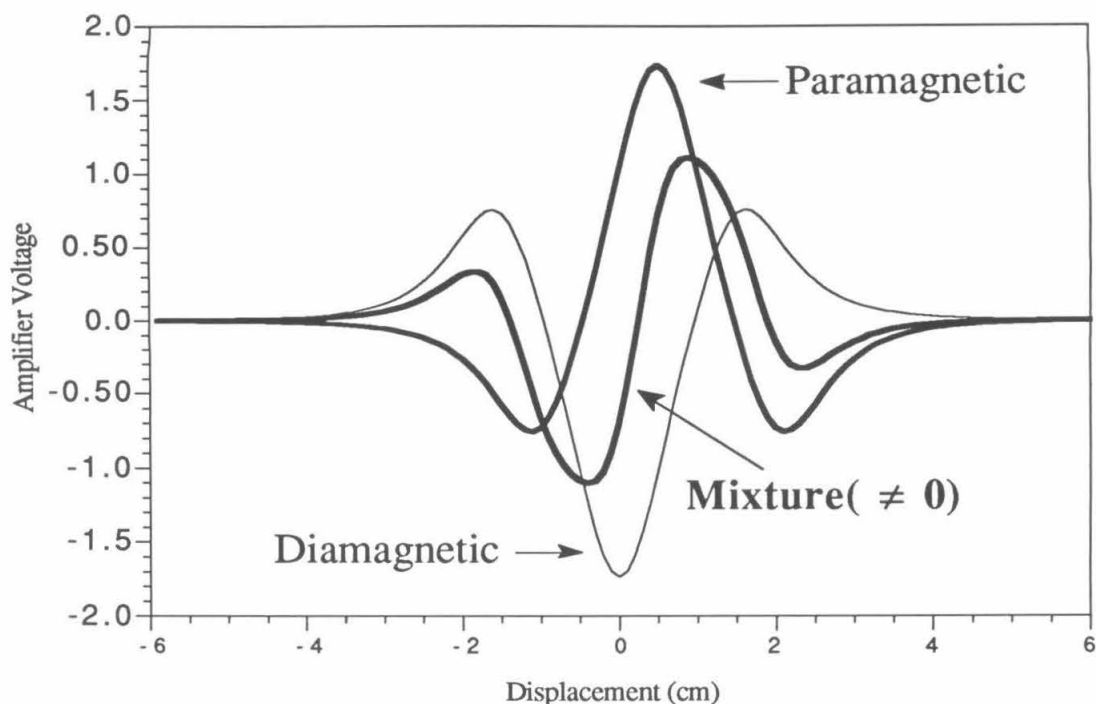


Figure 5-5. Trace produced by a sample of zero moment with spatially offset diamagnetic and paramagnetic contributions. Although the sample moment is zero, the mixture does behave according to the point-dipole approximation and thus the moment is calculated to be different from 0.

The meaning of S

For a doped paramagnetic polymer sample, or any other sample containing a mixture of spin states, a fit to a single Brillouin function is merely an approximation. It is useful to know the distributions of spin states that might give rise to a fit parameter S . We have computed the S -values that will be fit by the Marquardt minimization for various binary mixtures of spin states. The results are consistent with a relationship which has a linear component as its dominant term, and thus "average" in terms of "arithmetic mean" is a reasonable first-order interpretation for the single S -value obtained from a polymer sample. Figure 5-6 shows the S -value obtained from the program 3PFIT to a mixture of two species, one with $S=1$ and one with $S=2$, as a function of mole fraction. Although this function is biased toward the higher spin state, the error is $< 10\%$. We are interested only in distinguishing large differences in the behavior of our samples,

e.g., between a sample with $S = 4.3$ and one with $S = 3.1$. The S -value obtained from our simple model is thus entirely adequate.

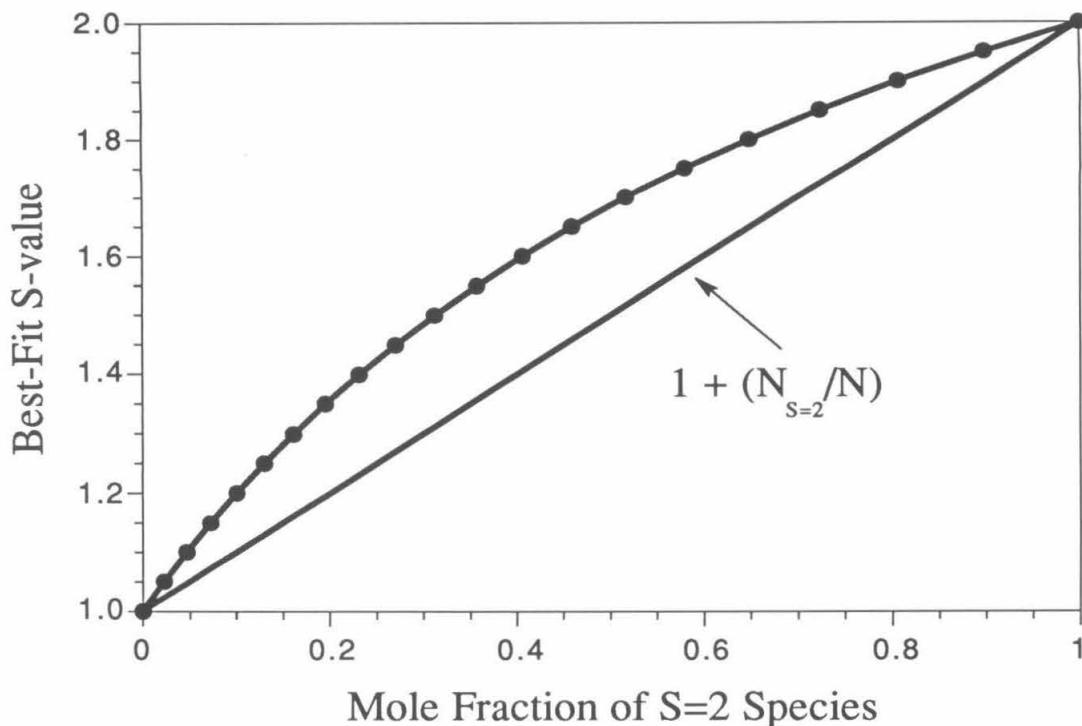


Figure 5-6. Plot of best-fit S -value for a mixture of quintet and triplet species vs. mole fraction of quintet. The mean S -value (straight line) is shown for comparison.

Creating Spins

Two general methods for creating spins in precursor polymers have been established. These are direct hydrogen atom abstraction by a highly reactive quinone,²² and oxidation of polycarbanions.²³ In the first case, we observe very little reaction under either thermal or photochemical conditions, while in the second case, the high molecular weights of these polymers greatly limits the solubilities of the corresponding polyanions, and very little spin communication is observed. A method that leads to some measure of success is the photolysis of **PDPMC-H** in the presence of iodine. In methylene chloride solution, this treatment (for 5 hours at an external temperature of 0 °C) yields a green, soluble polymer solid. We are able to achieve doping levels in this material of ~0.1%,

which is comparable to the success achieved by others in similar circumstances, as well as S -values between 1.07 and 2.2, indicating between three and five spins interacting cooperatively, on average. However, when commercial M.W. 45,000 polystyrene, **PS**, was subjected to the same treatment, similar S -value and spin concentration results were obtained. This intriguing result demonstrates that the behavior with iodine is not unique to our "designed" polymer. Furthermore, in both **PDPMC-H** and **PS**, the iodine doping is reversible over a period of a few days. Washing the methylene chloride solutions of the iodine-treated polymers removes all color from the organic layer. The "doped" polymers obtained after standing at room temperature for several days are diamagnetic. These results suggest that no permanent modification of the backbone occurs in either polymer on treatment with I_2 , and strongly suggests an associative phenomenon between I^\bullet or similar species in the polymer that may or may not be dependent on the polymer backbone. Iodine-atom and iodine-molecule complexes with aryl rings are well-known intermediates, having been studied by flash photolysis in the early 1960s.¹⁶² We suggest that a small number of I^\bullet radicals are generated which find host sites in both of these polymers, and that the radical complexes decompose over a few days at room temperature.

The evidence for generation of **PMPDC \bullet** upon treatment of **PDPMC-H** with iodine is weak in light of the reversibility and the results obtained with **PS**, and becomes more so when one considers the other treatments we have applied to **PDPMC-H**. In these experiments, we have used a number of well-precedented methods to generate radicals in the presence of this polymer, with limited evidence for spin generation and no evidence or negative evidence for the kinetic stability of the spins that are produced. Photolysis of mixtures of **PDPMC-H** in the presence of *t*-butyl hydroperoxide leads to an intriguing, broad EPR signal that may indicate cooperative interactions. However, when the matrix is thawed and recooled, the EPR signal disappears. This seems to indicate that the spins that form upon photolysis recombine in fluid media. Thermal or photochemical

decomposition of benzoyl peroxide, di-*t*-butyl peroxide, and *N*-bromosuccinimide in the presence of **PDPMC-H** all lead to polymers that exhibit no paramagnetism. Treatment of this polymer with nickel peroxide, lead dioxide, or silver(II) oxide also has no effect.

Rajca has prepared several polyarylmethyl polyradicals by the oxidation of polyarylmethyl polyanions with iodine.²³ This seems an ideal route to **PDPMC•**. Treatment of **PDPMC-H** with several amide bases in THF leads to the development of an intense green color which we attribute to anion formation. These mixtures have been treated with iodine after allowing the deprotonation to proceed for varying lengths of time; however, all of the polymers obtained in this manner are also diamagnetic. Although we believe deprotonation is occurring due to the color change observed, ¹H NMR spectra of D₂O-quenched anion suggest that deuterium incorporation is minimal, and thus the overall amount of deprotonation is low. The mixture of base and **PDPMC•** often develops a precipitate on its own, which we attribute to poor solubility of this polyanion in THF.

In addition, we have photolyzed this polymer in the presence of benzoquinone and DDQ.²² Reprecipitation in pentane again yields a polymer which is diamagnetic. In short, we have tried all of the radical generating reactions known to work in these systems that do not involve transition metals such as copper or iron, which would contaminate our magnetic analysis, and have failed to produce evidence for the generation of stable radical centers.

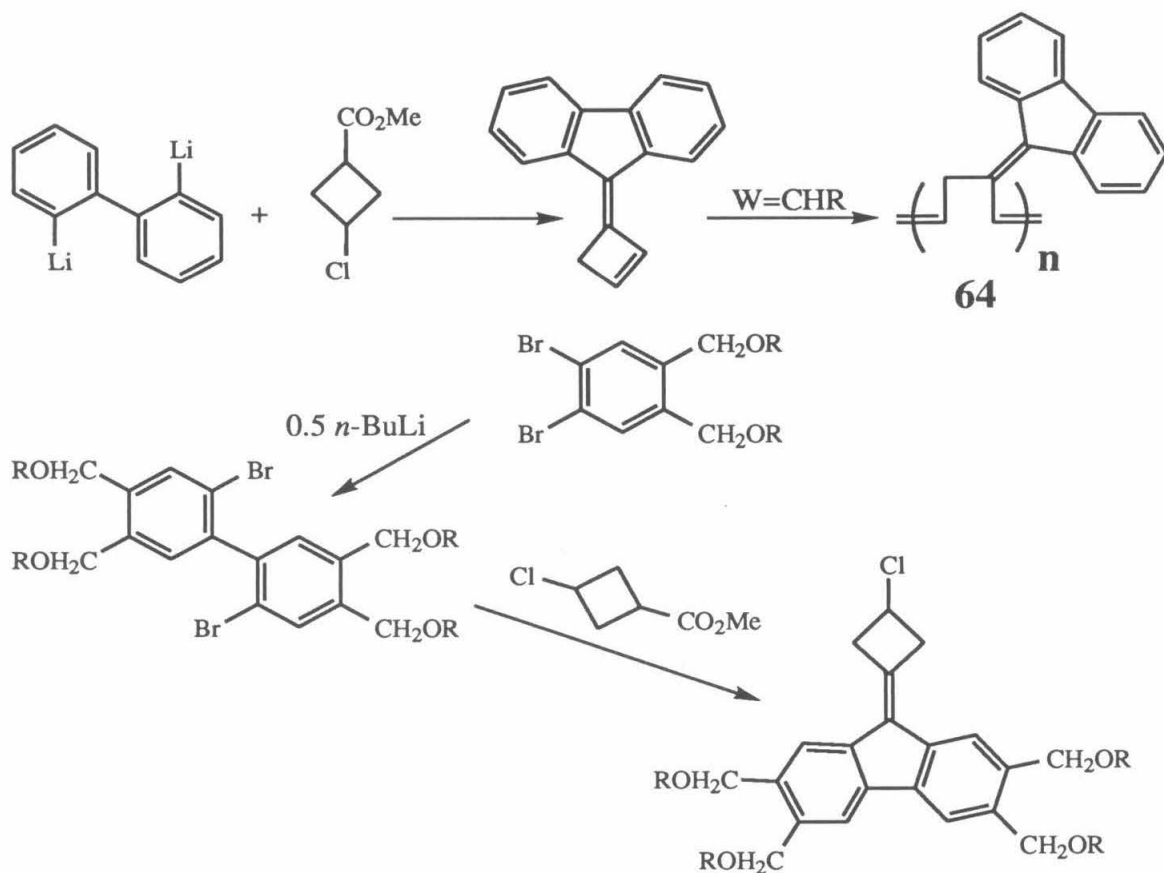
There are two possibilities. The first is that no radical generating reaction is taking place, and the second is that the spins produced in **PDPMC•** are not kinetically stable. Since in all of these materials there is very little difference in the NMR spectra of these polymers upon deprotonation and quenching, we have to conclude that the extent of radical generation upon oxidative treatment of this anion solution is small. The results of the *t*-butyl peroxide EPR experiment, in which we have directly observed a spin-

containing species that disappears upon matrix warming, seem to suggest the latter of the two possibilities. In this case, better radical stabilizing groups must be sought.

Modeling Studies.

In an attempt to rationalize our difficulty in the preparation of **PDPMC•**, we have turned to forcefield calculations using the program DISCOVER. The geometry which DISCOVER calculates for a 4-mer of **PDPMC-H** shows that the phenyl rings are severely twisted out of conjugation with the double bonds of the polymer (Figure 5-7). This computational result suggests that the aromatic stabilizations we expect to gain for the anions and radicals may be prevented from developing by steric constraints. In the structure shown, one phenyl/alkene torsional angle is roughly 90°, while the other averages 60°. A simple computational and synthetic modification of the polymer is to replace the two phenyl rings with a biphenylene to give **64** (Scheme 5-2).

Scheme 5-2



On inspection of the computational results (Figure 5-7), this structure seems to be much more promising in a number of regards. First, most of the dihedral torsion is eliminated, leading to better conjugation throughout the polymer. Second, the structure is highly regular, and the protons seem to be readily available for either deprotonation or atom abstraction. In addition, the acidity of the fluorenyl moiety should increase the acidity by approximately 10 pK units.¹⁶³ Studies of the autooxidation of fluorenyl anions also suggest that the anions produced may be susceptible to mild oxidation conditions. A simple route to derivatives of this structure with symmetrically displaced alkoxyalkyl groups is available (Scheme 5-2).¹⁶⁴ This family of polymers demands further investigation for its own structural and electronic properties.

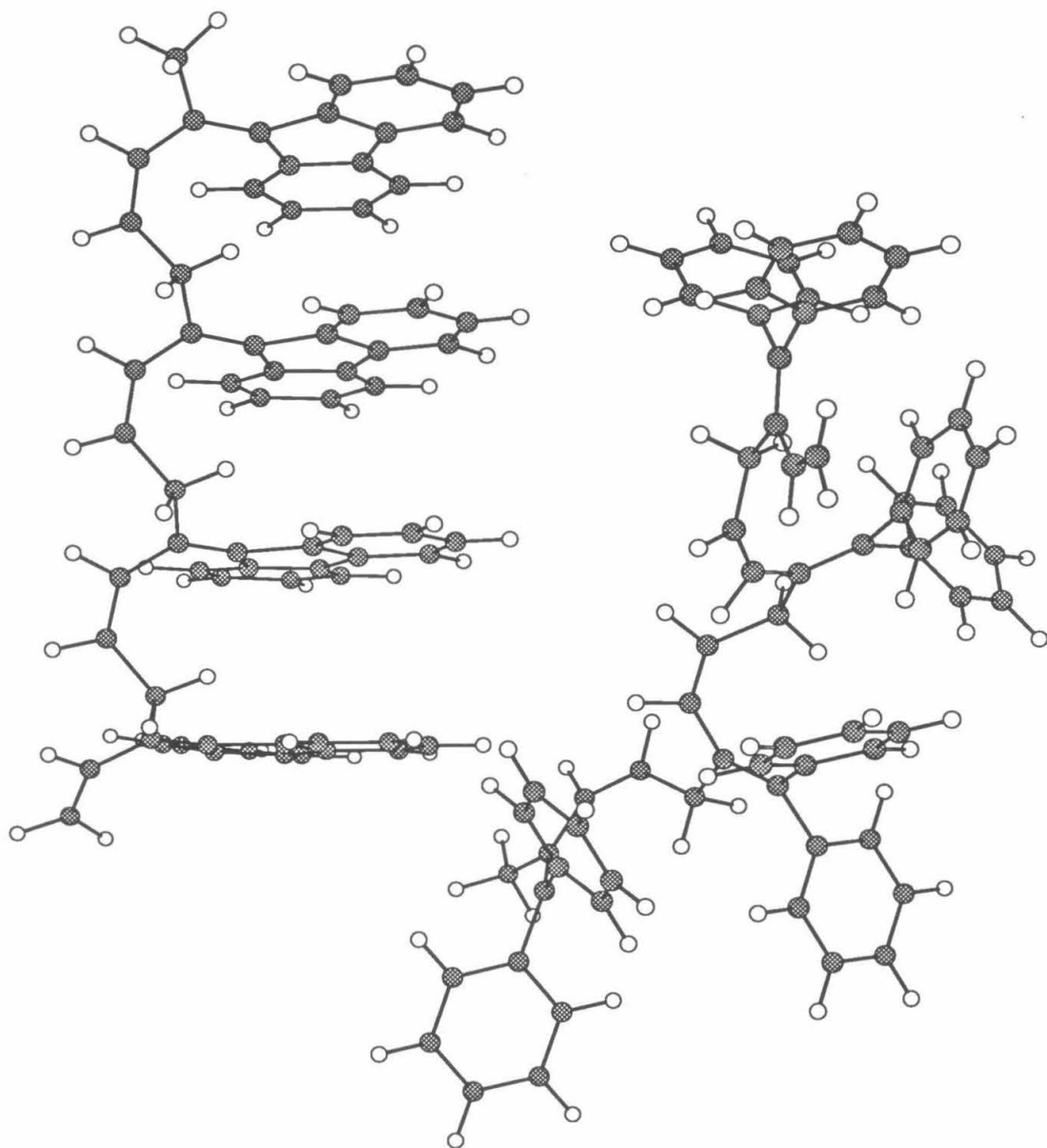


Figure 5-7. Calculated structures of **64** and **PDPMC-H**.

Experimental

p-Thioanisylmagnesium bromide: Magnesium chips (5.31 g; 0.230 mol) were placed in a 250 ml round-bottomed flask, which was then capped with a rubber septum, and flame-dried under a flow of argon. *p*-Bromothioanisole (20.11 g; 99.01 mmol) was added to a dry 100 ml pear-shaped flask. Dry THF was added to the magnesium (15 ml) and the bromide (75 ml). The magnesium was activated by the addition of a few drops of $\text{ClCH}_2\text{CH}_2\text{Br}$. The solution containing the bromide was then added dropwise. Careful addition was maintained so that the THF was nearly refluxing. After the addition was complete and the flask had cooled to room temperature, a few drops of $\text{ClCH}_2\text{CH}_2\text{Br}$ were added and bubbling near the surface of the magnesium was observed. The flask was then heated to near reflux, and allowed to stir for 1 h. The molarity of the solution (1.15 M) was determined by titration (85 ml; 99% yield).

p-(*N,N*-Dimethylamino)phenylmagnesium bromide: A typical synthesis involved the following steps. Magnesium chips (3.10 g; 0.128 mol) were placed in a 250 ml round-bottomed flask, which was then capped with a rubber septum, and flame-dried under a flow of argon. *p*-Bromo-*N,N*-dimethylaniline (10.01 g; 50.00 mmol) was added to a dry 100 ml pear-shaped flask. Dry THF was added to the magnesium (40 ml) and the bromide (50 ml). The magnesium was activated by the addition of a few drops of $\text{ClCH}_2\text{CH}_2\text{Br}$. The solution containing the bromide was then added dropwise. Careful addition was maintained so that the THF was nearly refluxing. After the addition was complete and the flask had cooled to room temperature, the mixture was allowed to stir for 1 h. The molarity of the solution (0.54 M) was determined by titration (85 ml; 92% yield).

Synthesis of methyl 3-chlorocyclobutanecarboxylate

The compounds 1-carboxy-3-chlorocyclobutane (51.99 g, 0.387 mol), 2,2-dimethoxypropane (75 ml, 63.5 g, 0.610 moles), methanol (11 mls), and methanesulfonic acid (0.506 g) were added together in a 250 ml round bottom flask equipped with a reflux condenser and flushed with argon. The solution was then heated to 65 °C under argon for 18 h. Upon completion, the volatiles were removed by rotary evaporation at 30 °C and the residue dissolved in diethyl ether. This solution was then washed with saturated sodium bicarbonate, water, and brine solutions. The diethyl ether layer was dried over magnesium sulfate and rotovapped to dryness. The resulting red oil was distilled at 45 torr in several fractions from 96 - 110 °C to give the colorless liquid product in 60% yield (a mixture of *cis* and *trans* isomers). ¹H NMR (CDCl₃): 4.58 (1H, m), 4.28 (1H, m), 3.69 (6H, d), 3.22 (2H, vbm), 2.8 (4H, vbm), 2.54 (4H, vbm).

Synthesis of 3-chlorocyclobutanecarbonyl chloride

A sample of 3-chlorocyclobutanecarboxylic acid was added to a 100 ml Schlenk flask fitted with a dropping funnel and the system purged with argon for 30 minutes. Thionyl chloride was then added dropwise to the flask. Upon addition, the flask was heated to 35 °C upon which the vigorous evolution of gases began and continued for 2 h. The flask was heated slowly to reflux and the reflux was maintained for 30 minutes after the evolution of gases had ceased. The thionyl chloride was removed by distillation at 75 - 78 °C and the system was left to cool. Further distillation at 30 torr allowed collection of three fractions, the product distilling at 70 ° at 18 torr as a clear liquid in 89% yield (a mixture of *cis* and *trans* isomers). ¹H NMR (CDCl₃): 4.38 (1H, m), 4.19 (2H, m), 3.68 (1H, m), 3.19 (2H, m), 2.83 (4H, m), 2.54 (4H, m).

Synthesis of the Monomer Precursors

3-Diphenylmethylenchlorocyclobutane: A sample of 1-methylcarbonate-3-chlorocyclobutane (3.50 g, 23.6 mmol) was dissolved in 25 ml of anhydrous diethyl ether in a dry 100 ml round bottom flask under argon. Two equivalents of phenylmagnesium bromide were added dropwise, via cannula, over the course of 1 h to the flask at 0 °C. Once the addition was complete, the reaction was stirred for 30 minutes at 0 °C, and then allowed to warm to room temperature and stirred an additional 2 h. A saturated solution of ammonium chloride (25 ml) was added dropwise to the reaction mixture and the pH adjusted to ~1 using aliquots of concentrated HCl and 1 N HCl. The layers were separated and the aqueous phase was then extracted twice with diethyl ether (2 X 50 ml). The organic phases were combined and dried (MgSO₄). Dropwise addition of 40 mls of concentrated sulfuric acid to the solution at 0 °C followed by stirring for 1 h at room temperature effected the dehydration. The mixture was transferred to a separatory funnel using diethyl ether and water. The layers were separated and the aqueous phase extracted twice with diethyl ether (2 X 200 ml). The organic phases were combined, dried with MgSO₄, and filtered. The volatiles were evaporated using rotary evaporation and pumped dry under dynamic vacuum to yield a light brown solid. Chromatography on silica gel using using 10:1 hexane:diethyl ether elutes the product ($R_f = 0.9$). Recrystallization from a mixture of diethyl ether and hexane gives the product as white needles (3.30 g; 55 %). ¹H NMR (CDCl₃): 7.30 (4H, t, $J = 7$ Hz), 7.22 (2H, t, $J = 7$ Hz), 7.13 (4H, d, $J = 7$ Hz), 4.48 (1H, quintet), 3.45 (2H, m), 3.23 (2H, m). ¹³C NMR (CDCl₃): 139.95, 135.35, 131.09, 128.71, 128.21, 126.80, 48.35, 44.64. Elemental Analysis: C: 80.15 (80.15) H: 5.97 (5.93).

Similar double Grignard additions were performed with p-tolylmagnesium bromide, p-chlorophenylmagnesium bromide, and p-fluorophenylmagnesium bromide:

1-Di(p-tolyl)methylene-3-chlorocyclobutane: yellow plates ¹H NMR (CDCl₃): 7.09 (4H, d, $J = 8$ Hz), 7.01 (4H, d, $J = 8$ Hz), 4.47 (1H, quintet), 3.43 (2H, m), 3.19 (2H,

m), 2.32 (6H, s). ^{13}C NMR (CDCl_3): 137.20, 136.39, 134.98, 129.73, 128.85, 128.59, 48.43, 44.60, 21.15. Elemental Analysis: C: 80.57 (80.69) H: 6.82 (6.77).

1-Di(p-chlorophenyl)methylene-3-chlorocyclobutane: white plates ^1H NMR (CDCl_3): 7.27 (4H, m), 7.03 (4H, m), 4.47 (1H, quintet), 3.41 (2H, m), 3.17 (2H, m). ^{13}C NMR (CDCl_3): 137.88, 133.24, 132.86, 132.53, 129.94, 128.54, 47.98, 44.47. Elemental Analysis: C: 63.51 (63.09) H: 4.24 (4.05).

1-Di(p-fluorophenyl)methylene-3-chlorocyclobutane: yellow squares ^1H NMR (CDCl_3): 7.07 (4H, m), 6.98 (4H, m), 4.47 (1H, quintet), 3.40 (2H, m), 3.17 (2H, m). ^{13}C NMR (CDCl_3): 156.87 (d, $J_{\text{C-F}} = 246$ Hz), 132.38 (d, $J_{\text{C-F}} = 3$ Hz), 130.18, 128.13, 127.20 (d, $J_{\text{C-F}} = 8$ Hz), 113.04 (d, $J_{\text{C-F}} = 21$ Hz), 49.71, 46.26. C: 70.04 (70.23) H: 4.57 (4.51).

1-Di(p-thioanisole)methylene-3-chlorocyclobutane: A 250 ml round-bottomed flask was charged with 3-chloro-1-cyclobutaneacetyl chloride (4.93 g; 32.2 mmol). The flask was capped with a rubber septum, purged with argon, and cooled to -78°C . To a flame-dried graduated cylinder was added under argon 26.0 ml of a solution of p-thioanisolemagnesium bromide (1.15 M in THF; 29.9 mmol). The solution was diluted to 100 ml total volume with dry THF. The Grignard solution was then added dropwise to the flask containing the acid chloride. After the addition was complete, the cream-colored slurry was allowed to warm to room temperature and stirred for 1 h. Water (25 ml) was added, and the mixture was transferred to a separatory funnel using water and diethyl ether. The layers were separated, and the aqueous phase was extracted with 50 ml of diethyl ether. The organic phases were combined, dried (MgSO_4), filtered, and evaporated to dryness. The resulting green oil was chromatographed on silica gel using 20:1 (and eventually 10:1) pentane:diethyl ether. Three UV-absorbing fractions were collected. The white fluffy solid from the first fraction ($R_f = 0.62$ using 4:1 pentane:diethyl ether) was recrystallized from diethyl ether to give 0.76 g of white needles. ^1H NMR (CD_2Cl_2): 7.19 (4H, d, $J = 8$ Hz), 7.06 (4H, d, $J = 8$ Hz), 4.52 (1H,

quintet), 3.45 (2H, m), 3.20 (2H, m), 2.47 (6H, s). ^{13}C NMR (CD_2Cl_2): 137.52, 136.96, 134.42, 131.31, 129.48, 126.35, 48.83, 44.92, 15.74. Elemental Analysis: C: 65.42 (65.78) H: 5.55 (5.52).

p-Thioanisole *trans*-3-chlorocyclobutyl ketone: The second UV-absorbing fraction ($R_f = 0.48$ using 4:1 pentane:diethyl ether) from the preceding paragraph was a white oily solid that was rechromatographed on silica gel using 25:1 pentane:diethyl ether. The product was recrystallized from diethyl ether to give 1.05 g of a white powdery solid. ^1H NMR (CD_2Cl_2): 7.78 (2H, d, $J = 8$ Hz), 7.28 (2H, d, $J = 8$ Hz), 4.50 (1H, m), 4.18 (1H, m), 2.92 (2H, m), 2.63 (2H, m), 2.52 (3H, s). ^{13}C NMR (CD_2Cl_2): 198.81, 146.64, 131.74, 128.99, 125.28, 51.62, 37.63, 36.94, 14.89. Elemental Analysis: C: 59.13 (59.87) H: 5.32 (5.44). The *trans* configuration was assigned to this isomer because no NOE enhancement was observed between the ring hydrogens *a* to the chloro group ($d = 4.50$) and *a* to the ketone group ($d = 4.18$). This observation contrasts that for the *cis* isomer (*vide infra*).

p-Thioanisole *cis*-3-chlorocyclobutyl ketone: The third UV-absorbing fraction ($R_f = 0.29$ using 4:1 pentane:diethyl ether) from the preceding reaction was a white fluffy solid that was recrystallized from diethyl ether to give 1.61 g of white needles. ^1H NMR (CD_2Cl_2): 7.78 (2H, d, $J = 9$ Hz), 7.28 (2H, d, $J = 9$ Hz), 4.49 (1H, m), 3.68 (1H, m), 2.85 (2H, m), 2.63 (2H, m), 2.52 (3H, s). ^{13}C NMR (CD_2Cl_2): 196.79, 146.08, 131.22, 128.35, 124.67, 48.36, 37.33, 35.82, 14.28. Elemental Analysis: C: 59.54 (59.87) H: 5.50 (5.44). The *cis* configuration was assigned to this isomer because an NOE enhancement was observed between the ring hydrogens *a* to the chloro group ($d = 4.49$) and *a* to the ketone group ($d = 3.68$). This observation contrasts that for the *trans* isomer (*vide supra*).

1-Di(p-phenyl methyl sulfone)methylene-3-chlorocyclobutane: A 100 ml round-bottomed flask was charged with 1-di(*p*-thioanisole)methylene-3-chlorocyclobutane (0.52 g; 1.50 mmol) and acetone (50 ml). Oxone (2.93 g; 4.7 mmol) was dissolved in 30 ml of

water. The flask containing the dithioether was cooled to 0 °C, and 10 ml of the Oxone solution were added via pipet. The reaction was allowed to warm to room temperature, and 5 ml of the Oxone solution were added every 15 min over the course of 1 h. The reaction mixture was allowed to stir an additional 3 h at room temperature. Analysis by TLC showed the formation of a product with $R_f = 0.07$ (4:1 ethyl acetate:hexane) and the disappearance of the starting dithioether ($R_f = 0.66$). A solution of 1 N NaOH was added until the mixture was basic (pH 10) as judged by pH paper. The mixture was transferred to a 500 ml separatory funnel using CH_2Cl_2 and water. The layers were separated and the aqueous phase was extracted with CH_2Cl_2 (3 X 100 ml). The organic phases were combined, dried (MgSO_4), filtered, and evaporated to dryness. The resulting white powder (0.57 g) was recrystallized from a mixture of CH_2Cl_2 and diethyl ether to give pale yellow crystals. ^1H NMR (CD_2Cl_2): 7.89 (4H, d, $J = 8$ Hz), 7.34 (4H, d, $J = 8$ Hz), 4.56 (1H, quintet), 3.52 (2H, m), 3.26 (2H, m), 3.05 (6H, s). ^{13}C NMR (CD_2Cl_2): 144.80, 139.61, 137.97, 132.90, 129.86, 127.90, 48.22, 44.91, 44.70.

*1-Di(3,5-di-*t*-butyl-4-trimethylsiloxyphenyl)methylene-3-chlorocyclobutane:* A flame-dried 250 ml round-bottomed flask was charged with 75 ml of dry THF under argon. The flask was cooled to -78 °C, and a solution of *t*-BuLi in pentane (10 ml; 17 mmol) was added via cannula. 3,5-Di-*t*-butyl-4-trimethylsiloxy-1-bromobenzene (2.85 g; 8.0 mmol) was dissolved in 25 ml of dry THF and added to the cooled solution via cannula. The solution was stirred for 1 h at -78 °C. A sample of 1-methylcarbonate-3-chlorocyclobutane (0.66 g, 4.4 mmol) was added dropwise via syringe. After the addition was complete, the mixture was stirred for 1 h at -78 °C and then allowed to warm to room temperature and stirred for 2 h. A solution of 1 N HCl (4 ml) was added, and the mixture was allowed to stir for 1 min. The mixture was dried with MgSO_4 , filtered, and evaporated to dryness. The residue was dissolved in CH_2Cl_2 (100 ml) and transferred to a dry Schlenk flask. The flask was cooled to -78 °C under argon, and Martin sulfurane (2.80 g; 4.20 mmol) was added through a flow of argon. The solution was allowed to

warm to room temperature and transferred to a separatory funnel. The solution was then washed with 100 ml of 5% NaOH solution and 100 ml of water. After drying (Na_2SO_4), the solution was filtered and evaporated to dryness. The residue was chromatographed on silica gel using 20:1 pentane:diethyl ether containing 1% triethylamine. Four UV-absorbing fractions were collected. The first fraction was recrystallized from a mixture of diethyl ether and methanol to give 0.55 g of yellow crystals. The crystals were rechromatographed on silica gel using pentane and 3% diethyl ether and 1% triethylamine. The resultant residue was recrystallized from a mixture of diethyl ether and methanol to give 0.46 g (0.76 mmol) of white needles. ^1H NMR (CD_2Cl_2): 7.00 (4H, s), 4.50 (1H, quintet), 3.48 (2H, m), 3.27 (2H, m), 1.34 (36H, s), 0.37 (18H, s). Elemental Analysis: C: 71.06 (71.46) H: 9.57 (9.69).

1-Fluorenylmethylene-3-chlorocyclobutane: A 100 ml round-bottomed flask was charged with 2,2'-dibromobiphenyl (1.72 g; 5.51 mmol). The flask was capped with a rubber septum and purged with argon. Dry diethyl ether (50 ml) was added and the solution was cooled to $-78\text{ }^\circ\text{C}$. A solution of n-BuLi in hexane (7.0 ml; 11 mmol) was added dropwise via cannula. The flask was then allowed to warm to room temperature and stirred for 4.5 h. 1-Methylcarbonate-3-chlorocyclobutane (0.817 g, 5.50 mmol) was dissolved in 50 ml of diethyl ether. This solution and that containing the dilithio reagent were added dropwise to a 250 ml round-bottomed flask containing 50 ml of diethyl ether under argon at $0\text{ }^\circ\text{C}$. The flask was allowed to warm to room temperature and stirred overnight. The solution was acidified to pH 1 by the addition of 1.0 N HCl. The mixture was transferred to a separatory funnel where the layers were separated. The aqueous phase was extracted with 50 ml of diethyl ether. The organic phases were combined, dried with MgSO_4 , filtered, and evaporated to dryness. The resulting yellow oil was chromatographed on silica gel using 4:1 hexane:diethyl ether. The fractions believed to contain the cis and trans alcohols ($R_f = 0.29$ and 0.21 using 4:1 hexane:diethyl ether) were combined and dried under vacuum to yield a white foam (1.17 g; 4.32 mmol). The

mixture of alcohols was dissolved in 25 ml of dry CH_2Cl_2 . The flask was cooled to 0 °C, and a solution containing Martin sulfurane (3.21 g; 4.77 mmol) in 25 ml of CH_2Cl_2 was added via cannula. The reaction was held at 0 °C for 4 h, and then allowed to warm to room temperature and stirred for 48 h. To the resulting yellow solution was added *ca.* 0.5 g of sodium ethoxide. The mixture was allowed to stir for 10 min, followed by the addition of water. The mixture was transferred to a separatory funnel using copious amounts of diethyl ether. The layers were separated and the aqueous phase was extracted twice with diethyl ether. The organic phases were combined and washed successively with 10% NaOH (2 X 100 ml), H_2O (1 X 100 ml), and brine (1 X 100 ml). The organic phase was dried with MgSO_4 , filtered, and the solvent was removed by rotary evaporation. The resulting yellow solid was chromatographed on silica gel using 4:1 hexane:diethyl ether. The yellow solid obtained was dissolved in CH_2Cl_2 and partially decolorized with activated charcoal. This material was recrystallized from CH_2Cl_2 to give 0.54 g (2.12 mmol) of white cotton-like fibers. ^1H NMR (CD_2Cl_2): 7.81 (2H, m), 7.51 (2H, m), 7.38 (4H, bm), 4.86 (1H, m), 4.15 (2H, m), 3.77 (2H, m). ^{13}C NMR (CD_2Cl_2): 139.84, 138.41, 137.69, 130.64, 127.71, 127.44, 123.50, 120.18, 50.10, 46.21.

1-(p-N,N-Dimethylaniline)(p-thioanisole)methylene-3-chlorocyclobutane: A 100 ml round-bottomed flask was charged with p-thioanisole cis-3-chlorocyclobutyl ketone (1.56 g; 6.48 mmol) and 20 ml of dry THF. The flask was cooled to 0 °C, and 10.0 ml of p-(N,N-dimethylaniline)magnesium bromide (0.66 M in THF) was added dropwise via cannula. The flask was allowed to warm to room temperature, and the orange solution was stirred for 3 h. Saturated ammonium chloride solution (25 ml) was added, and the mixture was transferred to a separatory funnel using diethyl ether. The layers were separated, and the aqueous phase was extracted with diethyl ether (2 X 50 ml). The organic phases were combined, dried with MgSO_4 , filtered, and evaporated to dryness. The resulting green oil was dissolved in diethyl ether and filtered through a glass frit.

The solvent was removed by rotary evaporation to give a green foam (2.34 g) presumably containing the cis and trans alcohols. The flask containing the foam was taken into the drybox and charged with Martin sulfurane (5.0 g; 7.4 mmol). The flask was then taken out of the drybox and cooled to 0 °C. Dry CH₂Cl₂ (~ 50 ml) was added via cannula to dissolve the materials. The resulting dark green solution was allowed to stir for 4 h at 0 °C. Sodium ethoxide (1.10 g; 16.2 mmol) was then added, and the mixture was stirred for ~ 10 min, after which the green color had dissipated. A solution of sodium hydroxide (1.0 N; 25 ml) was added and the mixture was transferred to a separatory funnel using copious amounts of diethyl ether. The layers were separated, and the aqueous phase was extracted with diethyl ether (2 X 50 ml). The organic phases were combined and washed with 10% NaOH (2 X 100 ml), water (100 ml) and brine (100 ml). The resulting clear yellow solution was dried with MgSO₄. Decolorizing carbon was added and the solution was filtered and evaporated to dryness. The resulting oil was chromatographed on silica gel using 6:1 pentane:diethyl ether. A UV-absorbing fraction with $R_f = 0.63$ (TLC using 4:1 pentane:diethyl ether) was collected and evaporated to give a white solid. The white solid was recrystallized in from diethyl ether to give 1.05 g (3.05 mmol) of a pale yellow powder. ¹H NMR (CD₂Cl₂): 7.19 (2H, d, $J = 8$ Hz), 7.07 (2H, d, $J = 8$ Hz), 6.99 (2H, d, $J = 9$ Hz), 6.66 (2H, d, $J = 9$ Hz), 4.51 (1H, quintet), 3.49 (1H, m), 3.41 (1H, m), 3.22 (1H, m), 3.16 (1H, m), 2.93 (6H, s), 2.48 (3H, s) ppm. ¹³C NMR (CD₂Cl₂): 149.82, 137.87, 137.09, 134.92, 129.72, 128.50, 128.23, 126.40, 112.27, 49.09, 45.06, 44.90, 40.59, 15.85. Elemental Analysis: C: 69.82 (69.85) H: 6.41 (6.45) N: 4.30 (4.07).

1-(p-N,N-dimethylaniline)(p-phenyl methyl sulfone)methylene-3-chlorocyclobutane: A 250 ml round-bottomed flask was charged with 1-(p-N,N-dimethylaniline)(p-thioanisole)methylene-3-chlorocyclobutane (0.72 g; 2.09 mmol) and acetone (40 ml). Oxone (2.06 g; 4.7 mmol) was dissolved in 20 ml of water. The flask containing the dithioether was cooled to 0 °C, and 5 ml aliquots of the Oxone solution were added via pipet over the course of 20 min. The reaction was allowed to warm to

room temperature and stirred an additional 2 h at room temperature. Analysis by TLC showed the formation of a product with $R_f = 0.64$ (2:1 ethyl acetate:hexane) and the disappearance of the starting thioether ($R_f = 0.82$). A solution of 1 N NaOH was added until the mixture was neutral as judged by pH paper. The mixture was transferred to a 500 ml separatory funnel using CH_2Cl_2 and water. The layers were separated and the aqueous phase was extracted with CH_2Cl_2 (3 X 100 ml). The organic phases were combined, dried (MgSO_4), filtered, and concentrated by rotary evaporation. The resulting solution chromatographed on silica gel (1:1 hexane:ethyl acetate) to give 0.12 g of crude product. This material was recrystallized from diethyl ether to give cream-colored needles. ^1H NMR (CD_2Cl_2): 7.84 (2H, d, $J = 8$ Hz), 7.35 (2H, d, $J = 8$ Hz), 6.97 (2H, d, $J = 9$ Hz), 6.66 (2H, d, $J = 9$ Hz), 4.53 (1H, quintet), 3.54 (1H, m), 3.42 (1H, m), 3.27 (1H, m), 3.16 (1H, m), 3.04 (3H, s), 2.94 (6H, s). ^{13}C NMR (CD_2Cl_2): 149.95, 146.83, 138.89, 134.19, 131.44, 130.07, 129.66, 127.53, 127.13, 112.24, 48.77, 45.06, 44.79, 44.77, 40.50.

Phenyl 3-chlorocyclobutyl ketone: A 100 ml round-bottomed flask was charged with 3-chloro-1-cyclobutaneacetyl chloride (4.48 g; 29.3 mmol). The flask was capped with a rubber septum, purged with argon, and cooled to -78 °C. To a flame-dried graduated cylinder was added under argon 10.0 ml of a solution of phenylmagnesium bromide (3.0 M in diethyl ether; 30 mmol). The solution was diluted into 50 ml of dry diethyl ether, cooled to 0 °C, and added dropwise to the flask containing the vigorously stirred acid chloride. After the addition was complete, the solution was allowed to warm to room temperature and stirred for 4 h. Ice and 1 N HCl were added, and the mixture was transferred to a separatory funnel using water and diethyl ether. The layers were separated, and the aqueous phase was extracted twice with 100 ml of diethyl ether. The organic phases were combined and washed successively with saturated bicarbonate solution, water, and brine (100 ml each). The solution was dried (MgSO_4), partially decolorized with activated charcoal, filtered, and evaporated to dryness. The resulting

tan oil was chromatographed on silica gel using 15:1 (and eventually 4:1) pentane:diethyl ether. The cis and trans isomers were separated and collected. The assignment of cis or trans to the isomers was made by analogy (e.g., relative R_f and ^1H NMR splitting patterns) to the p-thioanisole ketone isomers rigorously assigned above. Trans isomer: $R_f = 0.57$ (4:1 pentane:diethyl ether) ^1H NMR (CDCl_3): 7.88 (2H, m), 7.56 (1H), 7.45 (2H, m), 4.49 (1H, quintet), 4.23 (1H, m), 2.95 (2H, m), 2.63 (2H, m). Cis isomer: $R_f = 0.37$ (4:1 pentane:diethyl ether) ^1H NMR (CDCl_3): 7.88 (2H, m), 7.57 (1H), 7.45 (2H, m), 4.48 (1H, quintet), 3.70 (1H, m), 2.85 (2H, m), 2.69 (2H, m).

*1-(3,5-di-*t*-butyl-4-trimethylsiloxyphenyl)(phenyl)methylene-3-chlorocyclobutane:*

A flame-dried 100 ml round-bottomed flask was charged with 50 ml of dry THF under argon. The flask was cooled to $-78\text{ }^\circ\text{C}$, and a solution of *t*-BuLi in pentane (6.0 ml; 10 mmol) was added via cannula. 3,5-Di-*t*-butyl-4-trimethylsiloxy-1-bromobenzene (1.67 g; 4.67 mmol) was dissolved in 20 ml of dry THF and added to the cooled solution via cannula. The solution was stirred for 1 h at $-78\text{ }^\circ\text{C}$. A sample of phenyl trans-3-chlorocyclobutyl ketone (1.01 g, 5.19 mmol) was added dropwise via syringe. After the addition was complete, the solution was allowed to warm to room temperature and stirred for 3 h. A saturated solution of NH_4Cl (10 ml) was added, and the mixture was transferred to a separatory funnel using water and diethyl ether. The layers were separated and the aqueous phase extracted twice with 100 ml of diethyl ether. The organic phases were combined, dried with MgSO_4 , filtered, and evaporated to dryness. The resulting pale yellow oil was chromatographed on silica gel using 20:1 pentane:diethyl ether containing 1% triethylamine. The UV-absorbing fraction with $R_f = 0.72$ (4:1 pentane:diethyl ether) was recrystallized from a mixture of diethyl ether and methanol to give 0.64 g of clear crystals of the alcohol. ^1H NMR (CD_2Cl_2): 7.34 (2H, m), 7.30 (2H, m), 7.22 (1H, m), 7.16 (2H, s), 4.30 (1H, quintet), 3.02 (1H, m), 2.56 (1H, m), 2.35 (3H, bm), 1.34 (18H, s), 0.39 (9H, s). A sample of this alcohol (0.88 g; 1.86 mmol) was placed in a 100 ml round bottomed flask and taken into the drybox. The flask

was charged with Martin sulfurane (1.55 g; 2.30 mmol). The flask was then taken out of the drybox, and dry CH_2Cl_2 (~ 50 ml) was added via cannula to dissolve the materials. The resulting yellow solution was allowed to stir for 3 h. The mixture was transferred to a separatory funnel using copious amounts of diethyl ether. The organic phase was washed twice with 100 ml of 10% NaOH and dried with MgSO_4 . The solution was filtered and evaporated to dryness. The resulting oil was chromatographed on silica gel using 20:1 pentane:diethyl ether. A UV-absorbing fraction was collected and evaporated to give 0.300 g of a dark yellow oil. ^1H NMR (CDCl_3): 7.31 (2H, m), 7.25 (1H, m), 7.18 (2H, m), 6.99 (2H, s), 4.48 (1H, quintet), 3.0-3.5 (4H, bm), 1.37 (18H, s), 0.39 (9H, s).

General Polymerization Procedures

One step elimination and polymerization of dimethylenecyclobutene:

The 1-diphenylmethylene-3-chlorocyclobutane is dissolved in dry THF along with 0.98 equivalents of hexamethyldisilazide base to give a cloudy white solution. The chloride elimination is left to stir for 30 minutes at room temperature before an appropriate amount of the Grubbs and Johnson alkylidene catalyst¹⁶⁰ is added to this reaction mixture. Addition of the catalyst immediately turns the polymerization mixture a cloudy orange color that will not dissipate during the length of polymerization. The length of polymerization varies from 3 - 24 h, depending upon the inorganic base used, but is closely monitored by TLC for monomer depletion.

Upon completion, the pale orange and cloudy polymerization solution is precipitated gently in swirling methanol to give a slightly discolored, yellow solid. If desired, the polymer is easily redissolved and filtered through a silica plug. This purification step yields a pristine white polymer solid upon precipitation.

^1H NMR (CDCl_3): 6.71 - 7.11 (10H, bm), 5.66 (1H, d), 5.01 (1H, m), 2.16 (2H, bm) ppm. ^{13}C NMR (CDCl_3): 140.62, 134.74, 128.38, 127.66, 125.99, 36.00, 50.10 ppm. IR spectroscopy: 3050, 3020, 2970, 1600, 1490, 1440, 760, 695 cm^{-1} .

It is also possible to isolate the diphenylmethylene cyclobutene as a clear and colorless oil (after the first step) with filtration and chromatography of the reaction mixture.

^1H NMR (CDCl_3): 7.20 - 7.32 (10H, bm), 6.73 (1H, s), 6.47 (1H, s), 3.18 (1H, s) ppm.

Photochemical Doping Experiments

PDPMC-H is dissolved in methylene chloride, or THF with 1-10 equivalents of a radical-generating species such as di-*t*-butyl peroxide, benzoyl peroxide, or *N*-bromosuccinimide. The mixture is either heated under argon or photolyzed with vycor-filtered UV light. After varying periods of time, the polymer is collected by precipitation into pentane and centrifugation. The resulting polymers are normally white to yellow in color. The polymer is loaded into a SQUID sample holder and the paramagnetic moment determined by a saturation plot at 1.8 K. In all cases except those noted in the text and described below, only a linear response with the field is observed, indicating no paramagnetic component of the magnetization.

Experiments with Iodine

PDPMC-H (40 mg) was dissolved in CH_2Cl_2 and iodine (100 mg) was added. The solution was freeze-pump-thaw degassed 3x and photolyzed for 5 h using unfiltered light. The polymer was precipitated in pentane, washed, and dried. In three separate runs this procedure gave the results: $S=2.4$, 4.8×10^{20} spins/mole monomer; $S=1.84$, 1.22×10^{21} spins/mole monomer; $S=0$ (no paramagnetic response).

PDPMC-H (45 mg) was dissolved in C_6H_6 (6 ml) and iodine (42.4 mg) was added. After 10 h reaction, the polymer was precipitated into methanol, giving a yellow polymer solid. Magnetization studies indicate $S=1.07$, 1.18×10^{20} spins/mole monomer.

PS (1.13 g) was dissolved in C_6H_6 (25 ml) and degassed by purging with Ar. Solid I_2 (3 g) was added, and the mixture was stirred at room temperature for 40 h. The polymer was precipitated into pentane, which gave a brown-green polymer solid. This material was studied with the SQUID and revealed $S=2.19$, 1×10^{20} spins/mol monomer.

PS (140 mg) and I_2 (300 mg) were dissolved in CH_2Cl_2 under Ar and photolyzed using vycor-filtered light for 3 h. Precipitation into pentane and centrifugation gave a brown black sample that was analyzed with the SQUID and revealed: $S=2.21$, 1.3×10^{20} spins/mol monomer.

The oligomer structures were minimized with DISCOVER v. 2.8 using the CVFF forcefield. Oligomer chains were constructed using the Polymerizer module in InsightII version 2.1.0.

References.

- (1) *Free Radicals*; Kochi, J. K., Ed.; Wiley: New York, 1973.
- (2) Pryor, W. A. *Free Radicals*; McGraw-Hill: New York, 1966.
- (3) Proceedings of the Symposium on Ferromagnetic and High Spin Molecular Based Materials, 197th Meeting of the American Chemical Society, Dallas, TX, April 9-14, 1989. Miller, J.S.; Dougherty, D.A., Eds.; *Mol. Cryst. Liq. Cryst.* **1989**, 176, 1.
- (4) Buchachenko, A. L. *Russ. Chem. Rev.* **1990**, 59, 307.
- (5) Dougherty, D. A.; Kaisaki, D. A. *Mol. Cryst. Liq. Cryst.* **1990**, 183, 71.
- (6) Dougherty, D. A. *Acc. Chem. Res.* **1991**, 23, 88.
- (7) Iwamura, H. *High-Spin Organic Molecules and Spin Alignment in Organic Molecular Assemblies*; Academic Press Ltd: 1990; Vol. 26, pp 179-253.
- (8) Iwamura, H.; Koga, N. *Acc. Chem. Res.* **1993**, 27, 346.
- (9) Kittel, C. *Introduction to Solid State Physics*; 6th ed.; John Wiley & Sons, Inc.: New York, 1986, pp 395-460.
- (10) Carlin, R. L. *Magnetochemistry*; Springer-Verlag: Berlin, 1986.
- (11) Although "radical" is derived from Latin, the Greek prefixes "tetra-" and "poly-" have become popular in the literature and are used here with due apologies.
- (12) *Diradicals*; Borden, W. T., Ed.; John Wiley & Sons: New York, 1982.
- (13) Dougherty, D. A.; Grubbs, R. H.; Kaisaki, D. A.; Chang, W.; Jacobs, S. J.; Shultz, D. A.; Anderson, K. K.; Jain, R.; Ho, P. T.; Stewart, E. G. In *Magnetic Molecular Materials*; D. Gatteschi, O. Kahn, J. S. Miller and F. Palacio, Ed.; Kluwer Academic Publishers: The Netherlands, 1991; pp 105-120.
- (14) Iwamura, H. *Pure and Appl. Chem.* **1993**, 65, 57.
- (15) Wertz, J. E.; Bolton, J. R. *Electron Spin Resonance. Elementary Theory and Practical Applications*; Chapman and Hall: New York, 1986.
- (16) Dougherty, D. A. In *Research Frontiers in Magnetochemistry*; C. O'Connor, Ed.; World Scientific Publishing: Singapore, 1993, pp 327-349.

- (17) Chiang, L. Y.; Johnston, D. C.; Goshorn, D. P.; Bloch, A. N. *Synth. Met.* **1988**, 27, B639.
- (18) Caneschi, A.; Gatteschi, D.; Sessoli, R.; Rey, P. *Acc. Chem. Res.* **1989**, 22, 392.
- (19) Breslow, R. *Mol. Cryst. Liq. Cryst.* **1985**, 125, 261.
- (20) Kahn, O. In *Magnetic Molecular Materials*; D. Gatteschi, O. Kahn, J. S. Miller and F. Palacio, Ed.; Kluwer Academic Publishers: The Netherlands, 1991; pp 35-52.
- (21) Miller, J. S.; Epstein, A. J.; Reiff, W. M. *Science* **1988**, 240, 40.
- (22) Ota, M.; Otani, S.; Igarashi, M. *Chem. Lett.* **1989**, 1183.
- (23) Rajca, A.; Utamapanya, S.; Thayumanavan, S. *J. Am. Chem. Soc.* **1992**, 114, 1884.
- (24) Veciana, J.; Rovira, C.; Ventosa, N.; Crespo, M. I.; Palacio, F. *J. Am. Chem. Soc.* **1993**, 115, 57.
- (25) Novak, B. M.; Risse, W.; Grubbs, R. H. In *New Methods of Polymer Synthesis*; Wiley: New York, 1992; Vol. 102; pp 47-72.
- (26) Gomberg, M. *Berichte* **1900**, 33, 3150.
- (27) Ballester, M. *Acc. Chem. Res.* **1985**, 18, 380.
- (28) Carilla, J.; Juliá, L.; Riera, J.; Brillas, E.; Garrido, J. A.; Labarata, A.; Alcalá, R. *J. Am. Chem. Soc.* **1991**, 113, 8281.
- (29) Veciana, J.; Rovira, C. In *Magnetic Molecular Materials*; D. Gatteschi, O. Kahn, J. S. Miller and F. Palacio, Ed.; Kluwer Academic Publishers: The Netherlands, 1991; pp 121-132.
- (30) Coppinger, G. M. *J. Am. Chem. Soc.* **1957**, 79, 501.
- (31) Awaga, K.; Sugano, T.; Kinoshita, M. *Chem. Phys. Lett.* **1987**, 141, 540.
- (32) Chiang, L. Y.; Upasani, R. B.; Sheu, H. S.; Goshorn, D. P.; Lee, C. H. *J. Chem. Soc., Chem. Commun.* **1992**, 959.
- (33) Yang, N. C.; Castro, A. J. *J. Am. Chem. Soc.* **1960**, 82, 6208.

- (34) Bock, H.; John, A.; Havalas, Z.; Bats, J. W. *Angew. Chem. Int. Ed. Engl.* **1993**, 32, 416.
- (35) Koelsch, C. F. *J. Am. Chem. Soc.* **1957**, 79, 4439.
- (36) Tukada, H.; Mutai, K. *Tetrahedron Lett.* **1992**, 33, 6665.
- (37) Matsumoto, T.; Ishida, T.; Koga, N.; Iwamura, H. *J. Am. Chem. Soc.* **1992**, 114, 9952.
- (38) Rossitto, F. C.; Lahti, P. M. *J. Polym. Sci.* **1992**, 30, 1335.
- (39) Matsumoto, T.; Koga, N.; Iwamura, H. *J. Am. Chem. Soc.* **1992**, 114, 5448.
- (40) Chiarelli, R.; Rassat, A.; Rey, P. *J. Chem. Soc., Chem. Commun.* **1992**, 1081.
- (41) Yoshizawa, K.; Chano, A.; Ito, A.; Tanaka, K.; Yamabe, T.; Fujita, H.; Yamauchi, J.; Shiro, M. *J. Am. Chem. Soc.* **1992**, 114, 5995.
- (42) Nakazawa, Y.; Tamura, M.; Shirakawa, N.; Shiomi, D.; Takahashi, M.; Kinoshita, M.; Ishikawa, M. *Phys. Rev. B* **1992**, 46, 8906.
- (43) Berry, R. S.; Rice, S. A.; Ross, J. *Physical Chemistry*; Wiley: New York, 1980, pp 163-205.
- (44) Merzbacher, E. *Quantum Mechanics*; 2nd ed.; Wiley: New York, 1970, pp 251-275.
- (45) Mott, N. F.; Sneddon, I. N. *Wave Mechanics and its Applications*; Oxford University Press: Cambridge, 1957.
- (46) Uhlenbeck, G. E.; Goudsmit, S. *Physica* **1925**, 5, 266.
- (47) Uhlenbeck, G. E.; Goudsmit, S. *Nature* **1926**, 117, 264.
- (48) Pauli, W. *Z. Phys.* **1927**, 43, 601.
- (49) Dirac, P. A. M. *Proc. Roy. Soc. A* **1928**, 117, 610.
- (50) Itoh, K. *Pure & Appl. Chem.* **1978**, 50, 1251.
- (51) Dougherty, D. A. In *Kinetics and Spectroscopy of Carbenes and Biradicals.*; M. S. Platz, Ed.; Plenum Press: New York, 1990; pp 117-142.
- (52) Dowd, P. *Acc. Chem. Res.* **1972**, 5, 242.

- (53) Berson, J. A. *Acc. Chem. Res.* **1978**, *11*, 446.
- (54) Buchwalter, S. L.; Closs, G. L. *J. Am. Chem. Soc.* **1978**, *101*, 4688.
- (55) Snyder, G. J.; Dougherty, D. A. *J. Am. Chem. Soc.* **1989**, *111*, 3927.
- (56) Salem, L.; Rowland, C. *Angew. Chem. Int. Ed. Engl.* **1972**, *11*, 92.
- (57) Goldberg, A. H.; Dougherty, D. A. *J. Am. Chem. Soc.* **1983**, *105*, 284.
- (58) Jain, R.; Sponsler, M. B.; Coms, F. D.; Dougherty, D. A. *J. Am. Chem. Soc.* **1988**, *110*, 1356.
- (59) Borden, W. T.; Davidson, E. R. *J. Am. Chem. Soc.* **1977**, *99*, 4587.
- (60) Ovchinnikov, A. A. *Theoret. Chim. Acta (Berl.)* **1978**, *47*, 297.
- (61) Du, P.; Borden, W. T. *J. Am. Chem. Soc.* **1987**, *109*, 930.
- (62) Dowd, P. *J. Am. Chem. Soc.* **1970**, *94*, 1066.
- (63) Dowd, P.; Chang, W.; Paik, Y. H. *J. Am. Chem. Soc.* **1986**, *108*, 7416.
- (64) Nachtigall, P.; Jordan, K. D. *J. Am. Chem. Soc.* **1991**, *114*, 4743.
- (65) Nachtigall, P.; Jordan, K. D. *J. Am. Chem. Soc.* **1993**, *115*, 270.
- (66) Dixon, D. A.; Dunning, T. H., Jr.; Eades, R. A.; Kleier, D. A. *J. Am. Chem. Soc.* **1981**, *103*, 2878.
- (67) Dowd, P. *J. Am. Chem. Soc.* **1966**, *88*, 2587.
- (68) Dowd, P.; Chow, M. *J. Am. Chem. Soc.* **1977**, *99*, 6438.
- (69) Feller, D.; Davidson, E. R.; Borden, W. T. *Isr. J. Chem.* **1983**, *23*, 105.
- (70) Berson, J. A. In *Diradicals*; W. T. Borden, Ed.; John Wiley and Sons: New York, 1982; pp 151-194.
- (71) Snyder, G. J. Ph. D. Thesis, Caltech, 1988.
- (72) Rule, M.; Mondo, J. A.; Berson, J. A. *J. Am. Chem. Soc.* **1982**, *104*, 2209.
- (73) Mazur, M.; Berson, J. A. *J. Am. Chem. Soc.* **1982**, *104*, 2217.
- (74) Potter, S. E.; Berson, J. A. *J. Am. Chem. Soc.* **1976**, *98*, 5725.
- (75) Itoh, K. *Chem. Phys. Lett.* **1967**, *1*, 235.

- (76) Wasserman, E.; Murray, R.W.; Yager, W. A.; Trozzolo, A. M.; Smolinsky, G. J. *Am. Chem. Soc.* **1967**, *89*, 5076.
- (77) Iwamura, H.; Nakamura, N.; Koga, N.; Sasaki, S. *Mol. Cryst. Liq. Cryst.* **1992**, *218*, 207.
- (78) Itoh, K. In *Magnetic Molecular Materials*; D. Gatteschi, O. Kahn, J. S. Miller and F. Palacio, Ed.; Kluwer Academic Publishers: The Netherlands, 1991; pp 67-86.
- (79) Dvornitzky, M.; Chiarelli, R.; Rassat, A. *Angew. Chem. Int. Ed. Engl.* **1992**, *31*, 180.
- (80) Miura, Y.; Inui, K.; Yamaguchi, F.; Inoue, M.; Teki, Y.; Takui, T.; Itoh, K. *J. Polym. Sci.* **1992**, *30*, 959.
- (81) Kanno, F.; Inoue, K.; Koga, N.; Iwamura, H. *J. Am. Chem. Soc.* **1993**, *115*, 847.
- (82) Silverman, S. K.; Dougherty, D. A. *J. Phys. Chem.* submitted.
- (83) Jain, R.; Snyder, G. J.; Dougherty, D. A. *J. Am. Chem. Soc.* **1984**, *106*, 7294.
- (84) Sponsler, M. B.; Jain, R.; Coss, F. D.; Dougherty, D. A. *J. Am. Chem. Soc.* **1989**, *111*, 2240.
- (85) Buchwalter, S. L.; Closs, G. L. *J. Am. Chem. Soc.* **1975**, *97*, 3857.
- (86) Coss, F. D.; Dougherty, D. A. *Tetrahedron Lett.* **1988**, *29*, 3753.
- (87) Coss, F. D.; Dougherty, D. A. *J. Am. Chem. Soc.* **1989**, *111*, 6894.
- (88) Coss, F. D. Ph.D. Thesis, Caltech, 1989.
- (89) Stewart, E. G. Ph.D. Thesis, Caltech, 1992.
- (90) Kato, S.; Morokuma, K.; Feller, D.; Davidson, E. R.; Borden, W. T. *J. Am. Chem. Soc.* **1983**, *105*, 1791.
- (91) Wright, B. B.; Platz, M. S. *J. Am. Chem. Soc.* **1983**, *105*, 628.
- (92) Pranata, J.; Dougherty, D. A. *J. Phys. Org. Chem.* **1989**, *2*, 161.
- (93) Doubleday, C., Jr.; McIver, J. W., Jr.; Page, M. *J. Am. Chem. Soc.* **1982**, *104*, 6533.
- (94) Conrad, M.; Pitzer, R.; Schaefer, H., III *J. Am. Chem. Soc.* **1979**, *101*, 2245.

- (95) The synthesis of the azo precursor to 1,3-dimethyl-1,3-cyclohexanediyl has been reported, but no reports of EPR studies have appeared. Wilson, R. M.; Rekers, J. W.; Packard, A. B.; Elder, R. C. *J. Am. Chem. Soc.* **1980**, *102*, 1633.
- (96) Photolysis of the azo precursor to 2,4-adamantanediyl gave no EPR signal. Dowd, P.; Chang, W., personal communication.
- (97) Clites, J. A.; West, A. P., Jr.; Silverman, S. K.; Dougherty, D. A. unpublished results.
- (98) Seeger, D. E.; Lahti, P. M.; Rossi, A. R.; Berson, J. A. *J. Am. Chem. Soc.* **1986**, *108*, 1251.
- (99) Seeger, D. E.; Berson, J. A. *J. Am. Chem. Soc.* **1983**, *105*, 5144.
- (100) Kirste, B.; Harrer, W.; Kurreck, H. *Angew. Chem. Int. Ed. Engl.* **1981**, *20*, 873.
- (101) Grimm, M.; Kirste, B.; Kurreck, H. *Angew. Chem. Int. Ed. Engl.* **1986**, *25*, 1097.
- (102) Baumgarten, M.; Müller, U.; Bohnen; Müllen, K. *Angew. Chem. Int. Ed. Engl.* **1992**, *1992*, 448.
- (103) Tukada, H.; Mutai, K. *J. Chem. Soc., Chem. Commun.* **1991**, 35.
- (104) Dougherty, D. A.; Jacobs, S. J.; Silverman, S. K.; Murray, M.; Shultz, D. A.; West, A.P., Jr.; Clites, J. A. *Mol. Cryst. Liq. Cryst.* in press.
- (105) Kaisaki, D. A.; Chang, W.; Dougherty, D. A. *J. Am. Chem. Soc.* **1991**, *113*, 2764.
- (106) Murray, M.; Kaszynski, P.; Dougherty, D. A. unpublished results.
- (107) Kaszynski, P.; Dougherty, D. A. *J. Org. Chem.* submitted.
- (108) Neuenschwander, M. In *The Chemistry of Double Bonded Functional Groups*; S. Patai, Ed.; Wiley: Chichester, UK, 1989; Vol. 2; pp 1131-1268.
- (109) Stille, J. K.; Grubbs, R. H. *J. Org. Chem.* **1989**, *54*, 434.
- (110) Stone, K. J.; Little, R. D. *J. Org. Chem.* **1984**, *49*, 1849.
- (111) Freund, W.; Hünig, S. *J. Org. Chem.* **1987**, *52*, 2154.
- (112) Freund, H.; Hünig, S. *Helv. Chim. Acta* **1987**, *70*, 929.

- (113) Krapcho, A. P.; Horn, D. E.; Rao, D. R.; Abegaz, B. *J. Org. Chem.* **1972**, *37*, 1575.
- (114) Greidanus, J.; Schwalm, W. J. *Can. J. Chem.* **1969**, *47*, 3715.
- (115) Pedersen, B. S.; Scheibye, S.; Nilsson, N. H.; Lawesson, S. O. *Bull. Chim. Soc. Belg.* **1978**, *87*, 223.
- (116) Koli, A. K.; McClary, E. *J. Ind. Chem. Soc.* **1978**, *55*, 242.
- (117) Hamon, A.; Lacoume, B.; Plasquet, G.; Pilgrim, W. R. *Tetrahedron Lett.* **1976**, 211.
- (118) Nyström, J.-E.; McCanna, T. D.; Helquist, P.; Iyer, R. S. *Tetrahedron Lett.* **1985**, *26*, 5393.
- (119) Griffith, W. P.; Ley, S. V.; Whitcombe, G. P.; White, A. D. *J. Chem. Soc., Chem. Commun.* **1987**, 1625.
- (120) Mancuso, A. J.; Huang, S. L.; Swern, D. *J. Org. Chem.* **1978**, *43*, 2480.
- (121) Omura, K.; Swern, D. *Tetrahedron* **1978**, *34*, 1651.
- (122) Faulkner, D.; McKervey, M. A. *J. Chem. Soc. C* **1971**, 3906.
- (123) Eis, M. J.; Wrobel, J. E.; Ganem, B. *J. Am. Chem. Soc.* **1984**, *106*, 3693.
- (124) Little, R. D.; Carroll, G. L.; Petersen, J. L. *J. Am. Chem. Soc.* **1983**, *105*, 928.
- (125) Dervan, P. B.; Squillacote, M. E.; Lahti, P. M.; Sylwester, A. P.; Roberts, J. D. *J. Am. Chem. Soc.* **1981**, *103*, 1120.
- (126) George, M. V.; Balachandran, K. S. *Chem. Rev.* **1975**, *75*, 491.
- (127) Gassman, P. G.; Mansfield, K. T. *Org. Synth.* **1969**, *49*, 1.
- (128) Rose, M. E. *Elementary Theory of Angular Momentum*; Wiley: New York, 1957.
- (129) Weltner, W., Jr. *Magnetic Atoms and Molecules*; Dover Publications, Inc.: New York, 1983, pp 256-265.
- (130) Teki, Y.; Takui, T.; Itoh, K. *J. Chem. Phys.* **1988**, *88*, 6134.
- (131) Atkins, P. W. *Physical Chemistry*; 4th ed.; Freeman: New York, 1990, p 798.

- (132) Platz, M. S.; Senthilnathan, V. P.; Wright, B. B.; McCurdy, C. W., Jr. *J. Am. Chem. Soc.* **1982**, *104*, 6494.
- (133) Chang, M. H.; Dougherty, D. A. *J. Org. Chem.* **1981**, *46*, 4092.
- (134) Binkley, R. W. *J. Org. Chem.* **1976**, *41*, 3030.
- (135) Vedejs, E.; Marth, C. F.; Ruggeri, R. *J. Am. Chem. Soc.* **1988**, *110*, 3940; Vedejs, E.; Marth, C.F. *J. Am. Chem. Soc.* **1988**, *110*, 3948.
- (136) Davies, A. G.; Griller, D.; Ingold, K. U.; Lindsay, D. A.; Walton, J. C. *J. Chem. Soc., Perkin Trans. II* **1981**, 633.
- (137) Teki, Y.; Takui, T.; Itoh, K.; Iwamura, H.; Kobayashi, K. *J. Am. Chem. Soc.* **1986**, *108*, 2147.
- (138) Jain, R. Ph. D. Thesis, Caltech, 1987.
- (139) Hutchison, C. A., Jr.; Magnum, B. W. *J. Chem. Phys.* **1958**, *29*, 952.
- (140) Hutchison, C. A., Jr.; Magnum, B. W. *J. Chem. Phys.* **1961**, *34*, 908.
- (141) Swalen, J. D.; Gladney, H. M. *IBM J. Res. Dev.* **1964**, *8*, 515; Gladney, H.M. QCPE #68 and #69.
- (142) Kottis, P.; Lefebvre, R. *J. Chem. Phys.* **1963**, *39*, 393.
- (143) Kottis, P.; Lefebvre, R. *J. Chem. Phys.* **1964**, *41*, 739.
- (144) Wasserman, E.; Snyder, L. C.; Yager, W. A. *J. Chem. Phys.* **1964**, *41*, 1763.
- (145) Aasa, R.; Vänngård, T. *J. Magn. Reson.* **1978**, *91*, 30.
- (146) van Veen, G. *J. Magn. Reson.* **1978**, *30*, 91.
- (147) Stevenson, R. C. *J. Magn. Reson.* **1984**, *57*, 24.
- (148) Keijzers, C. P.; Reijerse, E. J.; Stam, P.; Dumont, M. F.; Gribnau, M. C. M. *J. Chem. Soc., Faraday Trans. I* **1987**, *83*, 3493.
- (149) Bonomo, R. P.; Di Bilio, A. J.; Riggi, F. *Chem. Phys.* **1991**, *151*, 323.
- (150) Nettar, D.; Villafranca, J. J. *J. Magn. Reson.* **1985**, *64*, 61.
- (151) Golub, G. H.; Van Loan, C. F. *Matrix Computations*; Johns Hopkins University Press: Baltimore, 1983, pp 136-321.

- (152) Iwasaki, M. *J. Magn. Reson.* **1974**, *16*, 417.
- (153) Teki, Y.; Takui, T.; Yagi, H.; Itoh, K.; Iwamura, H. *J. Chem. Phys.* **1985**, *83*, 539.
- (154) Press, W. H.; Flannery, B. P.; Teukolsky, S. A.; Vetterling, W. T. *Numerical Recipes (The Art of Scientific Computing)*; Cambridge University Press: New York, 1986.
- (155) Wilkinson, J. H. *Numer. Math.* **1962**, *4*, 368.
- (156) Kollmar, C.; Kahn, O. *J. Am. Chem. Soc.* **1991**, *113*, 7987.
- (157) McConnell, H. M. *J. Chem. Phys.* **1963**, *39*, 1910.
- (158) McConnell, H. M. In *Proc. R.A. Welch Fdn Conf.*; 1967; pp 144.
- (159) Manriquez, J. M.; Yee, G. T.; McLean, R. S.; Epstein, A. J.; Miller, J. S. *Science* **1991**, *252*, 1415.
- (160) Johnson, L.K.; Virgil, S.C.; Grubbs, R.H.; Ziller, J.W. *J. Am. Chem. Soc.* **1990**, *112*, 5384.
- (161) Lampman, G.M.; Aumiller, J.C. *Org. Synth.* **1988**, *Coll. Vol. 6*, 271.
- (162) Strong, R.L.; Rand, S.J.; Britt, J.A. *J. Am. Chem. Soc.* **1960**, *82*, 5053.
- (163) Matthews, W.S.; Bares, J.E.; Bartmess, J.E.; Bordwell, F.G.; Cornforth, F.J.; Drucker, G.E.; Margolin, Z.; McCallum, R.J.; McCollum, G.J.; Vanier, N.R. *J. Am. Chem. Soc.* **1975**, *97*, 7007.
- (164) Camenzind, M.J.; Hill, C.L. *J. Heterocycl. Chem.* **1985**, *22*, 575.

Appendix - Source Listings of Computer Programs

PROGRAM JQ

THIS PROGRAM CALCULATES THE STICK SPECTRUM FOR
A SYSTEM WITH SPIN 2 BY DIAGONALIZATION OF THE
SPIN HAMILTONIAN MATRIX:

$$H_{\text{spin}} = H * g * S + S * D * S$$

INPUT DESCRIPTION:

THE INPUT CONSISTS OF A FILE jq.inp WHICH CONTAINS THE
FOLLOWING INFORMATION IN FREE FORMAT

TITLE

D(cm-1) E(cm-1)

GZ GX GY MINFIELD(KILOGAUSS) MAXFIELD(KILOGAUSS)

THETAMIN THETAMAX DTHETA PHIMIN PHIMAX DPHI

FREQUENCY(GHz) SCREEN(BOOLEAN, FOR OUTPUT DISPLAY)

THE ORIENTATION OF THE PRINCIPAL AXES WRT THE MAGNETIC FIELD
IS VARIED AND THE RESONANT FIELDS AND TRANSITION PROBABILITIES
ARE CALCULATED FOR EACH TRANSITION AT EACH ORIENTATION.
SECANT METHOD ITERATIVE REGRESSION IS USED TO OBTAIN THE
RESONANT FIELDS. THE EIGENVALUES AND CORRESPONDING
EIGENVECTORS ARE COMPUTED USING STANDARD ROUTINES (WILKINSON).
THE TRANSITION MOMENT IS COMPUTED FROM THE EIGENVECTORS.
THE AASA-VAN GAARD FIELD SWEEP FACTOR IS APPROXIMATED AS
1/(G DELTA MS).

THE OUTPUT CONSISTS OF THE TRANSITION LABEL (I*J), THE RESONANT
FIELD IN KILOGAUSS, THE TRANSITION MOMENT (DIMENSIONLESS),
THE FIELD-SWEEP FACTOR (DIMENSIONLESS), THETA AND PHI. WHICH
ARE WRITTEN TO THE BINARY FILE jq.out. INFORMATION ON THE
PROGRAM'S PERFORMANCE IS WRITTEN TO THE FILE jq.log.

REFERENCES:

J.D. SWALEN, H.M. GLADNEY, IBM J.RES.DEV. 8,515 (1964)

R. AASA, T. VANNGARD, J.MAGN.RESON. 19,308 (1975).

G. VAN VEEN, J.MAGN.RESON. 30,91 (1978).

R.R. DE BIASI, J.A.M. MENDONCA, COMP.PHYS.COMMUN.
28,69 (1982).

R.P.BONOMO, A.J. DI BILIO AND F.RIGGI CHEM.PHYS.,(1990)
IN PRESS.

DIMENSION TRMT(300000),CAMPO(300000),HM(3),WE(5)
DIMENSION ICOMP(20),JCOMP(20),HCOMP(20),VAFAC(30
& 0000),TET(300000),PH(300000),LABEL(300000)
COMPLEX W(30,30)
LOGICAL SCREEN,ALLOWED
COMMON/EIGEN/WR(5,5)
COMMON/EVEC/W
COMMON/HPARAM/GZ,GX,GY,D1,E1,CTETA,STETA,CPhi,SPHI
CHARACTER*60 TITLE
REAL KK,HMIN,HMAX,HNEW,HOLD,H,DH,DM
INTEGER*4 NDT,NDTI,KL
* TOL --IN KILOGAUSS--

```

TOL=0.001
OPEN(UNIT=1,NAME='jq.inp',TYPE='old')
READ(1, '(A60)') TITLE
READ(1, *) D,E
*      CALCULATES ZERO-FIELD SPLITTING
GY=0.0
GX=0.0
GZ=0.0
H=0.0
NDIAG=0
D1=D/0.0333564
E1=E/0.0333564
CALL ENERGY(H,NDIAG)
ZFS1=0.0333564*ABS(WR(5,5)-WR(3,3))
ZFS2=0.0333564*ABS(WR(3,3)-WR(1,1))
DZZ=2.*D/3.
DXX=-D/3.+E
DYY=-D/3.-E
READ(1, *) GZ,GX,GY,HMIN,HMAX
READ(1, *) TMIN,TMAX,DTETA,PMIN,PMAX,DPHI
READ(1, *) FR,SCREEN
IF (SCREEN) TYPE 70
TYPE*, ''
NDT=0
NDTI=1
JMIN=2
JMAX=5
*
SWEEP POLAR ANGLES
DO 29 ATETA=TMIN,TMAX,DTETA
TETA=0.0174532*ATETA
DO 28 APhi=PMIN,PMAX,DPHI
PHI=0.0174532*APHI
IF (TETA.EQ.0.AND.PHI.GT.1E-6) GOTO 28
STETA=SIN(TETA)
CTETA=COS(TETA)
SPHI=SIN(PHI)
CPHI=COS(PHI)
*      LOOP OVER TRANSITIONS
DO 26 I=1,4
JMIN=I+1
JMAX=I+2
IF (JMAX.GE.5) THEN JMAX=5
DO 24 J=JMIN,JMAX
HOLD=HMIN
HNEW=HMAX
H=HNEW
CALL ENERGY(H,NDIAG)
XNEW=WR(6-J,6-J)-WR(6-I,6-I)-FR
H=HOLD
CALL ENERGY(H,NDIAG)
XOLD=WR(6-J,6-J)-WR(6-I,6-I)-FR
DO 16 L=1,20
DH=(HOLD-HNEW)*XNEW/(XNEW-XOLD)
HOLD=HNEW
XOLD=XNEW
HNEW=HNEW+DH
H=HNEW
CALL ENERGY(H,NDIAG)

```

```

XNEW=WR(6-J,6-J)-WR(6-I,6-I)-FR
IF(ABS(DH).LT.TOL.OR.XNEW.EQ.0) GO TO 20
IF(L.GE.19) GO TO 24
16    CONTINUE
20    NDT=NDT+1
DM=REAL(J-I)
CALL INTENSITY(TM,WR(6-J,6-J),WR(6-I,6-I),DHDHNU,DM)
IF (SCREEN) TYPE 60, I,J,H*1000,TM,ATETA,APHI,DHDHNU
LABEL(NDTI)=I*J
CAMPO(NDTI)=H
TET(NDTI)=STETA
PH(NDTI)=SPHI
TRMT(NDTI)=TM
VAFAC(NDTI)=DHDHNU
NDTI=NDTI+1
24    CONTINUE
26    CONTINUE
28    CONTINUE
29    CONTINUE
*
*    THE SPECTRUM IS STORED NUMERICALLY AND SAVED
*    AS BINARY FILE jq.out
*
    OPEN(UNIT=6,TYPE='UNKNOWN',NAME='jq.out'
& ,FORM='UNFORMATTED')
    NDTI=NDTI-1
    WRITE(6) TITLE
    WRITE(6) GZ,GX,GY,D,E,FR
    WRITE(6) HMIN*1000,HMAX*1000,NDTI
    DO 30 KL=1,NDTI
& ,TET(KL),CAMPO(KL),TRMT(KL),VAFAC(KL)
    ,TET(KL),PH(KL)
30    CONTINUE
    CLOSE(UNIT=6)
    OPEN(UNIT=6,TYPE='UNKNOWN',NAME='jq.log')
    WRITE(6, '(A60)') TITLE
    WRITE(6,*) GZ,GX,GY,D,E,FR,QUANTO
    WRITE(6,*) HMIN*1000,HMAX*1000
    WRITE(6,*) 'NUMBER OF TRANSITIONS FOUND=',NDT
    WRITE(6,*) 'NUMBER OF TRANSITIONS INCLUDED=',NDTI
    WRITE(6,*) 'NUMBER OF DIAGONALIZATIONS=',NDIAG
    CLOSE(UNIT=6)
70    FORMAT(3X,I1,'-',I1,5X,F7.1,4X,F8.5,4X,F5.1,4X,F5.1,4X,F5.3)
& 'TETA',6X,'PHI',4X,'dH/dhv')
80    FORMAT(X,I2,X,F6.1,X,F5.3,X,F5.3,X,F7.4,X,F7.4)
90    FORMAT(X,'gz=',F6.4,3X,'gx=',F6.4,3X,'gy=',F6.4)
100   FORMAT(X,'D=',F5.3,3X,'E=',F6.4,3X,'AlphaD=',F4.1,3X
& 'Fr.',F6.3,X,'GHz',X,(' ',F5.3,X,'cm-1','))
200   FORMAT(X,'Dzz=',F7.4,3X,'Dxx=',F7.4,3X,'Dyy=',F7.4)
300   FORMAT(X,'zfs1 =' ,F6.4,X,'cm-1',2X,'zfs2 =' ,F6.4,X,'cm-1')
    END
*
*    ENERGY
*
    SUBROUTINE ENERGY(H,NDIAG)
    DIMENSION ENER(5)
    COMPLEX W(30,30),CPA

```

```

COMMON/DGCOM2/DF6700,N,XMCHEP,TOL,CPA(30),TAU(2,30)
COMMON/EVEC/W
COMMON/EIGEN/WR(5,5)
COMMON/HPARAM/GZ,GX,GY,D,E,CT,ST,CP,SP
XMCHEP=1.0E-7
N=5
GHZ=1.39961*GZ*H*CT
GHX=1.39961*GX*H*ST*CP
GHY=1.39961*GY*H*ST*SP
W(1,1)=CMPLX(2.0*GHZ+2.0*D,0.0)
W(2,2)=CMPLX(GHZ-D,0.0)
W(3,3)=CMPLX(-2.0*D,0.0)
W(4,4)=CMPLX(-GHZ-D,0.0)
W(5,5)=CMPLX(-2.0*GHZ+2.0*D,0.0)
W(1,2)=CMPLX(GHX,-1.0*GHY)
W(1,3)=CMPLX(2.44949*E,0.0)
W(1,4)=CMPLX(0.0,0.0)
W(1,5)=CMPLX(0.0,0.0)
W(2,3)=CMPLX(1.224745*GHX,-1.224745*GHY)
W(2,4)=CMPLX(3.0*E,0.0)
W(2,5)=CMPLX(0.0,0.0)
W(3,4)=CMPLX(1.224745*GHX,-1.224745*GHY)
W(3,5)=CMPLX(2.44949*E,0.0)
W(4,5)=CMPLX(GHX,-1.0*GHY)
W(2,1)=CONJG(W(1,2))
W(3,2)=CONJG(W(2,3))
W(4,3)=CONJG(W(3,4))
W(5,3)=CONJG(W(3,5))
W(5,4)=CONJG(W(4,5))
W(3,1)=CONJG(W(1,3))
W(4,1)=(0.0,0.0)
W(5,1)=(0.0,0.0)
W(4,2)=CONJG(W(2,4))
W(5,2)=(0.0,0.0)
CALL HHERM (W,30)
CALL QRSTD (ENER,30)
DO I=1,5
  WR(I,I)=ENER(I)
END DO
NDIAG=NDIAG+1
END
*
```

```

* TRANSITION MOMENT
*
```

```

SUBROUTINE INTENSITY(TM,WHI,WLO,DHNU,DMS)
DIMENSION SPINZ(5),SPINXY(4)
COMPLEX CPA(30),W(30,30),VECTOR(30,2)
COMPLEX SPIU,SMENO,SZ,SX,SY
COMMON/EVEC/W
COMMON/DGCOM2/DF6700,N,XMCHEP,TOL,CPA,TAU(2,30)
COMMON/HPARAM/GZ,GX,GY,D,E,CTETA,STETA,CPhi,SPHI
CALL CORA(WHI,1,W,30)
DO 100 J=1,5
  VECTOR(J,1)=CPA(J)
  CALL CORA(WLO,1,W,30)
DO 200 J=1,5
  VECTOR(J,2)=CPA(J)
  SZ=(0.0,0.0)
```

100

200

```

SPIU=(0.0,0.0)
SMENO=(0.0,0.0)
*   Calcolo di <ilSzlj>
SPINZ(1)=2.0
SPINZ(2)=1.0
SPINZ(3)=0.0
SPINZ(4)=-1.0
SPINZ(5)=-2.0
DO 1 J=1,5
SZ=SZ+SPINZ(J)*VECTOR(J,2)*CONJG(VECTOR(J,1))
1  CONTINUE
*   Calcolo di <ilS+l> e <ilS-l>
SPINXY(1)=2.0
SPINXY(2)=2.44949
SPINXY(3)=2.44949
SPINXY(4)=2.0
DO 2 J=1,4
SPIU=SPIU+SPINXY(J)*VECTOR(J+1,2)*CONJG(VECTOR(J,1))
SMENO=SMENO+SPINXY(J)*VECTOR(J,2)*CONJG(VECTOR(J+1,1))
2  CONTINUE
SX=(0.5,0.0)*(SPIU+SMENO)
SY=(0.0,-0.5)*(SPIU-SMENO)
TM=CABS(GX*CTETA*CPHI*SX+GY*CTETA*STETA*SY
& -GZ*STETA*SZ)**2+CABS(GX*SPHI*SX-GY*CPHI*SY)**2
DHDHNU=SQRT((GX*CTETA)**2+(GX*STETA*CPHI)**2+(GY*STETA*SPHI)**2)
DHDHNU=1/DHDHNU/DMS
RETURN
END

*
*   SUBROUTINE HHERM
*
SUBROUTINE HHERM(A6700,NFORT)
*   SLIGHT MODIFICATION OF HHERM FOR EFFICIENT LINKING TO
*   NERULDA HHERM, QRSTD, TRIDIM, REVERSE AND QRHERM WERE
*   WRITTEN BY PETER A. BUSINGER AND WERE OBTAINED FROM
*   THE VIM PROGRAM LIBRARY ( F2 UTEX HERM F2 UTEX HERMQR).
*   THESE PROGRAMS ARE IN TURN TRANSLATIONS OF ALGOL PROCES-
*   DURES DUE TO WILKINSON (NUM. MATH. 4, 368 (1962)), AND
*   MUELLER (NUM. MATH. 8, 72 (1966)).
REAL A(2,30,30)
COMPLEX A6700(NFORT,NFORT)
INTEGER R,RM1
COMMON/DGCOM1/B(30),C(30),SKIPA,SKIP(30,6),SKIPFX(2)
COMMON/DGCOM2/DF6700
COMMON/DGCOM2/N,XMCHEP,TOL,CPA(30),TAU(2,30)
COMPLEX CPA,CTAU(30)
EQUIVALENCE (CTAU,TAU)
REAL MCHEPS
GAMMA=XMCHEP**2
DO 5 I=1,N
DO 5 J=1,N
A(1,I,J)=REAL(A6700(I,J))
A(2,I,J)=AIMAG(A6700(I,J))
5  CONTINUE
NM1=N-1
TOL=0.
DO 20 I=1,N
DO 20 J=1,I

```

```

DO 20 L=1,2
ABVAL=ABS(A(L,I,J))
IF (ABVAL-TOL) 20,20,10
10  TOL=ABVAL
20  CONTINUE
   IF (N.LE.2) GOTO 121
21  CONTINUE
   DO 121 R=2,NM1
   RM1=R-1
   VR=0.
   TAU(1,R)=0.
   TAU(2,R)=0.
   TAU(2,1)=0.
   DO L=R,N
   VR=VR+A(1,L,RM1)**2+A(2,L,RM1)**2
   END DO
   IF (VR-GAMMA*TOL**2) 121,121,30
30  IF (A(1,R,RM1)) 60,40,60
40  IF (A(2,R,RM1)) 60,50,60
50  A(1,R,RM1)=SQRT(VR)
   DELTA=VR
   TAU(1,1)=-A(1,R,RM1)
   GOTO 70
60  ROOT=SQRT((A(1,R,RM1)**2+A(2,R,RM1)**2)*VR)
   DELTA=VR+ROOT
   RATIO=VR/ROOT
   TAU(1,1)=-RATIO*A(1,R,RM1)
   TAU(2,1)=RATIO*A(2,R,RM1)
   A(1,R,RM1)=(RATIO+1)*A(1,R,RM1)
   A(2,R,RM1)=(RATIO+1)*A(2,R,RM1)
70  DO 90 J=R,N
   TAU(1,J)=A(1,J,RM1)/DELTA
   TAU(2,J)=A(2,J,RM1)/DELTA
   B(J)=0.
   C(J)=0.
   DO 80 L=R,J
   C(J)=C(J)+A(1,J,L)*A(1,L,RM1)-A(2,J,L)*A(2,L,RM1)
   B(J)=B(J)+A(1,J,L)*A(2,L,RM1)+A(2,J,L)*A(1,L,RM1)
80  CONTINUE
81  IF (J.EQ.N) GOTO 91
   JPLUS1=J+1
   DO 90 L=JPLUS1,N
   C(J)=C(J)+A(1,L,J)*A(1,L,RM1)+A(2,L,J)*A(2,L,RM1)
   B(J)=B(J)+A(1,L,J)*A(2,L,RM1)-A(2,L,J)*A(1,L,RM1)
90  CONTINUE
91  CONTINUE
   RHO=0.
   DO 100 L=R,N
   RHO=RHO+C(L)*TAU(1,L)+B(L)*TAU(2,L)
100 CONTINUE
   DO 110 I=R,N
   DO 110 J=R,I
   X1=TAU(1,I)*C(J)+TAU(2,I)*B(J)
   X2=TAU(2,I)*C(J)-TAU(1,I)*B(J)
   Q1=C(I)-RHO*A(1,I,RM1)
   Q2=B(I)-RHO*A(2,I,RM1)
   T1=Q1*TAU(1,J)+Q2*TAU(2,J)
   T2=Q2*TAU(1,J)-Q1*TAU(2,J)

```



```

      A(1,I,J)=A(1,I,J)-X1-T1
      A(2,I,J)=A(2,I,J)-X2-T2
110    CONTINUE
      TAU(1,R)=TAU(1,1)
      TAU(2,R)=TAU(2,1)
120    CONTINUE
121    CONTINUE
      DO 130 I=1,N
      C(I)=A(1,I,I)
130    CONTINUE
      IF (NM1) 150,150,140
140    TAU(1,N)=A(1,N,NM1)
      TAU(2,N)=-A(2,N,NM1)
150    TAU(1,1)=1.
      B(N)=0.
      TAU(2,1)=0.
152    IF (N.EQ.1) GOTO 200
      DO 180 I=2,N
      IM1=I-1
      BB=SQRT(TAU(1,I)*TAU(1,I)+TAU(2,I)*TAU(2,I))
      B(IM1)=BB
      IF (BB) 170,160,170
160    TAU(1,I)=1.
      BB=1.
170    TT1=TAU(1,I)*TAU(1,IM1)-TAU(2,I)*TAU(2,IM1)
      TT2=TAU(1,I)*TAU(2,IM1)+TAU(2,I)*TAU(1,IM1)
      TAU(1,I)=TT1/BB
      TAU(2,I)=TT2/BB
180    CONTINUE
200    CONTINUE
      DO 220 I=1,N
      DO 220 J=1,N
220    A6700(I,J)=CMPLX(A(1,I,J),A(2,I,J))
      RETURN
      END
      *
* SUBROUTINE QRSTD
*
      SUBROUTINE QRSTD(E,NFORT)
      REAL E(NFORT)
      COMMON/DGCOM1/BETA(30),ALPHA(30),RNORM,BB(60),SKIP(30,4)
      COMMON/DGCOM1/SKIPFX(2)
      COMMON/DGCOM2/DF6700
      COMMON/DGCOM2/N,ETA,TOL,SKIPA(30,4)
      DO I=1,N
      E(I)=ALPHA(I)
      BB(I+1)=BETA(I)**2
      END DO
      BB(1)=0.0
      BB(N+1)=0.0
      RNORM=0.0
      DO 5 I=1,N
5      RNORM=AMAX1(RNORM,SQRT(BB(I))+ABS(E(I))+SQRT(BB(I+1)))
      DELTA=ETA*RNORM
      EPS=DELTA**2
      IF (EPS.EQ.0) RETURN
      K=N
6      M=K

```

```

      IF (M.LE.0) GOTO 56
8      K=K-1
      IF (BB(K+1).GE.EPS) GOTO 8
      IF (K.NE.M-1) GOTO 13
      BB(K+1)=0.0
      GOTO 6
13     T=E(M)-E(M-1)
      R=BB(M)
      IF (K.GE.M-2) GOTO 22
      W=BB(M-1)
      C=T**2
      S=R/(C+W)
      IF (S*(W+S*C).GE.EPS) GOTO 22
      M=M-1
      BB(M+1)=0.0
      GOTO 13
22     IF (ABS(T).GE.DELTA) GOTO 25
      S=SQRT(R)
      GOTO 28
25     W=2.0/T
      S=W*R/(SQRT(W**2*R+1.0)+1.0)
28     IF (K.NE.M-2) GOTO 33
      E(M)=E(M)+S
      E(M-1)=E(M-1)-S
      BB(K+1)=0.0
      GOTO 6
33     SHIFT=E(M)+S
      IF (ABS(T).GE.DELTA) GOTO 37
      W=E(M-1)-S
      IF (ABS(W).LT.ABS(SHIFT)) SHIFT=W
37     S=0.0
      G=E(K+1)-SHIFT
      C=1.0
      GOTO 45
40     C=P/T
      S=W/T
      W=G
      EK1=E(K+1)
      G=C*(EK1-SHIFT)-S*W
      E(K)=(W-G)+EK1
45     IF (ABS(G).GE.DELTA) GOTO 48
      IF (G.GE.0.0) GOTO 47
      G=G-C*DELTA
      GOTO 48
47     G=G+C*DELTA
48     P=G**2/C
      K=K+1
      W=BB(K+1)
      T=W+P
      BB(K)=S*T
50     IF (K.LT.M) GOTO 40
      E(K)=G+SHIFT
      GOTO 6
56     IF (N.EQ.1) RETURN
      N1=N-1
      DO 70 I=1,N1
      K=I
      T=E(I)

```

```

I1=I+1
DO 62 J=I1,N
IF (E(J).LE.T) GOTO 62
T=E(J)
K=J
62  CONTINUE
IF (I.EQ.K) GOTO 70
E(K)=E(I)
E(I)=T
70  CONTINUE
RETURN
END
*
*  SUBROUTINE CORA
*
*      J.H. WILKINSON CALCULATION OF THE EIGENVECTORS OF A
*  SYMMETRIC TRIDIAGONAL MATRIX BY INVERSE ITERATION.
*  NUMERISCHE MATHEMATIK 4, 368 (1962).
SUBROUTINE CORA(EIGEN,NEIGEN,BBB,NFORT)
REAL LAMBDA,NORM,M,INT
COMPLEX BBB(NFORT,NFORT),CALPHA
COMMON/DGCOM1/B(30),C(30),NORM,M(30),P(30),Q(30),R(30)
COMMON/DGCOM1/INT(30),X(32)
COMMON/DGCOM2/DF6700
COMMON/DGCOM2/N,XMCHEP,TOL,CPA(30),TAU(2,30)
COMPLEX CPA,CTAU(30)
EQUIVALENCE (CTAU,TAU)
REAL MCHEPS
DATA LAMBDA/0./
MCHEPS=XMCHEP
GAMMA=MCHEPS**2
EPS=MCHEPS*NORM
IF (NEIGEN.NE.1) GOTO 10
LAMBDA=EIGEN
GOTO 20
10  LAMBDA=LAMBDA-EPS
IF (EIGEN.LT.LAMBDA) LAMBDA=EIGEN
20  CONTINUE
U=C(1)-LAMBDA
V=B(1)
IF (V.EQ.0) V=EPS
NMIN1=N-1
DO 60 I=1,NMIN1
BI=B(I)
IF (BI.EQ.0) BI=EPS
BI1=B(I+1)
IF (BI1.EQ.0) BI1=EPS
IF (ABS(BI).LT.ABS(U)) GOTO 50
M(I+1)=U/BI
IF ((M(I+1).EQ.0).AND.(BI.LE.EPS)) M(I+1)=1
P(I)=BI
Q(I)=C(I+1)-LAMBDA
R(I)=BI1
U=V-M(I+1)*Q(I)
V=-M(I+1)*R(I)
INT(I+1)=+1
GOTO 60
50  M(I+1)=BI/U

```

```

P(I)=U
Q(I)=V
R(I)=0
U=C(I+1)-LAMBDA-M(I+1)*V
V=BI1
INT(I+1)=-1
60  CONTINUE
P(N)=U
Q(N)=0
R(N)=0
X(N+1)=0
X(N+2)=0
H=0
ETA=1.0/N
DO II=1,N
I=N-II+1
U=ETA-Q(I)*X(I+1)-R(I)*X(I+2)
IF (P(I).NE.0) GOTO 65
X(I)=U/EPS
GOTO 66
65  X(I)=U/P(I)
66  H=H+ABS(X(I))
END DO
DO I=1,N
X(I)=X(I)/H
END DO
DO 75 I=2,N
IF (INT(I).LE.0) GOTO 70
U=X(I-1)
X(I-1)=X(I)
X(I)=U-M(I)*X(I-1)
GOTO 75
70  X(I)=X(I)-M(I)*X(I-1)
75  CONTINUE
H=0
DO II=1,N
I=N-II+1
U=X(I)-Q(I)*X(I+1)-R(I)*X(I+2)
IF (P(I).NE.0) GOTO 80
X(I)=U/EPS
GOTO 81
80  X(I)=U/P(I)
81  H=H+X(I)**2
END DO
H=SQRT(H)
GT2=GAMMA*TOL**2
CPA(1)=CMPLX(X(1)/H,0.)
DO J=2,N
CPA(J)=CMPLX(X(J)/H,0.)*CONJG(CTAU(J))
END DO
N2=N-2
DO 160 MR=1,N2
IR=N-MR
IRM1=IR-1
IF (B(IRM1).LE.GT2) GOTO 160
DELTA=B(IRM1)*CABS(BBB(IR,IRM1))
CALPHA=(0.,0.)
DO K=IR,N

```

150

CALPHA=CALPHA+CPA(K)*CONJG(BBB(K,IRM1))

END DO

CALPHA=CALPHA/DELTA

DO K=IR,N

CPA(K)=CPA(K)-BBB(K,IRM1)*CALPHA

END DO

160

CONTINUE

RETURN

END

Typical input file jq.inp
Rakesh's Quintet Simulation
0.0207 0.0047
2.0023 2.0023 2.0023 0.000 2.000
0.0 90.0 1.0 0.0 90.0 1.0
9.27 F

PROGRAM JQS

* Program jq reads the stick spectrum jq.out calculated
 * by means of program jq and adds a Gaussian lineshape to
 * each "single crystal transition"
 * Input:

* File jq.out -

* Stick spectrum.

* File jq.inp -

* WZ1,WX1,WY1 principal linewidth components (Gauss)

* HMIN,HMAX spectral limits (Gauss)

* NPOINT number of points (range=(HMAX-HMIN)/NPOINT)

* Single lines have 2*SIGMA peak-to-peak width in the
 * derivative spectra

* References:

* R.Aasa and T.Vanngard J.Magn.Reson., 19(1975)308.

* G.van Veen J.Magn.Reson., 79(1975)1129.

* R.P. Bonomo,A.J. Di Bilio and F. Riggi, Chem.Phys., (1991)

* CHARACTER*60 TITLE

* REAL H,HMIN,HMAX,NPOINT,HIFLD,LOWFLD

* REAL LOWNDP,HINDP,H1,MI,MI53

* DIMENSION VAFAC(150000),TM(150000)

* DIMENSION FIELD(150000),SPEC(10000),CAMPO(10000)

* DIMENSION ST(150000),SP(150000),LABEL(150000)

* DIMENSION WZ1(20),WX1(20),WY1(20)

* OPEN(UNIT=1,TYPE='OLD',NAME='jq.out',READONLY,FORM='UNFORMATTED')

* READ(1) TITLE

* READ(1) GZ,GX,GY,D,E,FR

* READ(1) HMIN,HMAX,NDT

* DO I=1,NDT

* READ(1) LABEL(I),FIELD(I),TM(I),VAFAC(I),ST(I),SP(I)

* END DO

* CLOSE(1)

* TYPE*, TITLE, D, E, FR, NDT

* *****

* Transitions are labelled as follows:

TRANSITION	LABEL
1-2	2
1-3	3
1-4	4
1-5	5
2-3	6
2-4	8
2-5	10
3-4	12
3-5	15
4-5	20

* *****

* OPEN(UNIT=2,TYPE='OLD',NAME='jq.inp',ACCESS='SEQUENTIAL')

```

READ(2,*) WZ1(2),WX1(2),WY1(2)
READ(2,*) WZ1(3),WX1(3),WY1(3)
READ(2,*) WZ1(4),WX1(4),WY1(4)
READ(2,*) WZ1(5),WX1(5),WY1(5)
READ(2,*) WZ1(6),WX1(6),WY1(6)
READ(2,*) WZ1(8),WX1(8),WY1(8)
READ(2,*) WZ1(10),WX1(10),WY1(10)
READ(2,*) WZ1(12),WX1(12),WY1(12)
READ(2,*) WZ1(15),WX1(15),WY1(15)
READ(2,*) WZ1(20),WX1(20),WY1(20)
READ(2,*) HMIN,HMAX,NPOINT
CLOSE(2)
DO I=1,4
  JK=I+1
  DO JL=JK,5
    JJ=I*JL
    WZ1(JJ)=WZ1(JJ)/1000.
    WX1(JJ)=WX1(JJ)/1000.
    WY1(JJ)=WY1(JJ)/1000.
  END DO
END DO
HMIN=HMIN/1000.
HMAX=HMAX/1000.
RANGE=(HMAX-HMIN)/NPOINT
*      *****
*      THE SPECTRUM IS ACTUALLY COMPUTED BETWEEN LIMITS
*      HMIN-LOWFLD AND HMAX+HIFLD
HIFLD=0.15/RANGE
IF (HMIN.LT.0.15) THEN
  LOWFLD=HMIN/RANGE
ELSE
  LOWFLD=HIFLD
END IF
HINDP=INT(HIFLD)
LOWNDP=INT(LOWFLD)
LOWFLD=LOWNDP*RANGE
HIFLD=HINDP*RANGE
HMAX=HMAX+HIFLD
HMIN=HMIN-LOWFLD
NPOINT=NPOINT+HINDP+LOWNDP
*      *****
DO I=1,NPOINT
  SPEC(I)=0.
END DO
DO 100 I=1,NPOINT+1
  CAMPO(I)=HMIN + (I-1)*RANGE
  DO 653 J=1,NDT
    H=FIELD(J)
    IF (H.LT.HMIN) GOTO 653
    IF (H.GT.HMAX) GOTO 653
    CT=SQRT(1-ST(J)*ST(J))
    CP=SQRT(1-SP(J)*SP(J))
    WZ=WZ1(LABEL(J))
    WX=WX1(LABEL(J))
    WY=WY1(LABEL(J))
    SIGMA=0.
    SIGMA = SQRT((WZ*CT)**2+(WX*CP*ST(J))
& **2 + (WY*ST(J)*SP(J))**2)

```



```

SIGMAI=5.*SIGMA
SIGMA2=SIGMA*SIGMA
SIGMA3=2.50663*SIGMA*SIGMA*SIGMA
IF (H-SIGMAI-HMIN) 65,67,67
65  IMIN=1
    GOTO 66
67  IMIN=IFIX(1.+(H-SIGMAI-HMIN)/RANGE)
66  IF (H+SIGMAI-HMAX) 64,68,68
68  IMAX=NPOINT+1
    GOTO 63
64  IMAX=IFIX(1.+(H+SIGMAI-HMIN)/RANGE)
63  TR=TM(J)*ST(J)*VAFAC(J)
    DO 650 INI=IMIN, IMAX
        VARH=CAMPO(INI)-H
91  CURVE=-TR*(VARH/SIGMA3)*EXP(-(VARH*VARH)/(2*SIGMA2))
93  SPEC(INI)=SPEC(INI)+CURVE
650  CONTINUE
653  CONTINUE
    OPEN(UNIT=3,TYPE='UNKNOWN',NAME='jqs.out')
    *      *****
    MAXPOINT=NPOINT-HINDP+1
    MINPOINT=LOWNDP+1
    HMAX=HMAX-HIFLD
    HMIN=HMIN+LOWFLD
    *      *****
    *      See Basic Library Function -WINDOW-
    DIFF=(HMAX-HMIN)/10
    DO I=MINPOINT,MAXPOINT
        CAMPO(I)=((CAMPO(I)-HMIN)/DIFF)-5
    END DO
    *      *****
    Y=0.
    DO I=MINPOINT,MAXPOINT
        IF (ABS(SPEC(I)).GT.Y) Y=ABS(SPEC(I))
    END DO
    HMIN=HMIN*1000
    HMAX=HMAX*1000
    *      WRITE(3,'(A60)') TITLE
    NPOINT=MAXPOINT-MINPOINT
    *      WRITE(3,*) HMIN,HMAX,NPOINT
    IF (MINPOINT.LT.0) THEN MINPOINT=0
    DO 33 KL=MINPOINT,MAXPOINT
        SPEC(KL)=SPEC(KL)/Y
        IF (SPEC(KL).LT.-1.0.OR.SPEC(KL).GT.1.0) SPEC(KL)=0
33  WRITE(3,899) CAMPO(KL),SPEC(KL)
899  FORMAT(X,2(F7.4,X))
    END

```

Typical input file jqs.inp

```
40.0 40.0 40.0
60.0 60.0 60.0
60.0 60.0 60.0
40.0 40.0 40.0
40.0 40.0 40.0
60.0 60.0 60.0
60.0 60.0 60.0
40.0 40.0 40.0
60.0 60.0 60.0
40.0 40.0 40.0
1300.0 5300.0 1000
```

PROGRAM JT

THIS PROGRAM CALCULATES THE STICK SPECTRUM FOR
A SYSTEM WITH SPIN 1 BY DIAGONALIZATION OF THE
SPIN HAMILTONIAN MATRIX:

$$H_{\text{spin}} = H \cdot g \cdot S + S \cdot D \cdot S$$

INPUT DESCRIPTION:

THE INPUT CONSISTS OF A FILE jt.inp WHICH CONTAINS THE
FOLLOWING INFORMATION IN FREE FORMAT

TITLE

D(cm-1) E(cm-1)

GZ GX GY MINFIELD(KILOGAUSS) MAXFIELD(KILOGAUSS)

THETAMIN THETAMAX DTHETA PHIMIN PHIMAX DPHI

FREQUENCY(GHz) SCREEN(BOOLEAN, FOR OUTPUT DISPLAY)

THE ORIENTATION OF THE PRINCIPAL AXES WRT THE MAGNETIC FIELD
IS VARIED AND THE RESONANT FIELDS AND TRANSITION PROBABILITIES
ARE CALCULATED FOR EACH TRANSITION AT EACH ORIENTATION.

SECANT METHOD ITERATIVE REGRESSION IS USED TO OBTAIN THE

RESONANT FIELDS. THE EIGENVALUES AND CORRESPONDING

EIGENVECTORS ARE COMPUTED USING STANDARD ROUTINES (WILKINSON).

THE TRANSITION MOMENT IS COMPUTED FROM THE EIGENVECTORS.

THE AASA-VAN GAARD FIELD SWEEP FACTOR IS APPROXIMATED AS
1/(G DELTA MS).

THE OUTPUT CONSISTS OF THE TRANSITION LABEL (I*J), THE RESONANT
FIELD IN KILOGAUSS, THE TRANSITION MOMENT (DIMENSIONLESS),
THE FIELD-SWEEP FACTOR (DIMENSIONLESS), THETA AND PHI. WHICH
ARE WRITTEN TO THE BINARY FILE jt.out. INFORMATION ON THE
PROGRAM'S PERFORMANCE IS WRITTEN TO THE FILE jt.log.

REFERENCES:

J.D. SWALEN, H.M. GLADNEY, IBM J.RES.DEV. 8,515 (1964)

R. AASA, T. VANNGARD, J.MAGN.RESON. 19,308 (1975).

G. VAN VEEN, J.MAGN.RESON. 30,91 (1978).

R.R. DE BIASI, J.A.M. MENDONCA, COMP.PHYS.COMMUN.
28,69 (1982).

R.P.BONOMO, A.J. DI BILIO AND F.RIGGI CHEM.PHYS.,(1990)
IN PRESS.

```

DIMENSION TRMT(150000),CAMPO(150000),HM(3),WE(4)
DIMENSION ICOMP(20),JCOMP(20),HCOMP(20),VAFAC(15
& 0000),TET(150000),PH(150000),LABEL(150000)
COMPLEX W(30,30)
LOGICAL SCREEN,ALLOWED
COMMON/EIGEN/WR(3,3)
COMMON/EVEC/W
COMMON/HPARAM/GZ,GX,GY,D1,E1,CTETA,STETA,CPhi,SPHI,UT,DT,URD
CHARACTER*60 TITLE
REAL KK,HMIN,HMAX,HMINI,HMAX1,HMIN1,HINCR,
& HSUP,HINF,H,HCOMP
*   TOL --IN KILOGAUSS--
TOL=0.001
OPEN(UNIT=1,NAME='jt.inp',TYPE='old')
READ(1, '(A60)') TITLE

```

```

READ(1,*) D,E
*      CALCULATES ZERO-FIELD SPLITTING
GY=0.0
GX=0.0
GZ=0.0
H=0.0
UT=1./3.
DT=2./3.
URD=SQRT(1./2.)
D1=D/0.0333564
E1=E/0.0333564
CALL ENERGY(H,NDIAG)
ZFS=0.0333564*ABS(WR(3,3)-WR(1,1))
DZZ=2.*D/3.
DXX=-D/3.+E
DYY=-D/3.-E
READ(1,*) GZ,GX,GY,HMIN,HMAX
READ(1,*) TMIN,TMAX,DTETA,PMIN,PMAX,DPHI
READ(1,*) FR,SCREEN
CLOSE(1)
IF (SCREEN) TYPE 70
TYPE*, ''
NDT=0
NDTI=1
JMAX=3
*      SWEEP POLAR ANGLES
DO 28 ATETA=TMIN,TMAX,DTETA
TETA=0.0174532*ATETA
DO 28 APhi=PMIN,PMAX,DPHI
Phi=0.0174532*APhi
IF (TETA.EQ.0.AND.Phi.GT.1E-6) GOTO 28
STETA=SIN(TETA)
CTETA=COS(TETA)
SPHI=SIN(PHI)
CPHI=COS(PHI)
*      LOOP OVER TRANSITIONS
DO 26 I=1,2
JK=I+1
DO 24 J=JK,JMAX
HOLD=HMIN
HNEW=HMAX
H=HNEW
CALL ENERGY(H,NDIAG)
XNEW=WR(4-J,4-J)-WR(4-I,4-I)-FR
H=HOLD
CALL ENERGY(H,NDIAG)
XOLD=WR(4-J,4-J)-WR(4-I,4-I)-FR
DO 16 L=1,20
DH=(HOLD-HNEW)*XNEW/(XNEW-XOLD)
HOLD=HNEW
XOLD=XNEW
HNEW=HNEW+DH
H=HNEW
CALL ENERGY(H,NDIAG)
XNEW=WR(4-J,4-J)-WR(4-I,4-I)-FR
IF(ABS(DH).LT.TOL.OR.XNEW.EQ.0) GO TO 20
IF(L.GE.19) GO TO 24
16    CONTINUE

```

```

20   NDT=NDT+1
    DM=REAL(J-I)
    CALL INTENSITY(TM,WR(4-J,4-J),WR(4-I,4-I),DHDHNU,DM)
    IF (SCREEN) TYPE 60, IJ,H*1000,TM,ATETA,APHI,DHDHNU
    LABEL(NDTI)=I*J
    CAMPO(NDTI)=H
    TET(NDTI)=STETA
    PH(NDTI)=SPHI
    TRMT(NDTI)=TM
    VAFAC(NDTI)=DHDHNU
    NDTI=NDTI+1
24   CONTINUE
26   CONTINUE
28   CONTINUE
    *
    *   THE SPECTRUM IS STORED NUMERICALLY AND SAVED
    *   AS BINARY FILE jt.out
    *
    OPEN(UNIT=7,TYPE='UNKNOWN',NAME='jt.out'
& ,FORM='UNFORMATTED')
    NDTI=NDTI-1
    WRITE(7) TITLE
    WRITE(7) GZ,GX,GY,D,E,FR
    WRITE(7) HMIN*1000,HMAX*1000,NDTI
    DO 30 KL=1,NDTI
    WRITE(7) LABEL(KL),CAMPO(KL),TRMT(KL),VAFAC(KL),TET(KL),PH(KL)
30   CONTINUE
    CLOSE(7)
    OPEN(UNIT=6,TYPE='UNKNOWN',NAME='jt.log')
    WRITE(6,'(A60)') TITLE
    WRITE(6,*) GZ,GX,GY,D,E,FR,QUANTO
    WRITE(6,*) HMIN*1000,HMAX*1000
    WRITE(6,*) 'NUMBER OF TRANSITIONS FOUND=',NDT
    WRITE(6,*) 'NUMBER OF TRANSITIONS INCLUDED=',NDTI
    WRITE(6,*) 'NUMBER OF DIAGONALIZATIONS=',NDIAG
    CLOSE(UNIT=6)
60   FORMAT(3X,I1,'-',I1,5X,F7.1,4X,F8.5,4X,F5.1,4X,F5.1,4X,F5.3)
70   FORMAT(X,'TRANSITION',2X,'FIELD',5X,'T.MOMENT',4X,
    !   'TETA',6X,'PHI',4X,'dH/dhv')
80   FORMAT(X,I2,X,F6.1,X,F5.3,X,F5.3,X,F7.4,X,F7.4)
90   FORMAT(X,'gz=',F6.4,3X,'gx=',F6.4,3X,'gy=',F6.4)
100  FORMAT(X,'D=',F5.3,3X,'E=',F6.4,3X,'AlphaD=',F4.1,3X
    !   'Fr.',F5.3,X,'GHz',X,'('F5.3,X,'cm-1',)')
200  FORMAT(X,'Dzz=',F7.4,3X,'Dxx=',F7.4,3X,'Dyy=',F7.4)
300  FORMAT(X,'zfs =',F6.4,X,'cm-1')
    END
    *
    *   ENERGY
    *
    SUBROUTINE ENERGY(H,NDIAG)
    DIMENSION ENER(3)
    COMPLEX W(30,30),CPA
    COMMON/DGCOM2/DF6700,N,XMCHEP,TOL,CPA(30),TAU(2,30)
    COMMON/EVEC/W
    COMMON/EIGEN/WR(3,3)
    COMMON/HPARAM/GZ,GX,GY,D,E,CT,ST,CP,SP,UT,DT,URD
    XMCHEP=1.0E-7
    N=3

```

```

NDIAG=NDIAG+1
GHZ=1.39961*GZ*H*CT
GHX=1.39961*GX*H*ST*CP
GHY=1.39961*GY*H*ST*SP
W(1,1)=CMPLX(GHZ + UT*D,0.0)
W(2,2)=CMPLX(-DT*D,0.0)
W(3,3)=CMPLX(-GHZ + UT*D,0.0)
W(1,2)=CMPLX(URD*GHX,-URD*GHY)
W(2,3)=CMPLX(URD*GHX,-URD*GHY)
W(1,3)=CMPLX(E,0)
W(2,1)=CONJG(W(1,2))
W(3,2)=CONJG(W(2,3))
W(3,1)=CONJG(W(1,3))
CALL HHERM (W,30)
CALL QRSTD (ENER,30)
DO I=1,3
  WR(I,I)=ENER(I)
END DO
END

```

```

*
```

```

* TRANSITION MOMENT

```

```

*
```

```

SUBROUTINE INTENSITY(TM,WHI,WLO,DHNU,DMS)
DIMENSION SPINZ(3),SPINXY(3)
COMPLEX CPA(30),W(30,30),VECTOR(30,2)
COMPLEX SPIU,SMENO,SZ,SX,SY
COMMON/EVEC/W
COMMON/DGCOM2/DF6700,N,XMCHEP,TOL,CPA,TAU(2,30)
COMMON/HPARAM/GZ,GX,GY,D,E,CTETA,STETA,CPhi,SPHI,UT,DT,URD
CALL CORA(WHI,1,W,30)
DO 100 J=1,3
100 VECTOR(J,1)=CPA(J)
CALL CORA(WLO,1,W,30)
DO 200 J=1,4
200 VECTOR(J,2)=CPA(J)
  SZ=(0.0,0.0)
  SPIU=(0.0,0.0)
  SMENO=(0.0,0.0)
  * Calcolo di <ilSzlj>
  SPINZ(1)=1.0
  SPINZ(2)=0.0
  SPINZ(3)=-1.0
  DO 1 J=1,3
1    SZ=SZ+SPINZ(J)*VECTOR(J,2)*CONJG(VECTOR(J,1))
    CONTINUE
    * Calcolo di <ilS+l> e <ilS-l>
    SPINXY(1)=1.414
    SPINXY(2)=1.414
    DO 2 J=1,2
    SPIU=SPIU+SPINXY(J)*VECTOR(J+1,2)*CONJG(VECTOR(J,1))
    SMENO=SMENO+SPINXY(J)*VECTOR(J,2)*CONJG(VECTOR(J+1,1))
2    CONTINUE
    SX=(0.5,0.0)*(SPIU+SMENO)
    SY=(0.0,-0.5)*(SPIU-SMENO)
    TM=CABS(GX*CTETA*CPhi*SX+GY*CTETA*STETA*SY
    & -GZ*STETA*SZ)**2+CABS(GX*SPHI*SX-GY*CPhi*SY)**2
    DHNU=SQRT((GZ*CTETA)**2+(GX*STETA*CPhi)**2+(GY*STETA*SPHI)**2)
    DHNU=1/DHNU/DMS

```

RETURN

END

THIS IS AN INCOMPLETE LISTING. THIS PROGRAM ALSO MUST HAVE THE THREE SUBROUTINES HHERM, QRSTD, AND CORA IN ORDER TO BE COMPLETE. THESE, HOWEVER, ARE IDENTICAL TO THE ROUTINES IN JQ AND HAVE NOT BEEN REPRODUCED HERE IN ORDER TO SAVE SPACE. SEE THE LISTING OF JQ ABOVE FOR A COMPLETE LISTING OF THESE SUBROUTINES.

A TYPICAL INPUT FILE JT.INP
Phenyl methyl TMM
0.0195 0.00175
2.0023 2.0023 2.0023 1.300 5.300
0.0 90.0 1.0 0.0 90.0 1.0
9.27 F

PROGRAM jts

Program jts reads the stick spectrum jt.out calculated
by means of program jt and adds a Gaussian lineshape to
each "single crystal transition"

Input:

File jt.out -

Stick spectrum.

File jts.inp -

WZ1,WX1,WY1 principal linewidth components (Gauss)
HMIN,HMAX spectral limits (Gauss)
NPOINT number of points (range=(HMAX-HMIN)/NPOINT)

Single lines have 2*SIGMA peak-to-peak width in the
derivative spectra

References:

R.Aasa and T.Vanngard J.Magn.Reson., 19(1975)308.
G.van Veen J.Magn.Reson., 79(1975)1129.
R.P. Bonomo,A.J. Di Bilio and F. Riggi, Chem.Phys., (1991)

```
CHARACTER*60 TITLE
REAL H,HMIN,HMAX,NPOINT,HIFLD,LOWFLD
REAL LOWNDP,HINDP,H1,MI,MI53
DIMENSION VAFAC(150000),TM(150000)
DIMENSION FIELD(150000),SPEC(5000),CAMPO(5000)
DIMENSION ST(150000),SP(150000),LABEL(150000)
DIMENSION WZ1(12),WX1(12),WY1(12)
OPEN(UNIT=1,TYPE='OLD',NAME='jt.out',FORM='UNFORMATTED')
READ(1) TITLE
READ(1) GZ,GX,GY,D,E,FR
READ(1) HMIN,HMAX,NDT
TYPE*, TITLE
DO I=1,NDT
READ(1) LABEL(I),FIELD(I),TM(I),VAFAC(I),ST(I),SP(I)
END DO
CLOSE(1)
```

Transitions are labelled as follows:

TRANSITION	LABEL
1-2	2
1-3	3
2-3	6

```
OPEN(UNIT=2,TYPE='OLD',NAME='jts.inp')
READ(2,*) WZ1(2),WX1(2),WY1(2)
READ(2,*) WZ1(3),WX1(3),WY1(3)
READ(2,*) WZ1(6),WX1(6),WY1(6)
READ(2,*) HMIN,HMAX,NPOINT
CLOSE(2)
```

```

DO I=1,2
JK=I+1
DO JL=JK,3
JJ=I*JL
WZ1(JJ)=WZ1(JJ)/1000.
WX1(JJ)=WX1(JJ)/1000.
WY1(JJ)=WY1(JJ)/1000.
END DO
END DO
HMIN=HMIN/1000.
HMAX=HMAX/1000.
RANGE=(HMAX-HMIN)/NPOINT
*      *****
*      THE SPECTRUM IS ACTUALLY COMPUTED BETWEEN LIMITS
*      HMIN-LOWFLD AND HMAX+HIFLD
HIFLD=0.15/RANGE
IF (HMIN.LT.0.15) THEN
LOWFLD=HMIN/RANGE
ELSE
LOWFLD=HIFLD
END IF
HINDP=INT(HIFLD)
LOWNDP=INT(LOWFLD)
LOWFLD=LOWNDP*RANGE
HIFLD=HINDP*RANGE
HMAX=HMAX+HIFLD
HMIN=HMIN-LOWFLD
NPOINT=NPOINT+HINDP+LOWNDP
*      *****
DO I=1,NPOINT
SPEC(I)=0.0
END DO
DO 100 I=1,NPOINT+1
CAMPO(I)=HMIN + (I-1)*RANGE
DO 653 J=1,NDT
H=FIELD(J)
IF (H.LT.HMIN) GOTO 653
IF (H.GT.HMAX) GOTO 653
CT=SQRT(1-ST(J)*ST(J))
CP=SQRT(1-SP(J)*SP(J))
WZ=WZ1(LABEL(J))
WX=WX1(LABEL(J))
WY=WY1(LABEL(J))
SIGMA=0.
SIGMA = SQRT((WZ*CT)**2+(WX*CP*ST(J))
& **2 + (WY*ST(J)*SP(J))**2)
SIGMAI=5.*SIGMA
SIGMA2=SIGMA*SIGMA
SIGMA3=2.50663*SIGMA*SIGMA*SIGMA
IF (H-SIGMAI-HMIN) 65,67,67
65 IMIN=1
GOTO 66
67 IMIN=IFIX(1.+(H-SIGMAI-HMIN)/RANGE)
66 IF (H+SIGMAI-HMAX) 64,68,68
68 IMAX=NPOINT+1
GOTO 63
64 IMAX=IFIX(1.+(H+SIGMAI-HMIN)/RANGE)
63 TR=TM(J)*ST(J)*VAFAC(J)

```

```

DO 650 INI=IMIN,IMAX
VARH=CAMPO(INI)-H
CURVE=-TR*(VARH/SIGMA3)*EXP(-(VARH*VARH)/(2*SIGMA2))
SPEC(INI)=SPEC(INI)+CURVE
650  CONTINUE
653  CONTINUE
      OPEN(UNIT=6,TYPE='UNKNOWN',NAME='jts.out',ACCESS='SEQUENTIAL',
&  FORM='FORMATTED')
      *      *****
      MAXPOINT=NPOINT-HINDP+1
      MINPOINT=LOWNDP+1
      HMAX=HMAX-HIFLD
      HMIN=HMIN+LOWFLD
      *      *****
      *      See Basic Library Function -WINDOW-
      DIFF=(HMAX-HMIN)/10
      DO I=MINPOINT,MAXPOINT
      CAMPO(I)=((CAMPO(I)-HMIN)/DIFF)-5
      END DO
      *      *****
      Y=0.
      DO I=MINPOINT,MAXPOINT
      IF (ABS(SPEC(I)).GT.Y) Y=ABS(SPEC(I))
      END DO
      HMIN=HMIN*1000
      HMAX=HMAX*1000
      NPOINT=MAXPOINT-MINPOINT
      DO 33 KL=MINPOINT,MAXPOINT
      SPEC(KL)=SPEC(KL)/Y
33  WRITE(6,899) CAMPO(KL),SPEC(KL)
      899  FORMAT(X,2(F7.4,X))
      END

```

A TYPICAL INPUT FILE JTS.INP

```
40.0 35.0 35.0  
70.0 70.0 70.0  
40.0 35.0 35.0  
1300.0 5300.0 1000
```

Program qtp

qtp is a minor modification of program jq. It provides the turning points of the quintet spectra by calculating the resonant fields for the orientations of the molecule that have one molecular axis aligned with the external field. qtp returns to the standard output the polarization (x,y,z) of the transition, the energy levels between which the transition occurs, and the magnetic field at which it occurs. qtp is useful for assigning lines in conjunction with full spectral simulation, because its output can be used to tell what parameters to adjust in the file jq.inp to closely reproduce experimental spectra

INPUT

The input for qtp is the same as for jq, namely the file jq.inp, which has the format

TITLE

D(cm-1) E(cm-1)
GZ GX GY MINFIELD(KILOGAUSS) MAXFIELD(KILOGAUSS)
THETAMIN THETAMAX DTHETA PHIMIN PHIMAX DPHI
FREQUENCY(GHz) SCREEN(BOOLEAN, FOR OUTPUT DISPLAY)

```

DIMENSION TRMT(300000),CAMPO(300000),HM(3),WE(5)
DIMENSION ICOMP(20),JCOMP(20),HCOMP(20),VAFAC(30
& 0000),TET(300000),PH(300000),LABEL(300000),HR(15),DIR(15)
COMPLEX W(30,30)
LOGICAL SCREEN,ALLOWED
COMMON/EIGEN/WR(5,5)
COMMON/EVEC/W
COMMON/HPARAM/GZ,GX,GY,D1,E1,CTETA,STETA,CPhi,SPHI
CHARACTER*60 TITLE
CHARACTER*1 AXIS
REAL KK,HMIN,HMAX,HNEW,HOLD,H,DH,DM
INTEGER AX,DIR
INTEGER*4 NDT,NDTI,KL
*      TOL --IN KILOGAUSS--
TOL=0.001
OPEN(UNIT=1,NAME='jq.inp',TYPE='old')
READ(1, '(A60)') TITLE
READ(1,*) D,E
*      CALCULATES ZERO-FIELD SPLITTING
GY=0.0
GX=0.0
GZ=0.0
H=0.0
NDIAG=0
D1=D/0.0333564
E1=E/0.0333564
CALL ENERGY(H,NDIAG)
ZFS1=0.0333564*ABS(WR(5,5)-WR(3,3))
ZFS2=0.0333564*ABS(WR(3,3)-WR(1,1))
DZZ=2.*D/3.
DXX=-D/3.+E
DYY=-D/3.-E
READ(1,*) GZ,GX,GY,HMIN,HMAX
READ(1,*) TMIN,TMAX,DTETA,PMIN,PMAX,DPHI

```

```

READ(1,*) FR,SCREEN
NDT=0
NDTI=1
JMIN=2
JMAX=5
*    SWEEP POLAR ANGLES
DO 29 ATETA=0.0,90.0,90.0
TETA=0.0174532*ATETA
DO 28 APhi=0.0,90.0,90.0
PHI=0.0174532*APHI
IF (TETA.EQ.0.AND.PHI.GT.1E-6) GOTO 28
STETA=SIN(TETA)
CTETA=COS(TETA)
SPHI=SIN(PHI)
CPHI=COS(PHI)
*    LOOP OVER TRANSITIONS
DO 26 I=1,4
J=I+1
HOLD=HMIN
HNEW=HMAX
H=HNEW
CALL ENERGY(H,NDIAG)
XNEW=WR(6-J,6-J)-WR(6-I,6-I)-FR
H=HOLD
CALL ENERGY(H,NDIAG)
XOLD=WR(6-J,6-J)-WR(6-I,6-I)-FR
DO 16 L=1,20
DH=(HOLD-HNEW)*XNEW/(XNEW-XOLD)
HOLD=HNEW
XOLD=XNEW
HNEW=HNEW+DH
H=HNEW
CALL ENERGY(H,NDIAG)
XNEW=WR(6-J,6-J)-WR(6-I,6-I)-FR
IF (ABS(DH).LT.TOL.OR.XNEW.EQ.0) GO TO 20
IF (L.GE.19) GO TO 26
16  CONTINUE
20  NDT=NDT+1
DM=REAL(J-I)
CALL INTENSITY(TM,WR(6-J,6-J),WR(6-I,6-I),DHDHNU,DM)
IF (ATETA.EQ.0) THEN
AX=0
ELSEIF (APHI.EQ.0) THEN
AX=1
ELSE
AX=2
ENDIF
DIR(NDTI)=AX
LABEL(NDTI)=I
CAMPO(NDTI)=H
HR(NDTI)=H
TET(NDTI)=STETA
PH(NDTI)=SPHI
TRMT(NDTI)=TM
VAFAC(NDTI)=DHDHNU
NDTI=NDTI+1
26  CONTINUE
CONTINUE

```

```

29      CONTINUE
        DO 31 I=1,12
        DO 30 J=1,12
        IF (HR(I).GE.HR(J)) GO TO 30
        A=HR(I)
        B=HR(J)
        HR(I)=B
        HR(J)=A
30      CONTINUE
31      CONTINUE
        TYPE 50, D, E
        DO 33 I=1,12
        DO 32 J=1,12
        IF (HR(I).NE.CAMPO(J)) GO TO 32
        IF (DIR(J).EQ.0) THEN
        AXIS='Z'
        ELSEIF (DIR(J).EQ.1) THEN
        AXIS='X'
        ELSE
        AXIS='Y'
        ENDIF
        TYPE 60, AXIS,LABEL(J),LABEL(J)+1,CAMPO(J)*1000
32      CONTINUE
33      CONTINUE
        50      FORMAT(X,'D='F6.5,X,'cm -1',X,'E='F6.5,X,'cm -1')
60      FORMAT(X,A1,X,I1,'-',I1,3X,F6.1)
70      FORMAT(X,'TRANSITION',2X,'FIELD',5X,'T.MOMENT',4X,
        !      'TETA',6X,'PHI',4X,'dH/dhv')
80      FORMAT(X,I2,X,F6.1,X,F5.3,X,F5.3,X,F7.4,X,F7.4)
90      FORMAT(X,'gz='F6.4,3X,'gx='F6.4,3X,'gy='F6.4)
100     FORMAT(X,'D='F5.3,3X,'E='F6.4,3X,'AlphaD='F4.1,3X
        !      'Fr='F6.3,X,'GHz',X,'('F5.3,X,'cm-1',')')
200     FORMAT(X,'Dzz='F7.4,3X,'Dxx='F7.4,3X,'Dyy='F7.4)
300     FORMAT(X,'zfs1 ='F6.4,X,'cm-1',2X,'zfs2 ='F6.4,X,'cm-1')
        END
        *
*      ENERGY
*
        SUBROUTINE ENERGY(H,NDIAG)
        DIMENSION ENER(5)
        COMPLEX W(30,30),CPA
        COMMON/DGCOM2/DF6700,N,XMCHEP,TOL,CPA(30),TAU(2,30)
        COMMON/EVEC/W
        COMMON/EIGEN/WR(5,5)
        COMMON/HPARAM/GZ,GX,GY,D,E,CT,ST,CP,SP
        XMCHEP=1.0E-7
        N=5
        GHZ=1.39961*GZ*H*CT
        GHX=1.39961*GX*H*ST*CP
        GHY=1.39961*GY*H*ST*SP
        W(1,1)=CMPLX(2.0*GHZ+2.0*D,0.0)
        W(2,2)=CMPLX(GHZ-D,0.0)
        W(3,3)=CMPLX(-2.0*D,0.0)
        W(4,4)=CMPLX(-GHZ-D,0.0)
        W(5,5)=CMPLX(-2.0*GHZ+2.0*D,0.0)
        W(1,2)=CMPLX(GHX,-1.0*GHY)
        W(1,3)=CMPLX(2.44949*E,0.0)
        W(1,4)=CMPLX(0.0,0.0)

```

```

W(1,5)=CMPLX(0.0,0.0)
W(2,3)=CMPLX(1.224745*GHX,-1.224745*GHY)
W(2,4)=CMPLX(3.0*E,0.0)
W(2,5)=CMPLX(0.0,0.0)
W(3,4)=CMPLX(1.224745*GHX,-1.224745*GHY)
W(3,5)=CMPLX(2.44949*E,0.0)
W(4,5)=CMPLX(GHX,-1.0*GHY)
W(2,1)=CONJG(W(1,2))
W(3,2)=CONJG(W(2,3))
W(4,3)=CONJG(W(3,4))
W(5,3)=CONJG(W(3,5))
W(5,4)=CONJG(W(4,5))
W(3,1)=CONJG(W(1,3))
W(4,1)=(0.0,0.0)
W(5,1)=(0.0,0.0)
W(4,2)=CONJG(W(2,4))
W(5,2)=(0.0,0.0)
CALL HHERM (W,30)
CALL QRSTD (ENER,30)
DO I=1,5
  WR(I,I)=ENER(I)
END DO
NDIAG=NDIAG+1
END
*
* TRANSITION MOMENT
*
SUBROUTINE INTENSITY(TM,WHI,WLO,DHHDHNU,DMS)
  DIMENSION SPINZ(5),SPINXY(4)
  COMPLEX CPA(30),W(30,30),VECTOR(30,2)
  COMPLEX SPIU,SMENO,SZ,SX,SY
  COMMON/EVEC/W
  COMMON/DGCOM2/DF6700,N,XMCHEP,TOL,CPA,TAU(2,30)
  COMMON/HPARAM/GZ,GX,GY,D,E,CTETA,STETA,CPhi,SPHI
  CALL CORA(WHI,1,W,30)
  DO 100 J=1,5
    VECTOR(J,1)=CPA(J)
    CALL CORA(WLO,1,W,30)
  DO 200 J=1,5
    VECTOR(J,2)=CPA(J)
    SZ=(0.0,0.0)
    SPIU=(0.0,0.0)
    SMENO=(0.0,0.0)
    *   Calcolo di <ilSzlj>
    SPINZ(1)=2.0
    SPINZ(2)=1.0
    SPINZ(3)=0.0
    SPINZ(4)=-1.0
    SPINZ(5)=-2.0
    DO 1 J=1,5
      SZ=SZ+SPINZ(J)*VECTOR(J,2)*CONJG(VECTOR(J,1))
    CONTINUE
    *   Calcolo di <ilS+lj> e <ilS-lj>
    SPINXY(1)=2.0
    SPINXY(2)=2.44949
    SPINXY(3)=2.44949
    SPINXY(4)=2.0
    DO 2 J=1,4

```



```

      SPIU=SPIU+SPINXY(J)*VECTOR(J+1,2)*CONJG(VECTOR(J,1))
      SMENO=SMENO+SPINXY(J)*VECTOR(J,2)*CONJG(VECTOR(J+1,1))
2      CONTINUE
      SX=(0.5,0.0)*(SPIU+SMENO)
      SY=(0.0,-0.5)*(SPIU-SMENO)
      TM=CABS(GX*CTETA*CPHI*SX+GY*CTETA*STETA*SY
&      -GZ*STETA*SZ)**2+CABS(GX*SPHI*SX-GY*CPHI*SY)**2
      DHDHNU=SQRT((GX*CTETA)**2+(GX*STETA*CPHI)**2+(GY*STETA*SPHI)**2)
      DHDHNU=1/DHDHNU/DMS
      RETURN
      END

```

THIS IS AN INCOMPLETE LISTING THIS PROGRAM ALSO MUST HAVE THE THREE
 SUBROUTINES HHHERM, QRSTD, AND CORA IN ORDER TO BE COMPLETE. THESE,
 HOWEVER, ARE IDENTICAL TO THE ROUTINES IN JQ AND HAVE NOT BEEN
 REPRODUCED HERE IN ORDER TO SAVE SPACE. SEE
 THE LISTING OF JQ ABOVE FOR A COMPLETE LISTING OF THESE SUBROUTINES

Program ttp

ttp is a minor modification of program jt. It provides the turning points of the triplet spectra by calculating the resonant fields for the orientations of the molecule that have one molecular axis aligned with the external field. ttp returns to the standard output the polarization (x,y,z) of the transition, the energy levels between which the transition occurs, and the magnetic field at which it occurs. ttp is useful for assigning lines in conjunction with full spectral simulation, because its output can be used to tell what parameters to adjust in the file jts.inp to closely reproduce experimental spectra

INPUT

The input for ttp is the same as for jt, namely the file jt.inp, which has the format

```

*      TITLE
*      D(cm-1) E(cm-1)
*      GZ GX GY MINFIELD(KILOGAUSS) MAXFIELD(KILOGAUSS)
*      THETAMIN THETAMAX DTHETA PHIMIN PHIMAX DPHI
*      FREQUENCY(GHz) SCREEN(BOOLEAN, FOR OUTPUT DISPLAY)
*
*      DIMENSION TRMT(150000),CAMPO(150000),HM(3),WE(4)
*      DIMENSION ICOMP(20),JCOMP(20),HCOMP(20),VAFAC(15
& 0000),TET(150000),PH(150000),LABEL(150000)
*      COMPLEX W(30,30)
*      LOGICAL SCREEN,ALLOWED
*      COMMON/EIGEN/WR(3,3)
*      COMMON/EVEC/W
*      COMMON/HPARAM/GZ,GX,GY,D1,E1,CTETA,STETA,CPhi,SPHI,UT,DT,URD
*      CHARACTER*60 TITLE
*      REAL KK,HMIN,HMAX,HMIN1,HMAX1,HMIN1,HINCR,
& HSUP,HINF,H,HCOMP
*      TOL --IN KILOGAUSS--
*      TOL=0.001
*      OPEN(UNIT=1,NAME='jt.inp',TYPE='old')
*      READ(1,'(A60)') TITLE
*      READ(1,*) D,E
*      CALCULATES ZERO-FIELD SPLITTING
*      GY=0.0
*      GX=0.0
*      GZ=0.0
*      H=0.0
*      UT=1./3.
*      DT=2./3.
*      URD=SQRT(1./2.)
*      D1=D/0.0333564
*      E1=E/0.0333564
*      CALL ENERGY(H,NDIAG)
*      ZFS=0.0333564*ABS(WR(3,3)-WR(1,1))
*      DZZ=2.*D/3.
*      DXX=-D/3.+E
*      DYY=-D/3.-E
*      READ(1,*) GZ,GX,GY,HMIN,HMAX
*      READ(1,*) TMIN,TMAX,DTETA,PMIN,PMAX,DPHI
*      READ(1,*) FR,SCREEN
*      CLOSE(1)

```

```

IF (SCREEN) TYPE 70
TYPE*, ''
NDT=0
NDTI=1
JMAX=3
*   SWEEP POLAR ANGLES
DO 30 ATETA=0.0,90.0,90.0
TETA=0.0174532*ATETA
DO 28 APhi=0.0,90.0,90.0
Phi=0.0174532*APhi
IF (TETA.EQ.0.AND.Phi.GT.1E-6) GOTO 28
STETA=SIN(TETA)
CTETA=COS(TETA)
SPHI=SIN(PHI)
CPHI=COS(PHI)
*   LOOP OVER TRANSITIONS
DO 26 I=1,2
J=I+1
HOLD=HMIN
HNEW=HMAX
H=HNEW
CALL ENERGY(H,NDIAG)
XNEW=WR(4-J,4-J)-WR(4-I,4-I)-FR
H=HOLD
CALL ENERGY(H,NDIAG)
XOLD=WR(4-J,4-J)-WR(4-I,4-I)-FR
DO 16 L=1,20
DH=(HOLD-HNEW)*XNEW/(XNEW-XOLD)
HOLD=HNEW
XOLD=XNEW
HNEW=HNEW+DH
H=HNEW
CALL ENERGY(H,NDIAG)
XNEW=WR(4-J,4-J)-WR(4-I,4-I)-FR
IF (ABS(DH).LT.TOL.OR.XNEW.EQ.0) GO TO 20
IF (L.GE.19) GO TO 26
16  CONTINUE
20  NDT=NDT+1
DM=REAL(J-I)
CALL INTENSITY(TM,WR(4-J,4-J),WR(4-I,4-I),DHDHNU,DM)
IF (CTETA.GT.0.1) TYPE 60, I,J,H*1000
IF (STETA*CPHI.GT.0.1) TYPE 61, I,J,H*1000
IF (STETA*SPHI.GT.0.1) TYPE 62, I,J,H*1000
LABEL(NDTI)=I*J
CAMPO(NDTI)=H
TET(NDTI)=STETA
PH(NDTI)=SPHI
TRMT(NDTI)=TM
VAFAC(NDTI)=DHDHNU
NDTI=NDTI+1
26  CONTINUE
28  CONTINUE
30  CONTINUE
60  FORMAT(2X,'Z',X,I1,'-',I1,5X,F7.1)
61  FORMAT(2X,'X',X,I1,'-',I1,5X,F7.1)
62  FORMAT(2X,'Y',X,I1,'-',I1,5X,F7.1)
70  FORMAT(X,'TRANSITION',2X,'FIELD',5X,'T.MOMENT',4X,'TETA',6X,'PHI',4X,'dH/dhv')
80  FORMAT(X,I2,X,F6.1,X,F5.3,X,F5.3,X,F7.4,X,F7.4)

```

```

90      FORMAT(X,'gz=' ,F6.4,3X,'gx=' ,F6.4,3X,'gy=' ,F6.4)
100     FORMAT(X,'D=' ,F5.3,3X,'E=' ,F6.4,3X,'AlphaD=' ,F4.1,3X,'Fr.=' ,F5.3,X,'GHZ' ,X,'(' ,F5.3,X,'cm-
1',')')
200     FORMAT(X,'Dzz=' ,F7.4,3X,'Dxx=' ,F7.4,3X,'Dyy=' ,F7.4)
300     FORMAT(X,'zfs=' ,F6.4,X,'cm-1')
      END
      *
*      ENERGY
*
      SUBROUTINE ENERGY(H,NDIAG)
      DIMENSION ENER(3)
      COMPLEX W(30,30),CPA
      COMMON/DGCOM2/DF6700,N,XMCHEP,TOL,CPA(30),TAU(2,30)
      COMMON/EVEC/W
      COMMON/EIGEN/WR(3,3)
      COMMON/HPARAM/GZ,GX,GY,D,E,CT,ST,CP,SP,UT,DT,URD
      XMCHEP=1.0E-7
      N=3
      NDIAG=NDIAG+1
      GHZ=1.39961*GZ*H*CT
      GHX=1.39961*GX*H*ST*CP
      GHY=1.39961*GY*H*ST*SP
      W(1,1)=CMPLX(GHZ + UT*D,0.0)
      W(2,2)=CMPLX(-DT*D,0.0)
      W(3,3)=CMPLX(-GHZ + UT*D,0.0)
      W(1,2)=CMPLX(URD*GHX,-URD*GHY)
      W(2,3)=CMPLX(URD*GHX,-URD*GHY)
      W(1,3)=CMPLX(E,0)
      W(2,1)=CONJG(W(1,2))
      W(3,2)=CONJG(W(2,3))
      W(3,1)=CONJG(W(1,3))
      CALL HHERM (W,30)
      CALL QRSTD (ENER,30)
      DO I=1,3
      WR(I,I)=ENER(I)
      END DO
      END
      *
*      TRANSITION MOMENT
*
      SUBROUTINE INTENSITY(TM,WHI,WLO,DHHDHNU,DMS)
      DIMENSION SPINZ(3),SPINXY(3)
      COMPLEX CPA(30),W(30,30),VECTOR(30,2)
      COMPLEX SPIU,SMENO,SZ,SX,SY
      COMMON/EVEC/W
      COMMON/DGCOM2/DF6700,N,XMCHEP,TOL,CPA,TAU(2,30)
      COMMON/HPARAM/GZ,GX,GY,D,E,CTETA,STETA,CPHI,SPHI,UT,DT,URD
      CALL CORA(WHI,1,W,30)
      DO 100 J=1,3
100     VECTOR(J,1)=CPA(J)
      CALL CORA(WLO,1,W,30)
      DO 200 J=1,4
200     VECTOR(J,2)=CPA(J)
      SZ=(0.0,0.0)
      SPIU=(0.0,0.0)
      SMENO=(0.0,0.0)
      *      Calcolo di <ilSzlj>
      SPINZ(1)=1.0

```

```

SPINZ(2)=0.0
SPINZ(3)=-1.0
DO 1 J=1,3
SZ=SZ+SPINZ(J)*VECTOR(J,2)*CONJG(VECTOR(J,1))
1 CONTINUE
*   Calcolo di  $\langle i|S+l_j\rangle$  e  $\langle i|S-l_j\rangle$ 
SPINXY(1)=1.414
SPINXY(2)=1.414
DO 2 J=1,2
SPIU=SPIU+SPINXY(J)*VECTOR(J+1,2)*CONJG(VECTOR(J,1))
SMENO=SMENO+SPINXY(J)*VECTOR(J,2)*CONJG(VECTOR(J+1,1))
2 CONTINUE
SX=(0.5,0.0)*(SPIU+SMENO)
SY=(0.0,-0.5)*(SPIU-SMENO)
TM=CABS(GX*CTETA*CPHI*SX+GY*CTETA*STETA*SY
& -GZ*STETA*SZ)**2+CABS(GX*SPHI*SX-GY*CPHI*SY)**2
DHDHNU=SQRT((GX*CTETA)**2+(GX*STETA*CPHI)**2+(GY*STETA*SPHI)**2)
DHDHNU=1/DHDHNU/DMS
RETURN
END

```

THIS IS AN INCOMPLETE LISTING THIS PROGRAM ALSO MUST HAVE THE THREE
 SUBROUTINES HHHERM, QRSTD, AND CORA IN ORDER TO BE COMPLETE. THESE,
 HOWEVER, ARE IDENTICAL TO THE ROUTINES IN JQ AND HAVE NOT BEEN
 REPRODUCED HERE IN ORDER TO SAVE SPACE. SEE
 THE LISTING OF JQ ABOVE FOR A COMPLETE LISTING OF THESE SUBROUTINES

PROGRAM ORDFIELDS

```

*
*   This program is a minor modification of jq that produces
*   a list of turning points of quintet spectra in increasing
*   value of the magnetic field. It is useful for assigning
*   D & E values to experimental spectra. The turning points
*   calculated correspond to molecular orientations that have
*   one molecular axis aligned with the external magnetic field
*   This program uses the input file jq.inp, which has the form
*
*   TITLE
*   D(cm-1) E(cm-1)
*   GZ GX GY MINFIELD(KILOGAUSS) MAXFIELD(KILOGAUSS)
*   THETAMIN THETAMAX DTHETA PHIMIN PHIMAX DPHI
*   FREQUENCY(GHz) SCREEN(BOOLEAN, FOR OUTPUT DISPLAY)
*
*   DIMENSION TRMT(300000),CAMPO(300000),HM(3),WE(5)
*   DIMENSION ICOMP(20),JCOMP(20),HCOMP(20),VAFAC(30
& 0000),TET(300000),PH(300000),LABEL(300000),HR(15),DIR(15)
*   COMPLEX W(30,30)
*   LOGICAL SCREEN,ALLOWED
*   COMMON/EIGEN/WR(5,5)
*   COMMON/EVEC/W
*   COMMON/HPARAM/GZ,GX,GY,D1,E1,CTETA,STETA,CPhi,SPHI
*   CHARACTER*60 TITLE
*   CHARACTER*1 AXIS
*   REAL KK,HMIN,HMAX,HNEW,HOLD,H,DH,DM
*   INTEGER AX,DIR
*   INTEGER*4 NDT,NDTI,KL
*   OPEN(6,CARRIAGECONTROL='FORTRAN')
*   TOL --IN KILOGAUSS--
*   TOL=0.001
*   OPEN(UNIT=1,NAME='jq.inp',TYPE='old')
*   READ(1, '(A60)') TITLE
*   READ(1,*) D,E
*   *   CALCULATES ZERO-FIELD SPLITTING
*   GY=0.0
*   GX=0.0
*   GZ=0.0
*   H=0.0
*   NDIAG=0
*   D1=D/0.0333564
*   E1=E/0.0333564
*   CALL ENERGY(H,NDIAG)
*   ZFS1=0.0333564*ABS(WR(5,5)-WR(3,3))
*   ZFS2=0.0333564*ABS(WR(3,3)-WR(1,1))
*   DZZ=2.*D/3.
*   DXX=-D/3.+E
*   DYY=-D/3.-E
*   READ(1,*) GZ,GX,GY,HMIN,HMAX
*   READ(1,*) TMIN,TMAX,DTETA,PMIN,PMAX,DPHI
*   READ(1,*) FR,SCREEN
*   NDT=0
*   NDTI=1
*   JMIN=2
*   JMAX=5
*   *   SWEEP POLAR ANGLES
*   DO 29 ATETA=0.0,90.0,90.0

```

```

TETA=0.0174532*ATETA
DO 28 APhi=0.0,90.0,90.0
PHI=0.0174532*APHI
IF (TETA.EQ.0.AND.PHI.GT.1E-6) GOTO 28
STETA=SIN(TETA)
CTETA=COS(TETA)
SPHI=SIN(PHI)
CPHI=COS(PHI)
*      LOOP OVER TRANSITIONS
DO 26 I=1,4
J=I+1
HOLD=HMIN
HNEW=HMAX
H=HNEW
CALL ENERGY(H,NDIAG)
XNEW=WR(6-J,6-J)-WR(6-I,6-I)-FR
H=HOLD
CALL ENERGY(H,NDIAG)
XOLD=WR(6-J,6-J)-WR(6-I,6-I)-FR
DO 16 L=1,20
DH=(HOLD-HNEW)*XNEW/(XNEW-XOLD)
HOLD=HNEW
XOLD=XNEW
HNEW=HNEW+DH
H=HNEW
CALL ENERGY(H,NDIAG)
XNEW=WR(6-J,6-J)-WR(6-I,6-I)-FR
IF(ABS(DH).LT.TOL.OR.XNEW.EQ.0) GO TO 20
IF(L.GE.19) GO TO 26
16  CONTINUE
20  NDT=NDT+1
DM=REAL(J-I)
CALL INTENSITY(TM,WR(6-J,6-J),WR(6-I,6-I),DHDHNU,DM)
IF (ATETA.EQ.0) THEN
AX=0
ELSEIF (APHI.EQ.0) THEN
AX=1
ELSE
AX=2
ENDIF
DIR(NDTI)=AX
LABEL(NDTI)=I
CAMPO(NDTI)=H
HR(NDTI)=H
TET(NDTI)=STETA
PH(NDTI)=SPHI
TRMT(NDTI)=TM
VAFAC(NDTI)=DHDHNU
NDTI=NDTI+1
26  CONTINUE
28  CONTINUE
29  CONTINUE
TYPE 50, E
DO 33 I=1,12
WRITE(6,60) CAMPO(I)*1000
33  CONTINUE
WRITE(6,61)
50  FORMAT('$',F6.5,'u')

```

```

60  FORMAT('$,F6.1,\n')
61  FORMAT(' ')
70  FORMAT(X,'TRANSITION',2X,'FIELD',5X,'T.MOMENT',4X,
!      'TETA',6X,'PHI',4X,'dH/dhv')
80  FORMAT(X,I2,X,F6.1,X,F5.3,X,F5.3,X,F7.4,X,F7.4)
90  FORMAT(X,'gz=',F6.4,3X,'gx=',F6.4,3X,'gy=',F6.4)
100 FORMAT(X,'D=',F5.3,3X,'E=',F6.4,3X,'AlphaD=',F4.1,3X
!      'Fr.',F6.3,X,'GHz',X,'('F5.3,X,'cm-1',')')
200  FORMAT(X,'Dzz=',F7.4,3X,'Dxx=',F7.4,3X,'Dyy=',F7.4)
300  FORMAT(X,'zfs1 =',F6.4,X,'cm-1',2X,'zfs2 =',F6.4,X,'cm-1')
END
*
*  ENERGY
*
SUBROUTINE ENERGY(H,NDIAG)
DIMENSION ENER(5)
COMPLEX W(30,30),CPA
COMMON/DGCOM2/DF6700,N,XMCHEP,TOL,CPA(30),TAU(2,30)
COMMON/EVEC/W
COMMON/EIGEN/WR(5,5)
COMMON/HPARAM/GZ,GX,GY,D,E,CT,ST,CP,SP
XMCHEP=1.0E-7
N=5
GHZ=1.39961*GZ*H*CT
GHX=1.39961*GX*H*ST*CP
GHY=1.39961*GY*H*ST*SP
W(1,1)=CMPLX(2.0*GHZ+2.0*D,0.0)
W(2,2)=CMPLX(GHZ-D,0.0)
W(3,3)=CMPLX(-2.0*D,0.0)
W(4,4)=CMPLX(-GHZ-D,0.0)
W(5,5)=CMPLX(-2.0*GHZ+2.0*D,0.0)
W(1,2)=CMPLX(GHX,-1.0*GHY)
W(1,3)=CMPLX(2.44949*E,0.0)
W(1,4)=CMPLX(0.0,0.0)
W(1,5)=CMPLX(0.0,0.0)
W(2,3)=CMPLX(1.224745*GHX,-1.224745*GHY)
W(2,4)=CMPLX(3.0*E,0.0)
W(2,5)=CMPLX(0.0,0.0)
W(3,4)=CMPLX(1.224745*GHX,-1.224745*GHY)
W(3,5)=CMPLX(2.44949*E,0.0)
W(4,5)=CMPLX(GHX,-1.0*GHY)
W(2,1)=CONJG(W(1,2))
W(3,2)=CONJG(W(2,3))
W(4,3)=CONJG(W(3,4))
W(5,3)=CONJG(W(3,5))
W(5,4)=CONJG(W(4,5))
W(3,1)=CONJG(W(1,3))
W(4,1)=(0.0,0.0)
W(5,1)=(0.0,0.0)
W(4,2)=CONJG(W(2,4))
W(5,2)=(0.0,0.0)
CALL HHERM (W,30)
CALL QRSTD (ENER,30)
DO I=1,5
WR(I,I)=ENER(I)
END DO
NDIAG=NDIAG+1
END

```



```

*
* TRANSITION MOMENT
*
SUBROUTINE INTENSITY(TM,WHI,WLO,DHNU,DMS)
DIMENSION SPINZ(5),SPINXY(4)
COMPLEX CPA(30),W(30,30),VECTOR(30,2)
COMPLEX SPIU,SMENO,SZ,SX,SY
COMMON/EVEC/W
COMMON/DGCOM2/DF6700,N,XMCHEP,TOL,CPA,TAU(2,30)
COMMON/HPARAM/GZ,GX,GY,D,E,CTETA,STETA,CPhi,SPHI
CALL CORA(WHI,1,W,30)
DO 100 J=1,5
100 VECTOR(J,1)=CPA(J)
CALL CORA(WLO,1,W,30)
DO 200 J=1,5
200 VECTOR(J,2)=CPA(J)
SZ=(0.0,0.0)
SPIU=(0.0,0.0)
SMENO=(0.0,0.0)
*   Calcolo di <ilSzl>
SPINZ(1)=2.0
SPINZ(2)=1.0
SPINZ(3)=0.0
SPINZ(4)=-1.0
SPINZ(5)=-2.0
DO 1 J=1,5
1 SZ=SZ+SPINZ(J)*VECTOR(J,2)*CONJG(VECTOR(J,1))
CONTINUE
*   Calcolo di <ilS+l> e <ilS-l>
SPINXY(1)=2.0
SPINXY(2)=2.44949
SPINXY(3)=2.44949
SPINXY(4)=2.0
DO 2 J=1,4
2 SPIU=SPIU+SPINXY(J)*VECTOR(J+1,2)*CONJG(VECTOR(J,1))
SMENO=SMENO+SPINXY(J)*VECTOR(J,2)*CONJG(VECTOR(J+1,1))
CONTINUE
SX=(0.5,0.0)*(SPIU+SMENO)
SY=(0.0,-0.5)*(SPIU-SMENO)
TM=CABS(GX*CTETA*CPhi*SX+GY*CTETA*STETA*SY
& -GZ*STETA*SZ)**2+CABS(GX*SPHI*SX-GY*CPhi*SY)**2
DHNU=SQRT((GZ*CTETA)**2+(GX*STETA*CPhi)**2+(GY*STETA*SPHI)**2)
DHNU=1/DHNU/DMS
RETURN
END

```

THIS IS AN INCOMPLETE LISTING THIS PROGRAM ALSO MUST HAVE THE THREE SUBROUTINES HHERM, QRSTD, AND CORA IN ORDER TO BE COMPLETE. THESE, HOWEVER, ARE IDENTICAL TO THE ROUTINES IN JQ AND HAVE NOT BEEN REPRODUCED HERE IN ORDER TO SAVE SPACE. SEE THE LISTING OF JQ ABOVE FOR A COMPLETE LISTING OF THESE SUBROUTINES

PROGRAM VIEW

* Program VIEW reads the stick spectrum calculated
 * by means of program JQ or JT and writes in to the
 * standard output

```

CHARACTER*60 TITLE
CHARACTER*20 FNAME
REAL H,HMIN,HMAX,NPOINT,HIFLD,LOWFLD
REAL LOWNDP,HINDP,H1,MI,MI53
DIMENSION VAFAC(150000),TM(150000)
DIMENSION FIELD(150000),SPEC(5000),CAMPO(5000)
DIMENSION ST(150000),SP(150000),LABEL(150000)
DIMENSION WZ1(20),WX1(20),WY1(20)
CALL GETARG(1,FNAME)
OPEN(UNIT=1,TYPE='OLD',NAME=FNAME,FORM='UNFORMATTED',READONLY)
READ(1) TITLE
READ(1) GZ,GX,GY,D,E,FR
READ(1) HMIN,HMAX,NDT
TYPE*, TITLE
TYPE*, D,E
DO I=1,NDT
  READ(1) LABEL(I),FIELD(I),TM(I),VAFAC(I),ST(I)
& ,SP(I)
  TYPE *, LABEL(I),FIELD(I),TM(I),VAFAC(I)
END DO
CLOSE(1)
80  FORMAT(X,I2,X,F6.1,X,F5.3,X,F5.3,X,F7.4,X)
END

```

PROGRAM PLOT

```

/*This program plots a simulated spectrum on the IRIS-4D*/
/*main terminal. Its command line is "plot <sfile> <pfile>"*/
/*where <sfile> is the XY-spectrum file jqs.out or jts.out and*/
/*<pfile> is the linewidth parameter file jqs.inp or jts.inp.*/

```

```

#include <gl.h>
#include <stdio.h>
#include <device.h>
#include <fmclient.h>

    fmfonthandle font1, font2;

main(argc, argv)
    int argc;
    char *argv[];

{
    int x,v,w,ls;
    float a,y,z;
    float var[1000][2],parm[10][3];
    short val;
    FILE *fopen(), *fin[3];

    fin[0] = fopen(argv[1], "r");
    fin[2] = fopen(argv[2], "r");
    x = 0;
    while (fscanf(fin[0], "%f %f", &y, &z) != EOF)
        { var[x][0] = y;
          var[x][1] = z;
          x++; }

    for(v=0;v<10;v++)
        { fscanf(fin[2], "%f %f %f", &a, &y, &z);
          parm[v][0] = a;
          parm[v][1] = y;
          parm[v][2] = z; }

    fminit();
    font1=fmfindfont("Times-Roman");

    prefposition(100,1200,100,900);
    w=winopen("simulation");
    minsize(21,21);
    winconstraints();
    drawit(var);
    valshow(parm);
    while(TRUE) {
        if (qread(&val) == REDRAW)
            { reshapeviewport();
              drawit(var);
              valshow(parm); }
    }
}

```

```

drawit(inp)
    float inp[1000][2];
{
    long vert[2];
    int i,j;
    float k,l;

    color(BLUE);
    clear();

    color(BLACK);
    for (i=0;i<11; i=i+1) {
        vert[0]=50+100*i;
        vert[1]=50;
        bgnline();
        v2i(vert);
        vert[1]=750;
        v2i(vert);
        endlne();
        vert[0]=50;
        vert[1]=50+70*i;
        bgnline();
        v2i(vert);
        vert[0]=1050;
        v2i(vert);
        endlne();
    }

    color(WHITE);
    for (i=0; i<4; i++) {
        bgnline();
        for (j=0; j<250; j++) {
            vert[0]= 50+(inp[(i*250+j)][0] +5) * 100;
            vert[1]= 50+(inp[(i*250+j)][1] +1) * 350;
            v2i(vert);
        }
        endlne();
    }
}

valshow(inp)
    float inp[10][3];
{
    char str0[17],str1[7],str2[7],str3[7];
    int q,r;
    long s,t;
    float sc;

    getsiz(&s,&t);
    sc = 24*(s/1101.0)*(t/801.0);
    font2 = fmscalefont(font1,sc);
    fmsetfont(font2);

    r=264;
    color(YELLOW);
    cmov2i (30,300);
    fmprstr("#");
    cmov2i (118,300);
    fmprstr("X");

```

```
cmov2i (268,300);
fmprstr("Y");
cmov2i (418,300);
fmprstr("Z");
for (q=0;q<10;q++) { if (inp[q][0] != 0) {
sprintf(str0,"%i",q+1);
sprintf(str1,"%4.1f",inp[q][0]);
sprintf(str2,"%4.1f",inp[q][1]);
sprintf(str3,"%4.1f",inp[q][2]);
cmov2i (30,r);
fmprstr(str0);
cmov2i (100,r);
fmprstr(str1);
cmov2i (250,r);
fmprstr(str2);
cmov2i (400,r);
fmprstr(str3);
r-=36;
}
}
}
```

PROGRAM HARDCOPY

```

#include <stdio.h>

/* This program reads two variables from the argument line*/
/* the first is the name of the xy-file of a simulated EPR spectrum, */
/* the second is the name of the lineshape parameter file used to */
/* generate the spectrum*/
/* The program then creates a postscript file tmp.ps which will print
/* the spectrum and lineshape parameters on the laserwriter and then */
/* calls lp to print it*/

main(argc, argv)
    int argc;
    char *argv[];

{
    int x,w,v,ls,q,r;
    float a,y,z;
    float parm[10][3];
    float var[1000][2];
    short val;
    FILE *fopen(), *fin[3];

    fin[0]= fopen(argv[1], "r");
    fin[1]= fopen("tmp.ps", "w");
    fin[2]= fopen(argv[2], "r");

    fprintf(fin[1], "%!\\n/Times-Roman findfont 12 scalefont      setfont\\n");
    fprintf(fin[1], "%i %i moveto\\n", 50, 16*14);
    fprintf(fin[1], "( Z      X      Y) show\\n");

    q = 0;
    while (fscanf(fin[2], "%f %f %f", &a, &y, &z) != EOF)
        {if (a > 0.0)
            {fprintf(fin[1], "%i %i moveto\\n", 50, (15-q)*14);
             fprintf(fin[1], "(%4.1f %4.1f %4.1f) show\\n",
              a, y, z);
              q++;}
        }

    fprintf(fin[1], "%s\\n%s\\n",
        "0 setgray 1 setlinewidth",
        "306 36 moveto");

    x = 0;
    while (fscanf(fin[0], "%f %f", &y, &z) != EOF)
        { var[x][0] = 36 + (y + 5) * 72;
          var[x][1] = 36 + (-z + 1) * 270;
          if (x>0) {fprintf(fin[1], "%6.2f %6.2f lineto\\n",
              var[x-1][1], var[x-1][0]);}
          x++;}

    fprintf(fin[1], "stroke\\nshowpage");
    r=system("lp tmp.ps");
}

```

```

program squid_data_converter;      { Version 1.1, 3-26-88 }

{ This program reads an ALL POINTS type MPMS data file }
{ and fits each SQUID response curve to the optimum moment }
{ by doing a chi-squared minimization by the Marquardt method }
{ (Numerical Recipes, section 14.3) }
{ It produces an output file consisting of the following columns }
{ FIELD  TEMP  MOMENT(MPMS) REAL MOMENT(THIS PROGRAM) CHISQ }
{ }
{ The fields are separated by tabs, and this output file is easily }
{ read by Kaleidagraph. For variable temperature data, use }
{ of this program is crucial to obtaining believable moments. }
{ The MPMS just can't calculate the thing right if the sample }
{ is off-center. Oh well, just like everything else QD does. }

{ The basis of this program is the Pascal Program Extract which }
{ came with the MPMS and the Marquardt minimization procedure }
{ that I simply copied letter-for-letter from Numerical Recipes }
{ }
{ This program could use a friendlier front end, because if it }
{ encounters an error (which it doesn't do if used correctly) }
{ it bombs and you have to restart. To avoid this difficulty, }
{ just make sure that the compiled version you're running and }
{ the data file you want to use are in the same folder. }
{ }
{ It would also be nice someday if this program could graph }
{ its results, but I'll leave that to someone else }
{ }
{ }

const
    PathLength = 65;
    TAB = chr(9);
const
    ModeLen = 9;
type
    WorkString = string[64];
    NumStr = string[12];
    TimeStr = string[8];
    FileName = string[PathLength];
    BlockType = (TTL, DAT, SUM, HYS, NUL);
    ColType = (FieldCol, TempCol, EMUCol, RealEMUCol, ChiSqCol, BlankCol);
    glndata = array[1..65] of double;
    glmma = array[1..5] of double;
    gllista = array[1..5] of integer;
    glcovar = array[1..5, 1..5] of double;
    glnpbymp = array[1..5, 1..1] of double;

var
    Fail: boolean;
    Delim: string[3];
    Name: FileName;
    Input_File: text;
    Output_File: text;
    LineBuffer: WorkString;
    Line_Ptr: integer;
    Block_Name: BlockType;
    Lines_In_Block: integer;
    Lines_To_Data: integer;

```

```

    Data_Points: integer;
    Line_Count: integer;
    Data_Number: integer;
    ColSpec: array[1..Modelen] of ColType;
    Mode: string[Modelen];
    Del: string[1];
{Data Elements}
    Field: NumStr;
    Temp: NumStr;
    DeltaT: NumStr;
    EMU: NumStr;
    RealEMU: NumStr;
    ChiSq: NumStr;
    RealEMU_Val, ChiSq_Val: double;
    Suscept: NumStr;
    Dev: NumStr;
    TimeI: TimeStr;
    TimeF: TimeStr;
    Start_Point: double;
    glochisq: double;
    glbeta: glmma;

procedure Initialize;

    var
        I, J: integer;
        Ch: char;

begin
    Fail := false;
    Line_Count := 0;
    Data_Number := 0;
    ColSpec[1] := FieldCol;
    ColSpec[2] := TempCol;
    ColSpec[3] := EMUCol;
    ColSpec[4] := RealEMUCol;
    ColSpec[5] := ChiSqCol;
    ColSpec[6] := BlankCol;
    ColSpec[7] := BlankCol;
    ColSpec[8] := BlankCol;
    ColSpec[9] := BlankCol;
    Delim := TAB;
end;

function Open_Input (var fp: text; Name: Filename): boolean;

    var
        Full_Name: FileName;

begin
    Full_Name := concat(Name, '.DAT');
    open(fp, Full_Name);
{$I-}
    reset(fp);
{$I+}
    if IOresult <> 0 then
        begin
            Open_Input := False;

```



```

{ close(fp); }
    end
else
    Open_Input := True;
end; { Open_Input }

procedure OpenFiles;
var
    Out_Name: FileName;
begin
    Write('Enter Data File Name (without extension): ');
    readln(Name);
    if not Open_Input(Input_File, Name) then
        begin
            Writeln('File "', Name, '.DAT" not found');
            Halt;           {Return an error code for batch files to see}
        end;
    Out_Name := concat(Name, '.OUT');
    rewrite(OutPut_File, Out_Name);
    writeln(Output_File, 'Field', TAB, 'Temp', TAB, 'Moment', TAB, 'Real Moment', TAB, 'ChiSq');
end; { OpenFiles}

procedure GetLine;
begin
    if not eof(Input_File) then
        begin
            Readln(Input_File, LineBuffer);
            Line_Count := Succ(Line_Count);
            Line_Ptr := 1;           {Reset the pointer}
        end;
end; {ReadLine}

function FindBlock: BlockType;

var
    Str: string[3];
    code: integer;

begin
    FindBlock := NUL;
    repeat
        GetLine;
        Str := Copy(LineBuffer, 1, 3)
    until ((Str = 'DAT') or (Str = 'SUM') or (Str = 'HYS') or (Str = 'TTL') or eof(Input_File));
    if eof(Input_File) then
        exit(FindBlock);
    Line_Count := 1;
    if Str = 'DAT' then
        FindBlock := DAT;
    if Str = 'SUM' then
        FindBlock := SUM;
    if Str = 'HYS' then
        FindBlock := HYS;
    if Str = 'TTL' then
        FindBlock := TTL;
    Str := Copy(LineBuffer, 5, 3);
    ReadString(Str, Lines_In_Block);
    if (Lines_in_Block = 0) then

```

```

        Fail := true; {must get at least}
end;                                {two good digits }

procedure DisplayTitle;
begin
    GetLine;
end;

function NextNumStr: NumStr;    {Isolates next number at LinePointer}
                                {and then resets LinePointer past number}
var
    StrLen: integer;
    StartPos: integer;

begin
    while ((Line_Ptr < Length(LineBuffer)) and (LineBuffer[Line_Ptr] = ' ') or (LineBuffer[Line_ptr]
= ',')) do
        Line_Ptr := Succ(Line_Ptr);
        StartPos := Line_Ptr;
        while (Line_Ptr <= Length(LineBuffer)) and (LineBuffer[Line_Ptr] <> ' ') and
(LineBuffer[Line_Ptr] <> ',') do
            Line_Ptr := Succ(Line_Ptr);    {now points to end of number}
        { If Line_Ptr < Length(LineBuffer) then}
        {   Line_Ptr:= Succ(Line_Ptr); }
        {now points to next number}
        StrLen := Line_Ptr - StartPos;
        NextNumStr := Copy(LineBuffer, StartPos, StrLen);

end;

procedure StoreLine;

var
    I, x: integer;
    Field_Val: double;
    Temp_Val: double;
    EMU_Val: double;
    Sus_Val: double;
    Line: NumStr;
    code: integer;

begin
    ReadString(Field, Field_Val);
    Field := StringOf(Field_Val : 10 : 2);
    ReadString(Temp, Temp_Val);
    Temp := StringOf(Temp_Val : 7 : 3);
    ReadString(EMU, EMU_Val);
    EMU := StringOf(EMU_Val : 11 : 8);
    RealEMU := StringOf(RealEMU_Val : 11 : 8);
    ChiSq := StringOf(ChiSq_Val : 11 : 8);

    for I := 1 to ModeLen do
        begin
            case ColSpec[i] of
                FieldCol:
                    Write(OutPut_File, Field);
                TempCol:

```

```

        Write(OutPut_File, Temp);
    EMUCol:
        Write(OutPut_File, EMU);
    RealEMUCol:
        Write(OutPut_File, RealEMU);
    ChiSqCol:
        Write(OutPut_File, ChiSq);
    end; {case}
    if ColSpec[I + 1] <> BlankCol then
        Write(OutPut_File, Delim);
    end; {for I}
    WriteLn(OutPut_File);
end; {storeline}

procedure gaussj (var a: glcovar; n, np: integer; var b: glnpbymp; m, mp: integer);
var
    big, dum, pivinv: double;
    i, icol, irow, j, k, l, ll: integer;
    indxc, indxr, ipiv: gllista;
begin
    for j := 1 to n do
        begin
            ipiv[j] := 0
        end;
    for i := 1 to n do
        begin
            big := 0.0;
            for j := 1 to n do
                begin
                    if (ipiv[j] <> 1) then
                        begin
                            for k := 1 to n do
                                begin
                                    if (ipiv[k] = 0) then
                                        begin
                                            if (abs(a[j, k]) >= big) then
                                                begin
                                                    big := abs(a[j, k]);
                                                    irow := j;
                                                    icol := k
                                                end
                                            end
                                        end
                                    else if (ipiv[k] > 1) then
                                        begin
                                            writeln('pause 1 in GAUSSJ - singular matrix');
                                            readln
                                        end
                                    end
                                end
                            end
                        end
                    end
                end
            end;
            ipiv[icol] := ipiv[icol] + 1;
            if (irow <> icol) then
                begin
                    for l := 1 to n do
                        begin
                            dum := a[irow, l];
                            b[irow, l] := b[icol, l];
                            b[icol, l] := dum
                        end
                    end
                end
            end;
        end
    end;
end;

```

```

        end;
        for l := 1 to m do
            begin
                dum := b[irow, l];
                b[irow, l] := b[icol, l];
                b[icol, l] := dum
            end
        end;
        indxr[i] := irow;
        indxc[i] := icol;
        if (a[icol, icol] = 0.0) then
            begin
                writeln('pause 2 in GAUSSJ - singular matrix');
                readln
            end;
        pivinv := 1.0 / a[icol, icol];
        a[icol, icol] := 1.0;
        for l := 1 to n do
            begin
                a[icol, l] := a[icol, l] * pivinv
            end;
        for l := 1 to m do
            begin
                b[icol, l] := b[icol, l] * pivinv
            end;
        for ll := 1 to n do
            begin
                if (ll <> icol) then
                    begin
                        dum := a[ll, icol];
                        a[ll, icol] := 0;
                        for l := 1 to n do
                            begin
                                a[ll, l] := a[ll, l] - a[icol, l] * dum
                            end;
                        for l := 1 to m do
                            begin
                                b[ll, l] := b[ll, l] - b[icol, l] * dum
                            end
                        end
                    end
                end
            end;
        end;
        for l := n downto 1 do
            begin
                if (indxr[l] <> indxc[l]) then
                    begin
                        for k := 1 to n do
                            begin
                                dum := a[k, indxr[l]];
                                a[k, indxr[l]] := a[k, indxc[l]];
                                a[k, indxc[l]] := dum
                            end
                        end
                    end
                end
            end;
        end;
    end;

procedure covsrt (var covar: glcovar; ncvm: integer; ma: integer; lista: gllista; mfit: integer);
var

```

```

    i, j: integer;
    swap: double;
begin
    for j := 1 to ma - 1 do
        begin
            for i := j + 1 to ma do
                begin
                    covar[i, j] := 0.0
                end
            end;
        end;
        for i := 1 to mfit - 1 do
            begin
                for j := i + 1 to mfit do
                    begin
                        if (lista[j] > lista[i]) then
                            begin
                                covar[lista[j], lista[i]] := covar[i, j]
                            end
                        else
                            begin
                                covar[lista[i], lista[j]] := covar[i, j]
                            end
                        end
                    end
                end;
            end;
            swap := covar[1, 1];
            for j := 1 to ma do
                begin
                    covar[i, j] := covar[j, j];
                    covar[j, j] := 0.0
                end;
            covar[lista[1], lista[1]] := swap;
            for j := 2 to mfit do
                begin
                    covar[lista[j], lista[j]] := covar[i, j]
                end;
            end;
            for j := 2 to ma do
                begin
                    for i := 1 to j - 1 do
                        begin
                            covar[i, j] := covar[j, i]
                        end
                    end
                end
            end;
        end;
    end;

    function resp (x: double; a: glmma): double;
    const
        C = 4192.07;
        Rsq = 0.9409;
        SEP = 1.507;
        Fudge = 0.993;
    var
        y, q: double;
    begin
        q := C * Fudge * (-1 / Exp(Ln((x - a[2] + SEP) * (x - a[2] + SEP) + Rsq) * 1.5) + 2 / Exp(Ln((x -
        a[2]) * (x - a[2]) + Rsq) * 1.5) - 1 / Exp(Ln((x - a[2] - SEP) * (x - a[2] - SEP) + Rsq) * 1.5));
        y := a[3] + a[4] * (x - a[2]) + a[5] * (x - a[2]) * (x - a[2]) + a[1] * q;
        resp := y
    end;
end;

```

```
procedure funcs (x: double; a: glmma; var y: double; var dyda: glmma);
```

```
  var
    I: integer;
    atemp: glmma;
begin
  y := resp(x, a);
  for I := 1 to 5 do
    begin
      atemp := a;
      a[I] := a[I] * 1.0001;
      dyda[I] := (resp(x, a) - y) / (a[I] - atemp[I]);
      a := atemp
    end
  end;
end;
```

```
procedure mrqcof (x, y, sig: glndata; ndata: integer; var a: glmma; mma: integer; lista: gllista; mfit:
integer; var alpha: glcovar; var beta: glmma; nalp: integer; var chisq: double);
```

```
  var
    k, j, i: integer;
    ymod, wt, sig2i, dy: double;
    dyda: glmma;
begin
  for j := 1 to mfit do
    begin
      for k := 1 to j do
        begin
          alpha[j, k] := 0.0
        end;
      beta[j] := 0.0
    end;
  chisq := 0.0;
  for i := 1 to ndata do
    begin
      funcs(x[i], a, ymod, dyda);
      sig2i := 1.0 / (sig[i] * sig[i]);
      dy := y[i] - ymod;
      for j := 1 to mfit do
        begin
          wt := dyda[lista[j]] * sig2i;
          for k := 1 to j do
            begin
              alpha[j, k] := alpha[j, k] + wt * dyda[lista[k]]
            end;
          beta[j] := beta[j] + dy * wt
        end;
      chisq := chisq + dy * dy * sig2i
    end;
  for j := 2 to mfit do
    begin
      for k := 1 to j - 1 do
        begin
          alpha[k, j] := alpha[j, k];
        end
      end
    end
  end;
end;
```

```

procedure mrqmin (x, y, sig: glndata; ndata: integer; var a: glmma; mma: integer; lista: gllista; mfit:
integer; var covar, alpha: glcovar; nca: integer; var chisq, alamda: double);
  label
  99;
  var
    k, kk, j, ihit: integer;
    atry, da: glmma;
    oneda: glnpbymp;

begin
  if (alamda < 0.0) then
    begin
      kk := mfit + 1;
      for j := 1 to mma do
        begin
          ihit := 0;
          for k := 1 to mfit do
            begin
              if (lista[k] = j) then
                ihit := ihit + 1
            end;
            if (ihit = 0) then
              begin
                lista[kk] := j;
                kk := kk + 1
              end
            else if (ihit > 1) then
              begin
                writeln('pause 1- in routine MQRMIN');
                writeln('improper permutation in LISTA');
                readln
              end
            end;
          end;
          if (kk > (mma + 1)) then
            begin
              writeln('pause 2- in routine MQRMIN');
              writeln('improper permutation in LISTA');
              readln
            end;
          alamda := 0.001;
          mrqcof(x, y, sig, ndata, a, mma, lista, mfit, alpha, glbeta, nca, chisq);
          glochisq := chisq;
          for j := 1 to mma do
            begin
              atry[j] := a[j]
            end
          end;
          for j := 1 to mfit do
            begin
              for k := 1 to mfit do
                begin
                  covar[j, k] := alpha[j, k];
                end;
                covar[j, j] := alpha[j, j] * (1.0 + alamda);
                oneda[j, 1] := glbeta[j]
            end;
            gaussj(covar, mfit, nca, oneda, 1, 1);
            for j := 1 to mfit do

```

```

    da[j] := oneda[j, 1];
    if (alamda = 0.0) then
        begin
            covsrt(covar, nca, mma, lista, mfit);
            goto 99
        end;
    for j := 1 to mfit do
        begin
            atry[lista[j]] := a[lista[j]] + da[j]
        end;
    mrqcof(x, y, sig, ndata, atry, mma, lista, mfit, covar, da, nca, chisq);
    if (chisq < glochisq) then
        begin
            alamda := 0.1 * alamda;
            glochisq := chisq;
            for j := 1 to mfit do
                begin
                    for k := 1 to mfit do
                        begin
                            alpha[j, k] := covar[j, k]
                        end;
                    glbeta[j] := da[j];
                    a[lista[j]] := atry[lista[j]]
                end
            end
        end
    else
        begin
            alamda := 10.0 * alamda;
            chisq := glochisq
        end;
99:
end;

procedure ProcessBlock;

const
    FIELDLINE = 8;    {Magnetic Field is on Line 8 in block}
var
    code: integer;
    LastData: integer;
{  Offset: integer; }
    I, J: integer;
    Date: NumStr;
    Field_Val: double;
    Start_Pos: double;
    Increment: double;
    Scan_Length: double;
    Startz: double;
    Num_Scans: integer;
    SQUID: NumStr;
    Range: integer;
    Gain: integer;
    Attenuation: double;
    Multiplier: double;
    Voltage: glndata;
    Zposition: glndata;
    sig: glndata;
    a, dummy: glmma;

```



```

    lista: gllista;
    mfit, ndata, mma, nca: integer;
    covar, alpha: glcovar;
    chisq, alambda, moment, oldmoment, yi, EMU_val: double;

begin
    GetLine;
    ReadString(NextNumStr, Lines_to_Data);
    ReadString(NextNumStr, Data_Points);
    ndata := Data_Points;
    repeat
        Getline;
    until Line_Count = FIELDLINE;
    Field := NextNumStr;
    ReadString(Field, Field_Val);

    GetLine;
    ReadString(NextNumStr, Start_Pos);
    ReadString(NextNumStr, Increment);
    Scan_Length := Increment * (Data_Points - 1);
    Startz := -Scan_Length / 2;

    Getline;

    GetLine;
    ReadString(NextNumStr, Num_Scans);

    GetLine;
    SQUID := NextNumStr;
    ReadString(NextNumStr, Range);
    ReadString(NextNumStr, Gain);
    case Gain of
        0:
            Attenuation := 1;
        1:
            Attenuation := 2;
        2:
            Attenuation := 5;
        3:
            Attenuation := 10;
    end; {case Gain}
    if Range > 10 then
        Range := Range - 8;

    Multiplier := Exp(Ln(10) * Range) / Attenuation;
    repeat
        Getline;
    until Line_Count = Lines_to_Data;
    Date := NextNumStr;
    TimeI := NextNumStr;
    Date := NextNumStr;
    TimeF := NextNumStr;
    Getline;
    if Length(LineBuffer) < 3 then
        Getline; { If blank, toss it !}
                { This allows reading old HYS files}
                { which had a blank line here    }
    if Block_Name = HYS then

```

```

    LastData := Data_Points
  else
    LastData := 1;
  { Writeln('Multiplier = ', StringOf(Multiplier : 7 : 4)); }
  for I := 1 to LastData do
    begin
      Temp := NextNumStr;
      if Block_Name = HYS then
        Field := NextNumStr
      else
        DeltaT := NextNumStr;
        EMU := NextNumStr;
        Readstring(EMU, EMU_val);
        Dev := NextNumStr;
        Data_Number := Succ(Data_Number);
        if I < LastData then
          Getline; { Get next line only if needed }
        end;
      for I := 1 to Num_Scans do
        GetLine;
      for I := 1 to ndata do
        begin
          GetLine;
          ReadString(NextNumStr, Voltage[I]);
          Zposition[I] := Startz + (I - 1) * Increment;
          sig[I] := 1.0;
        { Writeln(TAB, Zposition[I] : 4 : 3, TAB, Voltage[I] : 6 : 5); }
        end;

      mma := 5;
      a[1] := EMU_val / Multiplier;
      a[2] := 0.05;
      a[3] := 0.05;
      a[4] := 0.05;
      a[5] := 0.05;
      nca := 5;
      for I := 1 to 5 do
        lista[I] := I;
      mfit := 5;
      alamda := -1;
      chisq := 0;
      moment := 0;
      oldmoment := 0;
      repeat
        mrqmin(Zposition, Voltage, sig, ndata, a, 5, lista, 5, covar, alpha, 5, chisq, alamda);
        oldmoment := moment;
        moment := a[1] * Multiplier;
      until ((moment - oldmoment) / moment <= 0.0001);
      alamda := 0;
      mrqmin(Zposition, Voltage, sig, ndata, a, 5, lista, 5, covar, alpha, 5, chisq, alamda);
      moment := a[1] * Multiplier;
      RealEMU_Val := moment;
      ChiSq_Val := chisq;
      writeln(TAB, 'Field = ', Field, TAB, 'Temp = ', Temp);
      writeln(TAB, 'MPMS Moment=', EMU_Val : 8 : 7, TAB, 'Moment = ', TAB, moment : 8 : 7,
TAB, TAB, 'Chisq ', chisq : 7 : 5);
      writeln(TAB, 'Off-Center ', a[2] : 5 : 4, TAB, 'Baseline ', a[3] : 5 : 4, TAB, 'Linear ', a[4] : 5 : 4,
TAB, 'Quadratic ', a[5] : 5 : 4);

```

```

        StoreLine;
    end;

    procedure ProcessFile;

    begin {Process File}
        while not (eof(Input_File) or Fail) do
            begin
                Block_Name := FindBlock;
                case Block_Name of
                    TTL:
                        DisplayTitle;
                    DAT, SUM, HYS:
                        ProcessBlock;
                end; {case}
            end;
        close(Input_File);
        close(Output_File);
        if Fail then
            Writeln('Error found in file, extraction terminated');
        end; {Process File}

    begin
        OpenFiles;
        Initialize;
        ProcessFile;
    end.

```

```

program satfit;      { Version 1.0, 2-25-93 }
{ This program is designed to fit saturation data to S, Msat, and Xdia*T}
{ It uses as input a file with two columns, Mobs and H/T, in that order}
{ It is generally more robust than Kaleidagraph's implementation}
{}
{ The basis of this program is again the Marquardt minimization found}
{ in Numerical Recipes, Sec. 14.3}

```

```

const
  PathLength = 65;
  TAB = chr(9);
type
  WorkString = string[64];
  NumStr = string[12];
  TimeStr = string[8];
  FileName = string[PathLength];
  glndata = array[1..65] of double;
  glmma = array[1..3] of double;
  gllista = array[1..3] of integer;
  glcovar = array[1..3, 1..3] of double;
  glnpbymp = array[1..3, 1..1] of double;

```

```

var
  Fail: boolean;
  Delim: string[3];
  Name: FileName;
  Input_File: text;
  LineBuffer: WorkString;
  Line_Ptr: integer;
  Line_Count: integer;
  Data_Number: integer;
{Data Elements}
  glochisq: double;
  glbeta: glmma;
  I, J: integer;
  Num_Scans: integer;
  mobs: glndata;
  hovert: glndata;
  sig: glndata;
  a, dummy: glmma;
  lista: gllista;
  mfit, ndata, mma, nca: integer;
  covar, alpha: glcovar;
  chisq, alambda, newc, oldc, yi: double;

```

```

function Open_Input (var fp: text; Name: Filename): boolean;

```

```

begin
  open(fp, Name);
{$I-}
  reset(fp);
{$I+}
  if IOresult <> 0 then
    begin
      Open_Input := False;
    { close(fp); }

```

```

        end
    else
        Open_Input := True;
end; { Open_Input }

procedure OpenFiles;
begin
    Write('Enter Data File Name: ');
    readln(Name);
    if not Open_Input(Input_File, Name) then
        begin
            Writeln('File "', Name, ' not found');
            Halt;           {Return an error code for batch files to see}
        end;
end; { OpenFiles}

procedure GetLine;
begin
    if not eof(Input_File) then
        begin
            Readln(Input_File, LineBuffer);
            Line_Count := Succ(Line_Count);
            Line_Ptr := 1;    {Reset the pointer}
        end;
end; {ReadLine}

function NextNumStr: NumStr;    { Isolates next number at LinePointer}
                                {and then resets LinePointer past number}
var
    StrLen: integer;
    StartPos: integer;

begin
    while ((Line_Ptr < Length(LineBuffer)) and (LineBuffer[Line_Ptr] = ' ') or (LineBuffer[Line_ptr]
= TAB)) do
        Line_Ptr := Succ(Line_Ptr);
        StartPos := Line_Ptr;
        while (Line_Ptr <= Length(LineBuffer)) and (LineBuffer[Line_Ptr] <> ' ') and
(LineBuffer[Line_Ptr] <> TAB) do
            Line_Ptr := Succ(Line_Ptr);    {now points to end of number}
        { If Line_Ptr < Length(LineBuffer) then}
        {   Line_Ptr:= Succ(Line_Ptr); }
    {now points to next number}
    StrLen := Line_Ptr - StartPos;
    NextNumStr := Copy(LineBuffer, StartPos, StrLen);

end;

procedure gaussj (var a: glcovar; n, np: integer; var b: glnpbymp; m, mp: integer);
var
    big, dum, pivinv: double;
    i, icol, irow, j, k, l, ll: integer;
    indxc, indxr, ipiv: gllista;
begin
    for j := 1 to n do
        begin
            ipiv[j] := 0

```

```

end;
for i := 1 to n do
begin
  big := 0.0;
  for j := 1 to n do
    begin
      if (ipiv[j] <> 1) then
        begin
          for k := 1 to n do
            begin
              if (ipiv[k] = 0) then
                begin
                  if (abs(a[j, k]) >= big) then
                    begin
                      big := abs(a[j, k]);
                      irow := j;
                      icol := k;
                    end
                  end
                end
              else if (ipiv[k] > 1) then
                begin
                  writeln('pause 1 in GAUSSJ - singular matrix');
                  readln;
                end
              end
            end
          end
        end
      end;
      ipiv[icol] := ipiv[icol] + 1;
      if (irow <> icol) then
        begin
          for l := 1 to n do
            begin
              dum := a[irow, l];
              b[irow, l] := b[icol, l];
              b[icol, l] := dum;
            end;
          for l := 1 to m do
            begin
              dum := b[irow, l];
              b[irow, l] := b[icol, l];
              b[icol, l] := dum;
            end
          end;
          end;
          indxr[i] := irow;
          indxc[i] := icol;
          if (a[icol, icol] = 0.0) then
            begin
              writeln('pause 2 in GAUSSJ - singular matrix');
              readln;
            end;
            pivinv := 1.0 / a[icol, icol];
            a[icol, icol] := 1.0;
            for l := 1 to n do
              begin
                a[icol, l] := a[icol, l] * pivinv;
              end;
            for l := 1 to m do
              begin

```

```

        b[icol, l] := b[icol, l] * pivinv
    end;
    for ll := 1 to n do
    begin
        if (ll <> icol) then
        begin
            dum := a[ll, icol];
            a[ll, icol] := 0;
            for l := 1 to n do
            begin
                a[ll, l] := a[ll, l] - a[icol, l] * dum
            end;
            for l := 1 to m do
            begin
                b[ll, l] := b[ll, l] - b[icol, l] * dum
            end
        end
    end
    end;
    for l := n downto 1 do
    begin
        if (indxr[l] <> indxc[l]) then
        begin
            for k := 1 to n do
            begin
                dum := a[k, indxr[l]];
                a[k, indxr[l]] := a[k, indxc[l]];
                a[k, indxc[l]] := dum
            end
        end
    end
end;

procedure covsrt (var covar: glcovar; ncvm: integer; ma: integer; lista: gllista; mfit: integer);
var
    i, j: integer;
    swap: double;
begin
    for j := 1 to ma - 1 do
    begin
        for i := j + 1 to ma do
        begin
            covar[i, j] := 0.0
        end
    end;
    for i := 1 to mfit - 1 do
    begin
        for j := i + 1 to mfit do
        begin
            if (lista[j] > lista[i]) then
            begin
                covar[lista[j], lista[i]] := covar[i, j]
            end
            else
            begin
                covar[lista[i], lista[j]] := covar[i, j]
            end
        end
    end
end

```

```

    end;
    swap := covar[1, 1];
    for j := 1 to ma do
        begin
            covar[i, j] := covar[j, j];
            covar[j, j] := 0.0
        end;
    covar[lista[1], lista[1]] := swap;
    for j := 2 to mfit do
        begin
            covar[lista[j], lista[j]] := covar[i, j]
        end;
    for j := 2 to ma do
        begin
            for i := 1 to j - 1 do
                begin
                    covar[i, j] := covar[j, i]
                end
            end
        end
    end;
end;

function coth (x: double): double;

begin
    coth := (Exp(x) + Exp(-x)) / (Exp(x) - Exp(-x))
end;

function resp (x: double; a: glmma): double;
    const
        gbetaovertwok = 0.67326863;
begin
    if x = 0 then
        resp := 0
    else
        resp := a[3] * x + a[2] * ((a[1] + 0.5) * coth(gbetaovertwok * x * 2 * (a[1] + 0.5)) - 0.5 *
coth(gbetaovertwok * x))
    end;
end;

procedure funcs (x: double; a: glmma; var y: double; var dyda: glmma);
    var
        I: integer;
        atemp: glmma;
begin
    y := resp(x, a);
    for I := 1 to 3 do
        begin
            atemp := a;
            a[I] := a[I] * 1.0001;
            dyda[I] := (resp(x, a) - y) / (a[I] - atemp[I]);
            a := atemp
        end
    end;
end;

procedure mrqcof (x, y, sig: glndata; ndata: integer; var a: glmma; mma: integer; lista: gllista; mfit:
integer; var alpha: glcovar; var beta: glmma; nalp: integer; var chisq: double);
    var
        k, j, i: integer;

```



```

        ymod, wt, sig2i, dy: double;
        dyda: glmma;
begin
    for j := 1 to mfit do
        begin
            for k := 1 to j do
                begin
                    alpha[j, k] := 0.0
                end;
            beta[j] := 0.0
        end;
    chisq := 0.0;
    for i := 1 to ndata do
        begin
            func(x[i], a, ymod, dyda);
            sig2i := 1.0 / (sig[i] * sig[i]);
            dy := y[i] - ymod;
            for j := 1 to mfit do
                begin
                    wt := dyda[lista[j]] * sig2i;
                    for k := 1 to j do
                        begin
                            alpha[j, k] := alpha[j, k] + wt * dyda[lista[k]];
                        end;
                    beta[j] := beta[j] + dy * wt
                end;
            chisq := chisq + dy * dy * sig2i;
        end;
    for j := 2 to mfit do
        begin
            for k := 1 to j - 1 do
                begin
                    alpha[k, j] := alpha[j, k];
                end
            end
        end
    end;
end;

```

procedure mrqmin (x, y, sig: glndata; ndata: integer; var a: glmma; mma: integer; lista: glldata; mfit: integer; var covar, alpha: glcovar; nca: integer; var chisq, alambda: double);

```

    label
    99;
    var
        k, kk, j, ihit: integer;
        atry, da: glmma;
        oneda: glnpbymp;

begin
    if (alambda < 0.0) then
        begin
            kk := mfit + 1;
            for j := 1 to mma do
                begin
                    ihit := 0;
                    for k := 1 to mfit do
                        begin
                            if (lista[k] = j) then
                                ihit := ihit + 1
                        end;

```

```

        if (ihit = 0) then
            begin
                lista[kk] := j;
                kk := kk + 1
            end
        else if (ihit > 1) then
            begin
                writeln('pause 1- in routine MQRMIN');
                writeln('improper permutation in LISTA');
                readln
            end
        end;
    if (kk <> (mma + 1)) then
        begin
            writeln('pause 2- in routine MQRMIN');
            writeln('improper permutation in LISTA');
            readln
        end;
    alamda := 0.001;
    mrqcof(x, y, sig, ndata, a, mma, lista, mfit, alpha, glbeta, nca, chisq);
    glochisq := chisq;
    for j := 1 to mma do
        begin
            atry[j] := a[j]
        end
    end;
    for j := 1 to mfit do
        begin
            for k := 1 to mfit do
                begin
                    covar[j, k] := alpha[j, k];
                end;
            covar[j, j] := alpha[j, j] * (1.0 + alamda);
            oneda[j, 1] := glbeta[j]
        end;
    gaussj(covar, mfit, nca, oneda, 1, 1);
    for j := 1 to mfit do
        da[j] := oneda[j, 1];
    if (alamda = 0.0) then
        begin
            covsrt(covar, nca, mma, lista, mfit);
            goto 99
        end;
    for j := 1 to mfit do
        begin
            atry[lista[j]] := a[lista[j]] + da[j]
        end;
    mrqcof(x, y, sig, ndata, atry, mma, lista, mfit, covar, da, nca, chisq);
    if (chisq < glochisq) then
        begin
            alamda := 0.1 * alamda;
            glochisq := chisq;
            for j := 1 to mfit do
                begin
                    for k := 1 to mfit do
                        begin
                            alpha[j, k] := covar[j, k]
                        end;
                end;
        end;

```

```

                                glbeta[j] := da[j];
                                a[lista[j]] := atry[lista[j]]
                                end
                                end
                                else
                                begin
                                    alamda := 10.0 * alamda;
                                    chisq := glochisq
                                end;
99:
                                end;

begin
    OpenFiles;
    I := 0;
    GetLine;
    repeat
        I := I + 1;
        GetLine;
        ReadString(NextNumStr, mobs[I]);
        ReadString(NextNumStr, hovert[I]);
        sig[I] := 1.0;
        Writeln(TAB, hovert[I] : 4 : 3, TAB, mobs[I] : 8 : 7);
    until (eof(Input_File));

    ndata := I;
    mma := 3;
    a[1] := 0.5;
    a[2] := 0.001;
    a[3] := 0.0001;
    nca := 3;
    for I := 1 to 3 do
        lista[I] := I;
    mfit := 3;
    alamda := -1;
    chisq := 0.0;
    repeat
        mrqmin(hovert, mobs, sig, ndata, a, 3, lista, 3, covar, alpha, 3, chisq, alamda);
        writeln(TAB, 'S = ', a[1] : 6 : 5, TAB, 'Msat = ', a[2] : 10 : 9, TAB, 'Xdia*T=', a[3] : 10 : 9, TAB,
'Xsquared = ', chisq : 10 : 9, alamda);
        until (alamda > Exp(4 * Ln(10)));
        readln
    end.
end.

```